The Assessment and Optimization of Heat Transfer During Electrofusion Welding of Thermoplastic Composite Pipes: A Modelling and Experimental Study

Ameen AL Obedan

A thesis submitted in partial fulfilment of the requirements for the degree of Doctor of Philosophy

The University of Sheffield
Faculty of Engineering
Department of Mechanical Engineering

Submission Date
29/09/2023

To my mother, father and two younger sisters….

SUMMARY

The main goal of this project is to examine the heat transfer phenomenon that occurs during the electrofusion welding process of Glass PE Thermoplastic Composite Pipes (TCP). The aim is to optimize the electrofusion welding process and coupler design by finding the optimal parameters to achieve the long-term performance of 100 bar and 85°C. Ensuring fusion of TCP joints is crucial for maintaining structural integrity leak resistance and long-term reliability in various applications like oil and gas. What makes this project unique is that there has not been research done on these materials under the proposed pressure, so it offers a valuable contribution to the field.

The project objectives involve investigating heat transfer during electrofusion welding through both experimental testing and numerical simulation. A reliable model for heat transfer has been developed, considering factors such as welding time, temperature material properties and coupler design. This model helps optimize welding parameters and calibrate the heat source to achieve high quality fusion and strong joints for TCP.

During testing TCP specimens were prepared and temperature distribution was monitored using thermocouples and thermography while electrofusion welding took place. Visual inspection along, with characterization techniques were employed to assess the quality of the fusion process. The formed electrofusion joint underwent thorough analysis including CT scans to ensure accuracy and reliability of the results.
Numerical simulation using a technique called element analysis (FEA) was used alongside experimental findings to enhance the research. FEA models allowed for testing and optimization of welding parameters providing valuable insights into the distribution of temperature, thermal gradients and melting behaviour during electrofusion welding. The experimental data confirmed the accuracy of the simulation results boosting confidence in the model's capabilities.

The project also focused on studying how critical welding parameters affect heat transfer and temperature distribution in TCP joints. A sensitivity analysis was conducted to identify which parameters have the significant impact on the welding process. Additionally, measurements were taken to improve the accuracy of thermal properties used in the model.

To optimize the process further simulated temperatures were compared with measurements from tests using a method called least square difference. This analysis revealed four parameters that strongly influence electrofusion welding; power efficiency (97.2%) thermal contact resistance (0.017 W/m^2K) external convective heat transfer coefficient (12.27 W/m^2K) and internal convective heat transfer coefficient (9.7 W/m^2K). By applying these parameters in repeated tests there was agreement, between measured and simulated data. Based on a refined computational model for heat transfer and a thorough analysis of strength two new designs for electrofusion fittings in thermoplastic composite pipes were suggested. These designs have been found to be capable of meeting the demands of applications requiring 100 bar pressure and operating temperatures of 85°C.

To summarize this project significantly enhances the understanding of heat transfer during the electrofusion welding process for Glass-PE Thermoplastic Composite Pipes. By conducting experiments, utilizing simulations, and employing optimization techniques, optimized welding parameters were proposed, the computational model was validated, and a reliable, novel designs for electrofusion fittings which can withstand 100 bar pressure were recommended. The outcomes of this research directly contribute to advancements in joining technologies for TCP ultimately enhancing the quality, durability and performance of these pipes across various industries.

ACKNOWLEDGMENTS

I would like to express my gratitude to everyone who has played a significant role in helping me reach this crucial stage and continuously supported me throughout my research.

First and foremost, I am immensely thankful for the guidance and patience of Dr. Rachel Tomlinson, my supervisor. Her unwavering support has been invaluable on this journey.

I would also like to extend my appreciation to Dr. Abderrazak Traidia, my industrial supervisor. Moreover, I am grateful for the supervision provided by Professor Anthony Ryan Dr. Matt Smith and Dr. Mike Troughton over the four years. Their expertise and insights have greatly enriched my work.

My heartfelt thanks go to Saudi Aramco for sponsoring my research and to the Non-Metallic Innovation Center for funding the materials and testing facilities required for this project.

I would also like to acknowledge the team at the Mechanical Workshop, Basic Characterisation Lab, Microprep Lab and iForge for their professionalism and collaboration throughout my research process.

Lastly but not least I want to express my deepest gratitude, towards my friends and family who have been unwavering in their support, understanding and encouragement during the challenging phases of this Ph.D. Journey.

CONTENTS

LIST OF FIGURES

LIST OF TABLES

NOMENCLATURE

Cp	specific heat capacity
Cp_{eff}	effective specific heat capacity of composite
η	efficiency of the heat source
k	thermal conductivity
k_{eff}	effective thermal conductivity of composite
L	latent heat
L_{fz}	length of melting zone along the fusion zone
P	Power rating for electrofusion welding machine
Q	Volumetric heat generated in the wires
r	radial coordinate
S	space between wires
t	time
T	temperature
T_{deg}	degradation temperature
T_{meas}	measured temperature by thermocouple
T_{sim}	simulated temperature by FEA model
T_{welding}	temperature required for welding
w_{fz}	width of melting zone
z	axial coordinate
α	thermal diffusivity
f	phase fraction from solid to liquid
ρ	density
ρ_{eff}	effective density of composite

LIST OF ACRONYMS

DSC	Differential Scanning Calorimetry
ECU	Electrofusion control unit
EF	Electrofusion
EFW	Electrofusion welding
FE	Finite element
FEA	Finite element analysis
GF	Glass fiber
HDPE	High density polyethylene
LFA	Laser flash analysis
MTDSC	Modulated Temperature Differential Scanning Calorimetry
NDT	Non-destructive testing
PA	Polyamide
PE	Polyethylene
PE100	High density polyethylene with minimum required strength of 10 MPA
PEEK	Polyether ether ketone
PP	Polypropylene
PVDF	Polyvinylidene difluoride
RMSE	Root mean square error
RTD	Resistance Temperature Detector
SDR	Standard dimension ratio
TC	Thermocouple
TCP	Thermoplastic composite pipe
TMA	Thermomechanical Analysis

Chapter 1

INTRODUCTION

1.1 Background

Piping systems are commonly used in settings like industries, homes and businesses to transport liquids or gases. These piping systems can categorized into four types based on the materials they are made of; (i) metallic piping, (ii) thermoset piping, (iii) thermoplastic piping and (iv) composite piping consisting of two or more materials.

In times there has been a noticeable rise in the utilization of thermoplastic composite materials across various industries such as renewable energy, aircraft manufacturing, automotive sector and medical applications [1]. The oil and gas industry is one area where the use of composites is still evolving. Composite materials offer potential to replace traditional metallic structures due to their ability to customize performance according to structural requirements. Moreover, using composites provides numerous advantages like reducing weight and carbon emissions, high fracture toughness, resistance to chemicals, ductility and recyclability [2].

Thermoplastic Composite Pipes (TCP) have gained attention in different industries due to their exceptional mechanical properties, resistance against corrosion and ease of installation [3]. These pipes are composed of a polymer matrix reinforced with fibers that make them suitable for applications in oil and gas sector as well, as water distribution systems where durability and reliability are crucial factors.

The joining process is an aspect of manufacturing and installing polymer pipes. When it comes to joining these pipes electrofusion welding is the usually used technique. It involves applying heat and pressure to fuse the ends of the pipes using a designed coupler. This welding method ensures that the joints are strong and free from leaks, which is essential for the long-term performance of the pipes.

Traditionally metallic joints have been used for joining TCP (Thermoplastic Composite Pipe). This often leads to issues with corrosion. If the advantages of TCP are to be fully utilized for high pressure applications in the oil and gas industry, then non-metallic joints need more research.

The complexity of heat transfer during electrofusion welding depends on factors such as welding time, temperature, pressure and coupler design. While there have been developments in electrofusion welding techniques for TCPs most of these advancements primarily cater to low pressure applications and are not suitable for high pressure scenarios, like oil and gas flowlines.

To ensure long lasting joints it is crucial to identify the optimal combination of welding process parameters and coupler design. This will help minimize the risk of joint failures and extend the service life of TCP.

1.2 Problem statement

Electrofusion welding of composite pipes (TCP) is an emerging and promising technique that has the potential to greatly enhance the quality and reliability of joints in the oil and gas industry. However, there are still challenges to overcome in optimizing the heat transfer process and achieving long term performance. The current models and coupler designs fall short in capturing the mechanisms of heat transfer during electrofusion welding due to the complexity of physical processes such as multiphase interaction, temperature-dependent material properties and the need for coupled thermos-mechanical models along with the lack of detailed experimental validation data, resulting in suboptimal welding conditions and potential performance issues. Therefore, it is crucial to conduct a study to investigate and enhance the understanding of heat transfer during electrofusion welding of TCP.

1.3 Research Objectives

The primary aim of this research is to analyse the heat transfer in the electrofusion welding of Glass-PE Thermoplastic Composite Pipes (TCP). The goal is to optimize the process parameters and coupler design to ensure the desired long-term performance, specifically for 6" pipes operating at 100 bar pressure and 85°C temperature. The specific objectives of this study include:

1. To investigate existing commercial coupler designs to analyse their performance and identify potential areas for improvement.
2. To develop a reliable model for heat transfer during electrofusion welding of TCP, considering the complexities of the composite material and the welding process.
3. To measure the required material thermal properties to accurately incorporate them into the model and improve the accuracy of predictions.
4. To conduct experimental testing to validate the developed model and verify the effectiveness of the optimized process parameters.
5. To perform a sensitivity analysis on critical welding parameters to understand their influence on heat transfer and joint quality.
6. To analyse the melting area and define the temperature distribution and behaviour around the composite laminate during the welding process.
7. To optimize the welding process parameters to achieve the desired joint strength, integrity, and long-term performance.
8. To achieve a reliable design of electrofusion fitting for TCP based on the research findings, incorporating the optimized process parameters and coupler design recommendations.

By addressing these objectives, this research aims to contribute to the field of TCP manufacturing and welding by providing insights into the heat transfer process, optimizing the welding parameters, and enhancing the design of electrofusion fittings for improved performance and reliability.

1.4 Thesis Structure: Overview of Chapters and Their Content

This thesis consists of ten chapters that focus on aspects of studying heat transfer during the electrofusion welding of Glass PE Thermoplastic Composite Pipes (TCP) and optimizing process parameters and coupler design. The following is an overview of the chapters and their content:

Chapter 2: Literature Review & Research Methodology

This chapter critically examines the knowledge and research on TCP, electrofusion welding, heat transfer in welding processes and coupler design. It discusses the basics of TCP and its joining methods delves into the electrofusion welding process and explores the factors that affect heat transfer during welding. Additionally, it reviews current coupler designs and identify gaps in existing literature. This chapter also presents an approach to investigate heat transfer during electrofusion welding of TCP. It outlines the framework which includes material selection and preparation, characterization of material properties, installation of thermocouples, physical welding tests, development of simulation models, validation of results, data optimization and innovative fitting design optimization. This comprehensive methodology ensures an understanding of the steps taken to tackle the research problem.

Chapter 3: Materials and Thermal Properties

This chapter details the selection of materials for testing and the methods employed to measure their thermal conductivity, specific heat capacity, and melting temperature. It addresses the essential thermal properties required for incorporating accurate material data into the heat transfer model.

Chapter 4: Experimental EFW tests for validation

This chapter delves into the experimental procedure for the physical electrofusion welding (EFW) tests. It starts with pre-welding analyses, from pipe preparation, thermocouples installation, to test setup. It also describes two conducted welding tests and their outcomes. Additionally, it provides insights into welding post analysis particularly focusing on CT scans and identifying the melting zone. The knowledge gained from these experiments plays a role in verifying, validating and improving the simulation model discussed in Chapters 6 and 7.

Chapter 5: Modelling heat transfer during EFW of TCP

This chapter delves into the details of the Finite Element Analysis (FEA) model developed to simulate heat transfer during electrofusion welding of TCP. It elaborates on the selection of the governing equations, justify choices of boundary conditions, as well as assumptions made in constructing the model. Additionally, it explores numerical solution techniques employed to solve the heat transfer model. Verify it through comparison with experimental data, statistical analysis and sensitivity analysis.

Chapter 6: Optimization of welding process parameters

This chapter provides a comprehensive exploration of the optimization process within the context of electrofusion welding. It defines optimization's role, highlights key and assumed parameters, and introduces the least squares method for optimization. Formulation, procedural steps, and the algorithmic approach are explained, leading to post-optimization results validation.

Chapter 7: Recommendation of EF fitting design

This chapter builds upon the optimized welding parameters obtained in Chapter 6 and apply them to a new design optimization problem. The focus will be on enhancing the electrofusion fitting for Thermoplastic Composite Pipes (TCP). By considering constraints such as temperature limits and stress related issues, the aim is to create a fitting that is perfectly suited for TCP.

Chapter 8: Discussions, conclusions and future work

This chapter serves as the core of this thesis, where it analyses and interprets the research findings in relation to electrofusion welding for TCP applications. This chapter not only elucidates the significance of the results but also relates them to existing knowledge, drawing meaningful conclusions and implications . This chapter provides a platform for addressing important research questions exploring unforeseen challenges and suggesting directions for future investigations. This Chapter synthesies the findings from this study and draws important conclusions that underscore their implications for the field. Additionally, this chapter takes a stance towards the future, outlining possible directions for additional exploration, advancement and utilization of the findings from the research.

Chapter 2

BACKGROUND & RESEARCH METHODOLOGY

This chapter provides an overview of the existing knowledge in the field specifically focusing on heat transfer during electrofusion welding. It critically examines research and delves into various aspects such as material properties, techniques for electrofusion welding, factors that impact welding quality, methods for quality testing, mechanisms of heat transfer, techniques for measuring thermal properties and previous studies on electrofusion welding heat transfer models.

2.1 Thermoplastic Composite Pipe (TCP)

2.1.1 Introduction

Thermoplastic Composite Pipe (TCP) has emerged as an alternative to traditional metal and single layer thermoplastic pipes due to its unique mechanical properties, corrosion resistance and ease of installation. TCP consists of a polymer matrix reinforced with high strength fibers like glass or carbon fibers that enhance strength and durability. This section provides an overview of TCP by discussing its manufacturing process, mechanical properties and advantages over other pipe designs. TCP has gained popularity in the oil and gas industry due to its exceptional features and benefits outlined as follows.

Corrosion resistance

One key advantage of TCP is its resistance, to corrosion, a crucial factor considering the harsh environments encountered in oil and gas production. Unlike metallic pipes that require expensive corrosion protection, coatings or cathodic protection systems. TCP possesses inherent corrosion resistance capabilities that ensure long term durability while reducing maintenance costs.

Lightweight and easy installation

The lightweight nature of TCP makes it easier to handle, transport and install compared to metallic pipes. This advantage not reduces installation time but also minimizes the need for heavy equipment resulting in cost savings particularly in offshore and remote locations.

High-strength performance

TCP demonstrates mechanical properties that ensure high strength performance while still maintaining flexibility. This characteristic is crucial for withstanding the demands of pressures, dynamic loads and thermal expansions commonly encountered in oil and gas operations.

Reduced total cost of ownership

The combined benefits of corrosion resistance, lightweight construction and high strength performance contribute to a reduction in the overall cost of owning TCP within the oil and gas industry. TCPs lifespan, minimal maintenance requirements and ease of installation result in significant cost savings over its operational life cycle. Moreover, if glass fiber reinforced composite pipes were used instead of carbon steel in onshore flowlines an average reduction of 60% in lifecycle carbon footprint could be achieved [4].

In conclusion thermoplastic composite pipes offer advantages that make them highly desirable within the oil and gas industry. The corrosion resistance, lightweight construction, high strength performance, chemical resistance capabilities well as reduced total ownership costs address the critical need for reliable and durable piping systems, within this sector. Consequently, TCP has become increasingly. Embraced in a wide range of oil and gas applications playing a significant role in enhancing efficiency, safety and cost effectiveness, within the industry.

2.1.2 Materials, design, and production

TCP is composed of a thermoplastic matrix, such as polyethylene (PE), polypropylene (PP), or polyamide (PA), reinforced with high-strength fibers[5]. The choice of matrix and fibers depends on the specific application requirements, considering factors such as operating conditions, pressure, and temperature. The use of glass or carbon fibers imparts superior strength and stiffness, making TCP suitable for a wide range of industries. TCP consist of three layers which are usually made from the same thermoplastic compound; liner, reinforced layer and outer cover layer, as shown in figure 2-1.

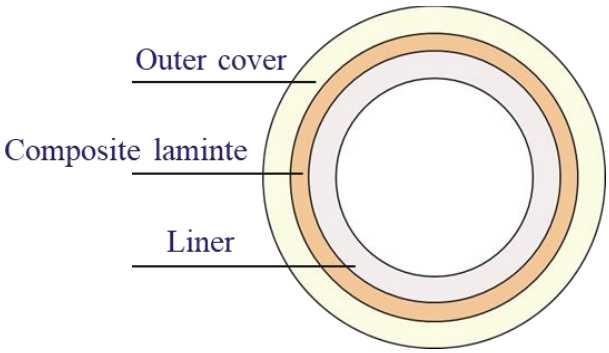

Figure 2-1 TCP configuration

The **liner** is the internal layer of the pipe with direct contact with the transported fluid. It provides sealing, resistance to the permeation of the fluid, and works as a smooth surface to allow for higher fluid flow rate [6]. The operational parameters (temperature, pressure and fluid type) play a significant role in the selection of the liner material. Typical thermoplastic polymers used in the oil and gas industry are polyethylene (PE), polyamide (PA), polyvinylidene difluoride (PVDF), polypropylene (PP), and polyether ether ketone (PEEK) [5].

The **reinforced layer** is the main element in the TCP structure [7], sandwiched between the liner and the outer protective layer. It provides the strength of the TCP structure and absorbs both internal and external loads on the pipe. The reinforced layer is built up in several layers of high-quality thermoplastic composite tapes, usually applied in opposite directions. Typical reinforcement used in oil and gas applications are glass or carbon fiber thermoplastic composites.

The **cover layer** provides protection from ultraviolet radiation, outside conditions and external damage [8]. In fact, the liner and cover layer work together to protect the middle reinforcement layers from corrosive environments that can come from the outside or the transported fluid.

The design and production of TCP involve several key considerations. The reinforcement fibers are typically arranged in a helical or cross-ply configuration to optimize mechanical properties and ensure balanced strength in different directions. The manufacturing process involves filament winding or tape laying techniques, where the fibers are impregnated with the thermoplastic matrix and wound or layered onto a mandrel. This process allows for the production of seamless pipes with controlled fiber orientations and thickness.

The thermoplastic composite pipe is typically made from discrete uni-directional high-end composite. The composite tapes contain several thousands of high-strength fibers with the size of microns in diameter impregnated with similar thermoplastic resin as the liner. The purpose of the resin is to hold the fibers in position to allow the fibers to carry loads.
An automated tape winding and placement process is used to build the pipe wall gradually out of layers of multiple tapes. The orientation of each layer can be changed with respect to the axis of the pipe to achieve the required structural strength properties. A heat source, such as a laser, is applied to each incoming tape and the one below to heat them above the resin melting temperature to fully fuse all layers, forming a fully bonded composite structure. [6]

2.1.3 Mechanical properties

TCP demonstrates mechanical characteristics by harnessing the strength of its fibers and the toughness and ductility of its thermoplastic matrix. The composite nature of TCP contributes to its tensile strength, stiffness and ability to withstand impact and fatigue. In contrast to singnle layer thermoplastic pipes TCP offers notable advantages. Single layer thermoplastic pipes often lack the necessary strength and durability required for demanding applications. On the other hand, TCP exhibits enhanced mechanical properties such as a higher strength to weight ratio improved resistance to external loads and reduced vulnerability to damage caused by external factors [9]. These superior mechanical properties make TCP well suited for challenging applications in industries, like oil and gas, water distribution and offshore structures..

2.1.4 Effect of Thermal Loading and Fluid Corrosivity on TCP

Thermal loading and fluid corrosivity are critical factors influencing the performance of TCP. TCP exhibits excellent resistance to high temperatures, with the thermoplastic matrix maintaining its structural integrity even under thermal cycling [10].

This characteristic makes TCP suitable for applications involving hot fluids or environments with fluctuating temperatures. Furthermore, TCP is highly resistant to corrosion from various fluids, including aggressive chemicals, acids, and saline solutions, ensuring their long-term reliability and durability in corrosive environments [11].

The distribution of temperature along the thickness of composite pipes plays a significant role in handling the high-temperature nature of the transported fluid. The thermal properties of the liner should be appropriate to protect the reinforced layer from higher temperature gradients and avoid any disturbance in the mechanical performance of the whole structure.

The temperature distribution under different internal temperatures was assessed by James ea al. (2019) for 24 mm thickness PEEK/Carbon composite riser as shown in figure 2-2. The temperature declines in approximately linear behaviour from the composite pipe liner to the external layer at dissimilar rates through each surface

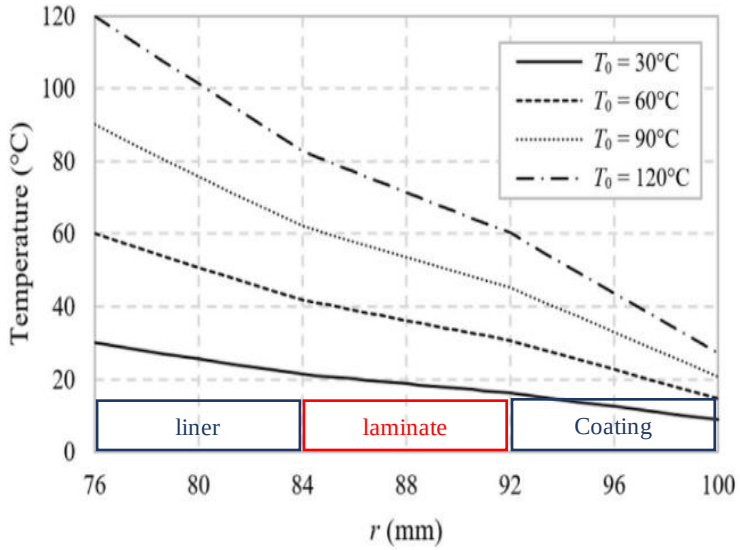

Figure 2-2 Temperature distribution of TCP for increasing internal temperature [10]

The steeper slope through both the liner and coating layers indicates lower thermal conductivity when compared to the laminate layer. Lower thermal conductivity materials are more efficient in terms of thermal insulation, thus protecting the laminate layer from high temperature gradients.

To simulate the effect of fluid corrosivity on the composite pipe internal layer, a polyethylene sample was examined by Qi et al (2015) in similar environment as the oilfields. This test aimed to determine changes in weight and the tensile strength of the sample subjected to H_2S and CO_2 with raising temperature.

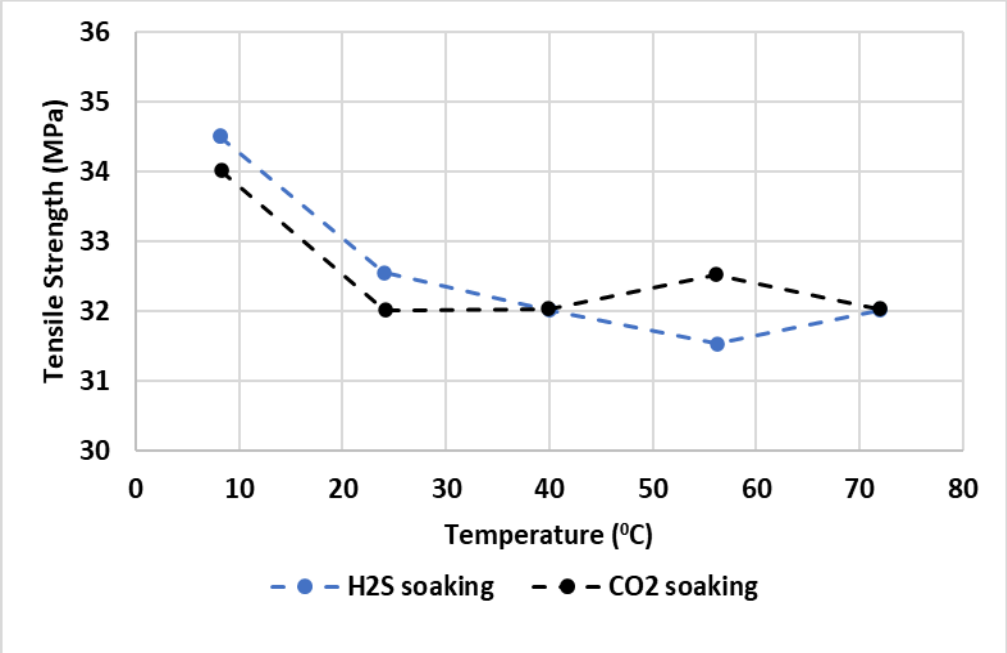

Figure 2-3 Impact of temperature change on tensile strength after corrosion [11]

It can be noticed from Figure 2-3 that the polyethylene tensile strengths decrease slightly with the increase in media temperature. With reduction rates around 5%, polyethylene shows satisfactory resistance to both H_2S and CO_2 corrosion. The low tensile strength reduction is obvious below glass transition temperature (approximately T_g=110 ^{0}C) as the polymer chains are in a more ordered, rigid state. However, above T_g the polymer chains gain mobility, becoming more flexible and less ordered where the material transitions to rubbery state which can be associated with higher reduction of the tensile strength.

2.1.5 TCP joining methods

The joining methods for three-layer thermoplastic composite pipes typically involve techniques that ensure a secure and leak-free connection between the layers. Here are three commonly used joining methods for three-layer thermoplastic composite pipes:

Mechanical Couplings

Mechanical couplings are the means of joining three layer thermoplastic composite pipes. These couplings use mechanisms like compression or interlocking to secure the layers together [12]. They eliminate the need for heat or welding processes. Allow for easy disassembly and reassembly. Mechanical couplings offer flexibility and ease of installation making them suitable for applications that require maintenance or repair. However, it is important to note that they may have some limitations in terms of strength, long term performance and resistance to corrosive environments.

Butt Fusion

Butt fusion serves as a technique for joining PE pipes and can also be adapted for TCP connections. This method involves heating the pipe ends to their melting point using a fusion machine, followed by applying pressure to join them together. As the material cools down. Solidifies, a strong and continuous joint is formed. Butt fusion offers joints, high joint strength and excellent chemical resistance. However, it requires fusion equipment and precise control over welding parameters to ensure proper fusion and maintain joint integrity. However, joining such pipes using butt fusion can be more challenging than joining solid-wall thermoplastic pipes. The reinforced layer can interfere with the fusion process and might not melt as uniformly as the outer thermoplastic layers. The result could be a joint that is not as robust or reliable. Kiani et al. (2022) found that a reduction in tensile strength (compared to the non-welded pipe) is approximately 82 % in butt fusion of HDPE pipes reinforced with glass fibers and carbon nano tubes. However, A butt fusion joint with armoured sleeve was proposed by Liu et al (2022) and studied through theoretical, FEA and experimental analysis. This study gave a promising result for HDPE/glass composite pipe and the joint performance under internal pressure.

Electrofusion Welding

Electrofusion welding is a widely employed technique for joining PE pipes [15], and it has potential use for connecting TCP. It involves the use of a specialized coupler with embedded heating elements. The heating elements generate heat by applying an electric current, melting the thermoplastic layers and facilitating fusion. Achieving intimate contact between the surfaces to be joined is essential for strong adhesion. The heating process is carefully regulated to ensure substantial pressure is attained through the ongoing melt expansion within the contained melt pool. Electrofusion welding provides seamless and integrated joints, high joint strength, and resistance to leakage. It requires specialized equipment and trained personnel for proper execution. However, joining TCP using EFW require special attention, as excessive heat may disturb the reinforced composite laminate structure and thus, disturb the mechanical integrity of the pipe.

Current research has begun to explore the implementation of electrofusion welding for TCP in low-pressure/temperature applications. Liu et al (2022) had designed an electrofusion joint for perforated steel skeleton reinforced thermoplastic composite pipe (PSS-RTP) and examined its strength through analytical and FEA model.

However, no literature is available on electrofusion welding for fully non-metallic TCP, underscoring the need for a deeper understanding of this welding process to optimize it for high-pressure applications, especially those prevalent in the oil and gas industry.

Whilst no research literature to join TCP using electrofusion welding, there are available products in the market. The first product is proposed by the company called Tega and claimed to withstand a pressure of 100 bar (1450 psi) [16]. As shown in Figures 2-4 and 2-5 the fitting has circular hole where pipe should be inserted unlike standard electrofusion fittings where pipe slides to the fitting bore. The figure clearly shows the fusion welding will take place at both the inner and outer layers of the pipe by having double heating coils placed on both sides of the fitting.

Figure 2-4 Tega electrofusion fitting [16]

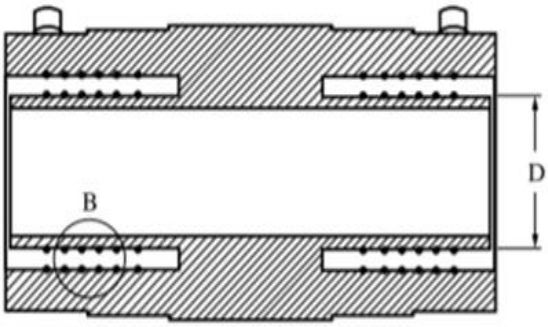

Figure 2-5 Cross section of Tega fitting [16]

The other product introduced by company called Soluforce is an electrofusion fitting designed for their own manufactured Reinforced thermoplastic pipes (RTP). It is a fully non-metallic joint with a combination of butt-welding and electrofusion welding. The electrofusion fitting shown in Figure 2-6, basically contains integrated copper wiring in reinforced plastic sleeve and can operate up to 90 bar/1305 psi for a 6-inch pipe [16].

Figure 2-6 Soluforce RTP Electrofusion fitting

The last product is an end-fitting flange produced by Soluforce as shown in Figure 2-7. It utilizes both mechanical joining and electrofusion welding methods. The solution is basically a stainless-steel flange attached to an electrofusion end fitting and can stand a pressure up to 125 bar/1813 psi [16]. This reusable solution enables the pipeline user to disassemble and reconnect the pipeline system when necessary.

Figure 2-7 Soluforce electrofusion end fitting [17]

Choosing the method to join three layer thermoplastic composite pipes depends on various factors, including pipe specifications, application requirements and desired joint strength and durability. Each joining method has its advantages and limitations so it is important to carefully consider the specific needs of the project as outlined in section 1.3.

2.1.6 Conclusion

Thermoplastic composite pipes (TCP) offer benefits in terms of mechanical properties, corrosion resistance and ease of installation. Designing and manufacturing TCP involves selecting materials arranging reinforcement fibers and employing production techniques. TCP provides advantages such as strength, durability and resistance to corrosive fluids. Additionally, TCP performs well under thermal conditions making them suitable for high temperature applications that involve thermal cycling. While metallic joints have traditionally been used to join TCP; recently there has been growing interest in using butt fusion and electrofusion welding, for low pressure applications based on literature reviews and emerging commercial products.

2.2 Electrofusion Welding Process

2.2.1 Introduction

The electrofusion welding technology is primarily used for joining PE pipes for water and gas transportation [18]. It has also been used in other industrial applications to join several other plastic pipes, such as Polyvinylidene fluoride (PVDF) and Polypropylene (PP). Electrofusion welding, while typical for plastic connections, has yet to be widespread in its application for joining composite oil & gas pipes. Introducing composite pipes reinforced with layers of carbon or glass fibers notably elevates their operating pressure capabilities. Thus, it amplifies concerns about the robustness of the electrofusion joint and the comprehensive quality of the assembled pipeline systems. In real-world scenarios, the benchmark for an excellent quality electrofusion joint is its ability to endure service loads for a minimum duration equal to the pipe's service life, typically 50 years [19]

Joining pipes by electrofusion requires three main elements; electrofusion fitting as shown in Figure 2-8, an electrofusion control unit (ECU), and a power source. For the electrofusion fitting, the joining is accomplished by the heat generated by circulating a current through an embedded resistance coil, usually at a fixed voltage of 40 to 80 Volt. These voltages reflect the specific requirements of the electrofusion process for different pipe sizes and materials to ensure a successful and durable joint. The supplied energy to the fitting is usually controlled by passing the current for a pre-specified fusion time [18]. The electrofusion control unit does not generate power; instead, it receives the power input from the power supply and ensures it passes in a stable manner to the fitting. [18]

The electrofusion fitting is usually made from polyethylene by injection molding [20]. The EF joint's schematic sketch is shown in Figures 2-8 and 2-9. The bore diameter of the fitting is larger than the pipe diameter and is constant along the fitting length. The clearance between the pipe and fitting considers the ovality of thermoplastic pipes and allows for a simple assembly process in the field. The fitting also has two terminal pins to take the regulated power input from the control unit to the embedded conductive wire on both sides of the fitting.

Figure 2-8 Electrofusion fitting [21]

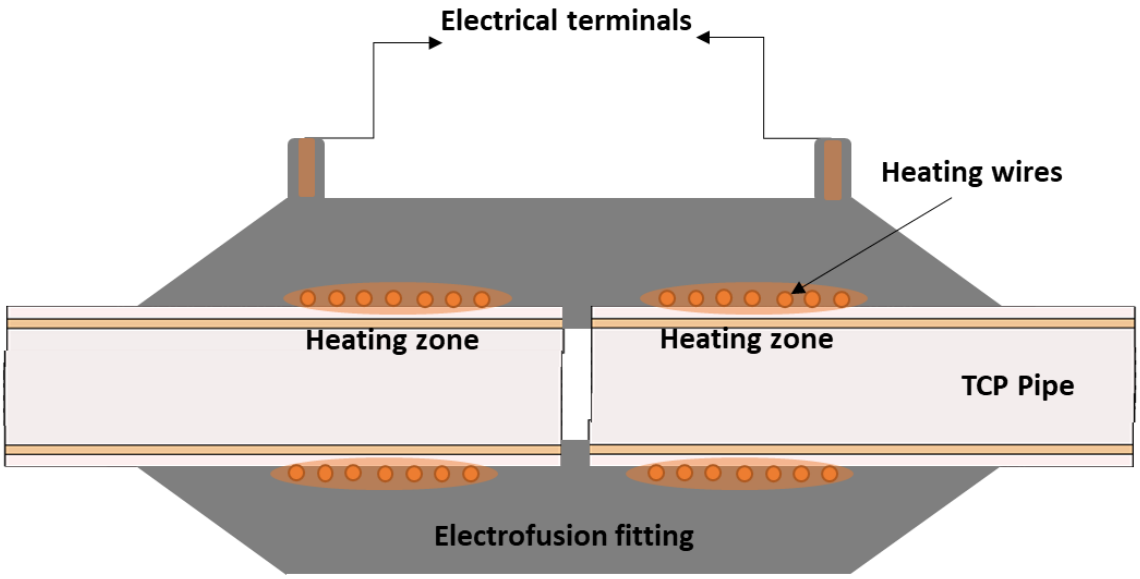

Figure 2-9 Electrofusion fitting cross-section

The electrofusion fitting can be divided into five different zones; two hot zones where the melting occurs, surrounded by three cold zones to stop the melted polymer from flowing out of the joint and ensure adequate pressure in the melting area. These cold zones are identified in Figure 2-10 located on the two sides of the hot zone and in the center of the fitting. There is also two melt indicators which are used to indicate a satisfactory welding process.

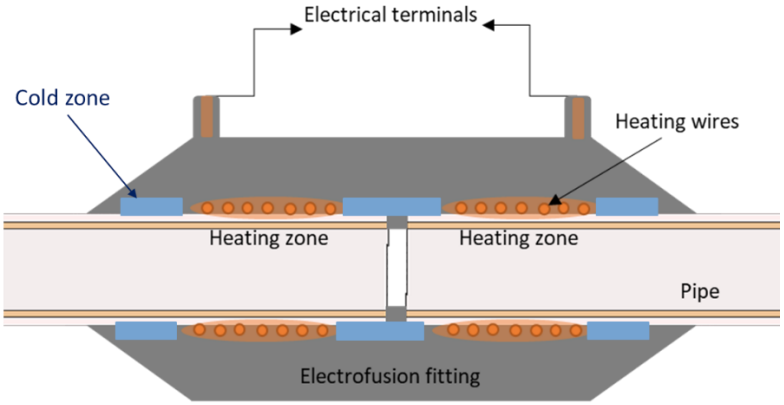

Figure 2-10 Electrofusion fitting heating and cold zones

Electrofusion welding offers an fully integrated connection eliminating the requirement for extra sealing substances or mechanical connectors. This creates a joint that is strong, dependable and resistant to leaks ensuring the long term effectiveness of PE pipes [18]. Electrofusion welding is also relatively fast and straightforward to execute necessitating training and expertise. The process can be automated, which boosts productivity and reduces labor expenses. Additionally the precise application of heat in electrofusion welding minimizes the risk of overheating or causing damage, to the surrounding pipe material.

2.2.2 EF welding process

The electrofusion welding process consists of several key steps. First, the pipe ends are prepared by cleaning and removing dirt, debris, or surface contaminants [18]. The coupler is then inserted between the pipe ends, ensuring proper alignment. Electrofusion fittings typically have an integrated heating coil and wires that connect to the welding machine. Once the fitting is correctly positioned, the physical welding process begins with a current circulating through the fitting coil causing thermal expansion in the surrounding material and contact between the fitting and pipe surfaces. The established contact then heats the pipe material, filling the initial clearance gap between the two surfaces. Figure 2-11 illustrates the EF joint formation was explained by Bowman (1997) in four steps.

Step 1 is where the pipe inserted into the fitting with an initial gap. The initial gap in electrofusion welding serves several essential roles. It facilitates uniform melt expansion and flow, ensuring even pressure distribution across the joint for strong adhesion. Additionally, it compensates for manufacturing tolerances, aids in achieving intimate contact between surfaces, and prevents overheating and material deformation during the welding process

Step 2 is where the current is applied to the coil, the gap is filled, a quantifiable melt pressure is present, and the material on both the pipe's external and fitting internal surface is melted and mixed. The flow of polymer material is crucial in electrofusion welding for promoting intimate contact between surfaces, facilitating fusion, eliminating voids, and ensuring uniform pressure distribution, all of which contribute to the formation of a strong and durable weld

Step 3 is where the fusion process closely reaches the standard fusion time, the temperature and melt pressure increase at the fusion interface. In addition, the volume of molten polymer and interface strength is increased. The mode of failure in the interface at this stage changes from brittle to ductile.

Step 4 is when the power is switched off, the joint is left clamped for cooling, where cooling of the molten polymer starts from the areas close to the cold zones to the center of the heated zones. [18]

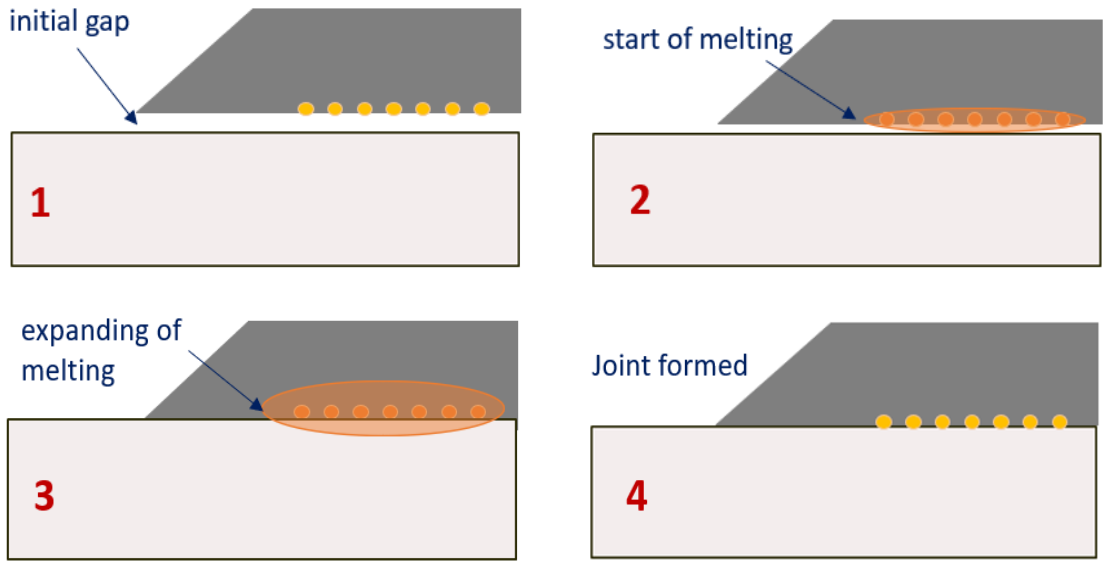

Figure 2-7 Electrofusion joint formation process [18]

During the melting phase thermoplastics experience increased mobility. This is crucial for the fusion or joining of two pieces during welding [22]. When the surfaces of these thermoplastics come into contact while in melting state, the polymer chains start to mix and spread across the interface. This mixing creates a bond between the surfaces effectively acting as a weld once it solidifies [23]. As the polymer chains interdiffuse, they also become entangled with each other, further strengthening the bond. This process of mixing and interdiffusion is commonly referred to as "healing". The healing period plays a role, in allowing polymer chains to penetrate and diffuse across the welding interface ensuring a strong weld. It is important to find an optimal welding time because too short duration might not allow sufficient macromolecular diffusion while excessively long times could lead to polymer degradation [24].

The entire welding process is controlled by a welding machine that monitors and regulates the temperature, heating time, and pressure applied during the fusion process. After the fusion, the joint can cool and solidify, forming a strong and leak-proof connection. The cooling phase is critical to achieve high-strength welded joints in the electrofusion process. In the cooling phase, the current stops flowing to the heating coil, and then both the temperature and melt pressure at the fusion interface begin to decline.

The cooling phase is required for crystallization and to allow proper organization of PE molecules on the welding interface. During cooling, the interface temperature stabilizes for some time due to the exotherm effect from PE crystallization. After the interface crystallization, the temperature starts to reduce until it reaches the ambient temperature, the PE volume formed at elevated temperature shrinks, and a high-strength joint is obtained [18]. Since the actual welding process is automated and controlled by the electrofusion control unit, the quality of the joint is mainly influenced by the preparation and cooling phases and the correct selection of the operation parameters.

2.2.3 Factors affecting the quality of EF joints

Boman (1997), Shi et al. (2011), Ge et al. (2021) have extensively studied the factors affecting electrofusion welding to optimize the process and improve joint quality. Investigations have focused on understanding the influence of surface preparation techniques, such as different cleaning methods and surface treatments, on the integrity of the fusion. Studies have also explored the effects of wire geometry and welding parameters, such as heating time [25], temperature, and pressure, on the strength and reliability of the joint.

Additionally, advancements in welding machine technology and automation have been made to ensure precise control and monitoring of the welding process, minimizing the risks of both lack of welding and over-welding.

Wire geometry

In electrofusion welding (EFW) the shape and dimensions of the wire are factors in determining the effectiveness, strength and overall quality of the joint. Figure 2-12 illustrates the wires geometry, including its size, pitch and depth [18]. The size and pitch of the wire play a role in distributing heat evenly during the fusion process. This even distribution is important to achieve a seamless fusion without any weak points in the joint. Additionally, variations, in wire depth can significantly impact how the polymer melts.

It is important to manage this melting rate to prevent material degradation or combustion, both of which can compromise the strength of the joint.

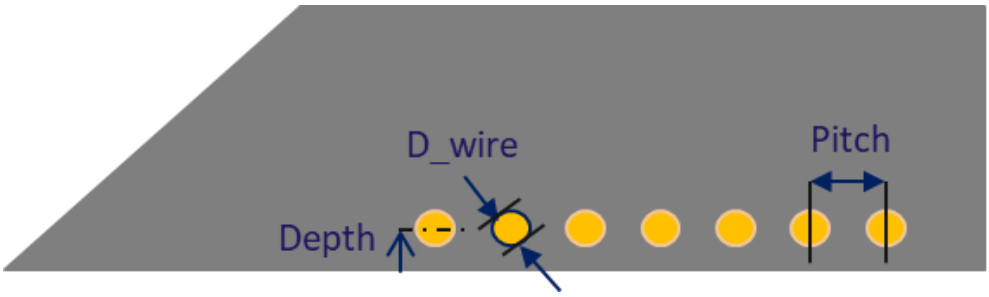

Figure 2-8 Heating wire geometry parameters

Surface Preparation

Properly preparing the surface is crucial to achieve an reliable fusion in electrofusion welding. The cleanliness of the pipe ends impacts the quality of the joint. Any impurities like dirt, grease or moisture can interfere with the fusion process. Compromise the strength of the joint [26]. Therefore, it is essential to clean the pipe ends before welding. Common methods such as using solvents scraping mechanically or wiping with lint free cloths are typically employed to ensure a clean and uncontaminated surface.

Lack of Welding

Inadequate welding, also referred to as "lack of welding " occurs when there is insufficient fusion between the pipe ends and the coupler. This can happen due to heating time insufficient pressure or misalignment of the pipe ends with the coupler [27]. Insufficient welding can result in joints, reduced strength and potential leaks or failures during service.

Hence it is crucial to control various welding parameters including heating time, temperature and pressure to ensure complete fusion and a strong joint. Bowman (1997) conducted an analysis, on how fusion time affects strength. The results depicted in Figure 2-13 illustrate that longer fusion times correlate with increased toughness of the joint. After about 200 seconds of fusion it was noticed that the toughness levels off suggesting that prolonging the fusion time, beyond this point does not noticeably improve the joints strength.

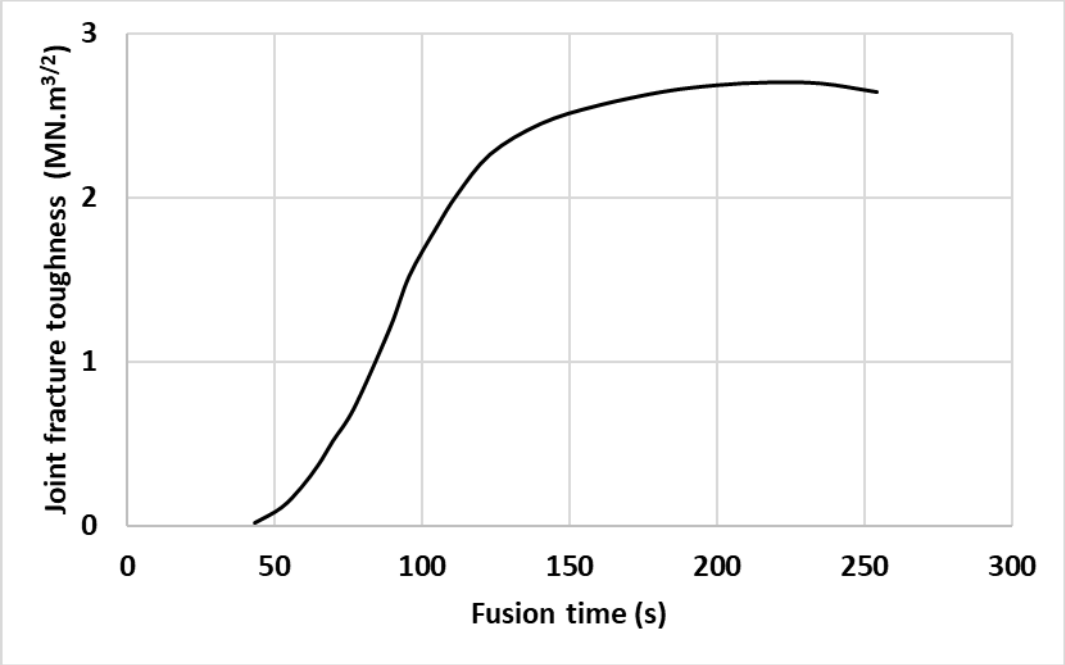

Figure 2-9 The effect of fusion time on the joint strength [18]

Over Welding

Excessive heat during electrofusion welding, also known as over welding or overheating can have an effect on the quality of the process. This occurs when both the pipe ends and the coupler are exposed to much heat causing material degradation, distortion or even melting. Overheating is typically caused by prolonged heating time temperatures or inadequate control of the welding process [27]. Over welding weakens the joint alters dimensions and compromises the long-term performance of the welded connection.

Therefore, it is crucial to have control and monitoring of welding parameters in order to prevent overheating and achieve optimal fusion without excessive exposure to heat. To summarize surface preparation, absence of welding techniques and over welding are crucial factors that significantly affect the quality and performance of electrofusion welding. Ensuring surface cleaning, meticulous control of welding parameters along with careful monitoring are essential for achieving strong and dependable joints. Additionally improving surface preparation techniques understanding how welding parameters impact results and exploring welding technologies will be pivotal, in enhancing the integrity of electrofusion joints.

2.2.4 Quality testing of EF joint

Researchers have proved the quality of the welded joint to be one of the most critical safety concerns in the pipeline system since any failure in the joint will directly fail the whole system. The quality of an electrofusion joint mostly depends on the entanglements of the polymer molecules close to the welding interface. It is important to mention that molecular entanglement considerably influences the toughness, intensity, and peeling energy of the welded joint [19]. Further to the quality of the electrofusion joint, plenty of work has been accomplished on the safety assessment and non-destructive inspection of polyethylene pipe systems during service, such as guided wave, ultrasonic inspection, phased array ultrasonics, and acoustic emission. [20].

However, one negative side of using electrofusion welding is the difficulty of inspecting the quality of the joint since the fitting covers the weld interface. The quality of electrofusion welding can be checked by three methods: visual examination, destructive testing, and non-destructive testing. Various testing methods are employed to assess the quality and integrity of electrofusion welds, and these are described as follows.

In **the visual examination**, it is impossible to assess the strength and defects of the formed joint; instead, some indicators are used to claim successful electrofusion welding. Visual examination is the first and most straightforward method to assess the quality of electrofusion welds [28]. It involves inspecting the joint for visible defects such as misalignment, pipe readiness, and unexpected behaviour during and after the welding such as surface cracks and excessive melt extrusion at the edges of the electrofusion fitting.

In **destructive testing**, the whole joint or small piece cut from the joints can be exposed to various short-term tests such as peel decohesion, crush, tensile, and hydrostatic pressure tests.

Destructive tests present different methods to evaluate the joint's quality based on the joint interface's strength. [29] However, such tests prevent further use of the joint.

Inspecting electrofusion joints using **non-destructive (NDT) methods** has been given considerable attention for many years. It was found that several NDT methods, such as ultrasonic, thermography, laser and x-ray [30], can detect some electrofusion welding defects. Unlike destructive testing, NDT techniques are not meant to provide an idea about the strength of the joint; instead, they are utilized to detect internal defects or discontinuities in the welds, such as incomplete fusion, voids, cracks, or irregularities, without damaging the joint.

2.2.5 Causes of failure associated with EF joint

Despite its benefits there are instances when electrofusion welding may encounter issues due to installation or improper design.. Common causes of failures are described briefly as follows.

Incomplete fusion occurs when the material of the pipe fails to fully bond with the coupler material leading to weakened or compromised joints. This kind of failure can be attributed to heating time inadequate pressure or misalignment between the ends of the pipe and the coupler [31].

Contamination during the welding process can result in failure. Contaminants like dirt moisture or grease can obstruct the fusion process. Hinder proper bonding between the pipe ends and coupler [32].

Overheating, caused by excessive heat application, can result in material degradation, distortion. Overheated welds may have reduced strength and compromised integrity, making them more susceptible to failure under operational conditions [26].

Improper installation practices, such as improper alignment, inadequate cleaning, or incorrect welding parameters, can lead to weak joints and compromised integrity. These practices may introduce defects or inconsistencies in welds thereby increasing the risk of failure [33].

Environmental factors, including exposure to aggressive chemicals, UV radiation, or high temperatures, can degrade the integrity of electrofusion welds over time [34]. Chemical attack, thermal degradation, or environmental stress cracking may weaken the joint and lead to failures in service [35].

To address these causes of failures there are ongoing efforts to improve welding techniques implement quality control measures and establish standardized testing procedures. Moreover, advancements, in welding equipment automated monitoring systems and operator training aim to improve the quality and reliability of electrofusion welds.

2.3 Modelling and validation of the electrofusion joining process

2.3.1 Introduction

In any manufacturing process it is crucial to determine the values of process parameters to achieve a successful outcome. Traditionally experimental methods and testing programs have been used to identify these parameters. They are often time-consuming and expensive. As a result, computational modelling of processes has become essential in various industries for simpler parameter optimization.

When it comes to modelling fusion welding processes the focus lies on heat transfer and consolidation. Other factors that directly impact strength, such as residual stresses and crystallinity content can also be considered [36]. Over the three decades there has been a growing interest among researchers in simulating the electrofusion process for joining polyethylene pipes due to its increasing applications.

Bowman [18] classified electrofusion simulation models into categories, with the goal of predicting heat transfer and temperature profiles during the joining process. These models are time dependent and vary based on the dimensions used in finite element modelling. Some models have improved accuracy by incorporating temperature dependent material properties and accounting for various physical phenomena associated with the process [36].

2.3.2 Electrofusion welding modelling

Electrofusion welding modelling employs computational methods to simulate the welding process. Electrofusion welding models have the capability to anticipate the temperature distribution, fluid flow and stress distribution of a weld joint [19,37]. Furthermore, they can optimize the welding process. Address any welding defects that may arise.

The significance of welding modelling, in electrofusion welding processes lies in two aspects.

Firstly, these models enable the prediction of the quality of a weld joint even before it is created. This helps to avoid errors and ensures that the weld joint meets the required specifications.

Additionally, these models allow the examination of how different welding parameters impact the quality of the weld joint. This valuable information can then be utilized to improve and optimize the welding process for weld joint quality.

Different models have been developed for electrofusion welding, which can be classified into three categories; thermal models, fluid flow models and structural models.

Thermal models primarily focus on understanding the heat transfer that occurs during the welding process. These models are typically based on the heat conduction equation. Provide insights into the temperature distribution within the weld joint [38,39].

Fluid flow models concentrate on studying the movement of fluids during welding. They often rely on equations like Navier Stokes or employ methods such as Lattice Boltzmann to predict flow patterns within the weld joint [40].

Structural models aim to analyze how a weld deforms throughout welding. These models are generally based on element methods and help in predicting stress distribution within the weld joint [19].

The history of modelling electrofusion welding dates back to the 1990s [38]. Initially simple analytical models were used to estimate temperature distribution in the weld area. However, these early models were built upon assumptions and did not account for the intricate physical processes associated with electrofusion welding.

In years more advanced numerical models started emerging during the late 1990s and early 2000s [19,41,42].These models were created using the element method to accurately simulate and analyze the various complex physical processes involved in electrofusion welding. These processes include heat transfer, mass transfer and fluid flow. Over time numerous other finite element models for electrofusion welding have been developed.

These models have proven valuable in studying a range of phenomena related to electrofusion welding. For instance they have helped understand how different welding parameters impact weld quality how pipe wall thickness affects weld strength and how pipe defects influence weld reliability. Additionally these finite element models have played a role in developing new welding techniques and optimizing welding parameters for different types of pipes and fittings.

Among the simplest models is the one proposed by Pitman [38]. This model focuses on a one dimensional heat transfer problem as its primary objective is to accurately represent temperature changes within welded parts during electrofusion welding. However, it is worth noting that this model requires consideration of the air gap between the pipe and fitting.
The basic heat transfer equation used by Pitman is:

$$\frac{\partial}{\partial x}\left(k(T)\frac{\partial T}{\partial x}\right) = \rho(T)C_P(T)\frac{\partial T}{\partial t} \quad (2.1)$$

where

k is the thermal conductivity,

ρ is the density,

And *Cp* is the specific heat capacity of the PE.

The Pitman model is an approach that can be employed to simulate the process of electrofusion welding. This model utilized the heat conduction equation to describe how heat is transferred during welding. It has been widely used to investigate the impact of factors on the welding process, such as the type of plastic material used, pipe thickness and welding parameters. However, it should be acknowledged that this study solely focused on the heat conduction equation while other factors like flow and plastic deformation might also influence the welding process. Therefore, a comprehensive model should take all these aspects into account.

Nakashiba et al. [41]. Nishimura et al. [42] developed two-dimensional finite element models to simulate temperature changes at the interface during electrofusion coupler welding with a diameter of 50 mm. They conducted a nonlinear heat transfer analysis. Constructed an axisymmetric finite element model to examine how heating duration, applied voltage, wire pitch and ambient temperature affect temperature distribution along the welded surfaces. Initially they neglected considering the gap between pipes and fittings for simplicity; however, they later realized its significance when dealing with electrofusion couplers larger than 75 mm, in size.

The electrofusion model developed by Fujikake et al. [43] is a FEA model that focuses on studying the process of electrofusion welding in two dimensions. This model takes into account aspects, including heat transfer, fluid flow and plastic deformation during the welding process. It also considers factors such as heat transfer between the pipes and fittings initial gap between the pipes, nonlinearity of heat transfer equations and temperature dependent thermal properties of the plastic material.

Fujikake et al. electrofusion model has been validated using data and is considered more accurate than previous models. It provides a tool for analyzing the impact of different factors on the electrofusion welding process, such as plastic type, pipe thickness, welding parameters, fluid flow conditions and initial gap size.

One of the models available is the model proposed by Rosala and his colleagues [19]. Rosala et al. Developed a FEA model that combines heat transfer analysis with thermal deformation analysis to simulate how the initial gap between the pipe and fitting closes over time. They also considered the movement of melted material into the interface.

To validate their FE model, Rosala et al. Compared its predicted results for temperature distribution in the weld region melt affected and gap closure time with experimental data (Figure 2-14). The findings showed agreement between the predicted results and experimental observations for welding polyethylene pipes.

However, it is important to note that this FE model has limitations. Firstly, it is specifically applicable to welding polyethylene pipes and is not directly extendable to other materials or pipe fitting geometries. Additionally other factors, like material properties of both pipe and fitting, joint geometry and electrical parameters of the welding process are not considered in this model.

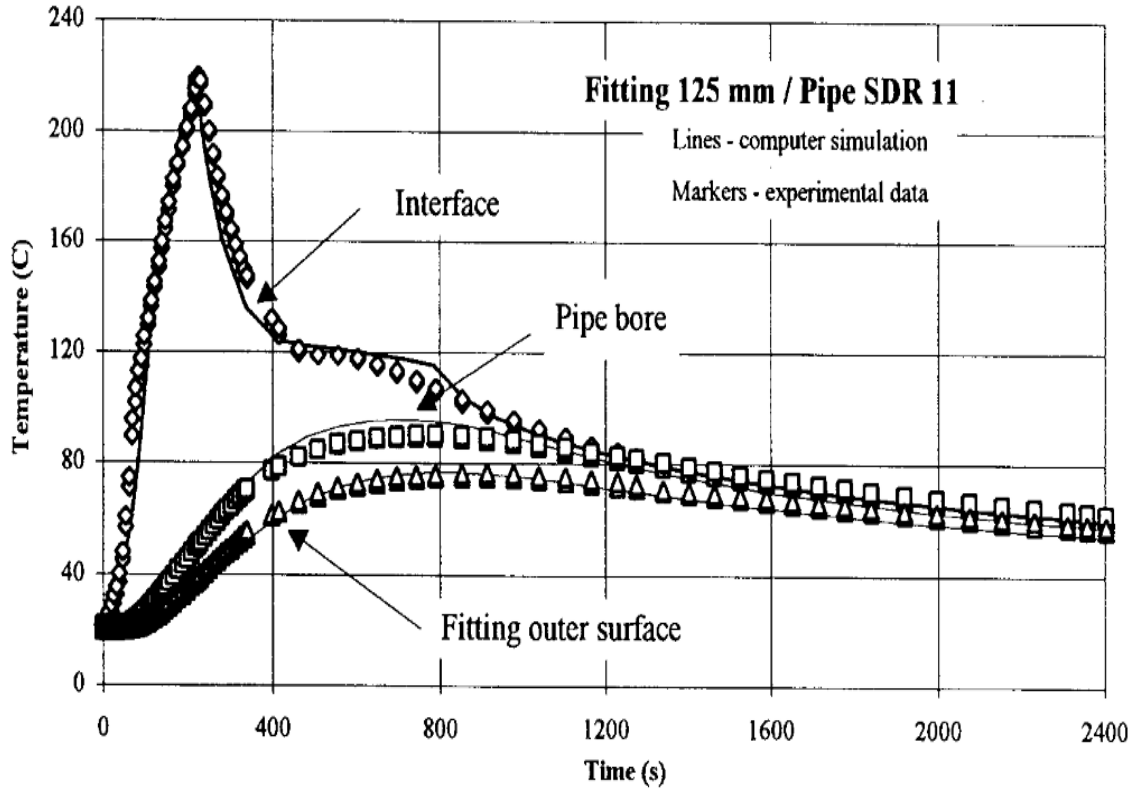

Figure 2-14 Predicted and experimental temperature through the EFW [19]

An axisymmetric one-dimensional heat transfer model was developed by Shi et al. [39]. This model utilizes the heat conduction equation in cylindrical coordinates to predict the temperature distribution considering the thermal contact conductivity of the contact surfaces. The impact of variation of power input, polyethylene material properties, and thermal contact resistance on the interface temperature was investigated.

Chebbo et al. [44] conducted a numerical simulation to study the electrofusion process. They focused on the welding of polyethylene using an experimental setup involving two PE100 plates. The simulation utilized a three finite element (FE) model considering various factors such as heat transfer, material deformation melting of polyethylene and electrical aspects of the welding process. The accuracy of the FE model was validated against data obtained from welding polyethylene pipes. Temperature distribution within the weld region was measured using thermocouples while weld quality was assessed through inspection and tensile testing of welded joints.

Earlier studies have also established the required conditions to achieve successful welding of PE100. To limit any thermal degradation, the maximum allowable welding temperature is 270 °C [45]. On the other hand, the minimum required temperature at the welding interface is 160 °C [25]. Additionally, to avoid thermal degradation around the heating wires, their temperature should not exceed 350 °C [45].

Table 1 summarizes the differences between the Pitman model, Nakashiba and Nishimura, Fujikake, Rosala, Shi and Chebbo model including the initial gap, number dimensional model type, temperature dependent thermal properties, thermal and mechanical stresses.

Table 1 Summary of the electrofusion welding heat transfer models

Model	**Heat transfer**	**Phase change**	**Initial gap**	**Temperature dependent thermal properties**	**Thermal and mechanical stresses**
Pitman model	One-dimensional	No	No	No	No
Nakashiba & Nishimura	Two-dimensional	No	No	Yes	No
Fujikake model	Two-dimensional	Yes	Yes	Yes	Yes
Rosala model	Three-dimensional	No	Yes	Yes	Yes
Shi model	One-dimensional	No	Yes	Yes	No
Chebbo model	Three-dimensional	Yes	Yes	Yes	No

In reviewing the methodologies developed for modelling electrofusion welding, it is evident that most prior research predominantly employed thermal heat transfer analysis. This approach, while foundational, often lacks a comprehensive representation of the actual welding behavior. Notably, Fukija and Rosala distinguished themselves by integrating heat transfer with solid mechanics, thereby achieving a more accurate thermomechanical analysis of the joint during welding.

Many models opted to simplify the problem by treating the heating wire as a heating layer. This simplification, however, overlooks the critical role of the heating wire as the primary heat source, which is a significant aspect that should be incorporated into the model for more accurate results. Additionally, the majority of these models failed to consider the thermal contact between the pipe and fitting, an omission that can lead to significant inaccuracies in the simulation of the welding process.

Chebbo's work stands out for its focus on the thermal contact resistance at both the wire/fitting and joint interfaces. His sensitivity analysis offered valuable insights into the impact of various factors such as fitting size, power, and thermal material properties on the welding process. This approach provides a more nuanced understanding of the thermal dynamics at play.

However, a common shortcoming across these studies is the validation mechanism, which predominantly relied on visual comparison with experimental temperature data. This method, using a limited number of measurement locations to represent different heat regions of the electrofusion joint, introduces a risk of inaccuracies. The accuracy of these readings is heavily dependent on the quality and stability of the thermocouples used, which can be compromised during the welding process.

All these models were concentrated on modelling single material pipes in EF welding. These models do not account for the unique properties of TCP, such as its multi-material composition and viscoelastic behaviour. There has been no published work investigating the EFW of thermoplastic composite pipes. Therefore, there is a need to develop new EFW models that are specifically tailored to TCPs. This will help to ensure the safe and reliable operation of TCP.

In summary, while significant strides have been made in modelling electrofusion welding, there are critical areas that require further refinement. Future research should focus on integrating comprehensive thermomechanical analysis, accurately representing the heating wire as the primary heat source and improving validation mechanisms to ensure more reliable and precise modelling outcomes.

2.3.3 Parameters affecting electrofusion modelling

Other than the factors that affect the quality of EF joints mentioned earlier in section 2.2.3, This section will discuss some other key parameters that influence the modelling of the welding process and the quality of the resulting joint.

Initial gap

The initial clearance between the fitting–pipe surfaces is one of the leading modelling parameters, mainly because the clearance creates a barrier to the heat transfer from the fitting to the pipe [19]. The initial clearance between the pipe and fitting closes gradually, and both the temperature and pressure at the fusion interface change dramatically with the spread of the contact region between both surfaces. A larger initial gap decreases the pressure magnitude at the fusion interface [18], as represented in Figure 2-15.

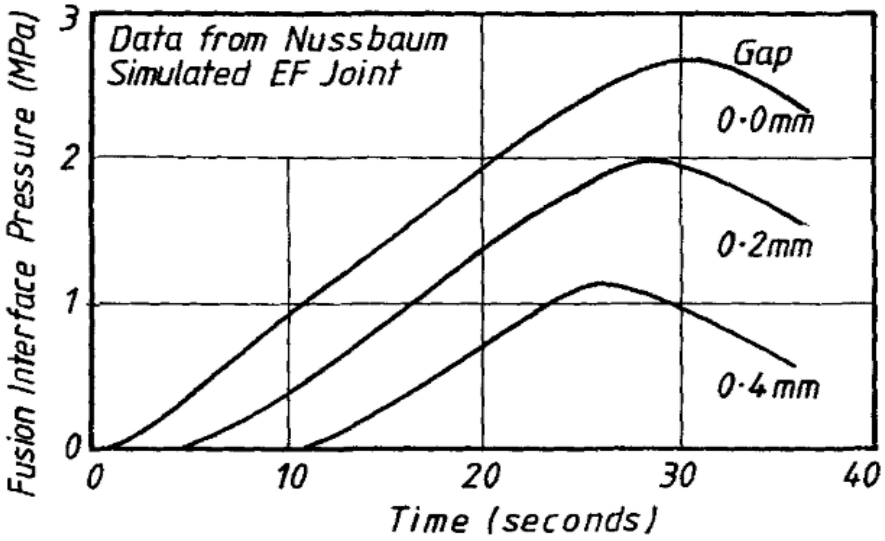

Figure 2-10 Influence of initial gap and fusion time on interface pressure [18]

Heating wire

The relation between the fusion interface temperature and the heating wire embedment depth is shown in Figure 2-16. The temperature gradient between the fusion interface and the polymer adjacent to the heating wire rises as the embedment depth of the heating wire increases. A larger wire diameter is unfavourable because it requires a deeper embedment depth and a larger pitch. Fittings with a larger pitch will degrade close to the wire before achieving the maximum fusion strength value [18]. Therefore, to reduce the distance between the fusion interface and the heating wire, the fitting design should follow a smaller wire diameter, smaller pitch, and shallower embedment depth.

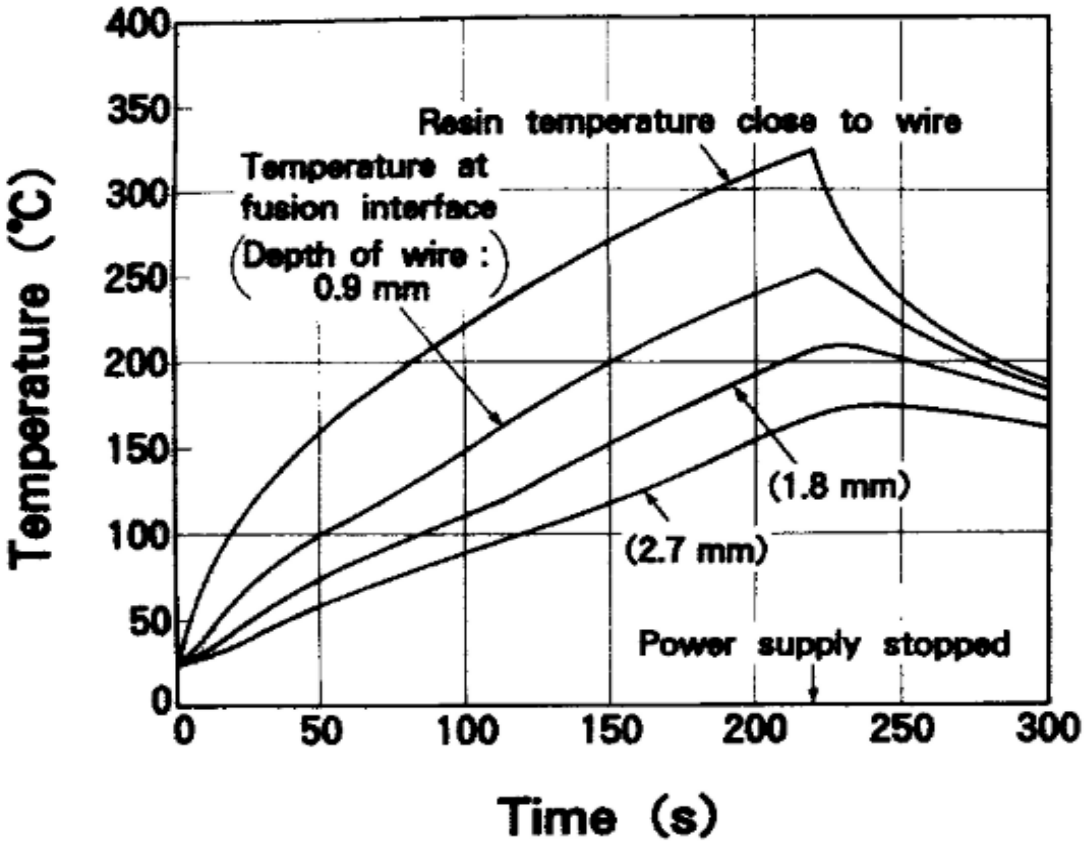

Figure 2-11 Influence of embedment depth on the interface temperature over time [18]

Ambient temperature

Additional power is needed to raise the joint and pipe temperature at low atmospheric temperatures. Therefore, it is required to increase the fusion time to compensate for the cold environment effect on the electrofusion welding. It was also noticed that wind had little impact on the welding process since the fusion interface is inside the joint [42,46]. The ECU often has temperature compensation features that adjust the welding parameters based on ambient temperature. In extremely cold conditions, pre-heat cycle may be employed before the actual fusion process [47]. This brings the fitting and pipe closer to the desired welding temperature, ensuring a more consistent and reliable weld.

2.3.4 Experimental measurement for validation

The primary objective of conducting an experimental investigation on electrofusion welding is to verify the predicted values obtained from numerical and finite element models. Temperature plays a role in electrofusion welding and accurately measuring it using both traditional and non traditional methods is of utmost importance.

Traditional methods typically involve the use of tools such as thermocouples or Resistance Temperature Detectors (RTDs) to measure temperature at points near the joint during the welding process [44,49]. While these methods provide readings they can be intrusive as they require drilling into the fitting and pipe. Moreover they only provide temperature data for areas rather than the entire joint.

Thermography, especially infrared (IR) thermography, has been a growing preference in recent years due to its non-invasive nature. IR thermography allows for mapping out the temperature distribution across the surface of the weld using infrared cameras [50,51]. It provides real time monitoring of temperature changes. Can identify areas that are excessively hot or cold aiding in evaluating weld quality and fusion efficiency. However, it is not without limitations. Factors like dirt on the surface reflections or changes, in surroundings can impact accuracy. Additionally, it primarily captures surface temperatures. May not capture deeper details within the joint.

Both traditional methods and infrared thermography will be employed to measure temperature during the electrofusion welding of TCP. Detailed experimental procedures and results will be presented in Chapter 5.

2.4 Material thermal properties

Accurate measurement of thermal properties is essential for understanding the heat transfer behaviour and optimizing the performance of thermoplastic materials. This section discusses various methods commonly employed to measure thermal conductivity, specific heat capacity, and melting temperature of these materials.

2.4.1 Heat transfer and Polyethylene

It is important to understand how polyethylene behaves when it is heated as this knowledge has applications in industries such as electrofusion welding. When polyethylene is heated its structure and material properties undergo changes that directly impact how it can be processed and the performance of the final product [18].

When polyethylene is heated the energy transferred to its polymer chains causes an increase in movement. At temperatures polyethylene exists in a crystalline form where the polymer chains are closely packed together. As the temperature rises the thermal energy affects the polymer chains leading to disruption of their crystalline structure. This weakening of forces results in the separation of polymer chains and what we commonly refer to as melting or softening of polyethylene [52].

With temperature increase the mobility of polymer chains increases along with increased chain slippage. The crystalline regions transition into a state above a specific temperature known as the melting point. In this state polymer chains are randomly arranged. This transformation causes polyethylene to change from a solid to a state making it more fluid and easier to manipulate during processes like electrofusion welding.

Heating also has an impact, on material properties of polyethylene including thermal conductivity, specific heat capacity and viscosity. As heating intensifies motion and facilitates heat transfer thermal conductivity increases [53].

The amount of heat energy needed to increase the temperature of a material, known as heat capacity also varies with temperature. As polyethylene shifts from being solid to becoming molten it generally experiences a decrease, in heat capacity.

2.4.2 Thermal conductivity measurement

Thermal conductivity plays a role in assessing how well a material can conduct heat. Various techniques are employed to measure conductivity in thermoplastic materials including;

Transient Hot Wire Method

This method involves inserting a wire probe usually made of a material with high thermal conductivity into the sample. A heat pulse is generated in the wire. By measuring the temperature response we can determine the thermal conductivity of the sample [54].

Transient Plane Source Method

In this method a disc or needle like sensor called a hot plate or hot needle is placed in contact with the sample. The sensor is. We record the temperature change over time to determine its thermal conductivity [55].

Guarded Hot Plate Method

This method sandwiches the sample between two plates, one heated and one cooled. By measuring the heat flow through the sample and considering its temperature difference along with known geometry we can calculate its conductivity [56].

2.4.3 Specific Heat Capacity Measurement

Specific heat capacity measures the amount of heat energy required to raise the temperature of a material per unit mass. Standard methods used for measuring specific heat capacity in thermoplastic materials include:

Differential Scanning Calorimetry (DSC)

DSC measures the heat flow either into or out of the sample as the temperature changes. By analysing the heat flow data during controlled heating or cooling we can determine the heat capacity [57].

Modulated Temperature Differential Scanning Calorimetry (MTDSC)

MTDSC is a variation of DSC that applies a temperature wave on top of the linear temperature program. This technique enhances accuracy in determining heat capacity especially for materials with multiple thermal transitions [58].

2.4.4 Melting Temperature Measurement

The melting temperature of a thermoplastic materials is a critical parameter that determines its processability and heat resistance. Standard methods for measuring the melting temperature include:

Differential Scanning Calorimetry (DSC)

By observing the endothermic peak associated with melting DSC can accurately determine the melting temperature. The sample is gradually heated at a controlled rate while monitoring the heat flow data [59].

Thermomechanical Analysis (TMA)

TMA measures changes in a sample, as temperature varies. By observing how thermal softening affects length or expansion of the sample we can determine its melting temperature [60].

Several methods are available to measure thermal properties in thermoplastic materials. In this research, PE samples from the fitting and pipe will be prepared for thermal investigation and to find their thermal properties as a requirement for the simulation model of EFW. The procedure of the thermal tests, methodology and results will be discussed in detail and presented in Chapter 4.

2.5 Conclusion

TCPs mechanical performance has been proven to withstand stress and thermal loading making it a viable replacement for pipes in oil and gas transportation both onshore and offshore. The lightweight and flexible nature of TCP also brings down the cost related to storage, transportation and installation.

While mechanical fittings are commonly used to join TCP **there has not been research on using electrofusion welding specifically for TCP until now**. The main concern with electrofusion welding is the impact of temperature gradients on TCPs mechanical properties. In Chapter 6 we will introduce a FEA model designed specifically for welding TCP. This model will examine the temperature profile. Investigate the melting zone during welding.

Electrofusion welding is a established method that has been used for joining polyethylene pipes for many years. Various computational models have been developed to study the heat transfer problem during the jointing process. Some of these models consider temperature material properties like crystallinity, density, thermal conductivity and specific heat. Additionally, these models address physical phenomena associated with welding such as phase changes, in materials and gap closure mechanisms.

Different factors such as the surrounding temperature, initial gap, size of the heating wire and depth of embedding were also examined. In Chapter 6 a detailed analysis will be presented to determine how these various factors affect the temperature during the welding process of composite pipes.

The strength of electrofusion welding primarily relies on surface preparation and appropriate heating and cooling times. Various tests, both destructive and non-destructive are used to assess the quality of electrofusion joints and identify any defects that may have occurred due to welding procedures.

To summarize electrofusion welding shows a promise for joining TCPs (Glass PE Thermoplastic Composite Pipes). Extensive research is crucial. This research focuses on understanding heat transfer in electrofusion welding specifically for 6" pipes operating under conditions. The research trajectory involves reviewing coupler designs virtually gathering accurate thermal property data and validating empirical models.

This study aims to develop a model for heat transfer in TCPs electrofusion welding process. It will conduct assessments to determine the sensitivity of key welding parameters and outline temperature behaviours during welding. The ultimate goal is to refine welding parameters that ensure joint strength and long-term performance while creating an improved design, for TCP electrofusion fittings.

2.6 Research methodology

This section presents the research methodology employed in this study to investigate the heat transfer during Thermoplastic Composite Pipe (TCP) electrofusion welding and optimize the fitting design for reliable TCP joints. The research procedure provides a systematic framework shown in Figure 2-17 for conducting experimental tests, developing a simulation model, and optimizing the fitting design based on the obtained results.

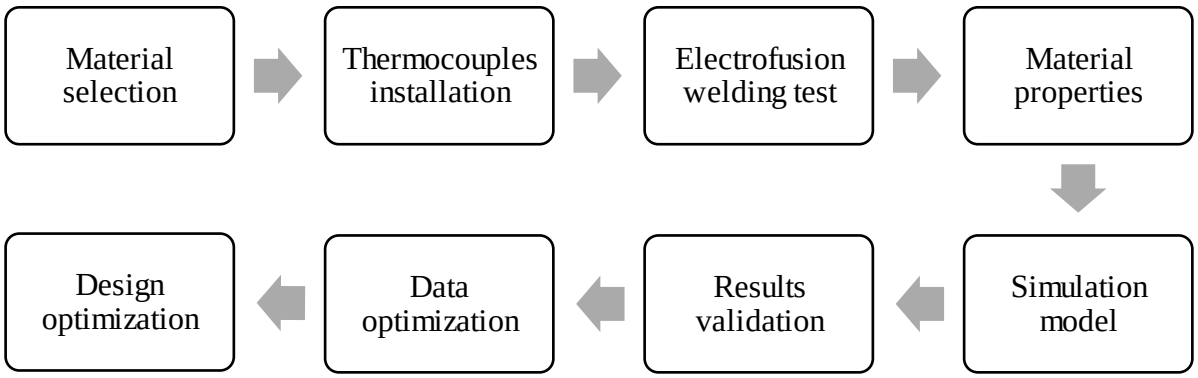

Figure 2-12 Methodological workflow

Material selection and preparation

The research starts by choosing suitable materials for Thermoplastic Composite Pipes (TCP) and EF couplers. The selection criteria include compatibility, mechanical properties, corrosion resistance and temperature resistance. Once the materials are chosen, the TCP specimens are prepared with dimensions and surface conditions to maintain consistency.

Thermocouples installation

placing thermocouples and temperature measurement devices on both TCP specimens and couplers is a crucial step. This allows to accurately capture temperature data during the electrofusion welding process. Novel Installation techniques are implemented to ensure consistent and reliable measurements throughout the welding process.

Electrofusion welding physical test

Electrofusion welding tests are carried out using TCP specimens along with selected EF couplers. In this research two tests are conducted under similar conditions. Throughout these tests parameters such as heating time and temperature are closely monitored. The electrofusion welding machine is operated using predetermined settings, which helps fuse the TCP specimens and create welded joints. The temperature data from the thermocouples is collected throughout the welding process.

Material thermal properties identification

To reflect the actual materials behaviour under thermal loading, the thermal properties of the TCP materials are identified. This involves conducting experiments or referring to existing literature to determine factors like thermal conductivity, specific heat capacity and melting temperature of the thermoplastic composite materials used in TCP. Measurement techniques are utilized and standard procedures are followed to obtain precise data on these thermal properties.

Simulation model

A simulation model based on data and material properties is developed using finite element analysis (FEA). This model aims to replicate the heat transfer behaviour and fusion process during electrofusion welding of TCP. It considers factors such as temperature distribution, thermal gradients and temperature dependent thermal properties. To ensure accuracy the simulation model, it is refined using experimental results.

Results comparison and validation

The results obtained from both testing and the simulation model are compared and analysed. The temperature profiles and other relevant data are examined to identify correlations and validate the simulation model against the findings. Any discrepancies or differences are thoroughly investigated to ensure the reliability and accuracy of the simulation model.

Data optimization

To improve the model accuracy and align it with experimental data, data optimization techniques are applied to fine tune the simulation model based on comparison and validation results. Adjustments are made to input parameters and variables in Test 1. Sensitivity analysis is carried out to identify parameters for heat transfer during electrofusion welding of TCP along, with their optimal values.

The optimized input parameters from Test 1 will be utilized to validate the simulation model using data obtained from Test 2.

New Fitting Design Optimization

Expanding on the optimization of EFW model process parameters this research aims to optimize the design of fittings for electrofusion joints in TCP. It involves exploring coupler geometries to enhance heat transfer and improve fitting strength based on outcomes obtained from a complementary stress analysis study. The simulation model is employed to evaluate and compare fitting designs enabling the selection of an optimal design that enhances the long term performance and reliability of electrofusion fittings for TCP.

By following this research procedure, this study will investigate heat transfer during electrofusion welding of TCP, tune the simulation model and validate it using experimental data and improve the design of electrofusion fittings for 3 layer TCP.

Chapter 3

MATERIALS AND THERMAL PROPERTIES

This chapter focuses on the testing of materials and the measurement of thermal properties for Thermoplastic Composite Pipes (TCP) used in electrofusion welding. It provides an essential foundation for understanding the behaviour of the materials and their thermal characteristics, over the range of temperatures expected in the EFW process, which are necessary for accurately modelling the heat transfer during the welding process in chapter 6.

The objectives of this chapter are to outline the procedures for material testing, provide an overview of the equipment and techniques used for thermal property measurement, and highlight the significance of obtaining accurate thermal property data. The chapter also emphasizes the importance of reliable material testing and thermal property measurement to ensure the validity of subsequent analysis and simulation.

3.1 Pipe and EF fitting selection

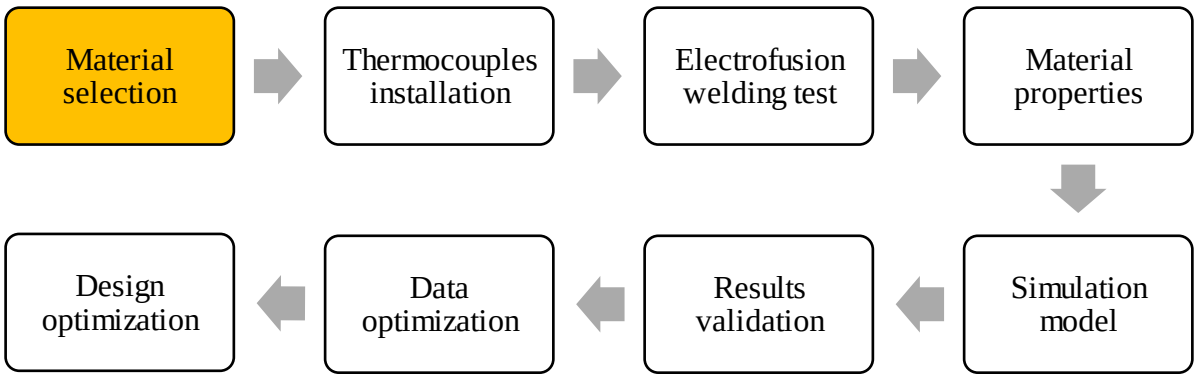

The TCP segments chose for the EFW test are 6” with pressure rating of 50 bar/750 psi due to their wide implementation in various industries. The liner was made from HDPE, the reinforcement was made from 10 layers of high-quality GF/HDPE tapes with 0.3 thickness for each layer, and the cover was made from HDPE. The dimensions of the TCP are specified in Figure 3-1 and Table 2.

Table 2 TCP dimensions

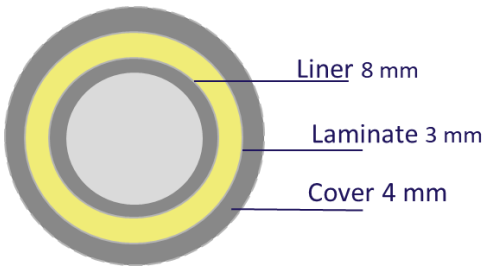

Inner diameter	150 mm
Outer diameter	180 mm
Total thickness	15 mm

Figure 3-1 TCP dimensions

A 180 mm commercial EF fitting made from PE100 was used in the physical testing of EFW of TCP. The pressure rating for this fitting is 10 bar/450 psi, fusion time is 220 seconds, and the cooling time is 12 minutes. The dimensions for the fitting are specified in Table 3 and shown by Figure 3-2. This fitting was chosen for its simple cylindrical design, with exposed wires and tight clearance, making it simpler for modelling, and its size with inner diameter equals to the pipe outer diameter. Although the pressure rating for this fitting is much lower than the required for this research, however, this will be good enough to build the knowledge for understanding the heat transfer during physical testing in laboratory environment and controlling environment parameters for the simulation model.

Table 3 Electrofusion fitting dimensions

Nominal diameter (mm)	H (mm)	L1 (mm)	L2 (mm)	W (mm)
180	229	102	102	215

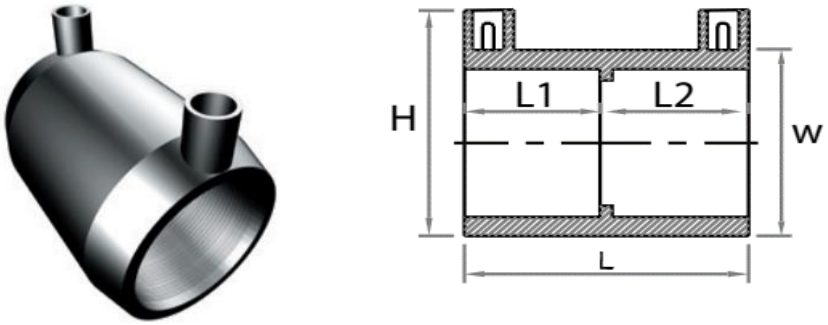

Figure 3-2 Electrofusion fitting and dimensions

3.2 Thermal properties measurements

This section detailed the tests, procedures and methods used to measure and calculate the thermal properties of the materials used in the test and will be utilized as input parameters in the FEA model in Chapter 6.

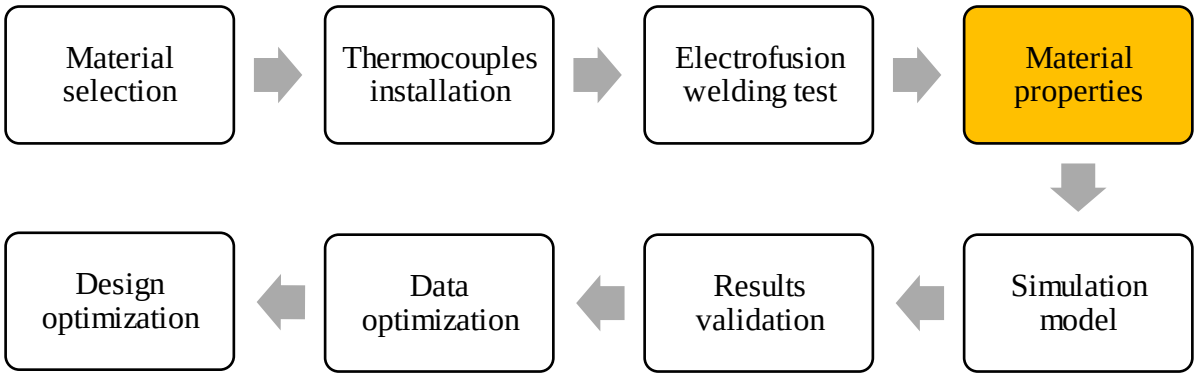

3.2.1 Laser Flash Analysis (LFA)

The technique known as Laser Flash Analysis as illustrated in Figure 3-3 is commonly used to measure the properties of materials. These properties include diffusivity, thermal conductivity, and specific heat capacity [61]. In LFA a small sample of the material is exposed to an intense burst of laser energy as depicted in Figure 3-4. This laser pulse causes an increase in temperature at the surface of the sample. As heat travels through the material, it creates a temperature gradient. This gradient leads to a temperature rise at the opposite surface of the sample. An infrared detector captures this temperature rise, records it over time providing valuable information, about how the material responds to thermal changes.

Figure 3-3 LFA467 device

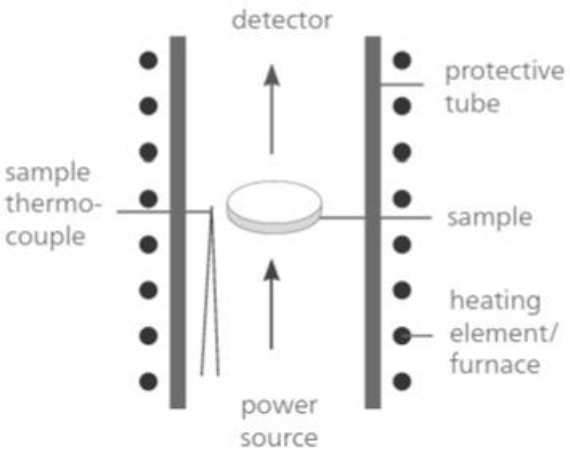

Figure 3-4 Flash technique

To determine the properties of a material one can analyse the temperature decay curve. This analysis involves using modelling and fitting techniques to extract relevant parameters. The main principle behind LFA is that the speed at which temperature spreads through a material is influenced by its diffusivity. By controlling experimental parameters and employing appropriate calibration LFA provides valuable insights into the heat transfer characteristics and thermal behaviour of materials. LFA is widely utilized in fields such as materials science, engineering and thermal management.

LFA procedure

This section provides an outline of the procedure for conducting a laser flash analysis experiment to measure the thermal properties of a material. The experiment aims to determine diffusivity, conductivity and specific heat capacity of layers of a pipe (liner, reinforcement and cover) at various temperatures. The laser flash technique is used to generate and measure the temperature response of these samples.

Sample preparation

Two samples were cut from each layer of the pipe as shown in Figure 3-5 with dimensions of 10 x 10 x 3(±0.01) mm. It was ensured that these samples were clean without any contaminants or surface irregularities that could affect measurements. If necessary, sample surfaces were polished to ensure uniform contact, with the measurement apparatus.

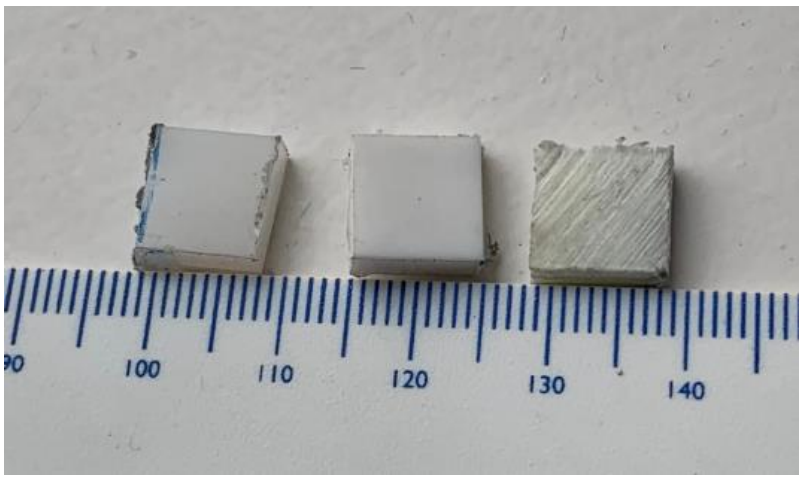

Figure 3-5 TCP sample for LFA

Experimental setup

The laser flash analysis setup was arranged, which typically includes a laser source, an infrared detector and a data acquisition system. the manufacturer's instructions were carefully followed while assembling and configuring the equipment. The sample was securely placed in the apparatus to ensure thermal contact with its components.

Temperature control

To maintain temperatures (30, 60, 90 & 100 ^{0}C) during the experiment a precise temperature control system was implemented. Depending on the desired temperature range a temperature-controlled chamber or a combination of heating and cooling elements was used. After setting each temperature increment, a time for the sample to reach thermal equilibrium was allowed before starting measurements. To avoid damaging the sample holder with molten polymer and rendering it unusable again, the properties at or beyond its melting temperature were not measured.

Measurement procedure

Firstly, the baseline temperature response of the sample without laser irradiation was measured. This served as a reference point, for measurements and helped to make necessary background corrections. To measure the temperature response of the sample a laser flash was initiated by delivering a brief pulse of laser energy to its surface. the duration of the laser pulse was kept as short as possible to minimize any thermal diffusion effects during the measurement process. Using a detector, the temperature decay curve was recorded, ensuring that enough data points for precise analysis had obtained. For each temperature point these measurements were repeated three times while maintaining consistent experimental conditions and sample positioning.

Data analysis

Once the recorded temperature decay curves were recorded, mathematical models and algorithms were applied to analyse them and derive important thermal properties of the material such, as diffusivity, thermal conductivity and specific heat capacity. The determination of diffusivity (a) was done through a mathematical analysis of the measured temperature/time function using specialized analysis software that includes different mathematical models tailored for specific applications.

The primary models involved in LFA as specified in ISO 22007-1 include the "half-time" method by Parker and its extension such as Cape-Lehmann model. The parker model introduced in 1961, assumes adiabatic conditions and uses the temperature rise at the rear surface of a thin sample following a laser pulse to calculate thermal diffusivity. The Cape-Lehmann model refines these calculations by considering heat losses and non-ideal pulse shapes. Algorithms used in LFA typically involve curve fitting of experimental temperature rise data to theoretical models utilizing least squares fitting or other optimization methos to extract the thermal diffusivity value from the observed data.

The thermal conductivity was calculated using Equation 3.1,

$$k(T)=a(T) \cdot \rho(T) \cdot Cp(T) \qquad (3.1)$$

where,

T - temperature

k - thermal conductivity

a - thermal diffusivity

ρ - bulk density

Cp - specific heat

Test results

The liner sample unfortunately failed the test twice (for 2 samples), thus, no data were generated for the material in this test. Additional tests in this chapter will compensate this failure.

The result of the diffusivity, specific heat capacity and thermal conductivity for repeated test of two samples of the composite laminate are listed in Table 4 and the pipe cover are listed in Table 5. The results, based on the average values obtained from three runs at each temperature, indicate notable trends in these thermal properties with respect to temperature in Figure 3-6. The measured density using Archimedes balance for the first sample was 1,690 kg/m^3 and 1,527 kg/m^3 for the second sample. The variation of the densities for the 2 samples could be attributed to variations in fiber distribution and void content within the material.

*Table 4 Composite laminate LFA results (1st sample)**

#run number	#Temperature ^{0}C	#Diffusivity (mm^2/s)	#Std_Dev/ (mm^2/s)	#*k* (W/(m*K))	#Cp (J/(g*K))
1..2..3	30	0.284	0.005	0.477	0.993
4..5..6	60	0.245	0.001	0.45	1.087
7..8..9	90	0.209	0	0.465	1.317
10..11..12	110	0.179	0.002	0.513	1.697

*Table 5 Composite laminate LFA results (2nd sample)**

#run number	#Temperature ^{0}C	#Diffusivity (mm^2/s)	#Std_Dev/ (mm^2/s)	*k* (W/(m*K))	*Cp* (J/(g*K))
1..2..3	30	0.319	0.003	0.495	1.016
4..5..6	50	0.287	0.003	0.458	1.045
7..8..9	70	0.253	0.003	0.452	1.168
10..11..12	90	0.234	0.004	0.479	1.34
13..14..15	110	0.191	0.001	0.487	1.672

** The volume fraction for the GF/HDPE laminate is 42%*

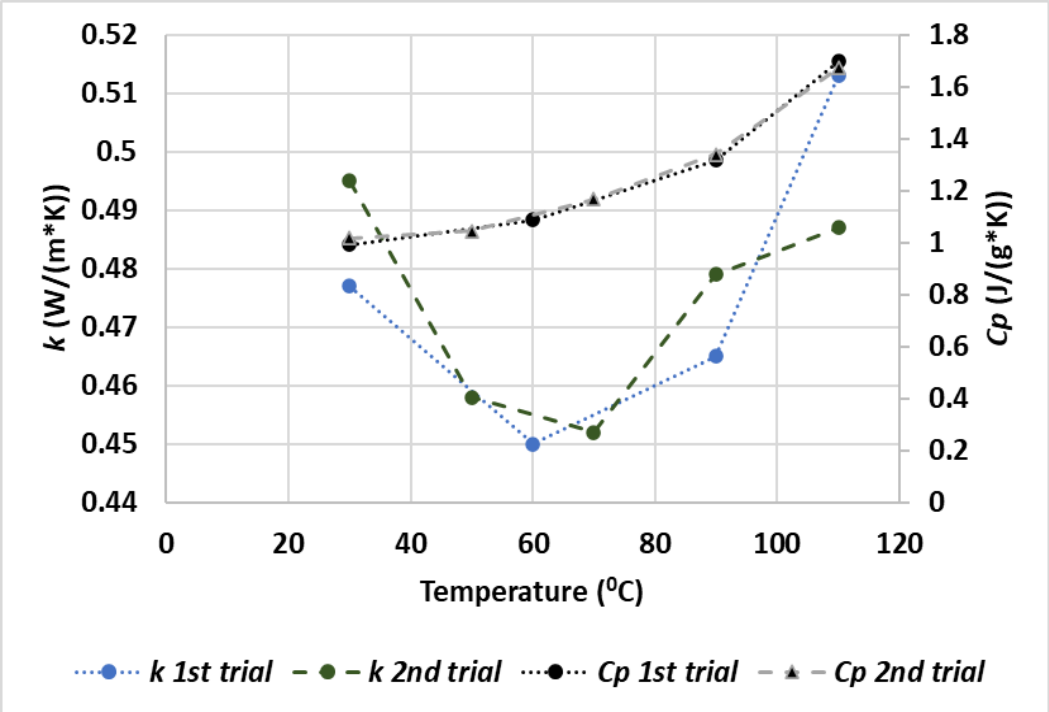

Figure 3-6 Thermal conductivity and specific heat capacity results for pipe's composite laminate

Composite Laminate Thermal Diffusivity

Across both trials, there is a consistent trend where the thermal diffusivity of the GF/HDPE laminate sample decreases with an increase in temperature. In the first trial, the values decrease from 0.284 mm^2/s at 30°C to 0.179 mm^2/s at 110°C. Similarly, in the second trial, they decrease from 0.319 mm^2/s at 30°C to 0.191 mm^2/s at 110°C. This suggests that the laminate's ability to conduct heat relative to its storage of heat diminishes as temperature increases.

Composite Laminate Thermal Conductivity

The thermal conductivity through the thickness exhibits a less consistent trend across the temperature range in both trials. In the first trial, starting at 0.477 W/(mK) at 30°C, it fluctuates and peaks to 0.513 W/(mK) at 110°C. The second trial shows a similar pattern, beginning at 0.495 W/(mK) at 30°C, dipping to 0.452 W/(mK) at 70°C, and rising again to 0.487 W/(mK) at 110°C. This behaviour suggests that other intrinsic or extrinsic factors, besides temperature, might be influencing the material's ability to conduct heat. The thermal conductivity in the plane could not be measured due to the small thickness of the pipe's laminate layer which is only 3 mm.

Composite Laminate Specific Heat Capacity

In both trials, the specific heat capacity of the laminate consistently increases with temperature. For the first trial, values rise from 0.993 J/(gK) at 30°C to 1.697 J/(gK) at 110°C. Similarly, in the second trial, it starts at 1.016 J/(gK) at 30°C and reaches up to 1.672 J/(gK) at 110°C. This trend indicates that the material requires more energy to increase its temperature by a unit degree as the temperature itself rises.

In conclusion, both trials demonstrate that with the rise in temperature, the thermal diffusivity of the GF/HDPE laminate tends to decrease and the specific heat capacity tends to increase. However, the thermal conductivity showcases a slightly varied behaviour across temperatures. These insights can be crucial for applications where the laminate may be subjected to variable temperature conditions.

The LFA results for diffusivity, specific heat capacity and thermal conductivity of the pipe's cover is summarized in Table 6.

Table 6 Pipe's cover (PE100) LFA results

#Shot number	#Temperature ^{0}C	#Diffusivity (mm^2/s)	#Std_Dev (mm^2/s)	#*k* (W/(m*K))	#*Cp* J/(g*K))
1..2..3	30	0.214	0.006	0.367	1.731
4..5..6	60	0.177	0.002	0.345	1.967
7..8..9	90	0.14	0.01	0.353	2.535
10..11..12	110	0.109	0.004	0.358	3.319

Cover Thermal Diffusivity

The results showed that the thermal diffusivity decreased as the temperature increased. At 30°C, the average diffusivity was 0.214 mm²/s, which decreased to 0.177 mm²/s at 60°C, 0.14 mm²/s at 90°C, and 0.109 mm²/s at 110°C

Cover Thermal conductivity

The thermal conductivity shown in Figure 3-7 shows a decrease as the temperature increases. At the lowest temperature of 30°C, the average thermal conductivity was found to be the highest, with a value of 0.477 W/(m·K). As the temperature increased to 110°C, the thermal conductivity decreased to 0.513 W/(m·K). This inverse relationship between thermal conductivity and temperature is consistent with the expected behaviour of most polymer materials.

Cover Specific heat capacity

The specific heat capacity shown in Figure 3-7 demonstrates a slight increase with increasing temperature. At 30°C, the average specific heat capacity was 0.993 J/(g·K), and it gradually increased to 1.697 J/(g·K) at 110°C. Although the change in specific heat capacity is relatively small, this trend suggests that the material requires more heat energy to raise its temperature as the temperature itself increases.

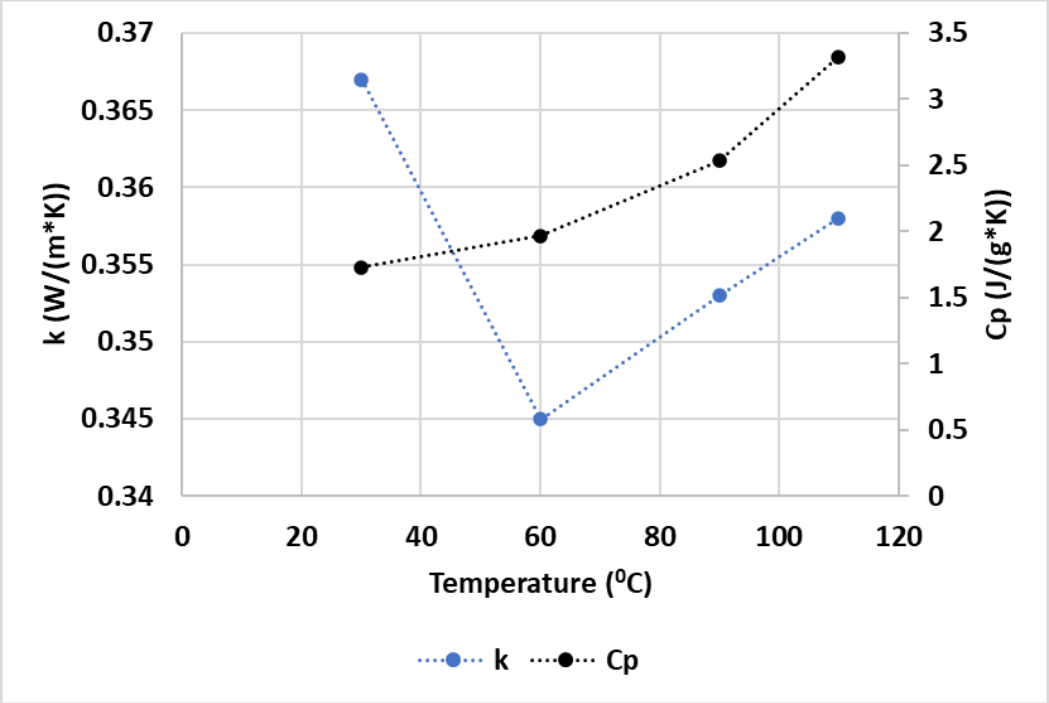

Figure 3-7 Thermal conductivity and specific heat capacity results for pipe's cover layer

Overall, the results indicate that the material exhibits a decrease in thermal conductivity and a slight increase in specific heat capacity with increasing temperature. These findings align with the expected behaviour of most materials and provide valuable insights into the thermal characteristics of the studied material. The collected values will be used in the simulation model in chapter 6.

3.2.2 Transient plane source method

The measurement of thermal conductivity changes in the pipe cover was conducted using the transient plane source (TPS) method at various temperature levels. These two materials are fused together to create the EF weld. The purpose of this test is to observe how thermal conductivity changes above the melting temperature, which could not be achieved through the LFA test. This section we provides an overview of the TPS method, including its principles, experimental setup and data analysis procedures.

Principles of the Transient Plane Source Method

The TPS method relies on analyzing how a material responds when it is exposed to a burst of heat generated by a flat heat source. This heat source is usually a disc or wire coated with a temperature sensitive substance. When this heat source comes into contact with the sample material it creates a lived burst of heat called a heat pulse.

This pulse causes an increase in temperature at the interface between the source and surface initiating the propagation of heat through the material.

As this heat travels through the material there are changes in its temperature distribution over time. The rate at which temperature increases or decreases, at locations depends on various thermal properties of the material primarily its thermal conductivity. To determine the conductivity of a material one can monitor the change in temperature over time.

Experimental Setup

The experimental setup for the TPS method typically involves three components: a TPS sensor, a temperature measurement system and a data acquisition system. The TPS sensor, sometimes referred to as the disk or hot wire sensor consists of a heat source and temperature sensors. Placing the sensor in contact with the sample material an electric current is applied to generate a heat pulse.

Temperature sensors integrated within the TPS sensor record temperature measurements during the transient response. These measurements are then captured using a data acquisition system that has temporal resolution. To ensure results it is essential to establish good thermal contact between the sensor and sample material to minimize thermal resistance at their interface. According to ISO 22007-2 [55] a test sample encloses the TPS sensor so that any heat generated by the sensor can freely disperse in all directions. However, when solving for conductivity it is important to consider that this assumes an infinite sample medium surrounding the TPS sensor. Therefore, any measurement and subsequent analysis must account for limitations imposed by small distances, between the TPS sensor and any boundaries of the sample. The TPS test device and the analysed samples are shown in Figures 3-8 and 3-9.

Figure 3-8 TPS test device by Thermtest

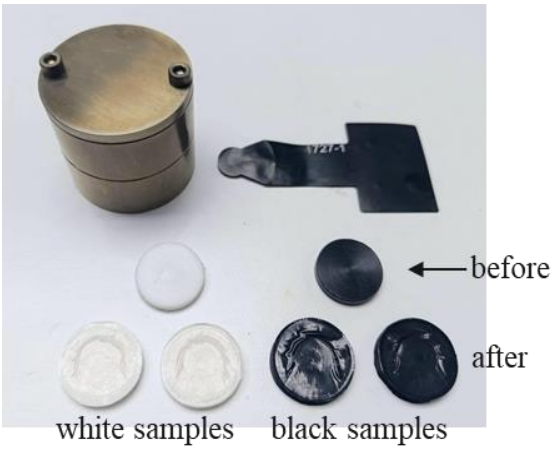

Figure 3-9 Samples prior and after test

It is important to note that the TPS method provides direct measurement of thermal conductivity (*k*) and not specific heat capacity (*Cp*). The *Cp* value is derived from the thermal conductivity value, along with the known density (ρ) and thermal diffusivity (*a*) of the sample material using Equation 3.1

Methodology

The purpose of this study was to assess how well heat travels through a type of polyethylene called PE100. To do this, sensor that acts as both a heater and a thermometer was used and placed within one sample of the plastic material. By sending a burst of heat through the sensor the temperature changed over time was observed and carefully analysed these temperature fluctuations. Various factors like the properties of the sample affected how quickly and intensely the temperature changed. By comparing the obtained data to a model and conducting thorough analysis, it was possible to determine exactly how well heat moves through PE100 in both its fittings and pipe cover. The accuracy of the results relied on maintaining sample thickness, precise calibration and ensuring optimal contact, between the sample and the sensor. While the TPS method itself is not displacement-controlled, the thickness of the sample is an important parameter. Accurate measurement of the sample thickness before and after a phase change is essential for correct data interpretation. This measurement was conducted manually prior to and after the test.

During the tests conductivity at four different temperatures was measured.
25 ^{0}C near room temperature, **120 ^{0}C** prior to melting temperature, **140 ^{0}C** after melting temperature and **180 ^{0}C** away from melting temperature

Results

The provided data in Table 7 and Figure 3-10 presents the results obtained through the Transient Plane Source (TPS) method for measuring the thermal conductivity, diffusivity, and heat capacity of two different materials: black (fitting material) and white (pipe jacket material). The data is presented at various temperatures (25°C, 120°C, 140°C, and 180°C) for each material. It is important to note that the melting temperature of materials is around 131°C.

Table 7 TPS results for the fitting and pipe's cover

Sample	Temperature [°C]		Conductivity *k* [W/(m·K)]	Diffusivity *a* [mm²/s]	Specific heat capacity *Cp* [MJ/(m³K)]
Black PE100 Fitting	25	Mean	0.469	0.244	1.992
		StdDev	0.002	0.008	0.055
	120	Mean	0.369	0.106	3.481
		StdDev	0.002	0.003	0.093
	140	Mean	0.254	0.120	2.112
		StdDev	0.001	0.001	0.008
	180	Mean	0.246	0.112	2.187
		StdDev	0.001	0.001	0.010
White PE100 Cover	25	Mean	0.471	0.226	2.082
		StdDev	0.002	0.004	0.091
	120	Mean	0.364	0.105	3.483
		StdDev	0.006	0.004	0.091
	140	Mean	0.266	0.133	2.005
		StdDev	0.000	0.001	0.009
	180	Mean	0.262	0.129	2.027
		StdDev	0.000	0.001	0.006

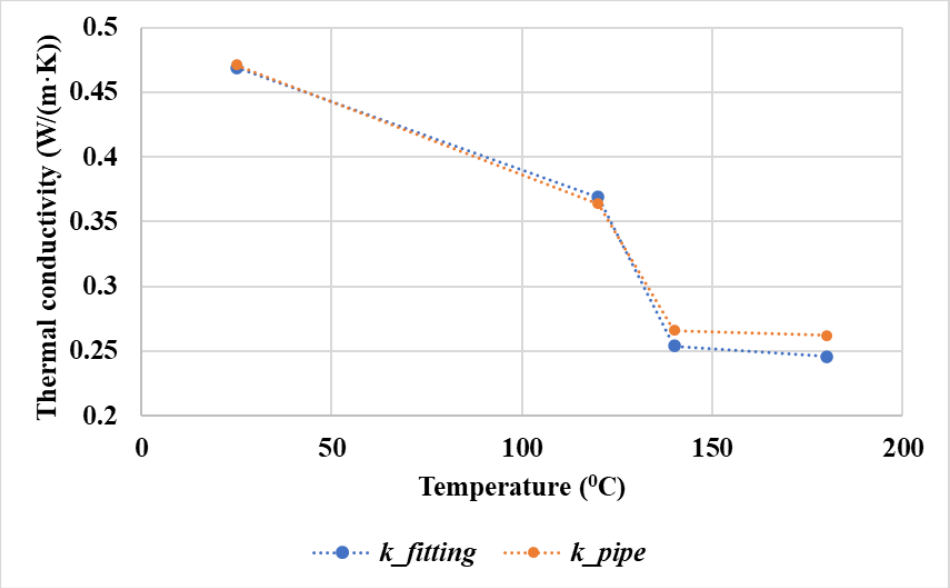

Figure 3-10 Thermal conductivity measurements for the fitting and pipe's cover

3.2.3 Differential scanning calorimetry (DSC)

DSC is an used method for studying the thermal properties of materials including phase transitions like melting and specific heat capacity. The SDT Q600 is a known DSC device that is recognized for its reliability and accuracy in measuring thermal events. In this study DSC was utilized to determine the melting temperature of the fitting and all layers of the pipe. Additionally it was employed to find the temperature specific heat capacity of PE100 for both the fitting and pipe's liner and cover.

Melting temperature

To determine the melting temperature a small sample of the material was placed in an airtight aluminium pan within the DSC instrument. The pan was then heated at a controlled rate while monitoring the heat flow into or out of the sample compared to a reference material. Any heat. Released during phase transitions, such as melting produced a distinct thermal signature.

Typically, the resulting DSC curve exhibits a peak corresponding to the melting transition. This peak represents the heat flow associated with changing from solid, to state. The position of this peak indicates the materials melting temperature.

The SDT Q600 instrument provides accurate measurements by monitoring heat flow throughout the heating process.

The software of the instrument enables the identification of the melting temperature by detecting the highest point on the DSC curve.

To ensure measurements it is important to consider various factors, such as proper sample preparation, optimal heating rate and instrument calibration. Careful attention should be given to preparing the sample in a way that ensures consistency and reproducibility. The heating rate should be adjusted to capture the melting process while maintaining a balance, between accuracy and efficient data collection.

Results

The DSC results for all joint materials are presented in Figure 3-11 for the pipe cover layer, Figure 3-12 for the pipe reinforcement layer, Figure 3-13 for the pipe liner layer and Figure 3-14 for the fitting.

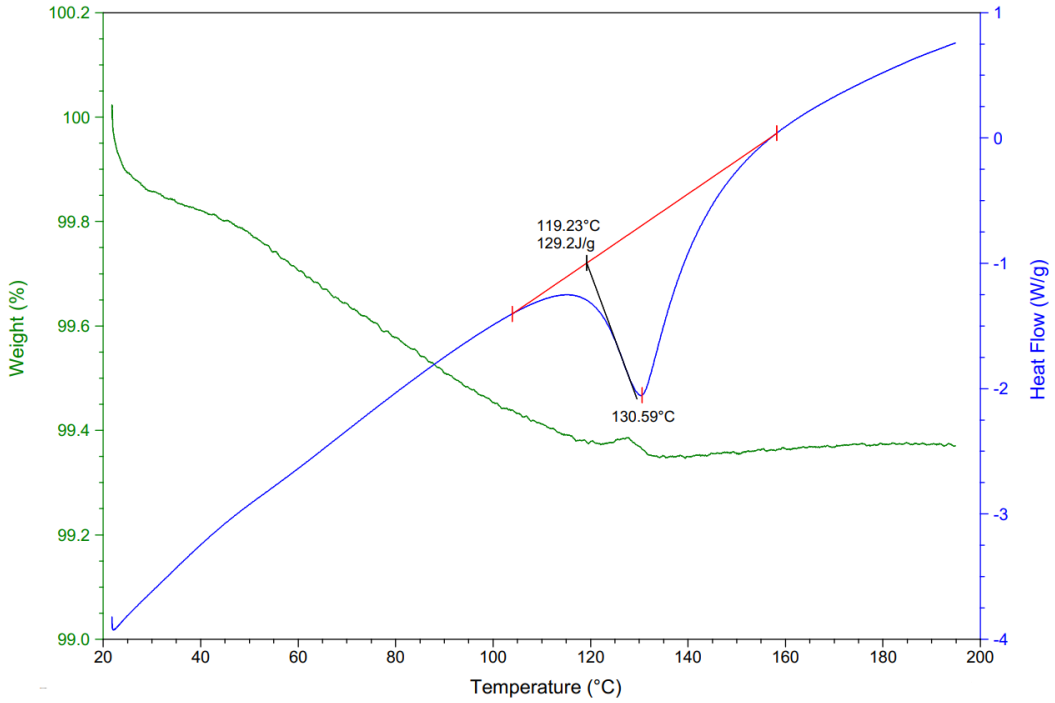

Figure 3-11 DSC results of the pipe's cover layer

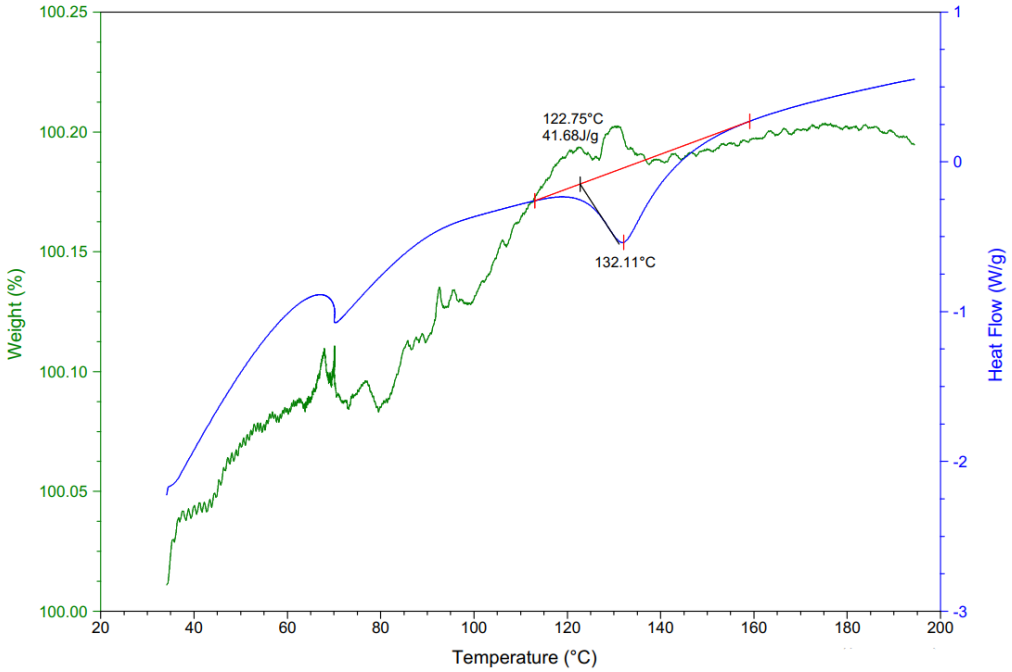

Figure 3-12 DSC results of the pipe's reinforcement layer

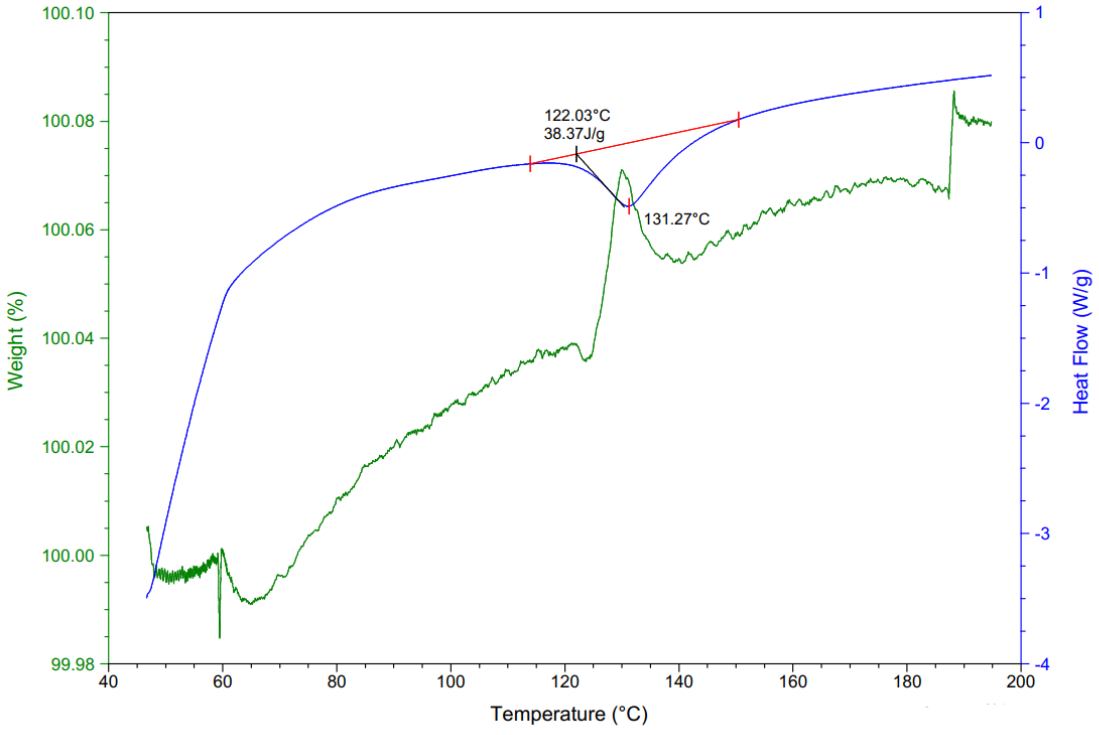

Figure 3-13 DSC results of the pipe's liner layer

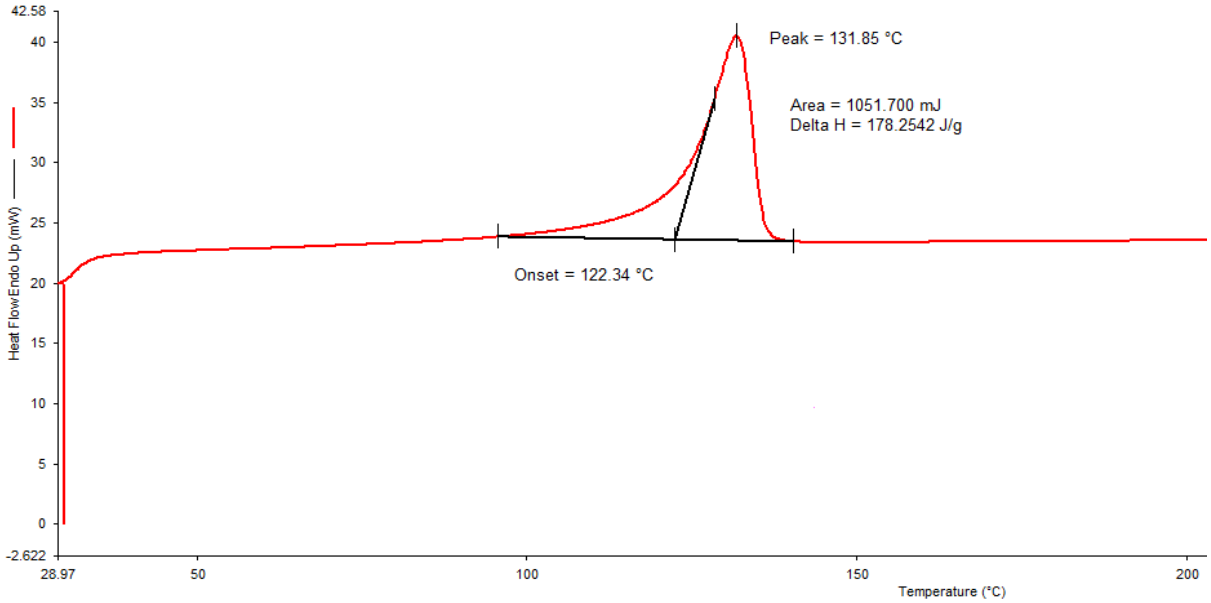

Figure 3-14 DSC results of the fitting

The outcomes of the DSC test are summarized and listed in Table 8 and several observations can be made.

Table 8 DSC onset and melting temperature for all materials

Sample Type	**T_{onset} (°C)**	**$T_{melting}$ (°C)**	**ΔH (J/g)**
Fitting PE100	122.34	131.85	178.254
Pipe Cover	119.23	130.59	129.2
Pipe Laminate	122.75	132.11	41.68
Pipe Liner	122.03	131.27	38.37

Onset temperature

The onset temperatures (T_{onset}) for the samples are relatively close, with the Pipe Cover exhibiting the lowest value at 119.23°C. The Fitting PE100, Pipe Laminate, and Pipe Liner samples all have onset temperature values around 122°C, indicating similar starting points for their thermal transitions.

Melting Temperatures

The melting temperatures are also closely grouped, with a range of just 1.52°C across all samples. The Pipe Laminate shows the highest melting point at 132.11°C, suggesting slightly different thermal characteristics or polymer chains compared to the other samples.

Enthalpy Changes

There is a noticeable variation in ΔH values. The Fitting PE100 displays the highest enthalpy change at 178.254 J/g, suggesting the greatest energy required for its phase transition. Conversely, the Pipe Laminate and Pipe Liner have significantly lower ΔH values, with the latter being the smallest at 38.37 J/g. This could imply differences in crystallinity, molecular orientation, or overall energy involved in their melting processes.

The four samples, while exhibiting similar onset and melting temperatures, show varying enthalpy changes during their phase transitions. The Fitting PE100 requires the highest energy for melting, indicating potential differences in its molecular structure or crystallinity compared to the other samples. The pipe laminate and pipe liner, despite their similar onset and melting points to the Fitting PE100, display much lower enthalpy changes, suggesting different thermal behaviours.

Further analysis might be needed to delve deeper into the molecular or compositional differences leading to these distinct thermal characteristics but there were out of the scope of this study.

Overall, these results emphasize the nuanced thermal behaviours exhibited by different PE materials, even when their basic transition temperatures are closely aligned.

Specific heat capacity

The specific heat capacity is a property that describes how much heat energy is needed to increase the temperature of a material by a certain amount. In this section we'll delve into the measurement of heat capacity for three different materials (fitting pipe liner and cover) using a precise technique called 3 run DSC. Unlike methods this technique accurately captures Cp values during the melting phase.

To determine the heat capacity of materials the widely used 3 run DSC method is employed. The DSC instrument, like the SDT Q600 has a heat flux sensor that measures how heat flows into or out of the sample as temperature changes.

To conduct heat capacity measurements three runs are performed on the same sample. In the first run an empty reference pan was used as a comparison point while the sample pan contains the material being studied. Both pans are subjected to a heating program typically with a linear heating ramp.

During the second run the sample pan was filled with a known reference material like sapphire or indium. Substances, with well-established specific heat capacity values. Again, both pans are subjected to the same heating program.

Finally in the third run, the sample pan contains the material of interest. The heating program used was the same as before. By comparing the heat flow patterns of the sample pan in the final runs with that of the reference pan the specific heat capacity of the material was obtained. The heat flow measured during the run represents a combination of factors such as the samples heat capacity and any energy absorption or release due to phase transitions or reactions. However, in the third run only the specific heat capacity of the material influences its heat flow pattern.

The specific heat capacity indicated in Figure 3-15 was calculated by dividing the difference in heat flow between the third runs, by both temperature difference and using known specific heat capacity values from a reference material used in the second run.

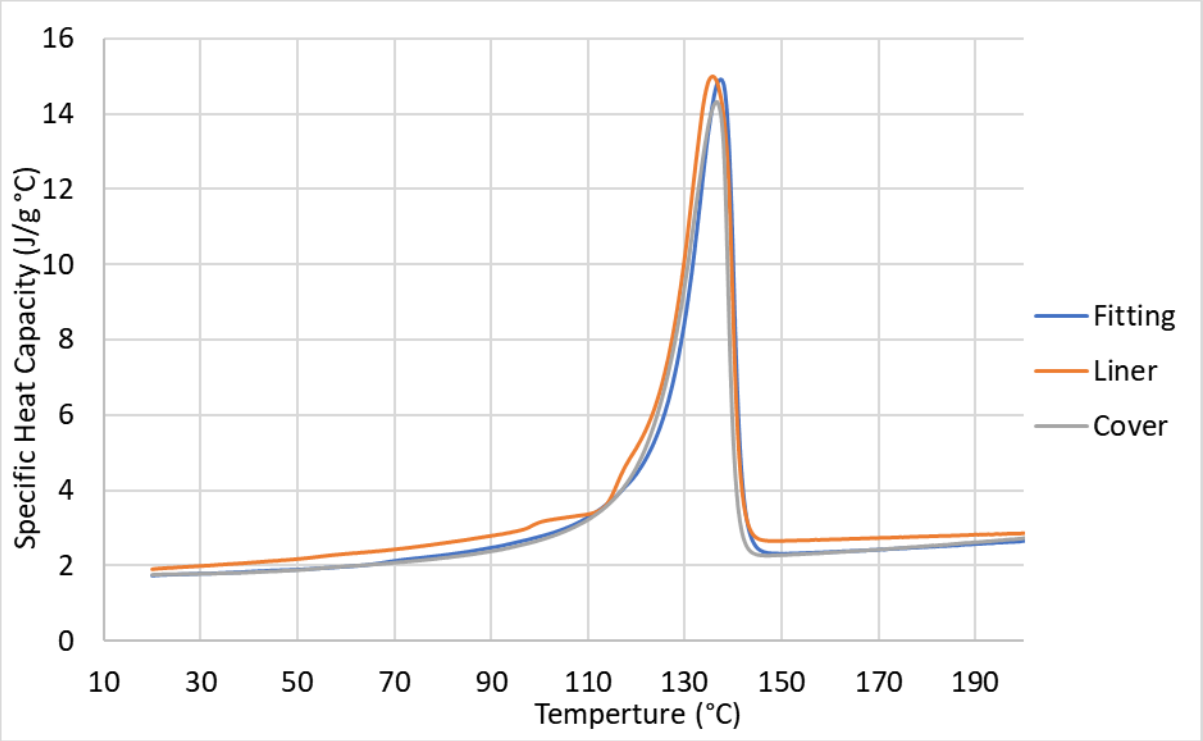

Figure 3-15 Cp results of the fitting, pipe's cover and liner

In the results shown in Figure 3-15 an increase in the specific heat capacity of the three HDPE materials can be observed when they reach their melting temperature. This notable increase is due to the phase change that HDPE undergoes from being a solid to becoming a liquid. During this transition the molecules of HDPE absorb energy to overcome the forces that hold them together in their rigid solid structure allowing them to move more freely as a liquid. The absorbed energy during this phase change is used for rearranging the structure rather than increasing the temperature of HDPE, which explains why there is a noticeable rise in specific heat capacity at the melting point, on the graph. After this transition phase the specific heat capacity of HDPE returns to levels representing the energy required to raise its temperature while it remains in its liquid state.

3.2.4 The rule of mixtures

Since the results of LFA test for the GF/HDPE composite laminate in Section 3.2.1 was unrealistic, where unexpected behaviour of increase in the thermal conductivity as the temperature increases, thus, to calculate the effective properties of the composite laminate at a specific temperature, the rule of mixtures was employed. The rule of mixtures assumes that the properties of the composite are a weighted average of the properties of the individual components based on their volume fractions (V_{HDPE} and V_{Glass}) of HDPE and glass fibers in the laminate, as well as the temperature at which the properties are to be evaluated. The properties of the glass fibers listed in Table 9 were assumed to remain constant throughout the study, as they are not subject to significant variations within the temperature range of the welding test.

Table 9 Properties of the glass fiber [62]

V_{Glass}	0.417
k_{Glass}	1.3 W/mK
ρ_{Glass}	2580 kg/m^3
Cp_{Glass}	810 J/kgK

The rule of mixtures was used to estimate the effective thermal conductivity (k_{eff}), specific heat capacity (Cp_{eff}), and density (ρ_{eff}) of the GF/HDPE laminate. For the thermal conductivity, using Equation 3.2, the result is presented in Figure 3-16.

$$k_{eff} = V_{HDPE} * k_{HDPE} + V_{Glass} * k_{Glass} \quad (3.2)$$

where k_{HDPE} and k_{Glass} are the thermal conductivities of HDPE and glass fibers, respectively.

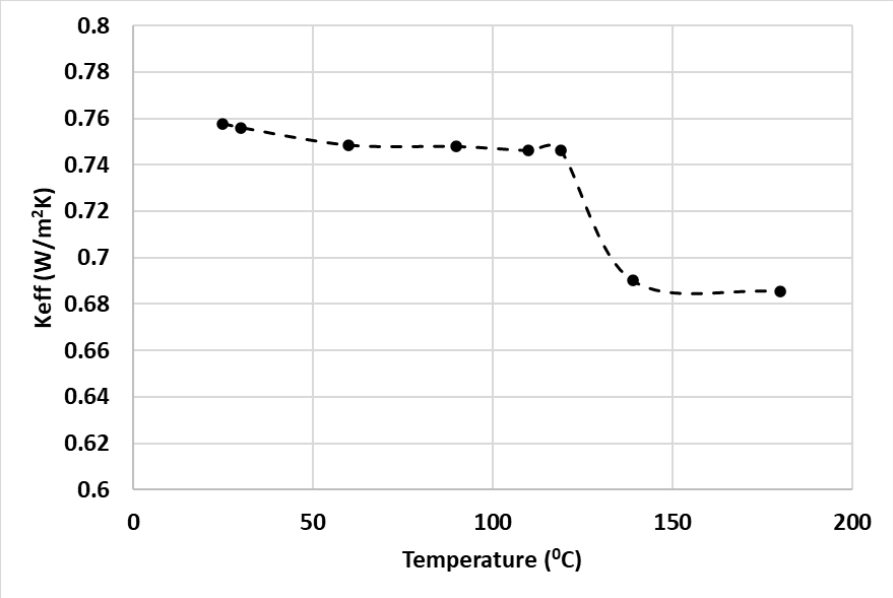

Figure 3-16 GF/HDPE effective thermal conductivity

For the specific heat capacity of the GF/HDPE laminate, using Equation 3.3, the result is shown in Figure 3-17.

$$Cp_{eff} = V_{HDPE} * Cp_{HDPE} + V_{Glass} * Cp_{Glass} \quad (4.3)$$

where Cp_{HDPE} and Cp_{Glass} are the specific heat capacities of HDPE and glass fibers, respectively. The HDPE specific heat capacities were taken from the DSC results presented earlier and for glass fibres were taken from literature.

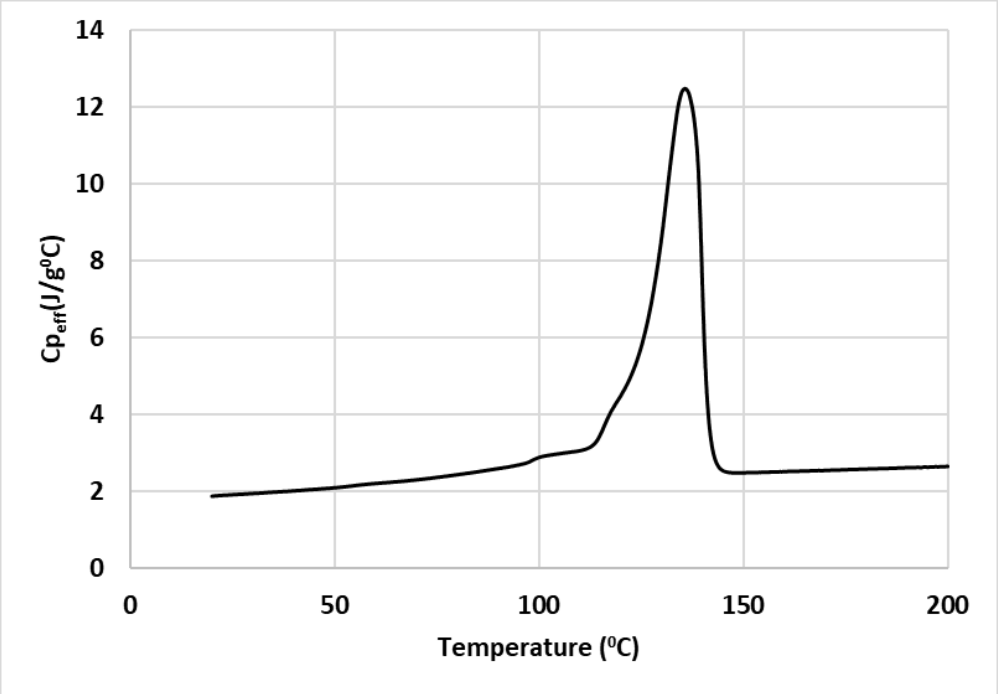

Figure 3-17 GF/HDPE effective specific heat capacity

The density of the GF/HDPE laminate using the rule of mixture can be calculated by Equation 3.4 and the result is presented in Figure 3-18.

$$\rho_{eff} = V_{HDPE} * \rho_{HDPE} + V_{Glass} * \rho_{Glass} \quad (3.4)$$

where ρ_{HDPE} and ρ_{Glass} are the densities of HDPE and glass fibers, respectively.

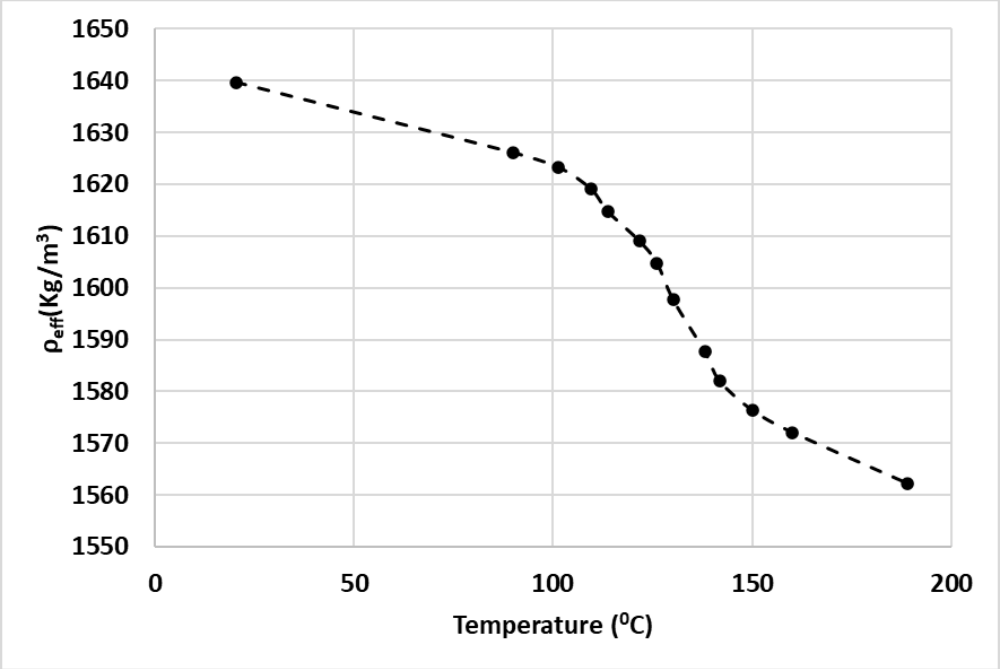

Figure 3-18 GF/HDPE effective density

The differences between the values obtained from the rule of mixtures and those determined by LFA are quite noticeable. This is evident in the conductivity values, where the rule of mixtures gives an approximate value of 0.75 while LFA reveals a significantly lower value of 0.47 showing a notable difference of around 59%.

These discrepancies arise because the rule of mixtures assumes that the components are evenly mixed and calculates properties based on their volume fractions and individual characteristics. However real composite materials like glass/HDPE laminate are often not uniformly mixed leading to deviations from predictions.

Furthermore the rule of mixtures does not take into account the interactions between phases in a composite material. The interface between glass and HDPE can greatly impact thermal properties especially when there is poor interaction between these phases. This can result in differences, between experimental and theoretical values.

The way the glass is distributed within the HDPE matrix greatly affects its properties. However, the rule of mixtures does not consider these distribution patterns, which can result in inconsistencies when comparing with findings.

To sum up the assumptions made in the rule of mixtures and factors like material heterogeneity, interface effects, arrangement of components and measurement techniques in LFA can all contribute to the variations observed between experimental values of Cp and k, for glass/HDPE laminate.

3.2.5 Conclusion

In order to simulate real world scenarios with the level of accuracy, Chapter 6 of the simulation model required specific input regarding critical thermal properties; specific heat capacity (*Cp*) thermal conductivity (*k*) and melting temperature. To obtain this information various testing methods were employed, including Laser Flash Analysis (LFA) Differential Scanning Calorimetry (DSC) and the Transient Plane Source (TPS).

The DSC analysis revealed peak melting temperatures for Fitting PE100 and identified significant shifts in Cp near the melting points. LFA provided insights into diffusivity by showing that the pipe cover had a value of 0.214 mm^2/s at 30°C. TPS results indicated a conductivity of 0.469 W/(mK) for Fitting PE100 at 25°C. Additionally, the effective thermal properties of the pipe reinforced laminate were determined using a combination of these data and the rule of mixtures resulting in a comprehensive understanding of their thermal profile.

When it comes to incorporating the properties of GF/HDPE into Chapter 6s simulation model to accurately reflect real world scenarios, data from LFA is generally preferred over relying solely on the rule of mixtures even if unexpected behaviour is observed in LFA data. This preference stems from LFA providing insights that capture the inherent complexities and interactions, within composite materials offering a nuanced perspective that aligns better with actual material behaviour.

In this research, an attempt was made to measure the temperature-dependent density of HDPE; however, due to the unavailability of the required instrumentation in the university labs, this objective could not be achieved. Consequently, to ensure the accuracy of the simulations and experiments, density values were adopted from reputable literature sources. The literature values, specifically those provided for PE100 in Section 2.3.4, were utilized as a reliable substitute for temperature-dependent density data in the absence of in-house measurements.

Chapter 4

EXPERIMENTAL EFW TEST FOR TCP

This chapter embarks on a journey through the stages of experimental electrofusion welding for validation, unveiling each crucial step undertaken to corroborate the theoretical insights gained earlier in Section 2.2. The process encompasses meticulous pre-test preparations, the strategic installation of thermocouples, the employment of infrared (IR) camera thermography, the execution of welding tests, and a meticulous post-welding analysis that includes computed tomography (CT) scanning and sample preparation to identify the extent of the melting zone. In the midst of these detailed experiments the main goal is to confirm the accuracy of the carefully crafted heat transfer model in Chapter 6 for electrofusion welding in TCP

Materials and tools required for the EFW test

3-Layer TCP/fittings

Thermocouples (appropriate for the desired temperature range)

Cutting tools (e.g., hacksaw, pipe cutter)

Pipe straightening machine

Drill machine

Drill bits (appropriate size for thermocouple placement)

Adhesive for the thermocouples' installation

Welding machine (ECU)

Extrusion welding machine

4.1 Electrofusion welding test preparation

4.1.1 Thermocouples installation

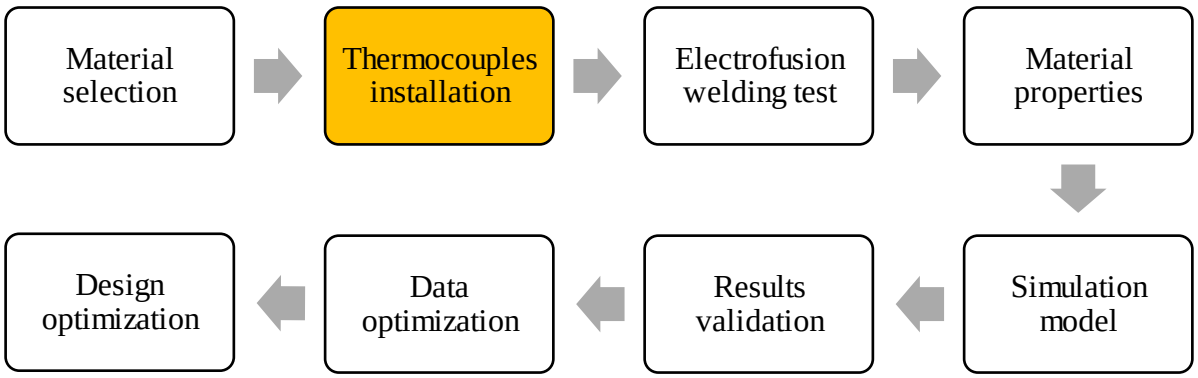

The procedure for the selection of the installation plan for thermocouples involves several steps to ensure optimal placement and accurate temperature measurements. Firstly, a thorough assessment of the test specimen or structure is conducted, considering factors such as expected temperature distribution, critical areas, and regions of interest.

In the scope of this research, two tests will be conducted, each involving the installation of 30 thermocouples. These thermocouples will be strategically distributed across five different axial sections and various depths within the pipe and fitting. The thermocouples used in these two physical tests were general purpose k-type thermocouples manufactured by TC Direct. The thermocouples length is 2 m with solid conductor of 0.2 mm diameter and operating temperature range of -75 to 220 ^{0}C. The selection of the installation plans was guided by a model analysis that considered the fundamental welding behaviour of PE pipes, utilizing literature data as a basis.

The detailed procedure for the installation of thermocouples will be elaborated upon in this section. To avoid any shorting with the copper heating wires and to ensure accurate temperature measurements, it is important to note that no thermocouples should be placed in the welding interface or the cover layer of the pipe. These areas have been excluded from the placement plans to maintain the integrity of the measurements and prevent any interference during the welding process.

The electrofusion joint during the heating process exhibits critical regions that require special attention. In this regard, five axial locations were carefully selected, to facilitate the installation of thermocouples. By strategically choosing these locations, the thermocouples can effectively monitor temperature variations within the critical regions of the electrofusion joint as shown in Figure 4-1. This approach enabled a comprehensive understanding of the joint's thermal behaviour and enhanced the reliability of the experimental data.

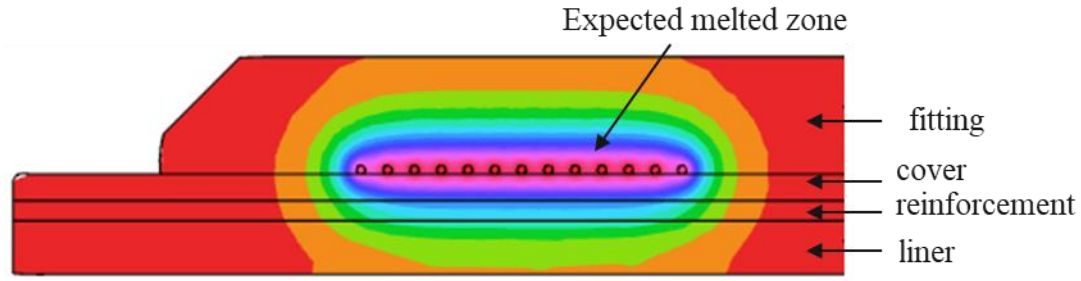

Figure 4-1 Electrofusion joint heat regions

Based upon the expected heat behaviour of the electrofusion joint during the welding, the locations of the thermocouples were selected for both tests. These locations are presented in Tables 10 and 11 for the first test. For the second test, the locations of thermocouples are presented in Table 12 and 13.

Test 1

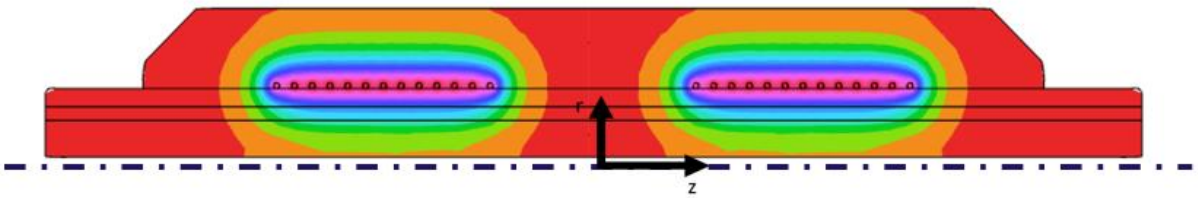

Table 10 Thermocouple locations in the pipe (Test 1)

Left Pipe			Right Pipe		
TC #	Axial position (mm)	Radial depth (mm)	TC #	Axial position (mm)	Radial depth (mm)
1	-20	11.5	11	25	10
2	-25	8	12	50	7.5
3	-50	8	13	60	10
4	-60	8	14	65	10.5
5	-65	10	15	50	10
6	-50	9.5	16	60	11
7	-25	9	17	20	12
8	-50	9	18	25	11
9	-60	9	19	50	10.5
10	-65	11	20	65	10.5

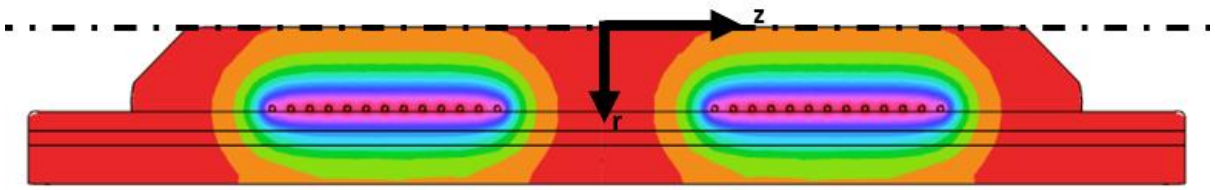

Table 11 Thermocouple locations in the EF fitting (Test 1)

Fitting left side			Fitting right side		
TC #	Axial position (mm)	Radial depth (mm)	TC #	Axial position (mm)	Radial depth (mm)
21	-20	14	26	25	12
29	-50	0	24	50	0
22	-50	12	27	50	10
23	-60	9	28	65	8
25	-60	11	30	65	6

Test 2

Table 12 Thermocouple locations in the pipe (Test 2)

Left pipe			Right pipe		
TC #	**Axial position (mm)**	**Radial depth (mm)**	**TC #**	**Axial position (mm)**	**Radial depth (mm)**
1	-20	12	9	20	12.5
2	-25	8	10	25	10
3	-50	8	11	50	11.5
4	-60	9	12	65	8.5
5	-50	9	13	65	9.5
6	-25	9	14	25	11
7	-50	10	15	60	11
8	-60	10	16	65	10.5

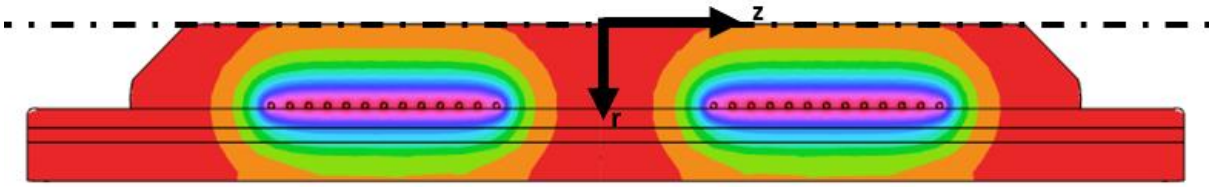

Table 13 Thermocouple locations in the EF fitting (Test 2)

Fitting left side			Fitting right side		
TC #	**Axial position (mm)**	**Radial depth (mm)**	**TC #**	**Axial position (mm)**	**Radial depth (mm)**
17	-20	14	24	25	12
18	-25	8	25	50	0
19	-60	6	26	65	7
20	-50	0	27	25	10
21	-60	10	28	60	8
22	-50	12	29	65	9
23	-60	12	30	65	11

4.1.2 Pipe and EF fitting preparation

Prior to welding, several steps were undertaken to prepare the 3-layer TCP. A suitable 3-layer 6" TCP made from PE100 liner and cover, HDPE/glass reinforcement was selected for the experiment. The desired length of the pipe was then measured and marked. Utilizing a cutting tool, either a hacksaw or pipe cutter, the pipe was divided into two 1-meter equal segments. It was of paramount importance to ensure that the ends of the pipes were cut squarely as shown in Figure 4-2.

Figure 4-2 Cutting the pipe to square ends

After the initial cutting, any burrs or sharp edges present on the cut ends of the pipes were carefully removed. In the straightening phase, should any of the pipe segments have appeared bent or deformed, they were straightened using a pipe straightening machine or another appropriate method as shown in Figure 4-3. It was crucial to ensure that the pipe segments were properly straightened to facilitate accurate thermocouple placement. To straighten the pipe samples a steel pipe/straightening jig was used and the assembly was inserted into a heating chamber at 80 ^{0}C for 5 to 8 hours until an acceptable level of pipe bending and ovality is achieved

Figure 4-3 Pipe straightening procedure

The ends of the pipes were scraped as shown in Figure 4-4 using a rotary scraper to achieve a circumference that was slightly less than the inner diameter of the fitting, which measured 180 mm.

Figure 4-4 Rotary scraping for the pipe end

It was ensured that the scraped end of the pipe could slide to the midpoint of the EF fitting as shown in Figure 4-5.

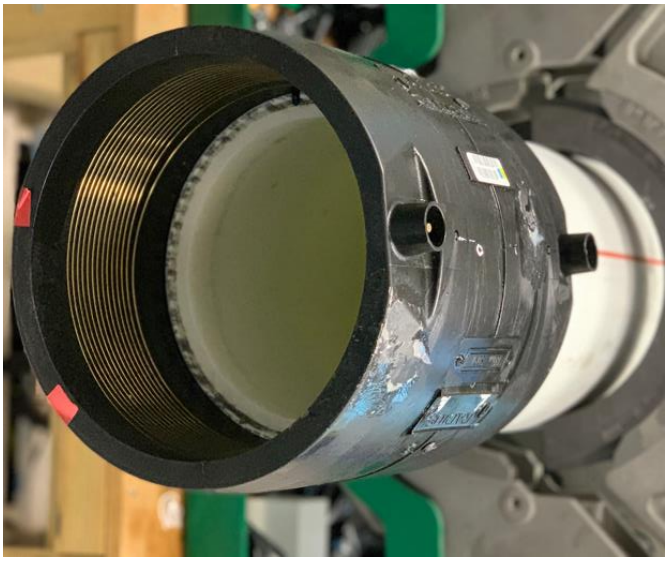

Figure 4-5 EF fitting sliding on pipe end

The pipe segments were then cut into two halves using jacksaw as shown in Figure 4-7 to facilitate the installation of thermocouples to the pipe's interior.

Figure 4-6 Pipe segments cut into halves

The locations of interest for the required holes were marked on each pipe half as shown in Figure 4-7.

Figure 4-7 Marking thermocouple's location on the pipe

Hole preparation:

During the hole preparation, the number and placement of thermocouples on each fitting and pipe half were determined. Subsequently, the positions for drilling holes were marked on the inner surface of the pipe halves. It was crucial to ensure that these marked positions were evenly spaced and would align correctly upon reassembling the pipe halves. This same procedure was also replicated for the EF fitting as shown in Figure 4-8.

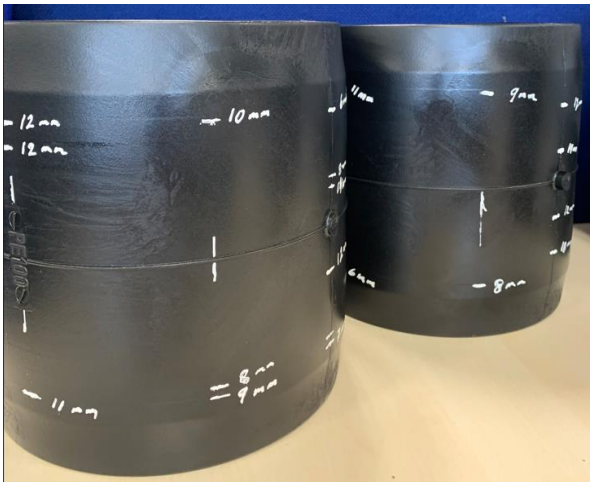

Figure 4-8 Marking thermocouple's location on the fitting

Drilling holes

During the drilling process, each pipe half was securely fastened using clamps or a vice to preclude any movement. An appropriate drill bit size, corresponding to the diameter of the

thermocouples, was selected. Holes were then drilled at the designated positions on the inner surface of each pipe half and the outer surface. This drilling procedure was consistently applied to all marked positions across both pipe halves and the EF fitting as shown in Figure 4-9.

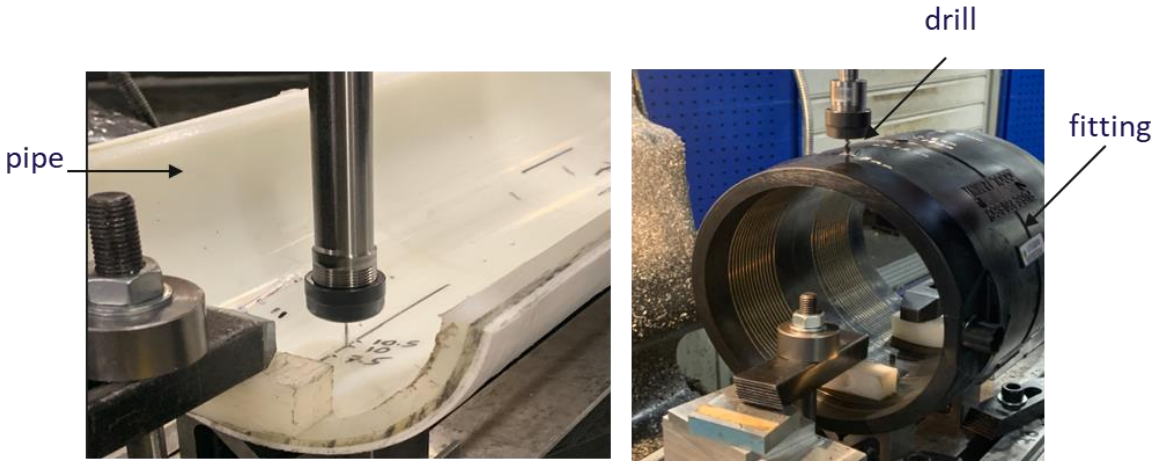

Figure 4-9 Hole drilling in pipe halves and fitting

Pipe reassembly

In the reassembly of the pipe, it was critical to ensure that the holes aligned accurately with their corresponding drilled positions. For meticulous alignment of the pipe halves, a plastic ring, with an inner diameter equating to the pipe's outer diameter, was employed. Welding fixtures or clamps were used to firmly hold the pipe halves in place for the duration of the re-welding process. The extrusion welding machine was configured based on the manufacturer's specifications, and welding parameters specific to the pipe material in use were meticulously followed. The welding commenced, with emphasis placed on achieving a continuous and uniform weld across the entirety of the conjoined pipe halves as shown in Figure 4-10. Throughout the welding operation, consistent speed and pressure were maintained to ensure an optimal weld joint. After welding, any excessive weld material was removed using an angle grinder as shown in Figure 4-11.

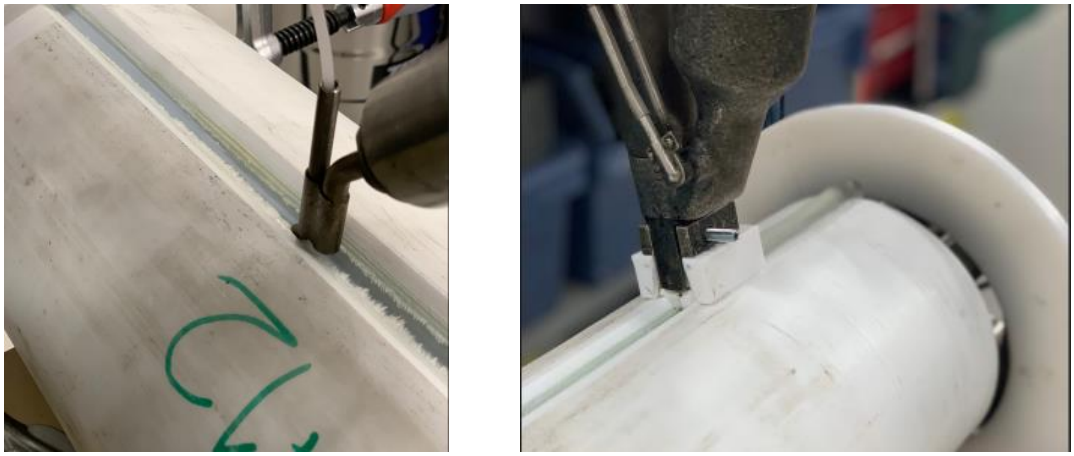

Figure 4-10 PE filling and extrusion welding reassembly

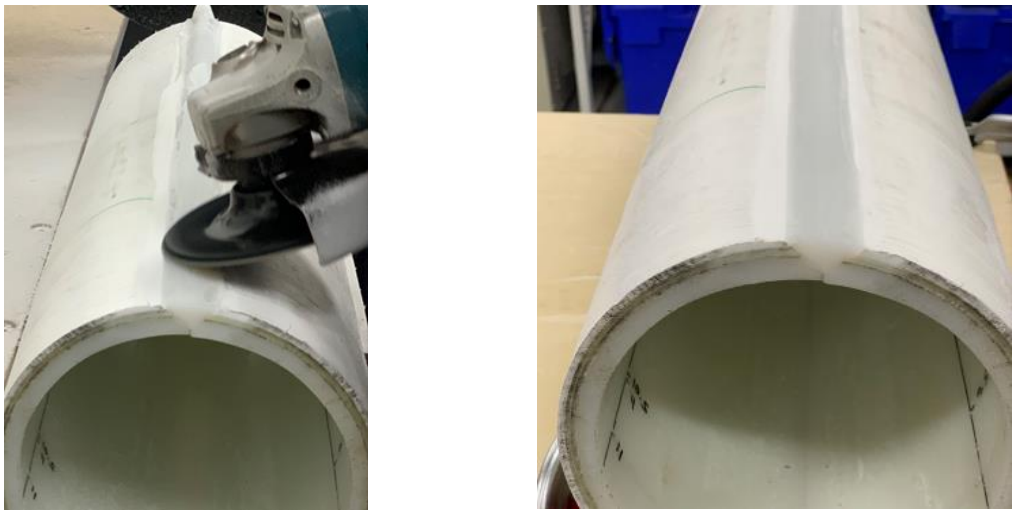

Figure 4-11 The excess material was ground away using an angle grinder

Thermocouple Placement

During the placement of thermocouples, the drilled holes were initially cleaned, ensuring the elimination of any debris or burrs. Each thermocouple was carefully inserted into its designated drilled hole. Subsequently, a black CT1 sealant and constructive adhesive was applied to the thermocouple to ensure its secure positioning. This method was replicated for all drilled locations on both pipe halves and the fitting as shown in Figure 4-12.

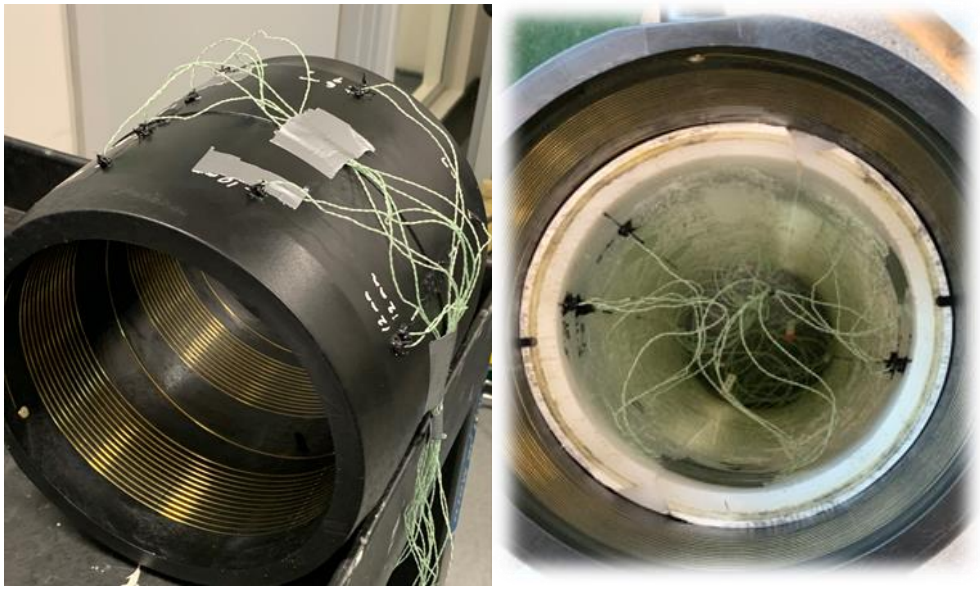

Figure 4-12 Thermocouples placement in both pipes and fitting

4.1.3 Electrofusion welding test setup

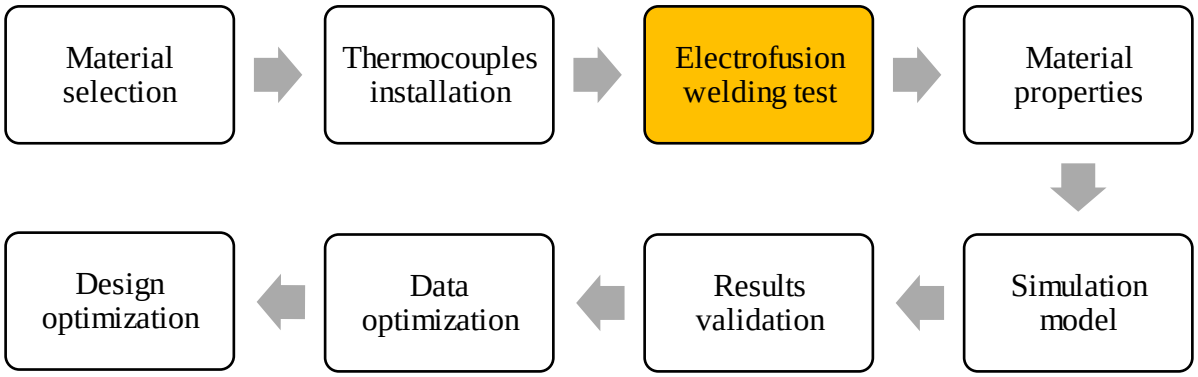

The electrofusion welding setup shown in Figure 4-13 had been thoughtfully constructed to ensure meticulous and controlled testing conditions. It had included clamps for uniform pressure distribution, securing the TCP and fitting consistently. A sophisticated data acquisition system, interconnected with strategically placed thermocouples, had recorded temperature changes at 0.5-second intervals throughout the welding cycle. Notably, the setup had also incorporated the electrofusion welding machine, which connected to both fitting terminals, facilitating the controlled application of heat and pressure. This integration of precise clamping, advanced temperature monitoring, and the electrofusion welding machine provided a comprehensive platform for analysing the fusion process dynamics and heat distribution patterns.

The input for the start of the physical welding was the EF fitting barcode to the ECU. The output of the test was voltage and current during during the heating cycle in addition to the 30 thermocouples readings during the whole welding cycle.

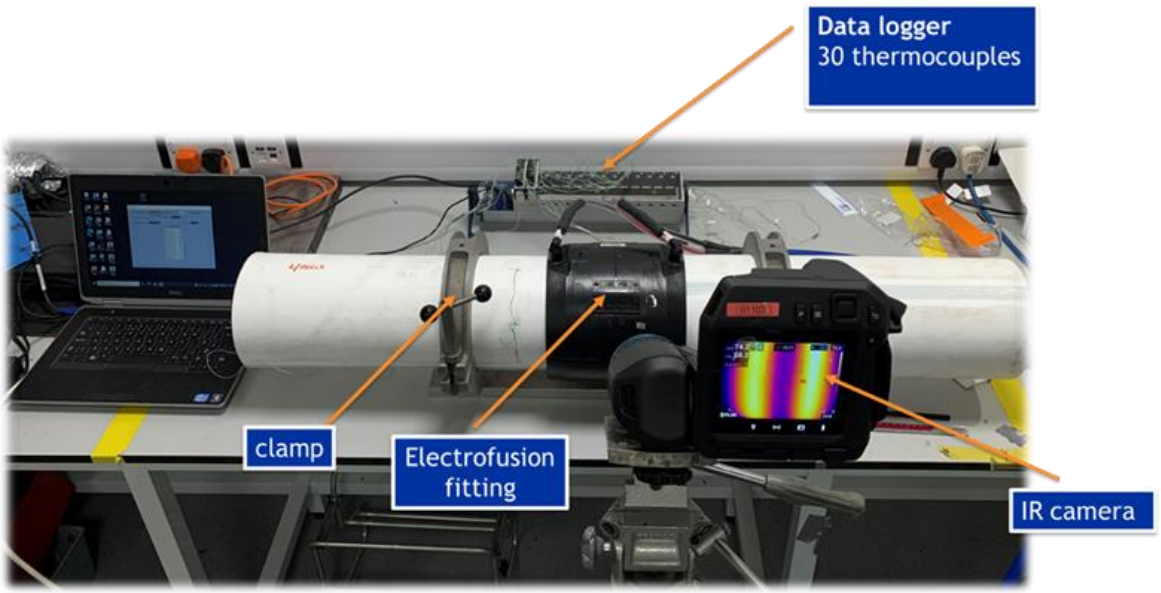

Figure 4-13 Electrofusion welding test setup

4.1.4 IR camera

The temperature profile on the external surface of the fitting during the electrofusion welding process was captured using a thermal FLIR T50 infrared camera. The collected data from thermography plays a crucial role in establishing a correlation between the simulation results and the temperature readings obtained from thermocouples. The emissivity of the polyethylene material was assumed to be 0.94, which is commonly accepted for this type of material. [63]

The thermal infrared camera utilized in the experiment was set at 1 meter distance from the fitting and was capable of capturing live temperature readings at a speed rate of 30 frames per second, enabling a detailed analysis of the temperature variations and distribution during the welding process. The integration of thermography data enhanced the understanding of the thermal behaviour of the process within the thermocouples and provided valuable insights for validating the simulation model's accuracy and reliability in predicting the temperature profiles during electrofusion welding of fittings.

4.2 EFW test results

4.2.1 EFW power result

In order to collect data on the power input during the electrofusion welding of TCP, voltage and current recordings from the electrofusion welding unit are captured and presented in Figure 4-14. The voltage measurements provide insight into the electrical energy supplied to the welding process, while temperature recordings help understand the thermal behaviour during the fusion process. These recorded values of voltage and current serve as essential inputs for the simulation model developed in chapter 6.

By collecting power data through voltage and temperature recordings, the simulation model can accurately replicate the actual power input during the welding process. This allows for a detailed analysis of the energy distribution and heat generation within the pipe, aiding in the optimization of welding parameters and the prediction of the resulting weld quality. The integration of experimental power data into the simulation model enhances its accuracy and reliability, ensuring that the model can effectively simulate and predict the behaviour of electrofusion welding for TCP.

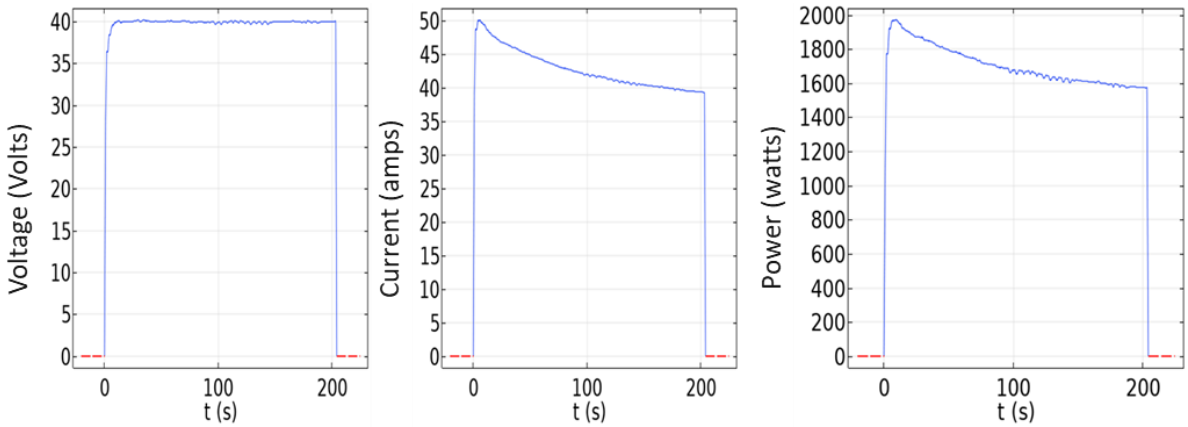

a) Voltage (Volts) *b) Current (amps)* *c) Power (Watts)*

Figure 4-14 Electrofusion welding input voltage, current and power

The utilization of power data as input for the simulation model provides valuable insights into the energy dynamics and thermal characteristics of the welding process. This information is instrumental in enhancing process control, optimizing welding conditions, and ultimately improving the quality and performance of the welded TCP.

4.2.2 EFW temperature results

The output results of all the 30 thermocouples in both tests are presented in Figures 4-15 and 4-16. It was noticed that the maximum temperature recorded at all times during the EFW did not exceed 100 ^{0}C and no danger is applied to the composite reinforcement in terms of the effect of heat transfer during the welding process since this is below the melting temperature of 131 ^{0}C as determine in Section 3.2.3.

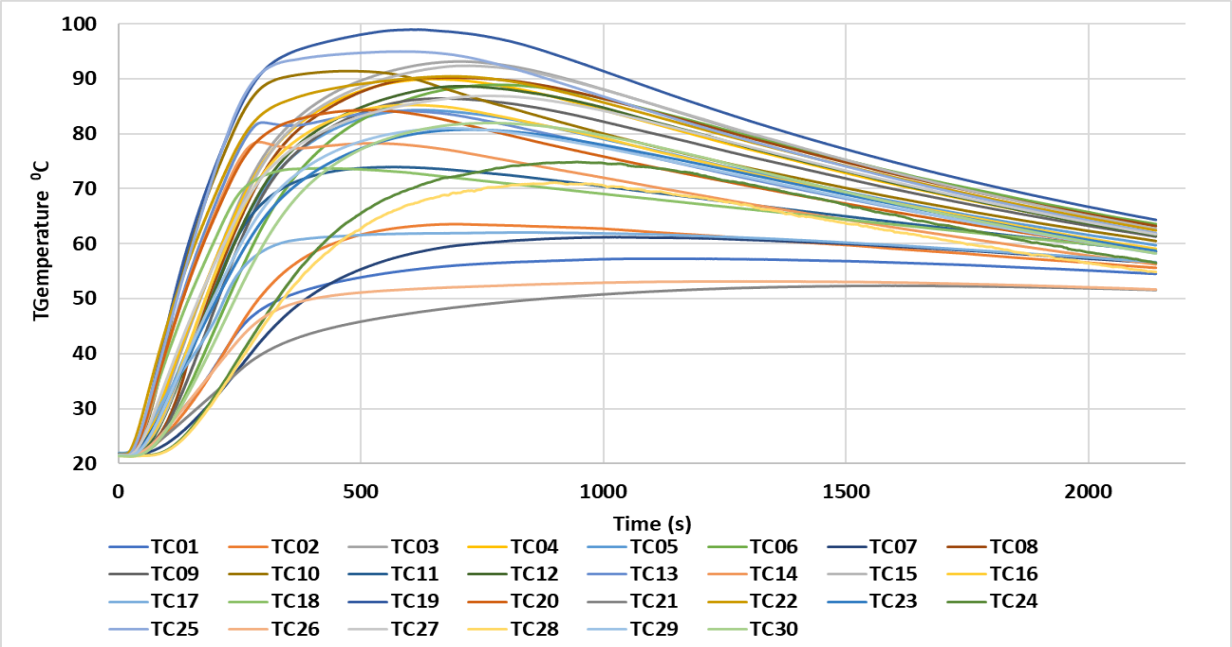

Figure 4-15 Temperature readings for all thermocouples in Test 1

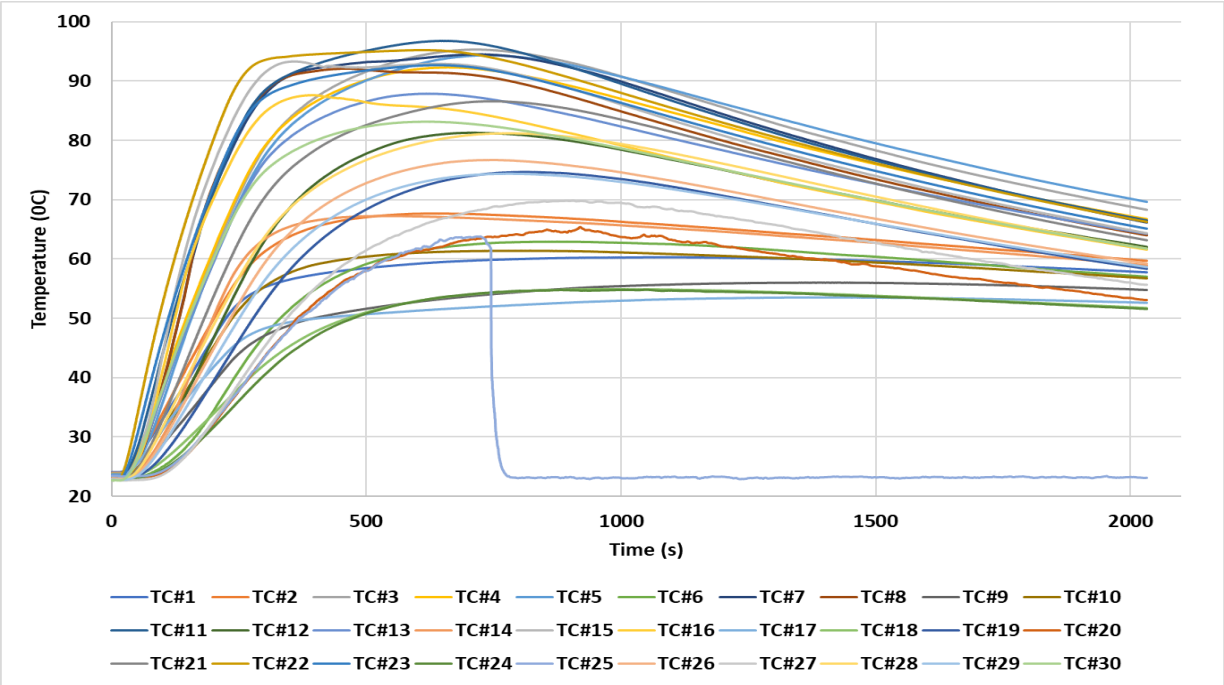

Figure 4-16 Temperature readings for all thermocouples in Test 2

During test 2, one of the installed thermocouples, TC#25 did fail as shown in Figure 4-16. At time 745 seconds with the maximum temperature of 61.7 ^{0}C reached, this thermocouple moved due to the increased of heat and fell from the external fitting surface, thus the temperature data of this thermocouple after time of 745 s is invalid.

The **heatmap plots** presented in Figures 4-17 and 4-18, provide a visual representation of how temperature is distributed across all the 30 thermocouples during the two welding tests. These heat maps are designed to offer an understanding of where and when heat is concentrated throughout the welding process. By aligning the temperature measurements of each thermocouple, a sequential representation of the thermal dynamics during electrofusion welding was created. Additionally, there are two accompanying line graphs that focus on the thermocouple with the maximum temperature and the thermocouple with the lowest maximum temperature. These line graphs depict how these specific thermocouples experience fluctuations, in temperature throughout the welding process.

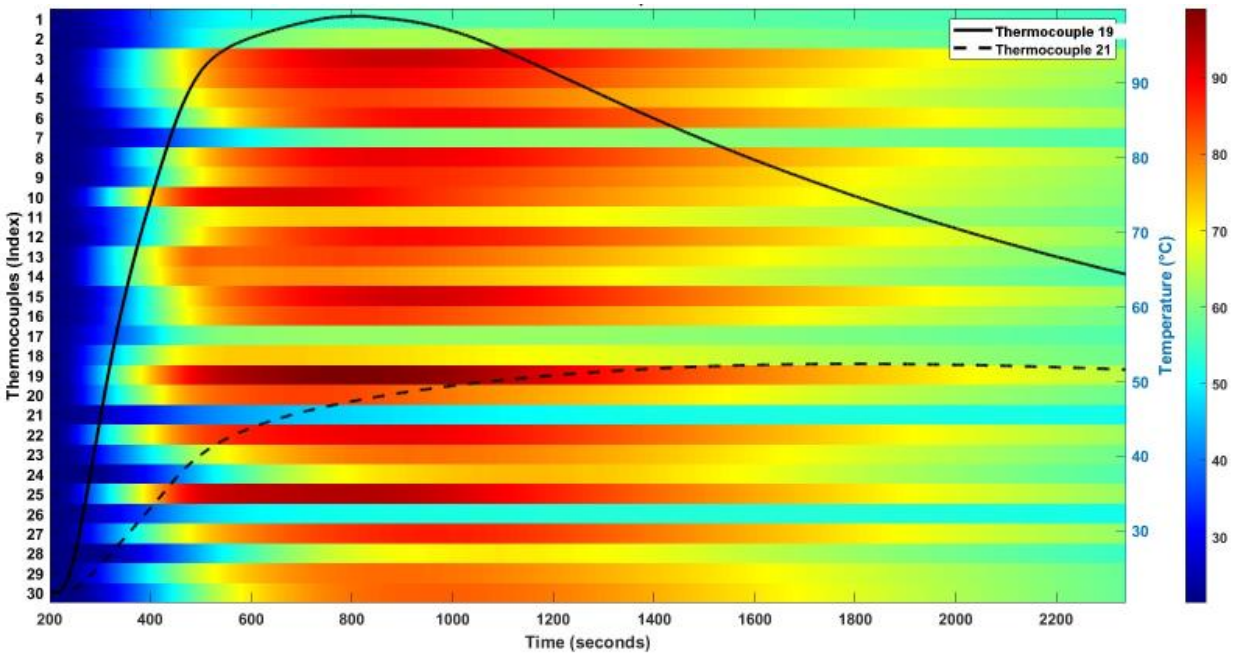

Figure 4-17 Heat map for Test 1

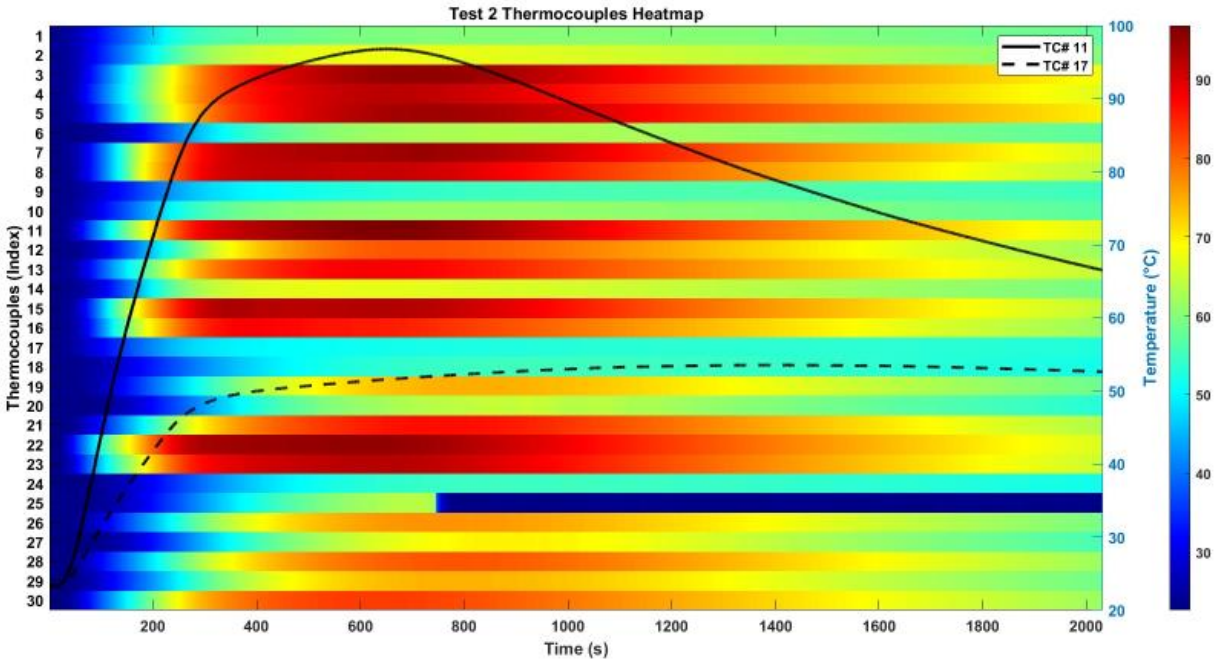

Figure 4-18 Heat map for Test 2

4.2.3 EFW thermography results

Figure 4-19 displays the thermography results, revealing the temperature pattern on the joint's external surface at its peak (83.8°C). The image distinctly identifies both hot and cold areas. There is a minor temperature fluctuation noticed around the circumference of the fitting at the same axial position. Such variations could be due to air gaps in certain parts, leading to greater heat resistance during welding. Consequently, more heat is needed for the joining process, which then gets redirected to the joint's exterior.

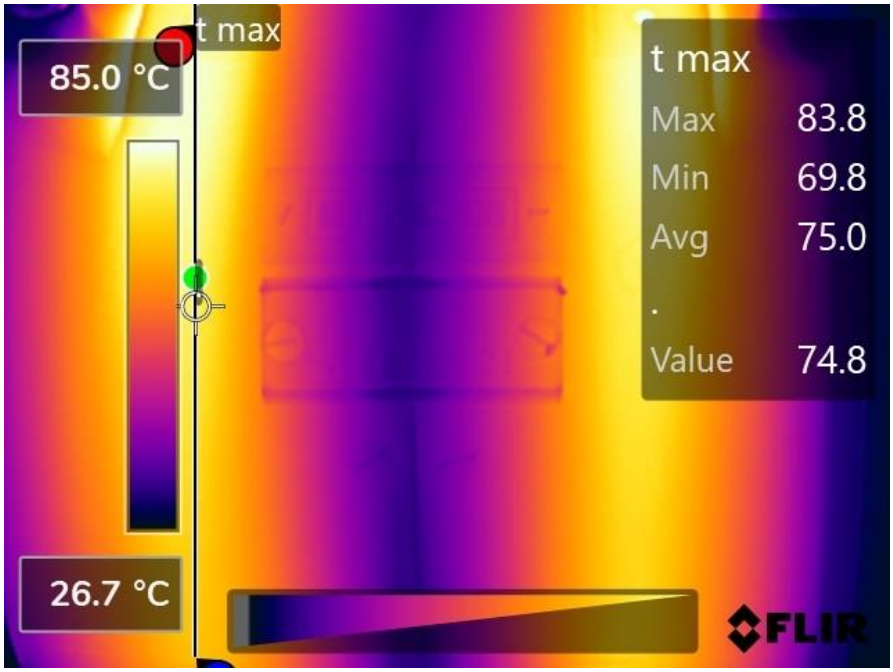

Figure 4-19 Thermography result at peak temperature of 83.8 °C

The temperature profile captured during the entire electrofusion welding process is displayed in Figure 4-20. This profile specifically represents a point near to the centre of the hot zone where the cursor is located.

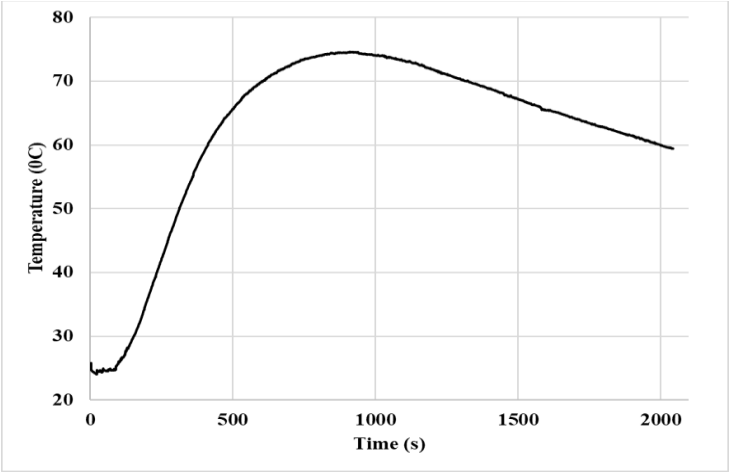

Figure 4-20 Thermography result at middle of heating zone at the point of the cursor indicated in

4.3 Post welding analysis

4.3.1 CT scan

A comprehensive X-ray computed tomography (CT) scan was conducted on the electrofusion joints of both tests subsequent to the welding process. The prime objective of this CT scan was to verify both the axial positioning and the radial depth of all the incorporated thermocouples, as depicted in Figure 4-21. However, due to transient factors encountered during the scanning procedure, including potential movement and dislodgment, obtaining a complete dataset directly from the thermocouples proved challenging. Instead, the obtained information pertained solely to the drilled holes, indicating the designated positions intended for the placement of the thermocouples. For this scan, the parameters in Table 14 were employed

Table 14 CT scan parameters

Parameter	Settings for the 450kV system
Energy (kV)	260
Current (µA)	300
Filter	2mm Copper
Source-Detector distance (mm)	996.943
Source-Specimen distance (mm)	664.5898
Number of projections	4600
Frames per projection	1
Exposure time (ms)	250
Effective voxel size (µm)	100
Magnification	1.5x
Binning	X1

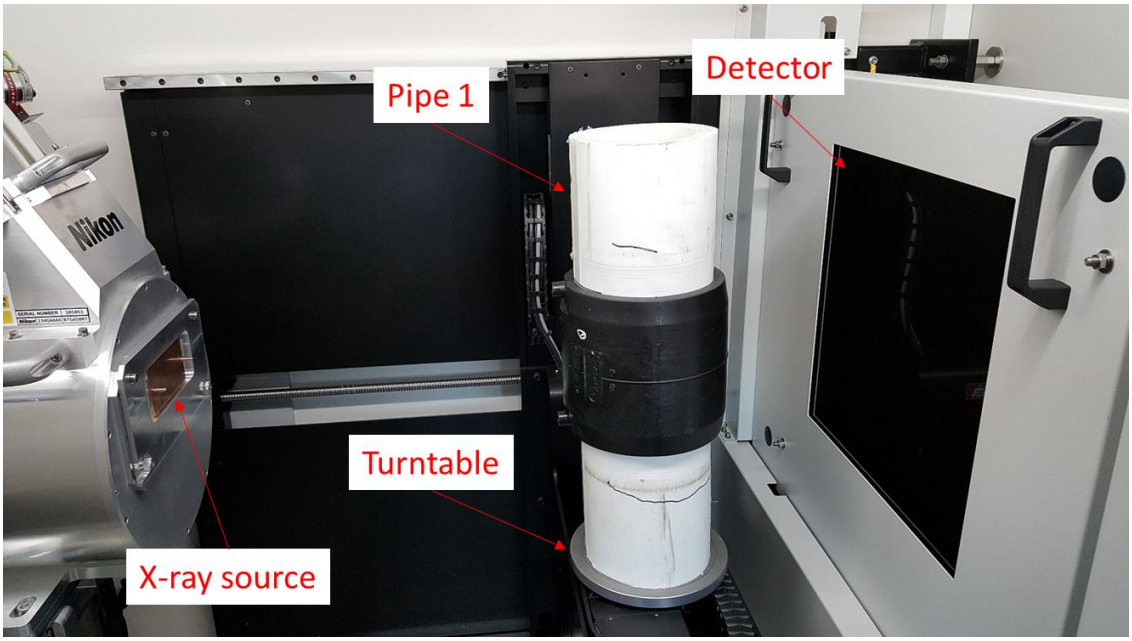

Figure 4-21 CT scan setup

Nonetheless, the acquired information was utilized to accurately determine the actual location and depth of the thermocouples within the developed computational model in Chapter 6. Unfortunately, some of the thermocouples were moved and other were fallen during transient as shown in Figure 4-22 and only the hole information can be collected. Aligning the collected hole information with the known design and intended positions of the thermocouples, an estimation of their true placement was achieved. This enabled the incorporation of more realistic and representative input parameters into the model, enhancing its predictive capabilities and providing a more accurate depiction of the thermal behaviour during the electrofusion welding process.

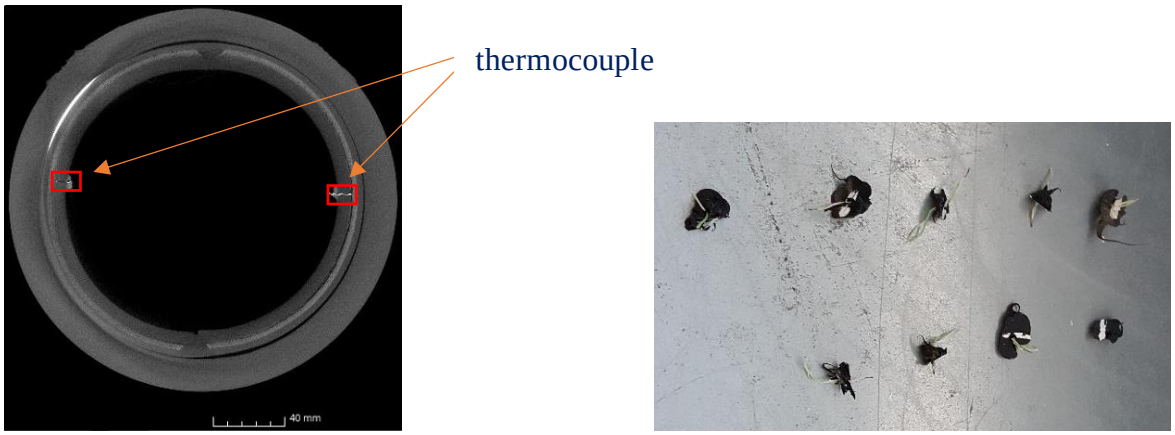

Figure 4-22 CT Scan of EF welding and falling thermocouples

The CT scan analysis revealed the manner in which the axial pipe was positioned into the EF fitting. This positioning affects the axial placement of the thermocouples in relation to the fitting. As shown in Figure 4-23, the left inner pipe from Test 1 has a 3.13 mm gap from the reference point, centred on the fitting. This gap has been accounted for by adjusting the measurements of the thermocouple's axial location, details of which will be discussed in Section 4.3.2.

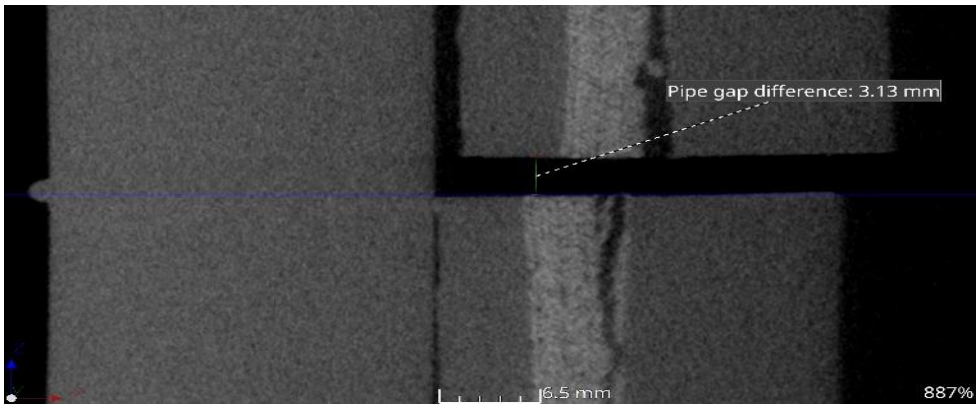

Figure 4-23CT Scan at the centre of EF joint of Test 1

Furthermore, the CT scan of served as a means to assess the joint's post-welding condition. Only scans of particular interest are presented here. Notably, instances of delamination were observed between the liner and the laminate reinforcement in certain regions as shown in Figure 4-24. This occurrence could potentially stem from inadequate bonding between these layers, possibly due to factors such as insufficient pressure during the welding process, uneven temperature distribution, or inconsistent material properties across the interface. These aspects could collectively contribute to weakened interlayer adhesion, warranting a comprehensive investigation to identify and rectify the underlying causative factors.

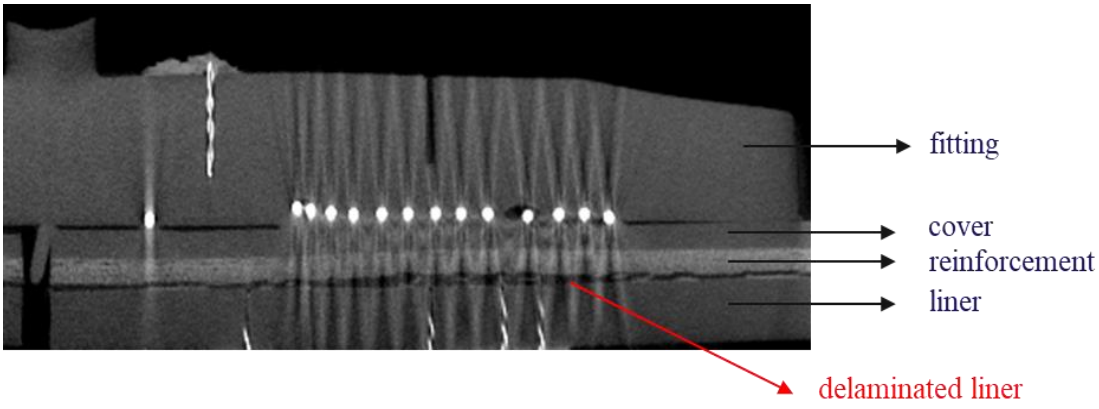

Figure 4-24 Liner delamination shown by CT scan

Despite the limitations encountered, this scan serves as a valuable contribution towards comprehending the precise positioning of the thermocouples. Moreover, it plays a key role in assuring the congruence between these thermocouple placements and the thermal profiles extracted from the experimental testing. Furthermore, the CT scan assumes a dual role by not only validating the thermocouple arrangement but also by inspecting the structural integrity of the joint itself. This multi-faceted utility underscores the efficacy of CT scanning in providing a comprehensive evaluation of both thermocouple accuracy and joint integrity.

4.3.2 Actual thermocouples' locations

The CT scans provided insights that necessitated a reassessment and adjustment of the thermocouples' positions in the pipe/fitting joint. Tables 15 and 16 detail the axial and radial positions for Test 1, as determined by the CT scan. Similarly, Tables 17 and 18 present the corresponding data for Test 2. These updated locations will serve as a reference for validating the heat transfer simulation model in Chapter 6

Table 15 Revised locations of thermocouples in the pipe (Test 1)

Left Pipe					Right Pipe				
TC #	Axial position (mm)		Radial depth (mm)		TC #	Axial position (mm)		Radial depth (mm)	
	Fitted	Measured	Fitted	Measured		Fitted	Measured	Fitted	Measured
1	20	20.93	11.5	9.78	11	25	24.77	10	9.89
2	25	26.29	8	6.57	12	50	49.87	7.5	6.75
3	50	50.87	8	7.42	13	60	59.97	10	9.69
4	60	60.83	8	7.02	14	65	64.47	10.5	10.14
5	65	65.75	10	6.69	15	50	50.17	10	8.92
6	50	50.57	9.5	6.18	16	60	59.87	11	8.94
7	25	26.69	9	7.99	17	20	20.57	12	10.3
8	50	51.31	9	8.12	18	25	25.57	11	9.88
9	60	61.63	9	7.77	19	50	50.37	10.5	9.82
10	65	66.25	11	9.82	20	65	65.47	10.5	9.3

Table 16 Revised locations of thermocouples in the fitting (Test 1)

Fitting left side					Fitting right side				
TC #	Axial position (mm)		Radial depth (mm)		TC #	Axial position (mm)		Radial depth (mm)	
	Fitted	Measured	Fitted	Measured		Fitted	Measured	Fitted	Measured
21	20	18.2	14	13.3	26	25	21.64	12	12.35
29*	50	N/A	0	N/A	24	50	49.99	0	0
22*	50	48.3	12	11.78	27*	50	51.39	10	10.55
23*	60	59.7	9	8.75	28*	65	64.63	8	8.05
25	60	60.05	11	11.13	30	65	64.18	6	5.68

** The thermocouple was missing, the depth of the hole was measured instead.*

Table 17 Revised locations of thermocouples in the pipe (Test 2)

Left pipe					Right pipe				
TC #	**Axial position (mm)**		**Radial depth (mm)**		**TC #**	**Axial position (mm)**		**Radial depth (mm)**	
	Fitted	Measured	Fitted	Measured		Fitted	Measured	Fitted	Measured
1	20	20.48	12	11.8	9	20	20.05	12.5	11.82
2	25	25.43	8	7.74	10	25	24.69	10	9.29
3	50	50.27	8	7.47	11	50	50.19	11.5	10.34
4	60	60.49	9	8.44	12	65	64.95	8.5	7.58
5	50	50.07	9	8.31	13	65	64.85	9.5	8.61
6	25	24.38	9	7.48	14	25	24.68	11	10.31
7	50	49.07	10	9.91	15	60	59.65	11	10.04
8	60	58.89	10	9.95	16	65	64.45	10.5	9.63

Table 18 Revised locations of thermocouples in the fitting (Test 2)

Fitting left side					**Fitting right side**				
TC #	**Axial position (mm)**		**Radial depth (mm)**		**TC #**	**Axial position (mm)**		**Radial depth (mm)**	
	Fitted	Measured	Fitted	Measured		Fitted	Measured	Fitted	Measured
17	20	20.79	14	13.07	24*	25	23.84	12	12.16
18	25	26.01	8	7.24	25*	50	34	0	N/A
19*	60	60.92	6	5.75	26*	65	63.57	7	6.99
20*	50	N/A	0	N/A	27*	25	N/A	10	N/A
21*	60	59.99	10	10.31	28	60	59.53	8	7.84
22*	50	48.83	12	12.2	29	65	64.27	9	6.5
23*	60	58.79	12	12.15	30*	65	65.62	11	11.2

** The thermocouple was missing, the depth of the hole was measured instead.*

4.3.3 Melting zone identification

Sample preparation

To facilitate extended analysis and to delineate the melting zone within the welded samples, a methodical cutting procedure was employed. This involved a sectioning of the welded specimens to reveal their internal composition. The samples underwent preparation and cutting using a bandsaw and a milling machine as shown in Figures 5-25, chosen for their ability to ensure precision and accuracy. This approach aimed to safeguard the structural integrity of the fusion zone while enabling an in-depth exploration of its internal characteristics. A set of different cut samples showing is shown in Figure 4-26.

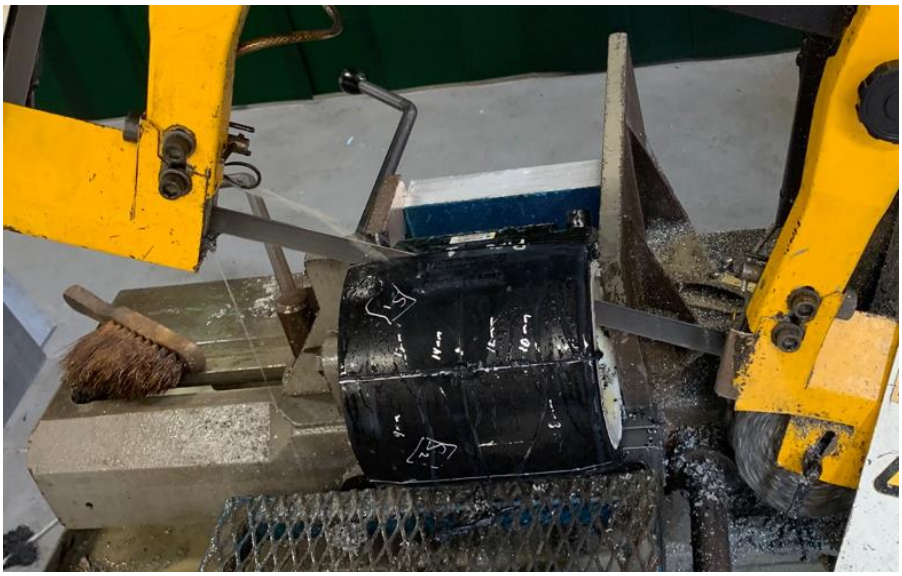

Figure 4-25 EF joint bandsaw cutting

Figure 4-26 EF joint cut samples

Observations from cut samples shown in Figure 4-27 revealed that in certain locations, the wires did not maintain contact with the pipe. This suggested the presence of an air gap between

the fitting and the pipe before welding. Conversely, in other regions as illustrated in Figure 4-28, the wires were in direct contact with the pipe, which likely indicated optimal contact between the fitting and the pipe prior to the welding process. This phenomena confirms the gap closure reported by Rosala et al. [18] where the polymer melt flows between the wires to the joint interface, while the wires stay in position. Additional observation from the cut samples shown in Figure 4-29 confirms the liner delamination that was observed earlier in the CT scan in Section 4.3.1.

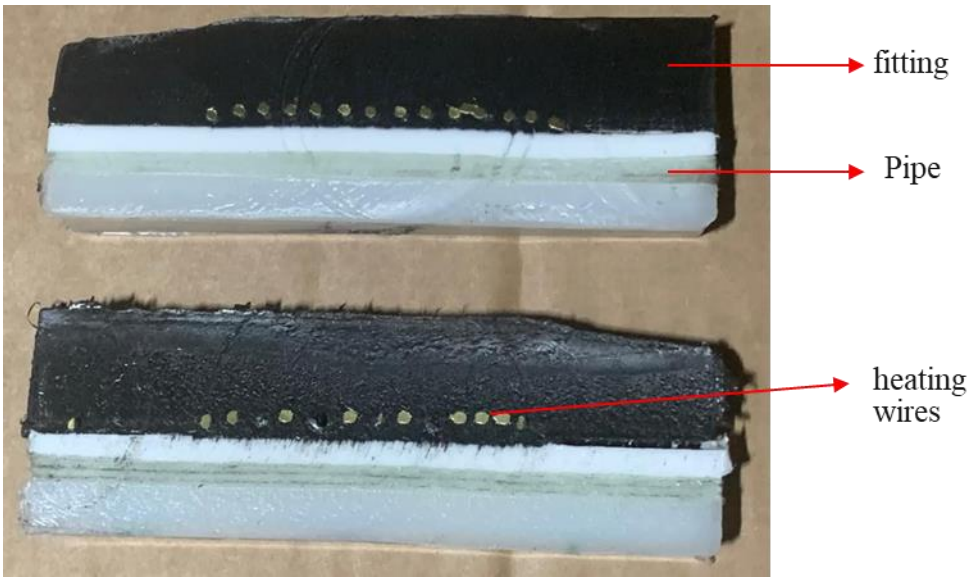

Figure 4-27 EF joint cut samples (non-contact wires) where potential air gap present between pipe and fitting

Figure 4-28 EF joint cut samples (contact wires) where potential full contact between pipe and fitting

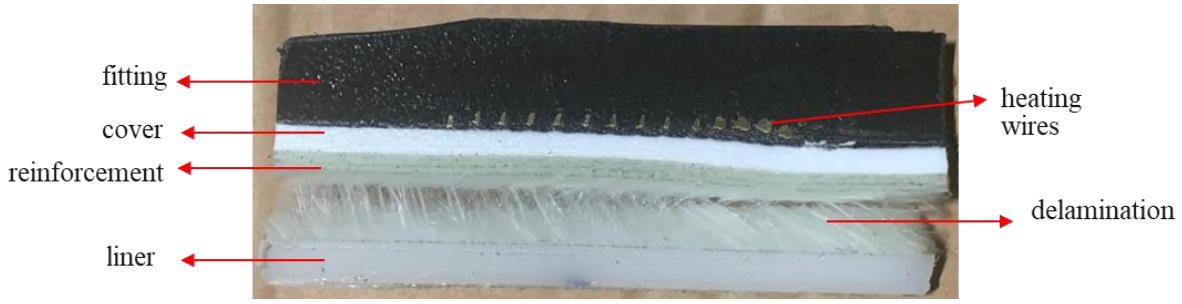

Figure 4-29 EF joint cut samples (delaminated liner

Afterward the surfaces that were cut were made smooth. Prepared for analysis using grinding and polishing techniques. This was done to remove any roughness or irregularities that could potentially impact the examination of the fusion zone. In order to obtain a surface, it was ideal to use epoxy resin to mount the samples. However, since the samples are too large for the automatic polisher, manual method was used.

Cold mounting

To securely embed the welded samples for analysis in this study epoxy resin in a cold mounting procedure was used. A mould made of material with a thickness of 3 mm was designed and created by utilizing a laser cutting machine. The acrylic pieces were then joined together to form a mould that perfectly fits the size and shape of the welded sample.

Mould Preparation

To ensure cleanliness and remove any dust or debris from the acrylic mould it underwent cleaning. The fit, between the mould pieces was checked to ensure a seal. Acrylic cement was applied along the edges of the mould pieces, which were then carefully joined together under pressure until a secure bond was achieved. Following manufacturers guidelines sufficient time was given for the acrylic cement to dry and cure completely.

Sample Placement:

In the process of sample placement, the welded sample was initially cleaned thoroughly to remove any impurities or loose particles. Then we carefully positioned it in the mould paying attention to cantering and alignment. Additionally, it was ensured that the sample was oriented appropriately for subsequent analysis.

Mixing Epoxy Resin:

A MetPrep (Ref 11 10 61) resin with a hardener (Ref 11 10 62) were used in this analysis . The epoxy and hardener were measured in a precise 4:1 ratio. In a clean container, both components were meticulously mixed, ensuring a homogeneous blend. Throughout the mixing, vigilant attention was given to prevent the introduction of air bubbles.

Pouring Epoxy Resin

During the process of pouring the epoxy resin, the mixed epoxy resin was methodically poured into the mould, ensuring the welded sample was fully submerged. Care was taken to guarantee that the resin filled the mould cavity without any spillage. Figure 4-30 shows the mould with the EF cut sample. The mould was then gently tapped to expel any entrapped air bubbles and to facilitate the resin's even distribution around the sample.

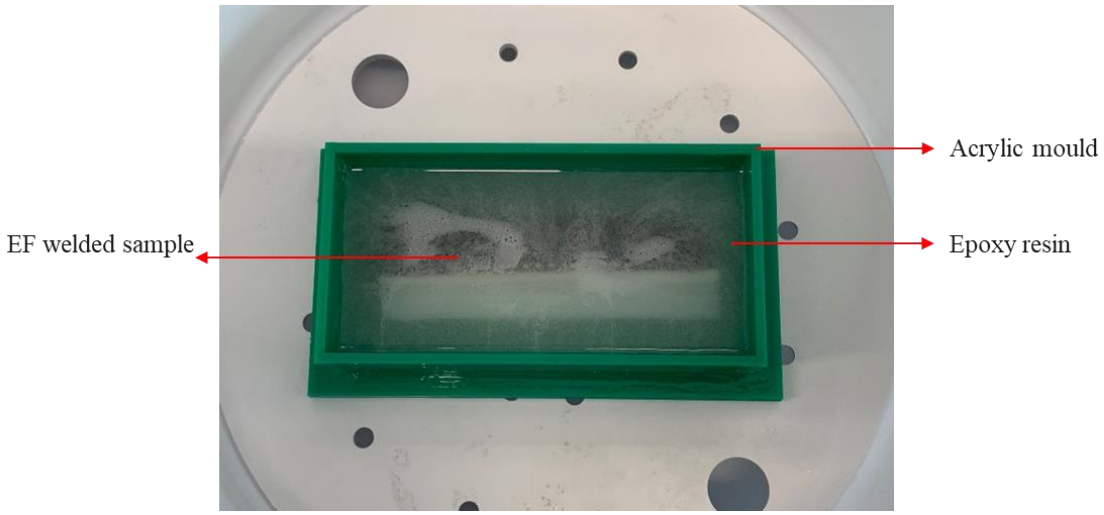

Figure 4-30 Cold mounted EF sample

Curing and Solidification:

In the curing and solidification stage, the mould embedded with the epoxy resin and sample was placed in a fume hood at room temperature for curing. The specific guidelines provided by the epoxy resin manufacturer were followed, which dictated a minimum curing time of 24 hours. This period was diligently observed to ensure the resin achieved full solidification and hardening.

Demoulding

During the demoulding phase, after ensuring the epoxy resin had fully cured, the mould pieces were meticulously removed to release the mounted sample. Utmost caution was exercised throughout this process to preclude any potential damage to the mounted sample.

The cold mounting procedure using epoxy resin enables embedding of the welded sample providing stability and support for subsequent analysis. The resulting mounted sample can undergo processing such as grinding and polishing which allows for exposure of the desired cross section, for other characterization techniques. This procedure ensures that the integrity of the welded sample is preserved while facilitating an investigation of its joint structure.

Manual Grinding

In carrying out manual grinding for EF cut samples as depicted in Figure 4-31. The process began with using a 10" backed grinding paper with a grit size of 120gt. To achieve the desired results a step-by-step approach was followed. Initially coarser grit sizes such as 320gt and 600gt were used, gradually progressing to finer grit sizes like 1200gt and finally concluding with a grinding paper.

Water was utilized as a lubricant throughout the process. It was applied carefully to avoid any slippage of the sample, which is similar to operating at high speeds. The speed of the grinding machine varied between 200rpm and 100rpm depending on the grit size.

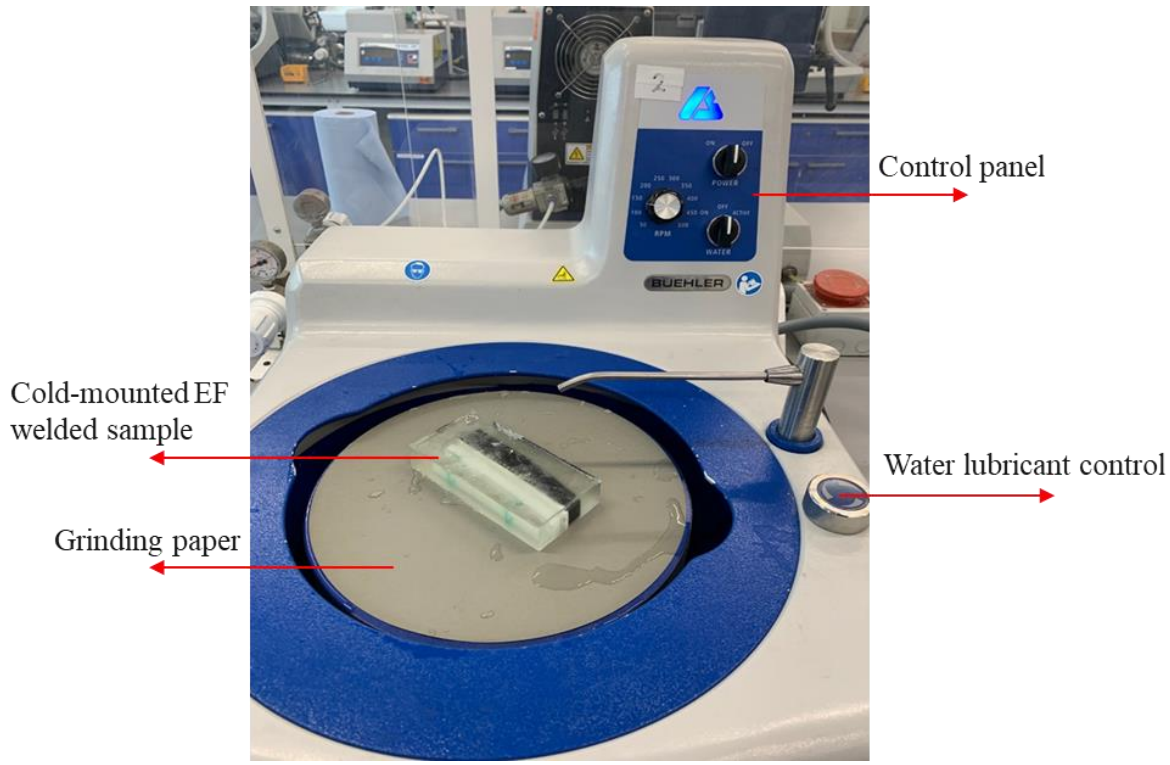

Figure 4-31 Manual grinding machine

Manual Polishing

A manual polishing technique was employed for composites. It involved following a sequence of steps. Initially a diamond paste with a particle size of 3 microns was applied on a cloth sourced from Metprep. An oil based lubricant facilitated the polishing process using this combination of paste and cloth. Then the setup transitioned to using a diamond paste with a particle size of 1 micron along with an alpha cloth from Metprep. The polishing continued consistently with the assistance of the oil based lubricant. Finally in the phase of polishing a diamond paste, with a particle size of 1/4 micron was used on Tournoire cloth from Metprep. Throughout all stages caution was taken to ensure that optimal results were achieved by using an amount of oil based lubricant without risking sample impregnation.

During the polishing process great care was taken not to compromise the integrity of the sample by using an extra amount of diamond paste. The speed of the polishing process was carefully regulated to ensure precision and prevent any loss of control. It was noted that high speeds could potentially compromise the quality of the polish. Additionally, it was important to maintain a motion of the sample in a direction opposite, to the polishing action as keeping it stationary for extended periods could result in comet like patterns appearing on the surface. The samples visual representation can be found in Figure 4-32.

Figure 4-32 Final polished sample

Fusion zone indication

To reveal the fusion zone clearly a procedure to detect the heat affected zone was followed [63]. A heavy-duty hot air gun was utilized, applying heat at a temperature of 400 ^{0}C on two welded cut samples. The heat caused the fusion zone to become more distinguishable, enhancing its visibility for detailed observation and analysis.

This comprehensive cutting, grinding, and polishing procedure, complemented by the application of heat using a heat gun, should facilitated the accurate identification and examination of the fusion zone in the welded samples. However, the type of heat gun used or the procedure applied did not actually showed the melting zone, rather, it melted the PE around the heating wires and this is clearly identified in Figures 4-33 and 4-34 for the sample with non-contact wires and with contact wires, respectively.

Figure 4-33 Heated sample (non-contact wires)

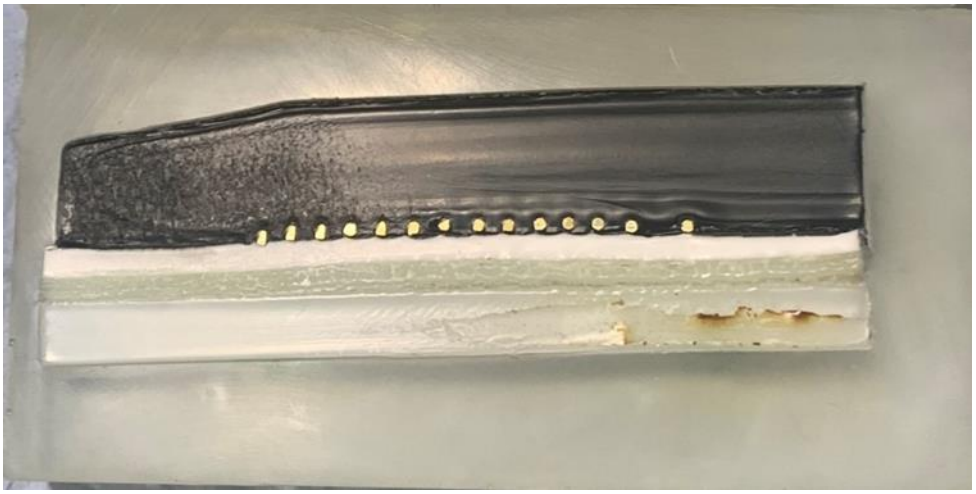

Figure 4-34 Heated sample (contact wires)

Results and Discussion

Upon completion of the cutting, grinding, and polishing procedures, the fusion zones in the two samples were examined. There was no clear indication of the melting zone with the method applied. However, other cut samples for example in Figure 4-35 at the extrusion welding of the two pipe halves clearly show the fusion zone length to be around 53 mm.

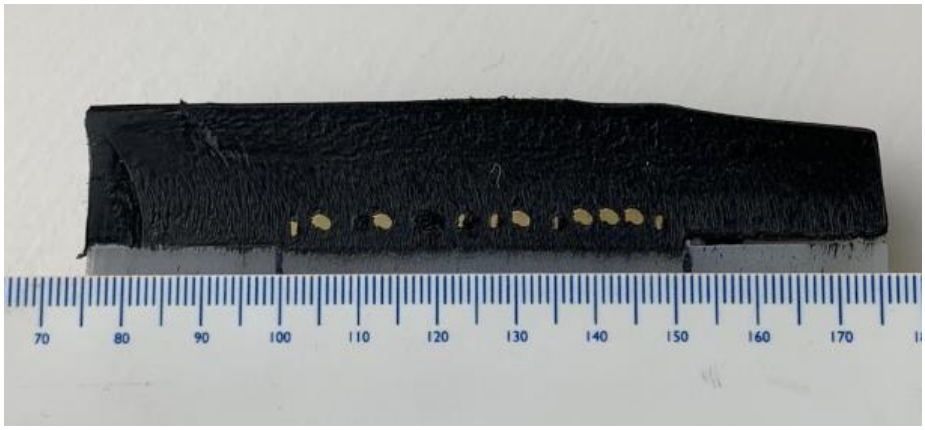

Figure 4-35 EF Cut sample at the extrusion welding

Another cut sample shown in Figure 4-36 confirmed this the same fusion length at different location taken in the EF joint with approximately 53 mm length.

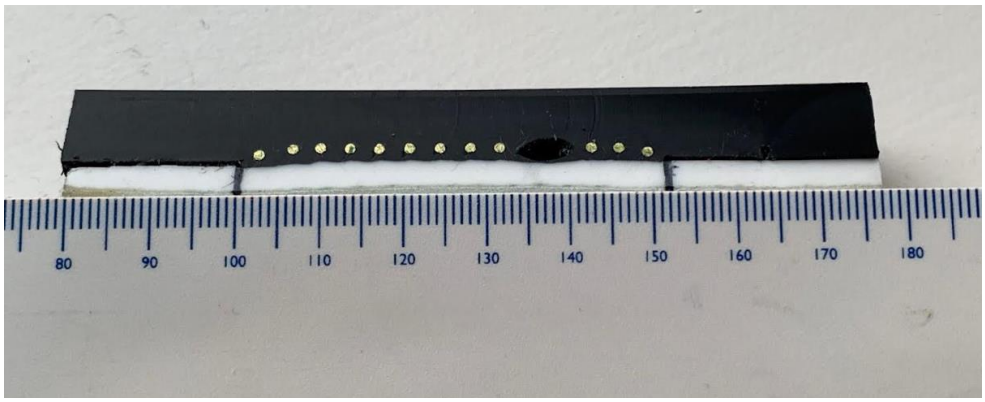

Figure 4-36 EFW cut sample

Moreover, the varied depths of the wires observed post-welding further indicated the possibility of non-uniform melting zones across different areas of the joint. To provide a more comprehensive understanding of the melting zone dynamics, an optimized simulation model will be employed in Chapter 6. This simulation is expected to offer a more in-depth insight into the melting zone characteristics, allowing for a comparative analysis with the observed samples.

4.4 Conclusion

This chapter have provided a detailed procedure for preparing TCP and fittings as well as the careful installation of thermocouples in preparation for the electrofusion test. A detailed description of the setup used for the physical tests was provided.

During both Test 1 and Test 2 it was interesting to note that the maximum temperature recorded by all thermocouples remained below 100°C. To further support these observations from the thermocouples a thermographic analysis showed that there was a distribution of temperature along a circular line of the fitting. This difference in temperature could possibly be due to gaps in regions leading to more heat dissipation compared to other areas. The subsequent CT scan examination provided alignment information between the pipe and fitting while also considering adjustments made to the thermocouple locations. It is worth mentioning that some thermocouples had moved before the CT scan. This movement has been considered when verifying the simulation model developed in Chapter 6.

The results from the CT scan also revealed areas where delamination had occurred within layers of the pipe. This topic will be further analysed in relation to upcoming simulation results discussed in Chapters 6 & 7. Additionally, procedure, for cutting, mounting, grinding and polishing larger welded samples manually was discussed.

Despite the efforts we were unable to definitively determine the melting zone in these samples. As a result, we will rely on measurements, from studies and the results of the simulations to gain further understanding of how the melting zone is characterized in this particular test.

`

Chapter 5

MODELLING HEAT TRANSFER DURING EFW OF TCP

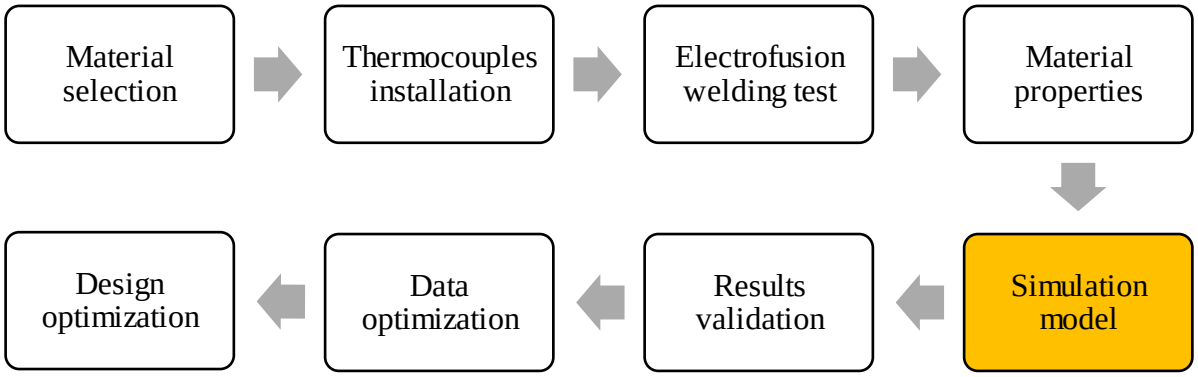

This chapter presents the Finite Element Analysis (FEA) of the physical electrofusion welding of TCP, utilizing material properties derived from measurements and adhering to the power input consistent with the physical welding test. The primary aim of this simulation is to comprehensively model the transient behaviour of heat transfer during the electrofusion welding process. This detailed modelling sets a solid foundation for the development of a tool/process, applicable to the welding of TCP and couplers with different configurations, materials, and operating conditions, and is intended to aid in the design of a new coupler for joining TCP. Throughout this description, the mathematical derivation is established, assumptions are clarified, and boundary conditions are defined. Additionally, this chapter offers a comprehensive examination of simulation results and engages in both model verification and a comparative analysis with experimental data.

5.1 Mathematical derivation

Modelling heat transfer during the electrofusion welding process of thermoplastic pipes involves solving the heat equation, which is a parabolic partial differential equation. This can be done by considering the three modes of heat transfer: conduction, convection, and radiation. Assuming a 2D axisymmetric model of the EF joint, the heat equation takes the following form [64]:

$$\frac{\partial T}{\partial t} = \alpha * \left(\frac{1}{r}\frac{\partial}{\partial r}\left(r\frac{\partial T}{\partial r}\right) + \frac{\partial^2 T}{\partial z^2}\right) + \frac{Q}{\rho C_p} \tag{5.1}$$

where,

T is the temperature

t is the time

α is the thermal diffusivity, which *is k/(ρCp), k* being the thermal conductivity, ρ the density, and *Cp* the heat capacity at constant pressure

r, z are the radial and axial coordinates, respectively

Q is the heat generation in wires per unit volume

Incorporating temperature-dependent properties (*k, Cp, ρ*), requires an extension of the earlier model. The heat equation changes slightly due to temperature-dependent properties to:

$$\rho(T)C_p(T)\frac{\partial T}{dt} = k(T)\left[\frac{\partial^2 T}{\partial r^2} + \frac{1}{r}\frac{\partial T}{\partial r}\right] \tag{5.2}$$

where *ρ(T), Cp(T*), and *k(T)* are temperature-dependent density, specific heat capacity, and thermal conductivity, respectively.

During the fusion process, the polymer undergoes phase change, thus, it is required to account for the latent heat, *L(T*), absorbed or released [66].

$$\frac{\partial T}{\partial t} = \frac{k(T)}{\rho(T)C_p(T)} * \left(\frac{1}{r}\frac{\partial}{\partial r}\left(r\frac{\partial T}{\partial r}\right) + \frac{\partial^2 T}{\partial z^2}\right) + \frac{Q}{\rho(T)C_p(T)} + L(T)\frac{\partial f}{\partial t} \tag{5.3}$$

where,

f is the phase fraction changing from solid to liquid.

∂f/∂t can be calculated using an appropriate phase-change model.

The temperature-dependent terms make it more challenging to solve these equations, and numerical methods are required. It is worth noting that material properties like density, specific heat capacity, thermal conductivity, and the heat source are often given in tabular form, requiring the use of interpolation during the simulation.

It is possible to model phase changes by using temperature-dependent specific heat capacity. This approach is often used in a simplified method known as the "apparent heat capacity method" [67].

The apparent heat capacity method, also known as the "effective heat capacity method," is a numerical technique used to model phase change problems, especially solid-liquid phase changes like melting and solidification. Instead of tracking the phase change interface directly, the method modifies the specific heat capacity to account for the latent heat of phase change.

The principle behind the apparent heat capacity method is to smear the phase change over a temperature range rather than a fixed temperature. This approach simplifies the equations and stabilizes the numerical computations. In this method, the heat capacity *Cp(T)* is modified such that it includes the effect of the latent heat of fusion.
When the temperature range reaches the melting point of the material, the heat capacity is increased dramatically to account for the latent heat of fusion. Mathematically, the heat capacity can be written as:

$$Cp(T) = Cp_{solid}(T) \qquad for\ T < T_{melt\_start} \tag{5.4}$$

$$Cp(T) = Cp_{solid}(T) + L_{fusion}/(T_{melt\_end} - T_{melt\_start}) \qquad for\ T_{melt\_start} \leq T \leq T_{melt\_end} \tag{5.5}$$

$$Cp(T) = Cp_{liquid}(T) \qquad for\ T > T_{melt\_end} \tag{5.6}$$

where,
L_{fusion} is the latent heat of fusion.
T_{melt_start} and T_{melt_end} are the temperatures at which melting starts and ends, respectively
$Cp_{solid}(T)$ and $Cp_{liquid}(T)$ are the heat capacities of the solid and liquid phases, respectively

Since the temperature dependent specific heat capacity was measured as in Section 3.2.3, the approximation of latent heat of fusion is already incorporated in the data and the final heat equation would be:

$$\rho(T)Cp(T)\frac{\partial T}{\partial t} = k(T)\left(\frac{\partial^2 T}{\partial z^2} + \frac{1}{r}\frac{\partial T}{\partial r} + \frac{\partial^2 T}{\partial r^2}\right) + \mathrm{Q} \tag{5.7}$$

This set of equations is generally difficult to solve analytically and is often solved numerically using methods such as the finite difference method, finite element method, The solution of this equation will provide the temperature distribution within the system at any given time. The temperature distribution will be compared with those obtained in Section 4.2.2 and with the best practices requirements from Section 2.3.2.

5.2 Electrofusion welding assumptions

The following assumptions based on literature methods [39] were considered when developing the electrofusion welding process for TCP and implemented in the FEA model.

- Axisymmetric 2D model
- Perfect contact between the pipe and electrofusion fitting (no air gap)
- Heat transfer is dominant; mechanical effects are ignored
- Temperature-dependent properties (density, heat capacity, thermal conductivity)
- Phase change modelled using the "apparent heat capacity" method
- Convective cooling on the outer surface and pipe inner surface *($h=10\ W/m^2K$)*
- Heat source only in the electrofusion fitting where the heating wire is located
- Initial temperature equal to the ambient temperature *($T_{env}=21.6\ ^0C$), this is equivalent to the temperature at which the test was conducted.*

5.3 Model setup

In this study, COMSOL Multiphysics version 6.0 was utilized to solve the EFW problem. COMSOL Multiphysics is a versatile simulation software known for its proficiency in addressing diverse physics-based problems through finite element analysis (FEA). This software is particularly advantageous for studying electrofusion welding due to its capability to model multiple interconnected physical phenomena accurately. It is well-suited for representing complex interactions like electrical heating and heat transfer inherent in electrofusion welding processes.

COMSOL provides an extensive library and customization options for material properties and boundary conditions, enabling precise modelling of the welding process's various materials and conditions. Its advanced numerical techniques ensure accurate and reliable solutions to the complex, nonlinear problems presented by electrofusion welding.

The software capability for parametric studies and post-processing is also invaluable, allowing for in-depth exploration of the impact of different welding parameters on the final outcomes. Thus, COMSOL Multiphysics stands out as a suitable choice for conducting sophisticated, yet clear and comprehensive, studies in electrofusion welding heat transfer modelling.

The electrofusion joint is symmetric at both ends, so only half of the joint was analysed in the model to speed up the computational time, as shown in Figure 6.1. The basic model for EFW of TCP can be divided into three bodies: fitting, heating wires and pipe.

The wires are made from copper, the fitting is made from PE100, and the pipe materials are as specified in section 3.1.

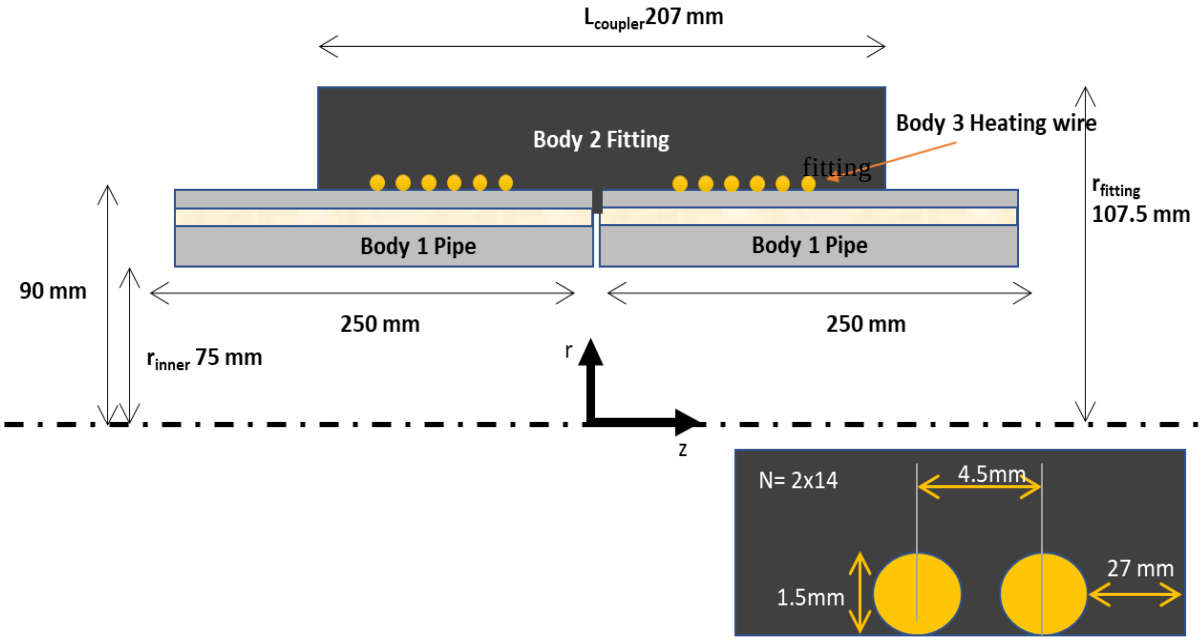

Figure 5-1 Schematic of the modelled joint

5.4 Initial and boundary conditions

Initial condition

$$T(r, z, 0) = T_{initial} \qquad \text{for all r, z at time } t=0 \qquad (5.8)$$

Boundary conditions

At the outer surface of the fitting ($r = r_{fitting}$), convective heat loss occurs to the environment:

$$-k\,\partial T/\partial r = h(T - T_{env}) \qquad (5.9)$$

At the inner surface of the pipe ($r = r_{inner}$), convective heat loss occurs to the environment:

$$-k\,\partial T/\partial r = h(T - T_{env}) \qquad (5.10)$$

where h is the convective heat transfer coefficient and T_{env} is the environment temperature.

At the interface between the two pipes and the electrofusion fitting ($r = r_{inner}$), continuity of heat flux is assumed:

$$k_{pipe}\,\partial T_{pipe}/\partial r = k_{fitting}\partial T_{fitting}/\partial r \qquad (5.11)$$

where the subscript "pipe" refers to pipe properties and "fitting" refers to the fitting properties.

At each interface between two consecutive layers, the heat flux and temperature should be continuous:

$$k_{cover}\,\partial T_{cover}/\partial r = k_{laminate}\partial T_{laminate}/\partial r \qquad (5.12)$$

$$k_{laminate}\partial T_{laminate}/\partial r = k_{liner}\,\partial T_{liner}/\partial r \quad (5.13)$$

At the left and right boundaries ($z = \pm L_{pipe}/2$), the heat flux can be assumed to be zero:

$$\partial T/\partial z = 0 \quad (5.14)$$

The heat source term Q is nonzero only within the electrofusion fitting heating wires is located, and zero elsewhere.

5.5 Model mesh and solver settings

The meshing strategy employed for this study involved the utilization of linear triangular elements with an automatic (physics-controlled) adaptive fine meshing approach. This approach ensured that the mesh adaptation was guided by the underlying physics, particularly focusing on areas surrounding the heating wires where intricate thermal behaviour occurs. The mesh generator segments domains into triangular mesh elements to approximate the original, potentially curved, geometries. The sides of these triangles are known as mesh edges, and their corners are identified as mesh vertices. Boundaries within the geometry are discretized, forming edge elements, which serve as approximated mesh edges, while vertex elements denote the geometry vertices. The meshing statistics for the developed model were as follows:

- **Mesh vertices:** 35007
- **Element types:** triangles: 69313, edge elements: 3106, vertex element: 186
- **Average element quality:** 0.6922, and it represents the average quality of the mesh element with a scalar value between 0 and 1
- **Element area ratio:** 4.941e-5, and it represents the ratio between the areas of the largest and smallest element.
- **Mesh area:** 0.007399 m², and it represents the total area of the mesh.

The chosen linear triangular elements provided a balanced compromise between computational efficiency and accuracy. The adaptive fine meshing strategy ensured higher element density in regions of interest, such as the vicinity of heating wires labelled in Figure 6.2 and 6.3, where precise temperature predictions are critical. This approach allowed the capture of intricate temperature variations accurately while optimizing computational resources. The mesh quality statistics demonstrate the overall quality and distribution of the elements within the mesh, reflecting the mesh suitability for accurately simulating the complex heat transfer behaviour during electrofusion welding of TCP.

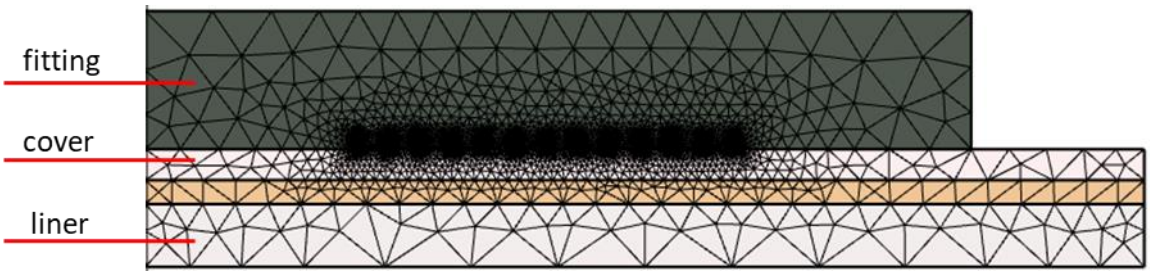

Figure 5-2 Mesh for the modelled joint

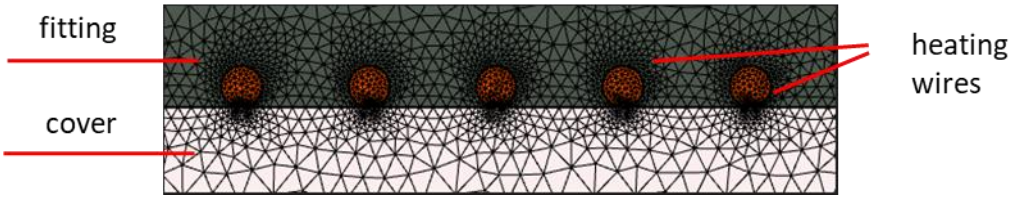

Figure 5-3 Mesh around the heating wires

To accurately model the transient behaviour of heat transfer during electrofusion welding, a time-dependent solver is chosen, with the backward differentiation formula (BDF) method being particularly well-suited for stiff partial differential equations (PDEs) like the heat equation. The study is configured as a transient analysis, allowing the simulation to capture dynamic temperature changes over time. The simulation is conducted with a time step of 1 second, ensuring that the temporal evolution of temperature is adequately represented.

In total, the solver was responsible for handling 164,940 degrees of freedom, generally refers to the number of independent variables in the model, which can indeed be associated with the number of all internal and boundary nodes in the mesh. This included 91,695 internal degrees of freedom, assigned to only the internal nodes of the mesh, excluding the boundary nodes. This configuration enables the simulation to effectively model the intricate thermal behaviour that occurs during the electrofusion welding process for TCP.

5.6 Simulation results

The electrofusion welding problem was solved by finite element modelling using COMSOL Multiphysics software with a Heat Transfer Module. Using the power input from Section 4.2.1, the simulation profile taken in the centre of the heating zone for various points in the electrofusion joint, is shown in Figure 5-4.

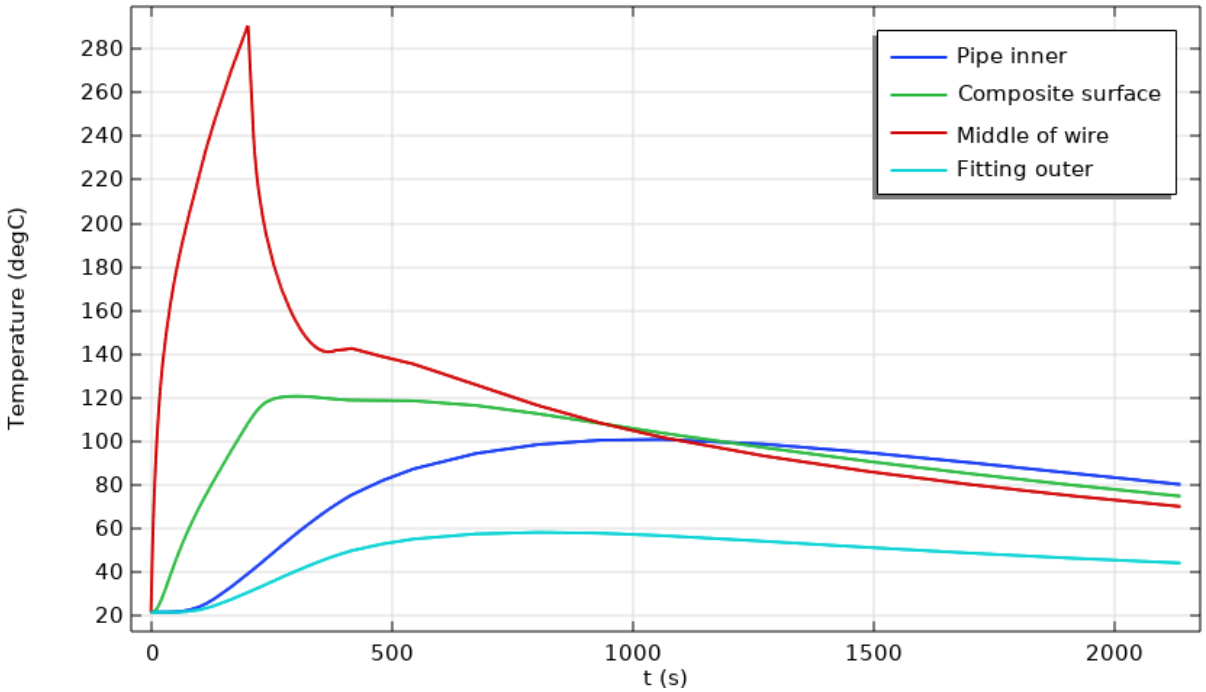

Figure 5-4 Simulated temperature history at selected probe locations

The temperature exhibited distinct peaks across various components: it reached around 300 °C in the heating wires, peaked first at 121 °C in the composite laminate (reinforcement layer), followed by 60 °C on the fitting external surface, and lastly peaked at 102 °C on the pipe inner surface.

At the end of the heating duration (203 seconds) and the cooling period (15 minutes), the temperature across the thickness of the joint—from the pipe's inner surface to the fitting's outer surface—was calculated. The temperature variation throughout the joint's thickness is depicted in Figure 5-5.

The non-linear cooling behaviour of the wire temperature during the cooling stage is primarily due to the interplay between different material properties and the effect of latent heat. The surrounding PE material undergoes solidification which involves the release of latent heat. This phase change occurs at a constant temperature causing a plateau in the temperature profile. As the PE material transitions to the solid phase, the release of latent heat affects the temperature distribution and cooling rate in the wires.

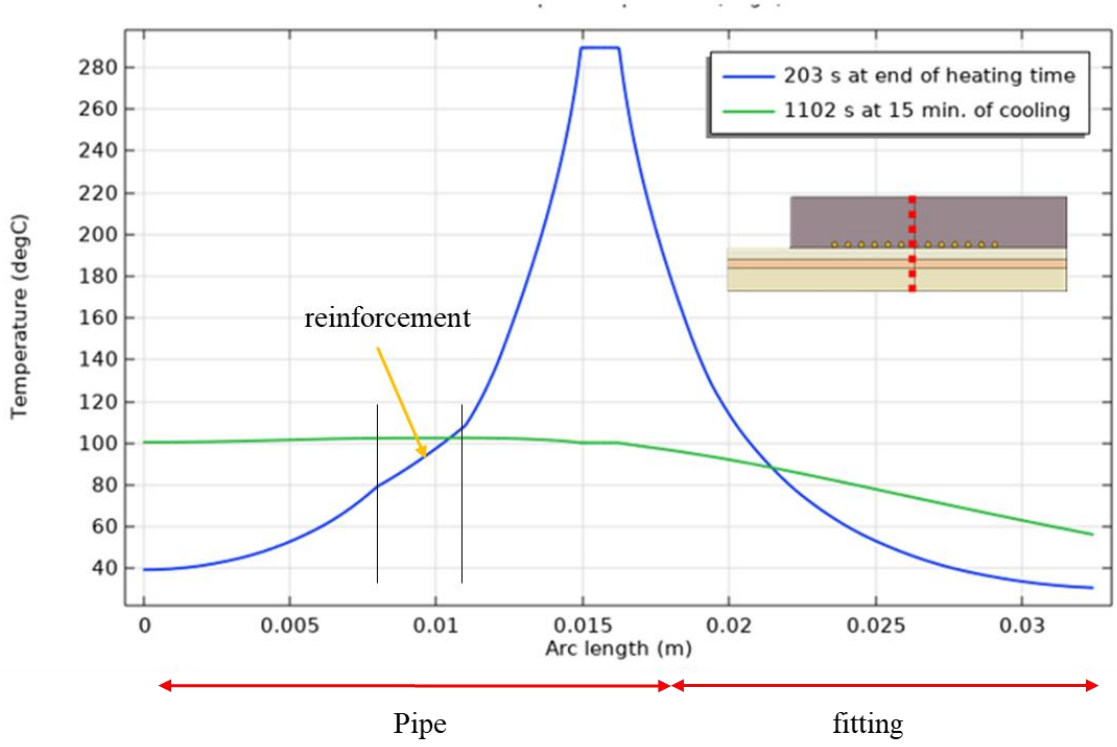

Figure 5-5 Simulated cross-thickness joint temperature at selected times

The simulated data in Figure 5-5 shows the behaviour of temperature across the EF joint, the temperature at the at the end of heating peaked at the welding interface at 290 ^{0}C, it is also noticed the different temperature curves at the heating cycle when comparing the pipe reinforcement with the HDPE liner and fitting indicating the different thermal properties of these layers. At the end of the cooling period, a stable temperature was reached in the pipe, however, a reduction in temperature in the fitting side was observed, which can be justified by the heat loss due convection at the fitting side.Model verification and experimental comparison

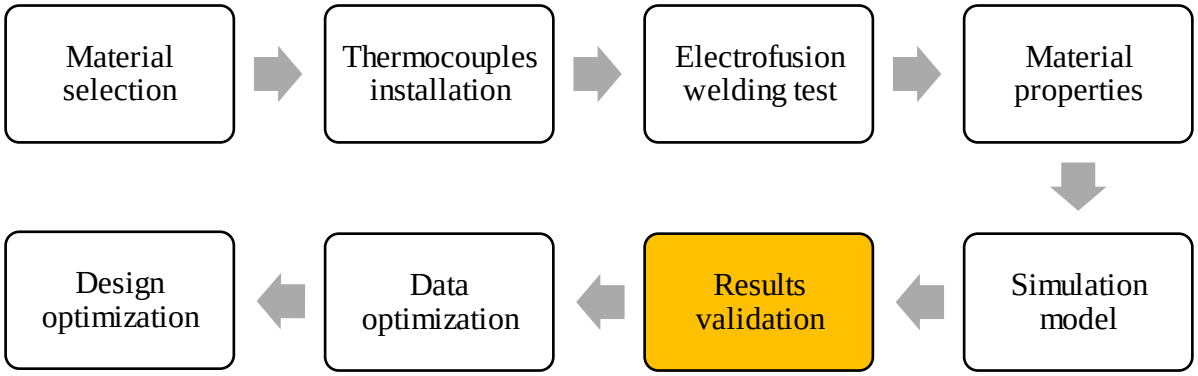

5.6.1 Visual comparison

An essential step in validating the developed heat transfer model for electrofusion welding of TCP involves a comprehensive visual comparison between simulated and experimental temperature profiles. This comparative analysis provides a robust platform to assess the accuracy and reliability of the simulation results against the empirical data obtained from the experimental testing.

This comparison is pivotal in determining the model's fidelity in replicating the actual thermal behaviour during the electrofusion welding process. Any deviations between the simulated and experimental profiles are meticulously scrutinized and analysed. Factors contributing to disparities, such as variations in material properties, boundary conditions, model assumptions or welding parameters, are carefully assessed to ascertain the source of differences.

The visual comparison involves overlaying the simulated and experimental temperature profiles on a single graph as shown in Figures 5-6 to 5-10, facilitating a direct visual assessment of their concurrence. The model diagram included in each figure illustrates the location where the comparison was made. If a high level of agreement is observed between the profiles, it enhances the confidence in the developed heat transfer model and its ability to predict the thermal dynamics during electrofusion welding accurately.

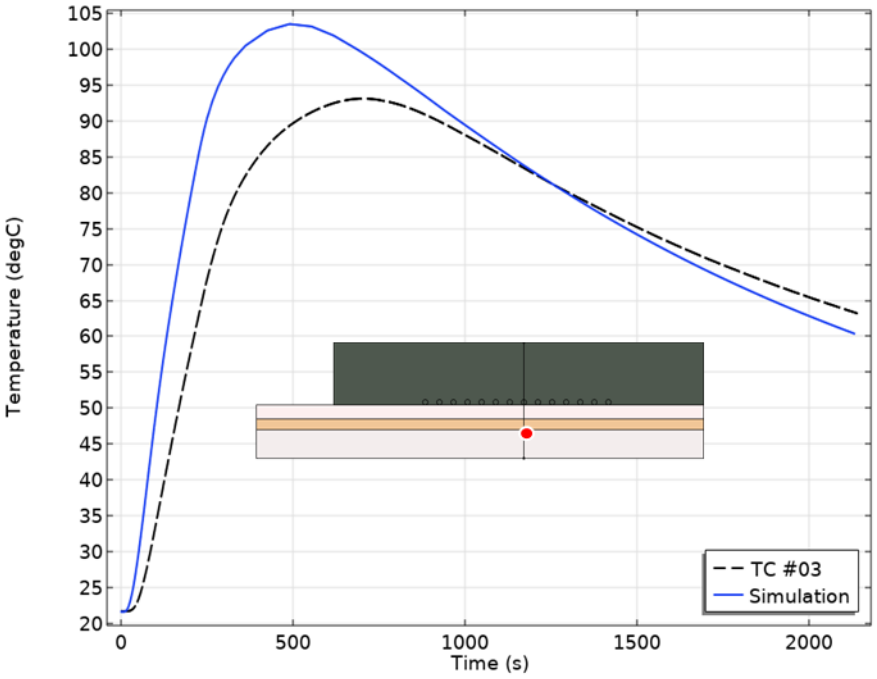

Figure 5-6 Comparison of simulated and measured temperatures at TC#03

The simulation data presented in Figure 5-6 indicates variability during the heating phase. Compared to the experimental measurements, the model demonstrates a pronounced heat dispersion. Several elements could account for these accelerated heating rates, including the material's thermal attributes. Heat loss from thermal contact resistance at the welding juncture or diminished heat production efficacy from the heating wires might also play a part. In the cooling stage, a discernible disparity exists between the two data sets, with the simulated values reflecting a steeper temperature decline than the empirical measurements. This discrepancy can likely be attributed to convective heat loss.

This pattern is consistently observed at various points along the pipe at locations TC#13 and TC#19, as illustrated in Figures 5-7 and 5-8, which reinforces the earlier discussed hypotheses.

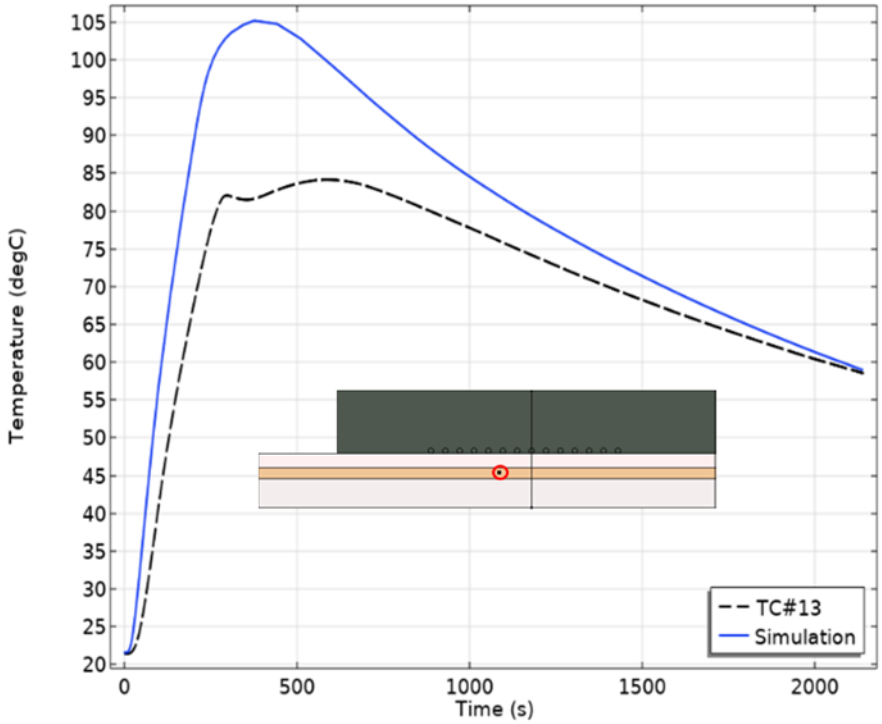

Figure 5-7 Comparison of simulated and measured temperatures at TC#13

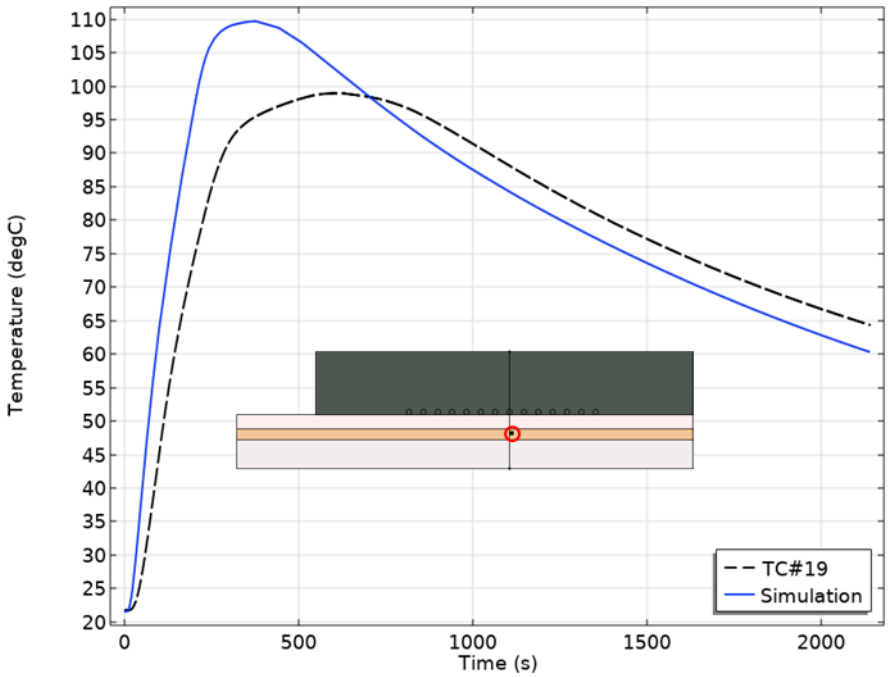

Figure 5-8 Comparison of simulated and measured temperatures at TC#19

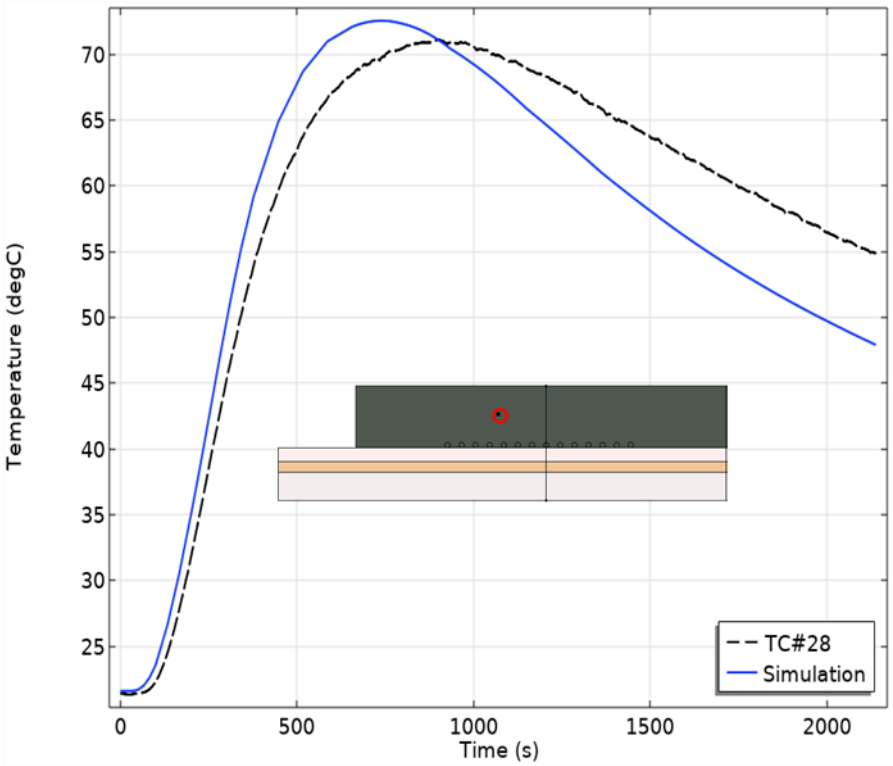

Figure 5-9 Comparison of simulated and measured temperatures at TC#28

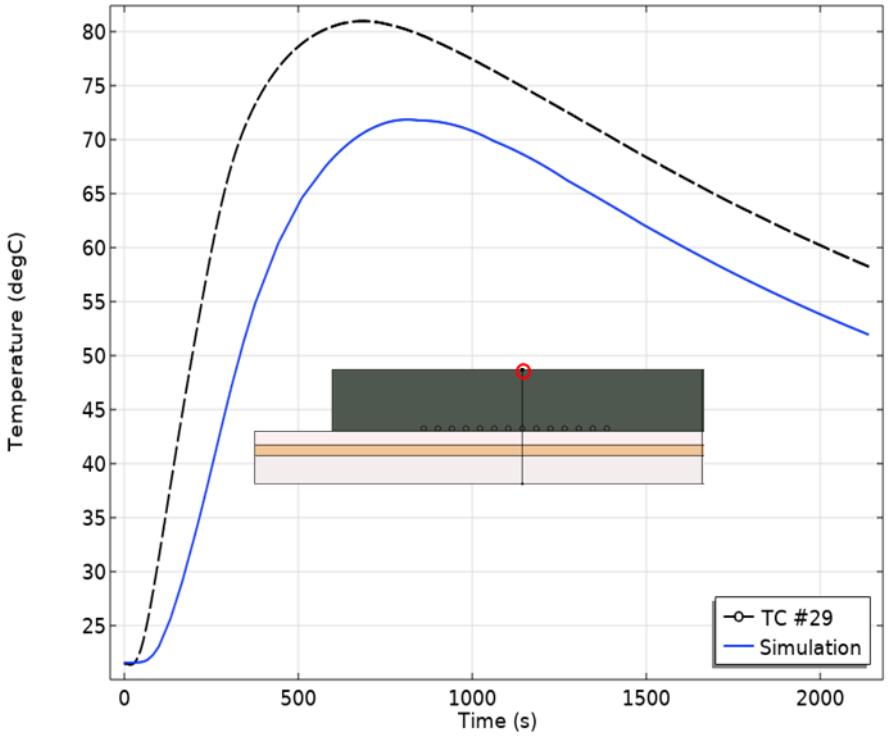

Figure 5-10 Comparison of simulated and measured temperatures at TC#29

This comparison process underscores the iterative nature of research and underscores the importance of refining the simulation model based on experimental insights. It also serves as a tangible demonstration of the successful integration of theoretical modelling and empirical

experimentation, driving advancements in the understanding and optimization of electrofusion welding processes for a TCP system. The following steps will further analyze both data in depth by looking at statistical analysis and testing the hypothesis by looking at the influence of multiple parameters on the heat transfer model. Detailed comparison of all 30 thermocouples in both tests is consdered in Chapter 7.

5.6.2 Statistical analysis

Comprehensive comparison between the temperatures obtained from numerical modelling and experimental measurements were presented through rigorous statistical analysis. The goal was to assess the accuracy and reliability of the simulation model in replicating real-world conditions. To quantify the agreement (or otherwise) between the two datasets, the Root Mean Square Error (RMSE) was employed as a robust metric. The following procedure outlines the steps undertaken for defining and calculating the RMSE for the 30 thermocouples within Test 1, while Test 2 data will be used later on Chapter 7 to validate the optimized model obtained from Test 1.

Data Preparation and Alignment

To ensure an accurate comparison, the simulated and experimental temperature datasets were meticulously aligned. Given that these datasets originated from different starting points and time steps, interpolation techniques were employed to synchronize them onto a common time grid. This alignment procedure was executed individually for each of the 30 thermocouples. It was noticed from this process that the experimental measured data was leading by 6 seconds. This is the time between the start of temperature recording and the start of the physical test.

RMSE Calculation

For each Thermocouple (i) at time t, the root mean square error can be calculated through the following formula:

$$RMSE(i) = \sqrt{\frac{1}{N_i}\sum\left(T_{\exp(i,t)} - T_{sim(i,t)}\right)^2} \tag{6.15}$$

where,

$Texp_{i,t}$ is the observed (measured) temperature for thermocouple i at time t.

$Tsim_{i,t}$ is the predicted (simulated) temperature for thermocouple i at time t.

The result of RMSE values for Test 1, encompassing all 30 thermocouples, have been illustrated in Figure 5-11.

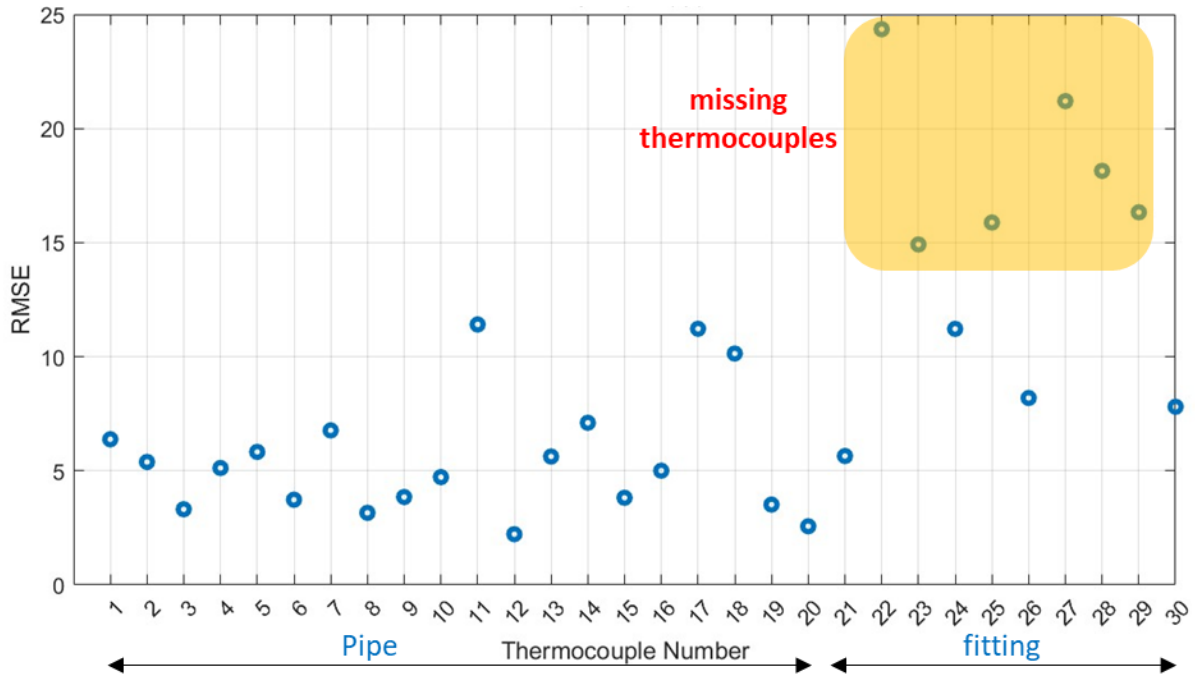

Figure 5-11 RMSE values for all thermocouples of Test 1

The RMSE values vary across a range of values from 2.22 ^{0}C to 24.35 ^{0}C. This indicates a significant variation in the agreement between the simulated and experimental temperature readings for the different thermocouples. Lower RMSE values, such as 2.22 ^{0}C, indicate a higher level of accuracy and precision in the agreement between the simulated and experimental data. On the other hand, higher RMSE values, such as 24.35 ^{0}C, indicate a lower level of agreement and indicative of potential issues with simulation accuracy or experimental measurements. The highlighted RMSE values represent the missing or fallen thermocouples during CT scan as indicated in Sections 4.3.1 & 4.3.2. These were all located in the coupler and had higher RMSE. This suggests that small variations in the thermocouple placement as discussed earlier in Sections 4.3.1 & 4.3.2 may have a large effect on temperature, especially if they were close to the heating source, thus a lack of agreement between the simulation and measured data was noticed.

Thermocouples with lower RMSE values, indicating a better agreement between the simulated and experimental data, and can be considered for optimization processes. These locations have a higher level of accuracy and are more reliable in the refinement process of the simulation model.

Overall RMSE

The individual thermocouple RMSE values were averaged, generating an aggregate RMSE for Test 1. This overall RMSE value signified the combined agreement between the simulated and experimental data across all thermocouples. The overall RMSE value is approximately 7.69 ^{0}C. This is still not considered bad as it is less than 10% of the lowest maximum temperature reading during the test, however, this can be improved by proper process parameter optimization described in Chapter 7.

The RMSE analysis played a pivotal role in optimization considerations. Thermocouples with lower RMSE values, signifying accurate simulations, emerged as prime candidates for optimization processes. These thermocouples offered dependable data for refining the model's parameters and enhancing its predictive capabilities.

Throughout this research, the procedure was iteratively revisited through an optimization process acted in Chapter 7. Any modifications to the simulation model or adjustments to simulation parameters were systematically evaluated by measuring their impact on the RMSE values. This iterative approach enabled the gradual minimization of RMSE, thereby enhancing the alignment between simulated and experimental data. This rigorous analysis shed light on the strengths and weaknesses of the simulation model and offered valuable insights for further model refinement and optimization.

5.6.3 Sensitivity analysis

The sensitivity analysis serves as a crucial part of understanding how different parameters influence heat transfer during the electrofusion welding process. For the purpose of the developed model, the considered parameters were the internal and external convective heat transfer coefficients, heat source calibration, and the thermal contact resistance between the pipe and the fitting. It was assumed that the power input and material properties are constant for this analysis.

Internal and External Convective Heat Transfer Coefficients

Convective heat transfer plays a significant role in the electrofusion welding process. Variations in the internal and external convective heat transfer coefficients can significantly impact the heat transfer behaviour and thus the welding quality. A lower heat transfer coefficient implies a slower rate of heat dissipation, which could result in higher temperatures and potentially affect the integrity of the joint.

On the other hand, a high heat transfer coefficient might lead to rapid cooling, affecting the fusion process. Sensitivity analysis of these parameters would thus help in comprehending their impact and identifying an optimal range for the convective heat transfer coefficients.

While a convective heat transfer coefficient of 10 W/m²K was initially assumed, for this analysis, values between 8 and 15 W/m²K were selected to define the boundaries of this value, in accordance with those referenced in the literature [19,43].

Thermocouple TC#19, placed on the fitting's external surface, serves as a key indicator of the influence of different convective heat transfer coefficients on the simulated temperature profile. In contrast, TC#29, situated within the composite reinforcement, provides insights into the combined effects of external and internal convective cooling. Moreover, both of these strategically chosen locations will play a key role in conducting sensitivity analyses, enabling a comprehensive exploration of the impact of various parameters on the electrofusion welding process.

The observation from Figure 5-12 elucidates that altering the external convective heat transfer coefficient (h_o) at the centre of the external fitting surface induces a minimal effect on the heating side relative to its noticeable impact on the peak temperature and cooling steepness. This influence is manifested by an elevation in peak temperature and a reduction in cooling rates as the value of h_o reduces.

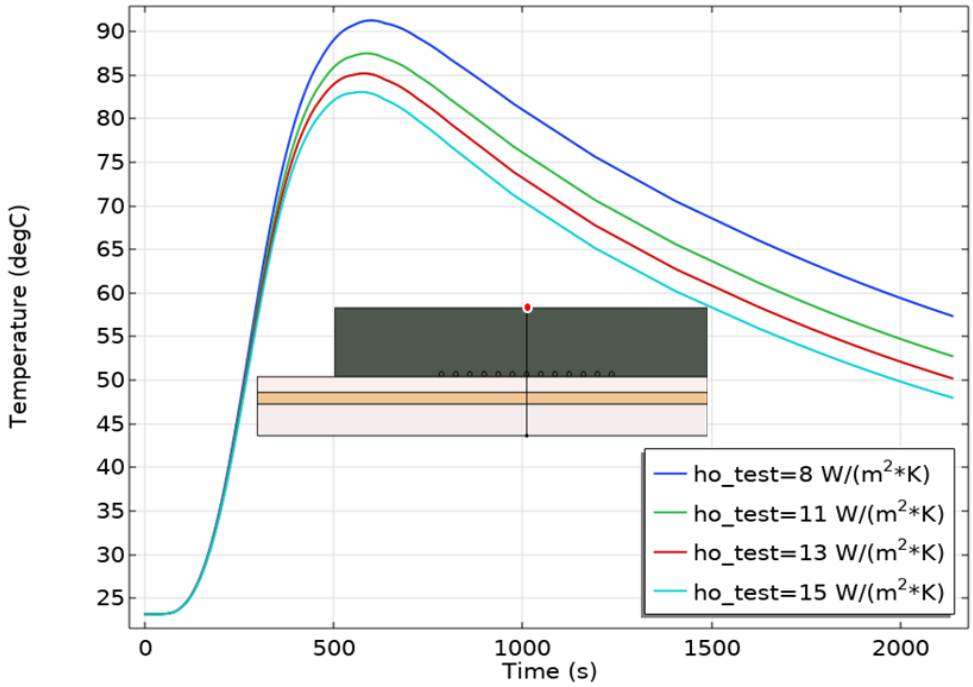

Figure 5-12 Sensitivity analysis of h_o at TC#29

As depicted in Figure 5-13, altering the external convective heat transfer coefficient yields no notable impact on the heating side or the peak temperature in the laminate.

However, a minor change is discernible, starting approximately at the mid-point of the cooling phase, indicating a slightly accelerated cooling rate concomitant with a reduction in the external convective heat transfer coefficient.

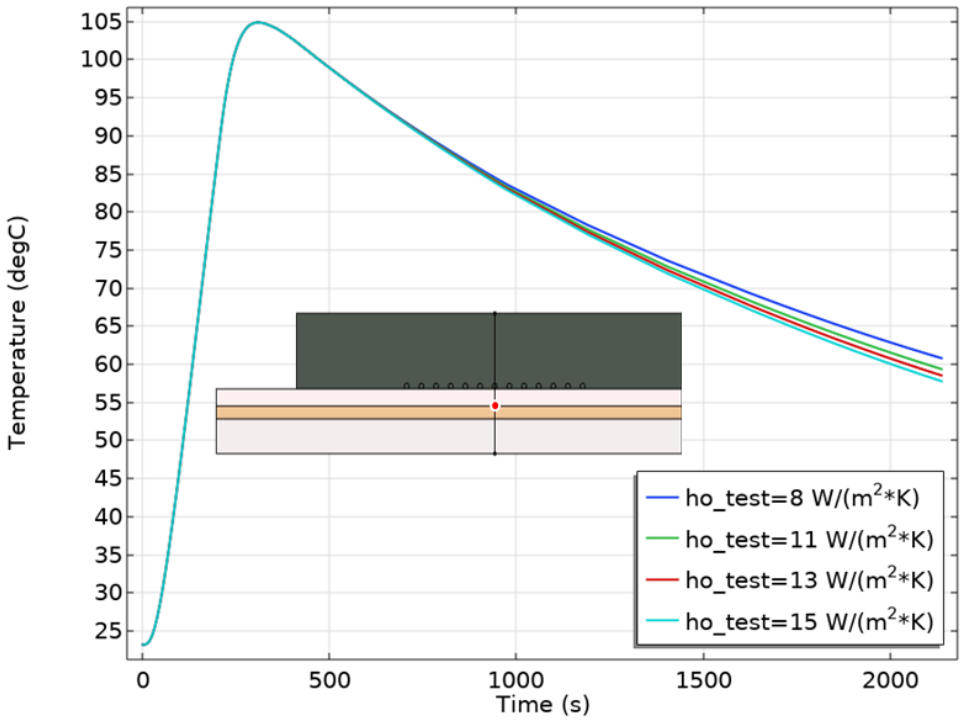

Figure 5-13 Sensitivity analysis of h_0 at TC#19

Additionally, as shown in Figure 5-14, changing the internal convective heat transfer coefficient on the laminate did lead to earlier start and slightly faster cooling rates compared to changing the external convective heat transfer coefficient.

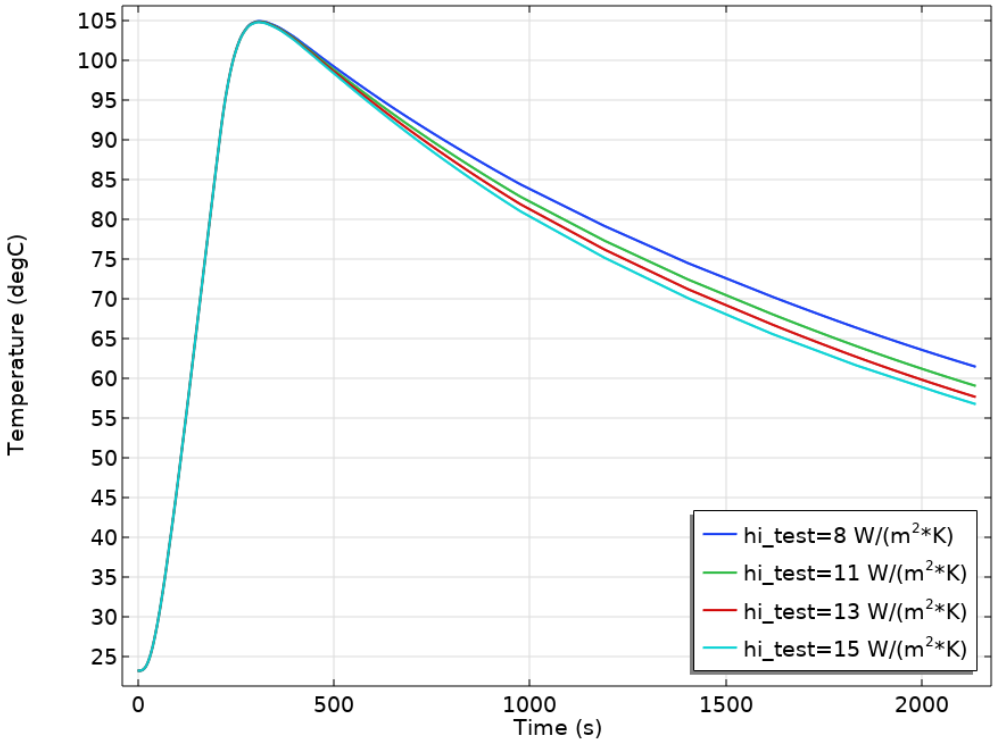

Figure 5-14 Sensitivity analysis of h_i at TC#19

Heat Source Calibration

Heat source calibration, which represents the level of heat generated during the welding process, plays a vital role in heat transfer and overall welding quality. Under-calibration could lead to insufficient heat, affecting the joint quality due to inadequate fusion. On the other hand, over-calibration could cause excessive heat, potentially damaging the material and compromising the joint integrity. Therefore, understanding the sensitivity of the welding process to this parameter would help in determining the optimal calibration for the heat source. To account for the heat loss in the heat source it is assumed that:

$$Q_{generated} = \eta * Q_{input} \tag{6.18}$$

where η *is* the efficiency of the heat source and represents the percentage of heat loss during the welding process.

In this analysis, varying values were assumed, ranging from 80% to 95% efficiency, to observe their impact on the resultant temperature profiles at the specifically selected points, TC#29 & TC#19. The outcomes presented in Figures 5-15 and 5-16, show that there is a reduction in heat transfer to those locations corresponding with the decrease in efficiency.

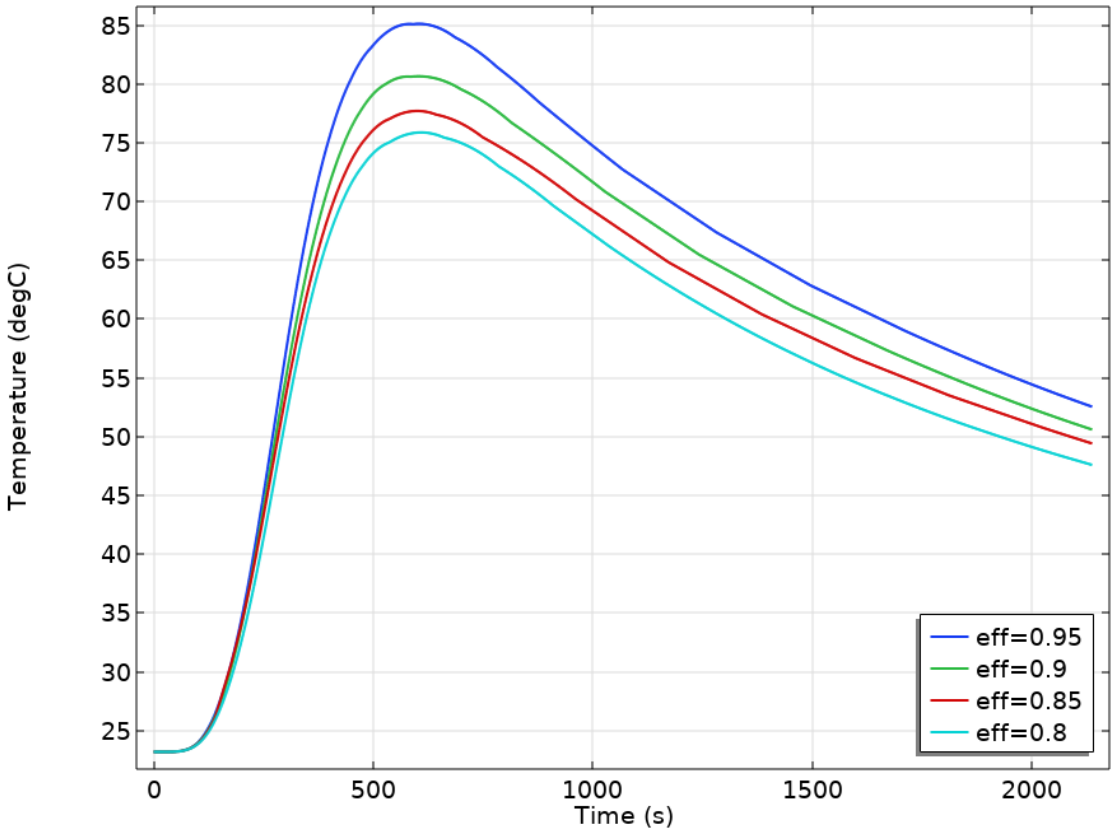

Figure 5-15 Sensitivity analysis of heat efficiency at TC#29

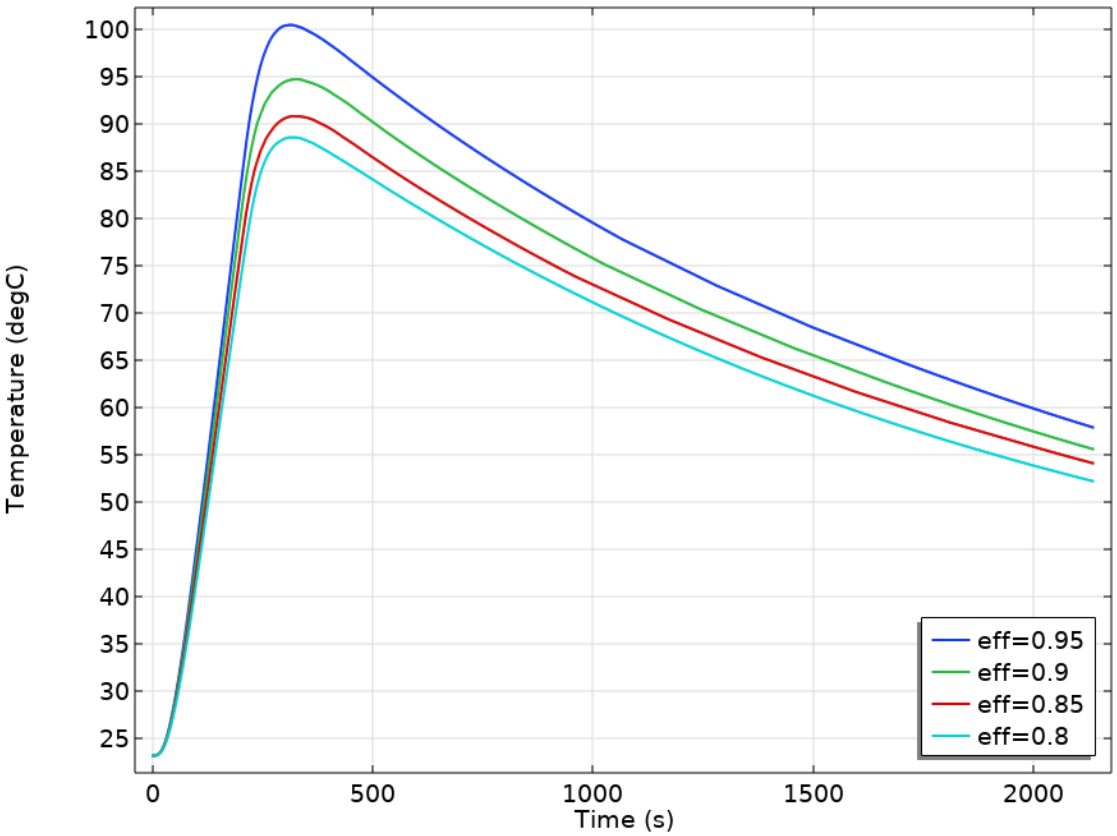

Figure 5-16 Sensitivity analysis of heat efficiency at TC#19

Thermal Contact Resistance

The thermal contact resistance between the pipe and the fitting is another parameter that could influence the welding process significantly [19,44,69]. A high thermal contact resistance could result in lesser heat transfer, potentially affecting the fusion between the pipe and the fitting. Lower thermal contact resistance, on the other hand, would promote heat transfer, potentially enhancing the fusion quality. However, it is crucial to identify an optimal thermal contact resistance as excessive heat transfer might also harm the joint integrity. Therefore, conducting a sensitivity analysis on this parameter could provide insights into achieving the ideal thermal contact resistance. The thermal contact resistance of PE100 surfaces does not have a fixed value as it can vary depending on several factors like material properties, surface roughness, and contact pressure. Therefore, in this procedure, values differing from those derived from preceding studies are employed to examine their impact on the resultant temperature.

The results shown in Figure 5-17 and 5-18 shows an increase in the heat transfer rate to the fitting, while a decrease to the pipe, with increasing the thermal contact resistance between the pipe/fitting during welding. This indicates that the thermal contact resistance act as a barrier to the heat transfer to the pipe, causing the heat to be redirected to the fitting.

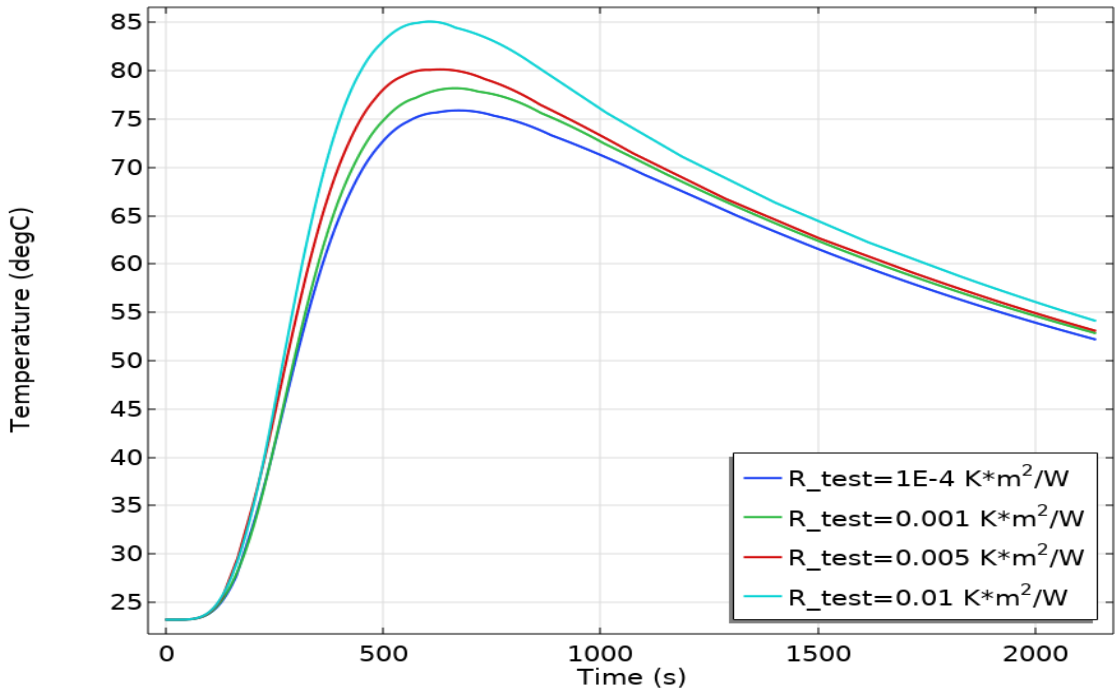

Figure 5-17 Sensitivity analysis of thermal contact resistance at TC#29

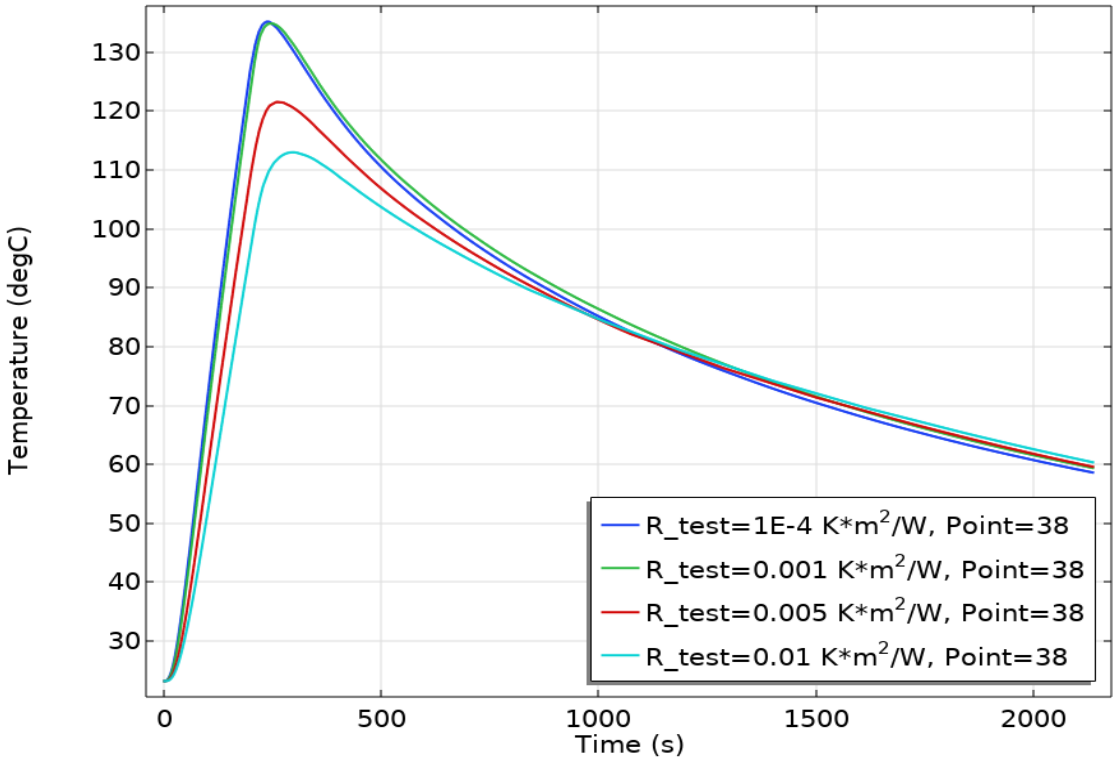

Figure 5-18 Sensitivity analysis of thermal contact resistance at TC#19

Meshing

Mesh Sensitivity Analysis was conducted to assess the model's response to changes in mesh element size. By systematically altering the mesh density and observing its impact on results, the model's sensitivity was gauged to mesh variations. To validate this, two critical temperatures were examined: the maximum temperature at the joint's external layer (fitting) and within the laminate layer (composite). Through this analysis, the aim was to determine how changes in mesh size influence temperature predictions and establish the level of confidence in the model's accuracy and robustness. The employed method involved varying the discretization of the domain by utilizing meshes of different sizes, to observe their impact on computational time and resultant temperatures.

The results of the mesh sensitivity analysis are summarized in Table 19, showcasing the influence of different mesh sizes on the maximum temperatures observed at the fitting and laminate layers. The variations in temperature values across varying mesh densities highlight the sensitivity of the model to mesh element size.

Table 19 Summary of effect of mesh size on the computational time and resultant temperatures

Mesh type	Mesh size (mm)	# of elements	Computational time	Tmax fitting (^{0}C)	Tmax laminate (^{0}C)
Coarse	25.4	10,604	8 min	84.38	102.60
Normal	17	44,791	19 min 30 s	84.36	102.59
Fine	13.5	44,971	19 min 11 s	85.52	104.09
Finer	9.4	31,957	17 min 21 s	85.51	104.08
Extra fine	5.08	58,661	25 min	85.52	104.1
Extremely fine	2.54	146,730	68 min	85.53	104.11

The data illustrates that as the mesh size becomes finer, there is a slight increase in the maximum temperatures at both the fitting and laminate layers. This trend indicates that the finer mesh allows for more accurate representation of heat transfer, leading to slightly higher temperature predictions. However, beyond a certain point, the temperature values stabilize as shown in Figure 5-19, suggesting that the model's sensitivity to mesh size diminishes and the extra computational time for finer mesh as shown in Figure 5-20 is not necessary. These results contribute to the understanding of how mesh size impacts temperature predictions and guide the selection of an appropriate mesh density for accurate and efficient simulations.

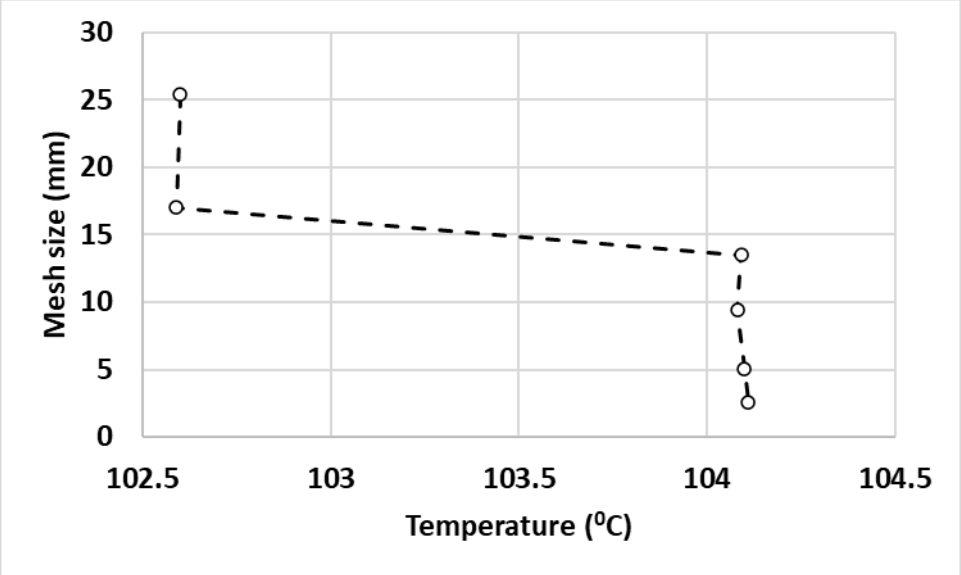

Figure 5-19 Mesh size against resultant peak temperature at the laminate

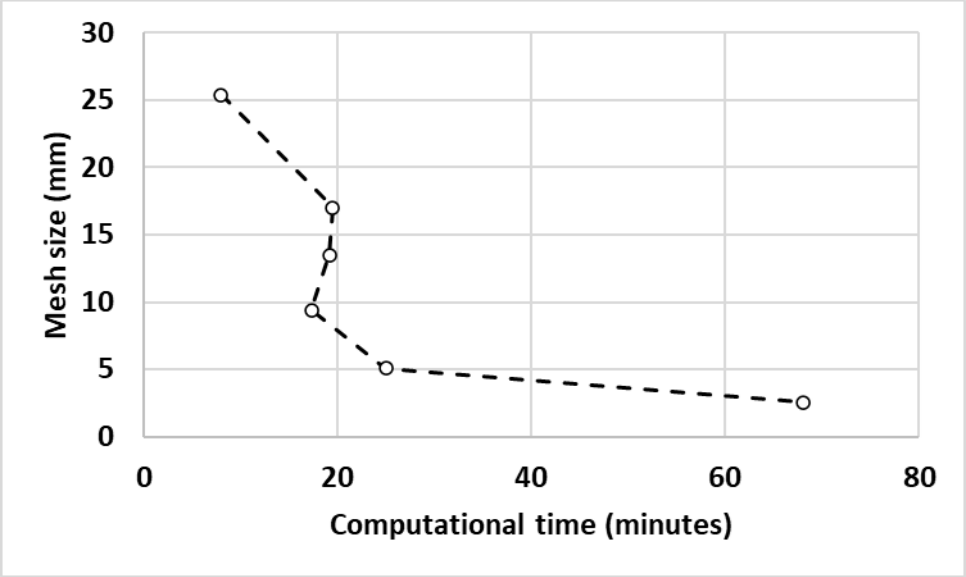

Figure 5-20 Mesh size against the computational time

Additionally, the temperature profile was computed for a specific point (TC#19) across various mesh sizes. This analysis allowed us to observe the variations in temperature prediction as the mesh element size was altered. The resulting temperature profiles were compared and contrasted, revealing the model's response to different mesh densities. The findings are visually represented in Figure 6.21, providing a clear illustration of how changes in mesh size affect temperature distribution at a single point within the joint.

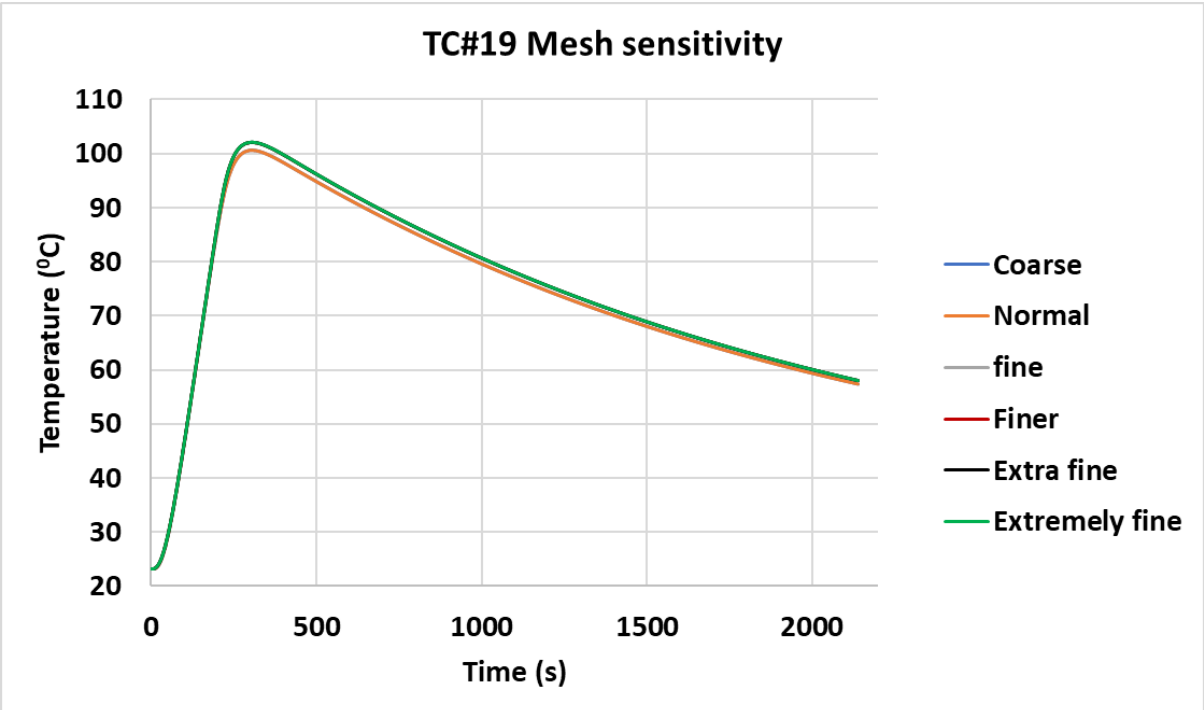

Figure 5-21 Sensitivity analysis of mesh size at TC#19

This sensitivity study ensures that the simulation outcomes remain consistent and reliable across varying mesh densities, enhancing the credibility of the simulation results. Based on the presented outcomes Finer mesh will be used for the remaining of this study.

In conclusion, conducting a sensitivity analysis provides crucial insights into discerning how alterations in these parameters affect heat transfer throughout the electrofusion welding procedure. This is instrumental in establishing limits to pinpoint an optimal parameter set, ensuring the attainment of the highest quality in joint formation.

5.7 Thermomechanical EFW model

This section delves into the thermomechanical modelling of electrofusion welding of Thermoplastic Composite Pipes (TCP). Thermomechanical modelling is an essential tool that provides insights into the complex interactions between thermal and mechanical factors during welding. By simulating heat distribution, temperature evolution, and the resultant mechanical stresses and deformation, a clear understanding of the behaviour of both the pipe and fitting during the electrofusion welding process is achieved. Thermal stresses can arise in a heated body due to a non-uniform temperature distribution, external constraints, or a combination of both. This section outlines the theoretical foundations, modelling approach, and key findings from the thermomechanical analysis of electrofusion welding.

5.7.1 Assumptions and boundary conditions

The following assumptions were considered when developing the thermomechanical model for electrofusion welding of TCP and implemented in the FEA model.

- Axisymmetric 2D model
- Perfect contact between the pipe and electrofusion fitting (no air gap)
- Heat transfer and mechanical effects are accounted for
- Linear elastic material
- Temperature-dependent thermal properties (density, heat capacity, thermal conductivity)
- Temperature-dependent mechanical properties (Modulus of elasticity, Poisson's ratio, coefficient of thermal expansion)
- Convective cooling on the outer surface and pipe inner surface
- Heat source only in the electrofusion fitting where the heating wire is located
- Initial temperature equal to the ambient temperature
- Initial displacement = 0
- Roller boundary condition on the fitting external to account for the holding clamps
- Symmetry and spring foundation on the pipe's free ends
- The heating wire and composite laminate were given identical mechanical properties to HDPE to avoid restriction to thermal deformation by the higher stiff material of both.

5.7.2 Results

The thermomechanical electrofusion model was solved by coupling Heat Transfer and Solid Mechanics modules in COMSOL Multiphysics through Thermal Expansion sub node. The mesh and solver settings kept as presented in this chapter. In this section, the thermal stresses and deformation are presented at three important times, in the middle of the heating, end of the heating and end of the cooling.

- **At the middle of the heating time (102 s)**

Thermal stresses begin to develop due to non-uniform temperature distribution. Stresses are higher at the interface of the heating elements and the material, gradually decreasing outward as shown in Figure 5-22. The material at the heating zone expands more than the surrounding material causing bulging in pipe as shown in figure 5-23.

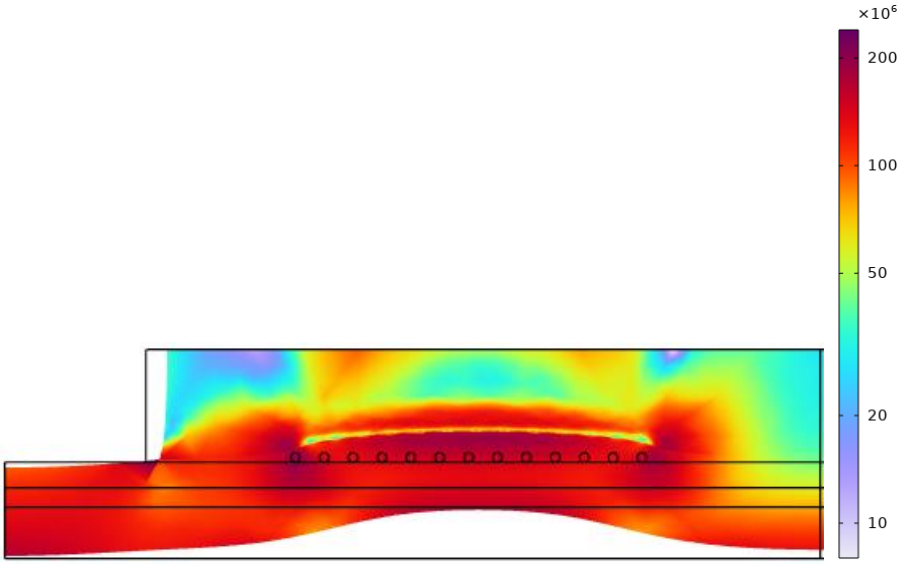

Figure 5-22 Von mises stress at middle of heating time (N/m²)

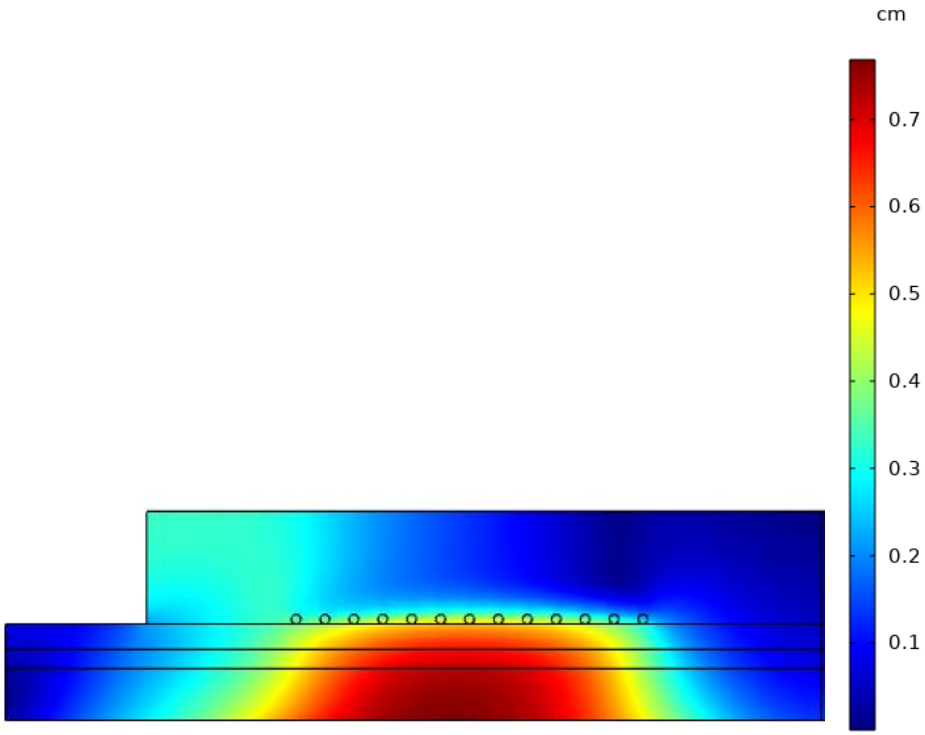

Figure 5-23 Displacement at middle of heating time (cm)

- **At the end of the heating time (203 s)**

Thermal stresses reach their maximum at the end of welding time as the temperature gradient is at its steepest as shown in Figure 5-24. The material has expanded to its maximum extent due to the peak temperatures. Larger displacement differences were observed between the heated and unheated zones as shown in Figure 5-25. At this stage, Displacement might cause some misalignment if the expansion is not uniform.

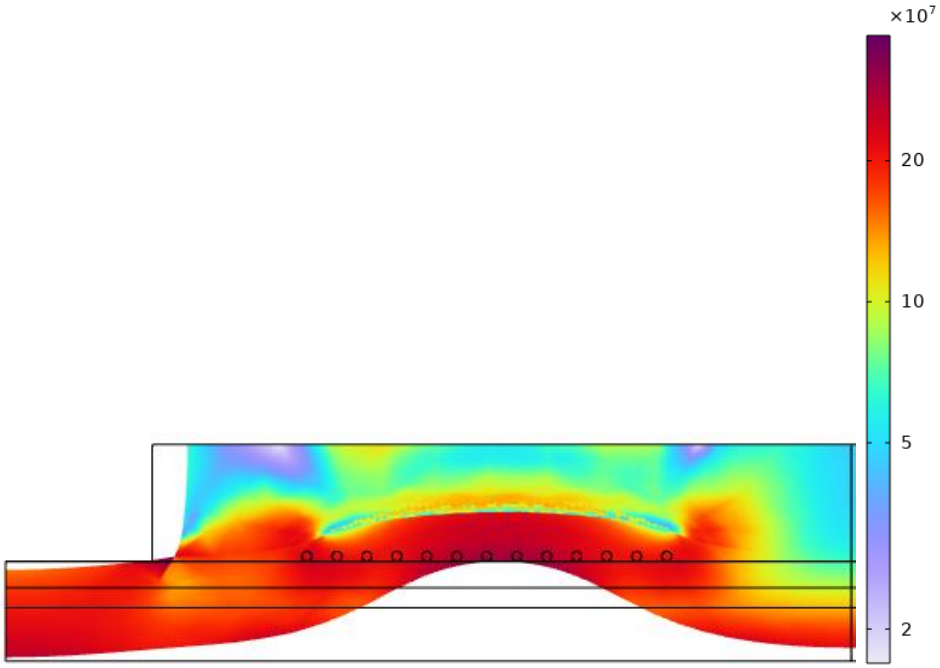

Figure 5-24 Von mises stress at end of heating time (N/m2)

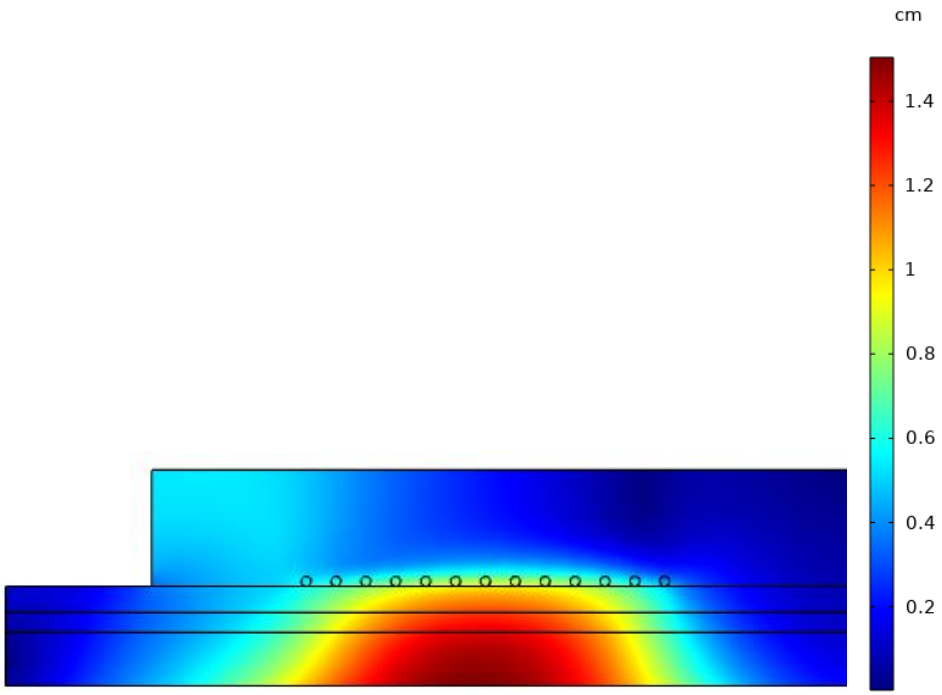

Figure 5-25 Displacement at end of heating time (cm)

- **At the end of cooling**

As the material cools, residual stresses develop due to the differential contraction of previously expanded regions. Stresses begin to redistribute and may lead to stress relaxation in some areas as shown in Figure 5-26. The material contracts, but not uniformly, leading to potential warping or distortion. Some displacement may become permanent, leading to residual deformation as shown in Figure 5-27. It is worth to mention that cooling can result in the final alignment of the welded components being different from the initial setup due to thermal shrinkage.

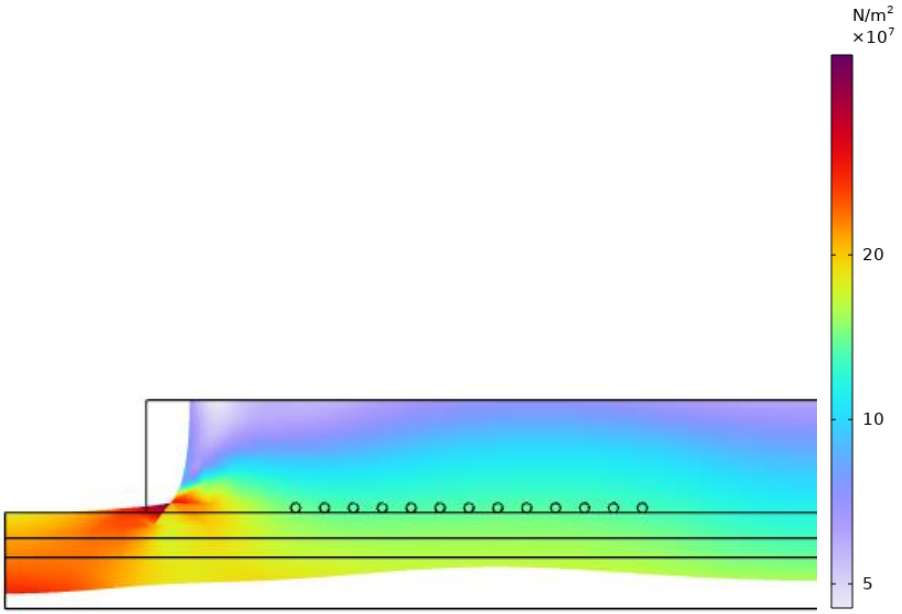

Figure 5-26 Von mises stress at end of cooling time (N/m2)

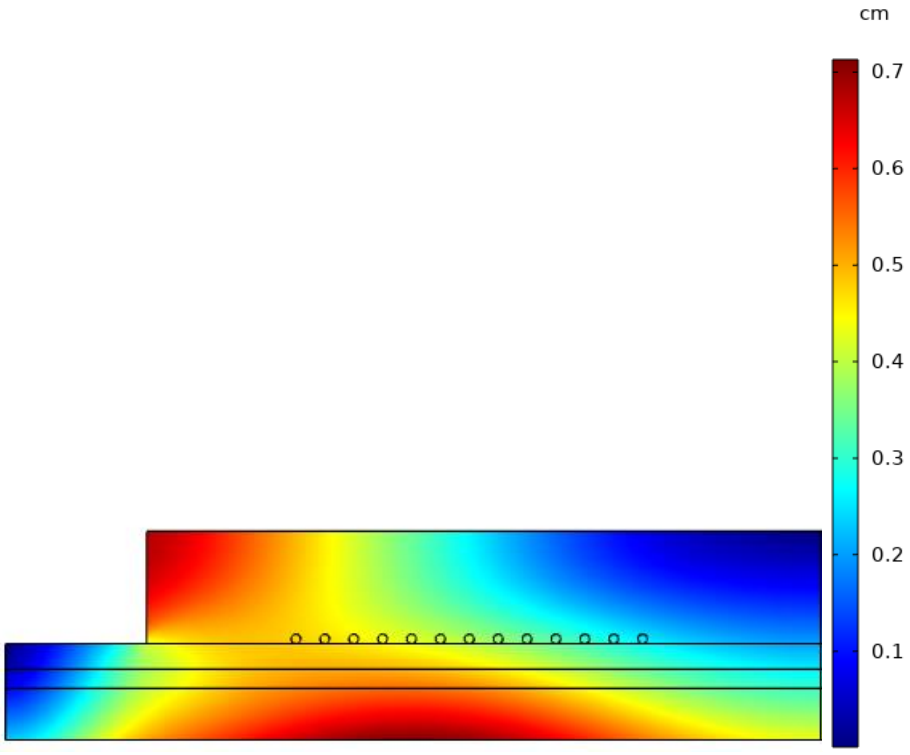

Figure 5-27 Displacement at end of cooling time (cm)

5.8 Conclusion

This chapter outlined the application of Finite Element Analysis (FEA) in examining the physical electrofusion welding of TCP. It employed material properties inferred from measurements and conformed to the power input in alignment with the actual welding test. The fundamental objective of this simulation was to thoroughly characterize the transient behaviour of heat transfer throughout the electrofusion welding process. Such meticulous modelling established a robust base for crafting a tool/process pertinent to welding TCP and couplers with varying configurations, materials, and operating conditions. This was aimed at assisting in the conceptualization of a novel coupler to join TCP. Additionally, a simple thermomechanical model to assess the thermal stresses and deformation was discussed.

The simulation model was verified pre-optimization using visual comparison and statistical analysis to compare both simulated and measured data. The visual comparison suggested the model was more adapted to points in the fusion zone rather than the cold zone. A sensitivity analysis was conducted to set the boundaries for the control parameters with the aim to find their optimal values in the next chapter with an enhanced optimized heat transfer simulation model for the EFW of TCP.

Chapter 6

OPTIMIZATION OF WELDING PROCESS PARAMETERS

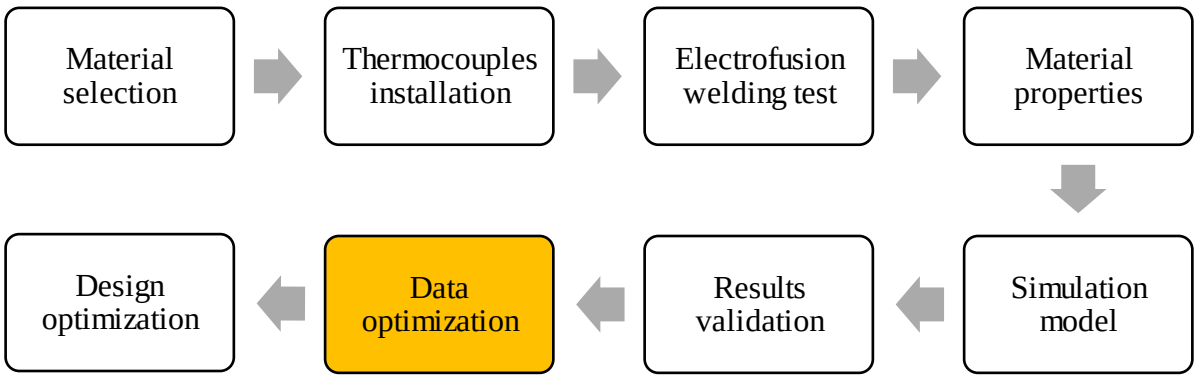

This chapter provides an extensive exploration of optimizing electrofusion welding process parameters. It begins by defining the significance of optimization in welding and pinpointing essential parameters. It delves into different optimization techniques, with a special emphasis on the least squares method. The formulation of the optimization problem, procedural steps, and algorithmic approach are systematically outlined. The chapter culminates in a thorough analysis of post-optimization results, emphasizing their accuracy and reliability through experimental validation. The outcomes of the optimization process will subsequently be utilized in the design of electrofusion fittings detailed in Chapter 8.

6.1 Introduction

Optimization refers to the systematic approach of finding the best possible solution to a problem by adjusting controllable variables. In the realm of simulating heat transfer, optimization seeks to improve thermal efficiency, reduce energy losses, and achieve desired temperature distributions within a system [70].

Optimization plays a crucial role in advancing various industries, including manufacturing, transportation, and energy systems. In the specific context of electrofusion welding, optimization of welding parameters becomes paramount in ensuring the highest quality of joints, maximizing energy utilization, and minimizing defects.

The optimization of welding parameters in electrofusion welding for TCP offers numerous benefits to both industry and research.

By identifying the optimal combination of heating time, power input, and coupler geometry, the joint integrity can be enhanced, joint failure rates can be reduced, and the overall efficiency of TCP systems can be improved. Moreover, optimization efforts aim to enhance the understanding of the complex heat transfer behaviour during electrofusion welding. This understanding is vital for developing accurate simulation models that replicate real-world welding scenarios.

The identification of unknown parameters in mathematical formulation or physical problems can be achieved using inverse optimization problems. The inverse optimization method in heat transfer problems is often concerned with minimizing the least squares difference between the observed and calculated temperatures by adjusting the heat transfer parameters of the system. The least of squares difference approach is used to estimate the missing welding parameters by matching the temperature profile from a simulated model to experimental data at different locations in the pipe/fitting assembly.

6.2 Selection of Process Parameters

At this stage of the research, the focus is on identifying the critical process parameters that require exploration to optimize the electrofusion welding process for TCP. For this optimization process, it was acknowledged that certain welding parameters, such as power input and heating time, are directly copied from the experimental setup to match the conditions of the physical welding tests. These parameters were predetermined to maintain consistency with the experimental design and ensure accurate validation of the simulation model.

6.2.1 Key Input Parameters for the Welding Process

In this section, we discuss the welding parameters that remain fixed and are directly taken from the experimental setup. The key input parameters include:

Power input is an essential welding parameter that governs the amount of energy delivered to the welding interface. It is predetermined and matched with the experimental values to replicate the real-world welding conditions accurately. Maintaining a consistent power input ensures that the heat generated during the welding process remains consistent between the simulation and experiments.

Heating time represents the duration for which the heating element applies heat to the welding interface. Similar to the power input, heating time is preestablished and maintained to match the experimental setting. This ensures that the energy input and temperature profiles align between the simulation and physical welding process.

Coupler geometry plays a significant role in determining the joint's integrity and strength. The geometrical dimensions of the coupler are directly copied from the experimental specimens to ensure that the simulated joints closely resemble the physical welded joints.

6.2.2 Assumed process parameters in the simulation model

While certain welding parameters are fixed to match the experiment, there are other parameters, known as assumed process parameters, that need to be explored during the optimization process. These parameters are not directly measured during the experimental tests but are essential in the simulation model to accurately represent the heat transfer behaviour during electrofusion welding. The effect of these parameters was discussed in the sensitivity analysis conducted in Section 5.7.3.

The **thermal contact resistance** represents the resistance to heat transfer at the interface between the thermoplastic composite pipe and the fitting during welding. This is combination of air resistance if there is a gap clearance in addition to the contact surfaces resistance. This parameter influences the efficiency of heat transfer and fusion bonding at the joint interface. Variations in thermal contact resistance can significantly affect the temperature distribution and fusion quality of the welded joint.

The **coefficient of convective heat transfer** represents the rate of heat transfer through convection on the external and internal surfaces of the fitting. The external fitting surface interacts with the environment, while the internal fitting surface comes into contact with the molten polymer during the welding process. Proper exploration of the convective heat transfer coefficient is crucial in accurately representing the heat loss or gain from these surfaces.

Power efficiency reflects how efficiently the input power is converted into heat for melting and fusing the materials. A higher power efficiency indicates that a larger portion of the input power is being utilized for the intended welding process rather than being lost as waste heat. Power efficiency is influenced by several factors, including the electrical properties of the materials, the design of the electrofusion machine, and the welding parameters.

By investigating and optimizing the assumed process parameters in the simulation model, the aim in this research is to achieve the best possible representation of the heat transfer behaviour during electrofusion welding. These optimizations will lead to improved accuracy of the simulation results, enabling to identify the optimal welding conditions for TCP joints more effectively. The results of Test 2 then will be used to validate this optimized model.

6.3 Optimization Techniques

This section illustrates the optimization technique employed to calibrate the simulation model with experimental data and identify the optimal welding conditions for TCP electrofusion welding. The objective is to enhance the accuracy of the simulation model by adjusting the assumed process parameters, such as thermal contact resistance and the coefficient of convective heat transfer, to match the experimental temperature profiles. Least squares method for model calibration

The least squares method is a widely used optimization technique for model calibration [71]. It seeks to minimize the sum of the squared differences between the simulated temperature profiles and the experimental temperature data obtained from the thermocouples. By finding the best-fit parameters that minimize the sum of the squared residuals, the simulation model becomes more accurate and aligns more closely with the experimental data.

The primary goal of the optimization process is to minimize the differences between the simulated and experimental temperature profiles at various locations on the TCP joint. This involves iteratively adjusting the assumed process parameters to achieve the best possible fit between the simulated and measured temperature data. The process continues until the simulation model closely matches the experimental data within a predefined tolerance of 5% to match the peak temperature at the single objective function.

6.3.1 Optimization problem formulation

To implement the optimization process effectively, the optimization problem must be properly formulated. This involves defining an objective function and imposing relevant constraints to ensure realistic and physically meaningful results. The objective function represents the mathematical expression that needs to be minimized during the optimization process. In this case, the objective function is the sum of the squared differences between the simulated and experimental temperature profiles at thermocouple location on the TCP joint.

$$Single\ Objective\ function: \left|T_{exp,i} - T_{sim,i}\right| \tag{7.1}$$

For the case in this study with more than one thermocouple, the objective function can be written as,

$$Multiple\ Objective\ function: \sum_{i=1}^{N} \left| T_{exp,i} - T_{sim,i} \right| \quad (7.2)$$

6.3.2 Optimization procedure

To provide a systematic approach to the optimization process, a flowchart is developed to guide the iterative adjustments of the assumed process parameters. The flowchart in Figure 6-1 outlines the steps of the optimization process and illustrates the convergence towards the optimal solution.

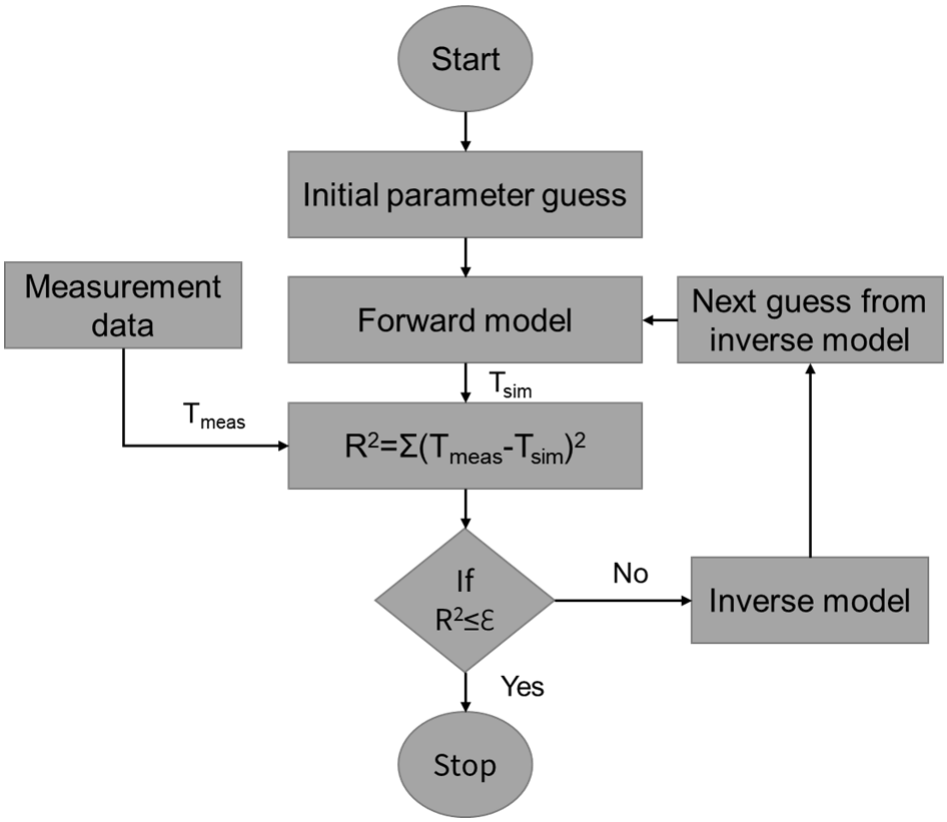

Figure 6-1 Optimization process steps flowchart

The optimization process starts with the initialization of the assumed process parameters. These initial values are based on previous knowledge and may be obtained from literature, theoretical models, or preliminary experiments. The optimization algorithm iteratively modifies the assumed process parameters based on the objective function and constraints. In each iteration, the simulation model is recalibrated, and the temperature profiles are compared with the experimental data. The assumed process parameters are adjusted to minimize the objective function, bringing the simulated and experimental temperature profiles into closer agreement.

Constraints are additional conditions that must be satisfied during the optimization process. The assumed control parameters have physical limits or predefined ranges based on the sensitivity analysis outcomes from Section 5.7.3. Imposing these constraints ensures that the optimization process remains realistic and within feasible bounds. The control parameters details including initial guess, lower and upper bounds are presented in Table 20

Table 20 Control parameters

Parameter	Initial value	Lower bound	Upper bound
η	0.9	0.8	1
$R_{contact}$	0.01 $(Km^2)/W$	0.0005	0.02
h_o	10 $W/(m^2K)$	7	15
h_i	10 $W/(m^2K)$	7	15

6.3.3 Algorithm Selection for Optimization

Different optimization algorithms can be utilized to address the calibration problem. The selection of the algorithm depends on factors such as the complexity of the function, the number of parameters to optimize and the desired computational efficiency. In this study, the Nelder Mead algorithm was employed to determine the optimal process parameters.

The Nelder Mead algorithm is a derivative free optimization technique that falls into the category of search methods [72]. It takes a geometric approach by iteratively refining a simplex (a multi-dimensional shape) within the parameter space to converge towards an optimal solution. The algorithm adjusts this simplex based on function values at its vertices guiding it towards finding an optimal solution. This algorithm was implemented using COMSOL built in Optimization Module.

Throughout the optimization process it is crucial to monitor convergence to ensure that a stable and optimal solution is reached. We establish convergence criteria that stop iterations after a defined number or when a desired level of accuracy is achieved. Furthermore, the robustness of optimization results we assess to ensure that small variations, in conditions do not significantly impact or invalidate the optimal solution.

By implementing these optimization techniques, the simulation model for TCP electrofusion welding can be calibrated to closely match the experimental temperature profiles.

The calibrated model will accurately represent the heat transfer behaviour during the welding process, leading to improved predictions of joint quality and enhanced optimization of welding parameters.

6.4 Final Optimized Results

In this section, the outcomes of the optimization process for the electrofusion welding of TCP are presented. The focus is on the final values obtained for the assumed process parameters, such as thermal contact resistance and the coefficient of convective heat transfer. Additionally, the results were compared before and after optimization to demonstrate the improvements achieved through the calibration of the simulation model.

6.4.1 Optimal values for welding process parameters

After completing the optimization process, the final values for the assumed process parameters are obtained and the results are listed in Table 21. These values represent the optimal settings that best align the simulated temperature profiles with the experimental temperature data from the thermocouples.

Table 21 Updated process parameters following optimization process

Parameter	Symbol	Optimized value
Power Efficiency	η	0.973
Thermal contact resistance	$R_{contact}$	0.017 $(Km^2)/W$
External convective heat transfer coefficient	h_o	12.27 $W/(m^2K)$
Internal convective heat transfer coefficient	h_i	9.7 $W/(m^2K)$

The primary value gained from the optimization process was to improve the accuracy of the model by finding the optimal values of the earlier assumed parameters that has not been measured experimentally. Additionally, the optimal parameters allow for further study analysis by being able to repeat the heat transfer analysis for electrofusion welding through the developed FEA model for different sets of geometry, boundary conditions, power and time without having to repeat the actual test. Thus, a reduction in the associated time and costs for conducting actual welding tests can be achieved by conducting an optimization analysis.

6.4.2 Comparison of results before and after optimization

To evaluate the effectiveness of the optimization process, a comparative analysis was conducted of the results obtained before and after calibration.

Temperature Distribution Profiles

The temperature profiles obtained from the simulation model was compared before and after optimization with the experimental temperature data obtained from Test 1. By visually inspecting the profiles and quantitatively analysing the differences, the level of improvement achieved through calibration can be assessed. The simulation data from Test 1, following process parameter optimization, underwent statistical analysis, with the Root Mean Square Error (RMSE) values post-optimization being calculated and illustrated in Figure 6-2. Notably, there is an increase in RMSE values in certain locations when compared to the pre-optimization RMSEs discussed in Section 5.7.2. This phenomenon can be attributed to the fact that, in some areas, the simulated temperature data closely aligned with experimental readings but failed to capture the true thermal behaviour of the thermocouples particularly in the cooling phase.

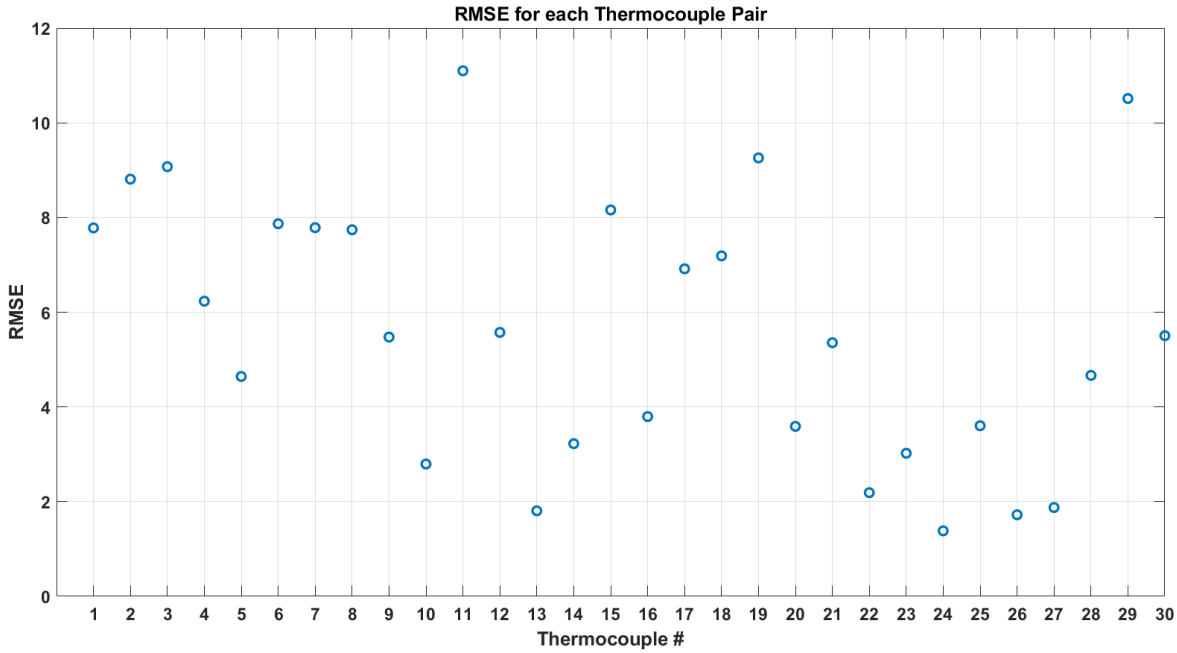

Figure 6-2 RMSE values for Test 1 after optimization

Despite this, the overall RMSE values remain lower than those observed pre-optimization. This is evident when comparing the Overall RMSE values, which decreased from 7.69 before optimization to 6.25 after optimization.

This demonstrates an improved agreement between simulated and measured temperature values before and after optimization. Figures 6-3 to 6-6 further elucidate this comparison, for some thermocouples and the remaining results for all 30 locations in Test 1, both pre and post optimization can be found in the Appendix.

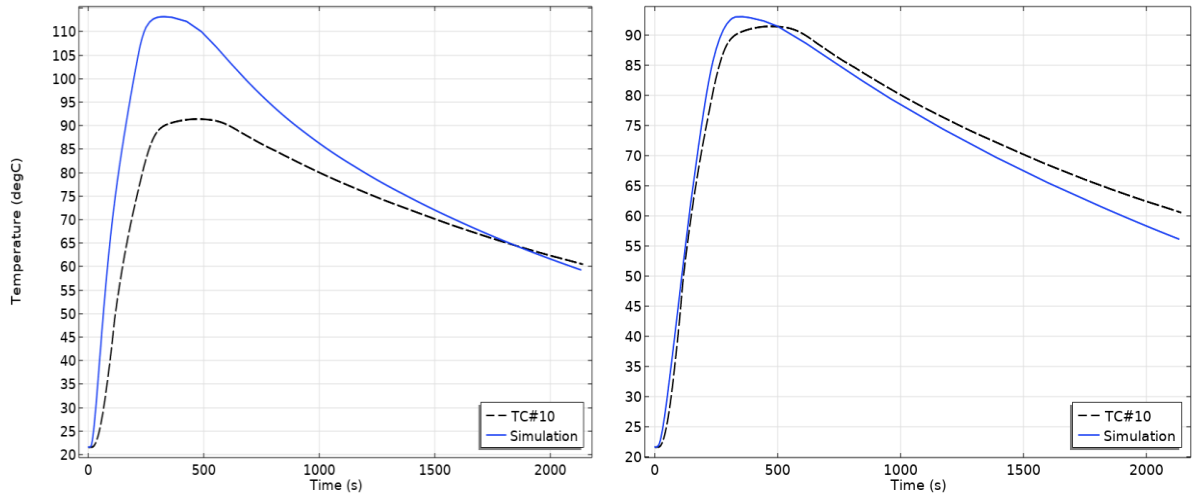

Figure 6-3 TC#10 Simulated and experimental temperature over time a) before b) after optimization

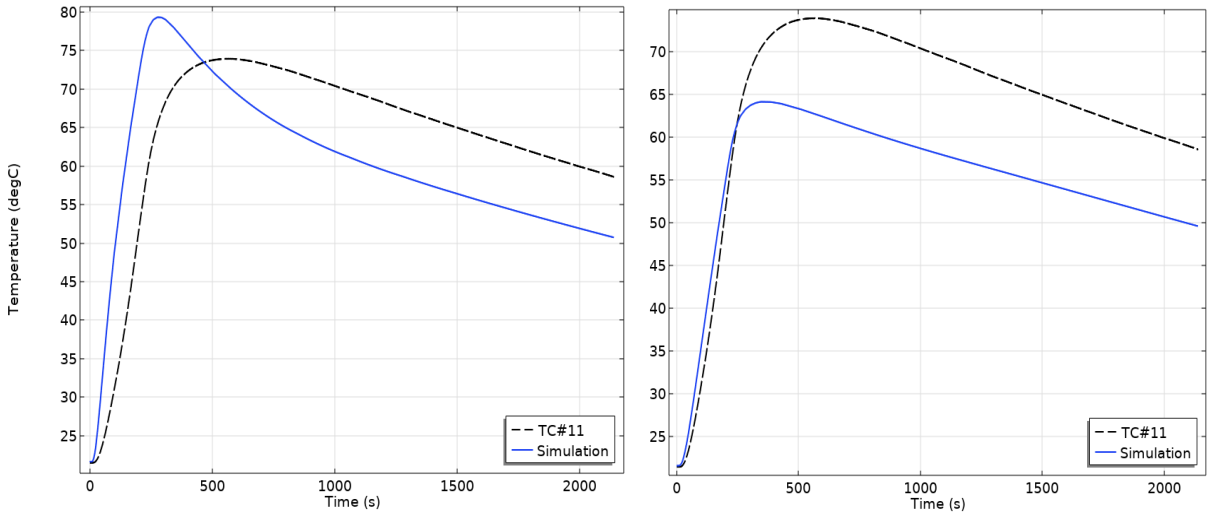

Figure 6-4 TC#11 Simulated and experimental temperature over time a) before b) after optimization

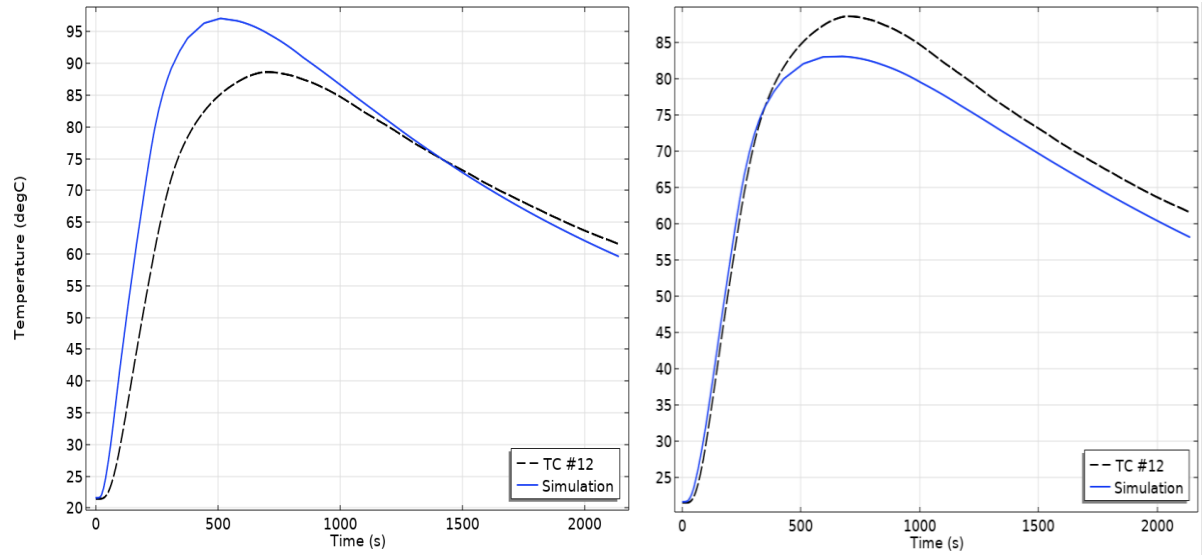

Figure 6-5 TC#12 Simulated and experimental temperature over time a) before b) after optimization

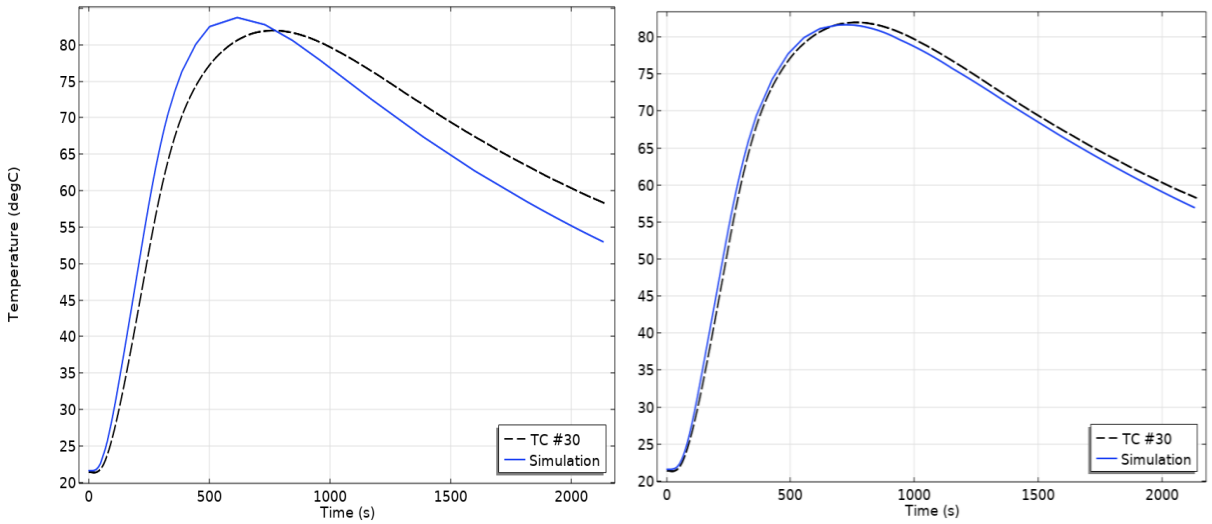

Figure 6-6 TC#30 Simulated and experimental temperature over time a) before b) after optimization

The simulation was not accurately capturing the actual temperature profile for those thermocouples placed in the cold zone (away from the fusion zone) in both the pipe and fitting. The difference is clearly found in TC#21,26 in the fitting and TC#1,2,7,11,17,18 in the pipe. This tells that the assumptions made for the model were not valid on the cold zones. Additionally, the peak temperature for most of the thermocouples placed in the pipe, went from higher pre-optimization into lower post-optimization when compared to the peak temperatures for those obtained experimentally. This suggests that the thermal contact resistance is not equivalent along the welding interface.

By presenting the final optimized values for the welding process parameters and comparing the results before and after optimization, this section demonstrates the effectiveness of the optimization process in improving the accuracy of the simulation model. The optimized simulation model closely aligns with experimental data, especially those located in the fusion zone, providing a reliable tool for facilitating better decision-making in the design and manufacturing of TCP joints. To strengthen the credibility of the optimized process parameters, they were employed as inputs in the simulation, and the outcomes were compared with the results of Test 2. The next section will evaluate these results to assess the repeatability and consistency of the optimization process.

6.4.3 Repeatability of the optimized welding parameters

In this section, the application of the optimized welding parameters was explored in a repeated experiment. To evaluate the repeatability of the optimized welding parameters, an additional welding experiments (Test 2) was conducted under the same conditions as the initial experimental setup. The optimized welding parameters, including the values of thermal contact resistance and the coefficient of convective heat transfer, were implemented in this repeated experiment. A statistical analysis was carried out to assess the RMSE values for Test 2, as depicted in Figure 6-7. These RMSE values hover around 5°C and are even lower than those obtained for Test 1. This indicates that the optimized process parameters have been effectively established and are applicable with consistency in the repeatability demonstrated in Test 2. Notably, the overall RMSE value for Test 2 is 6.1°C, and this value drops to 3.8°C when excluding thermocouple 25. This suggests that the optimized process parameters are were accurately determined and the optimized model is a good representation of the electrofusion welding process.

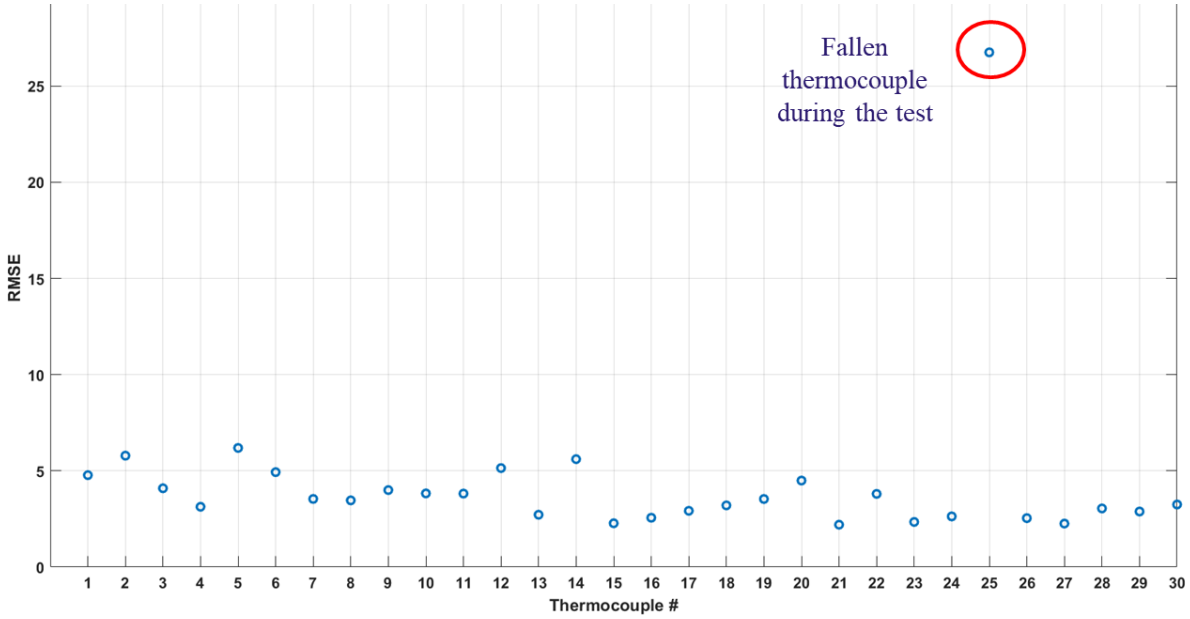

Figure 6-7 RMSE values for Test 2 with optimized parameters

The comparison between measured and simulated temperatures using the optimized process parameters is illustrated in Figures 6-8 for all 30 thermocouples in Test 2.

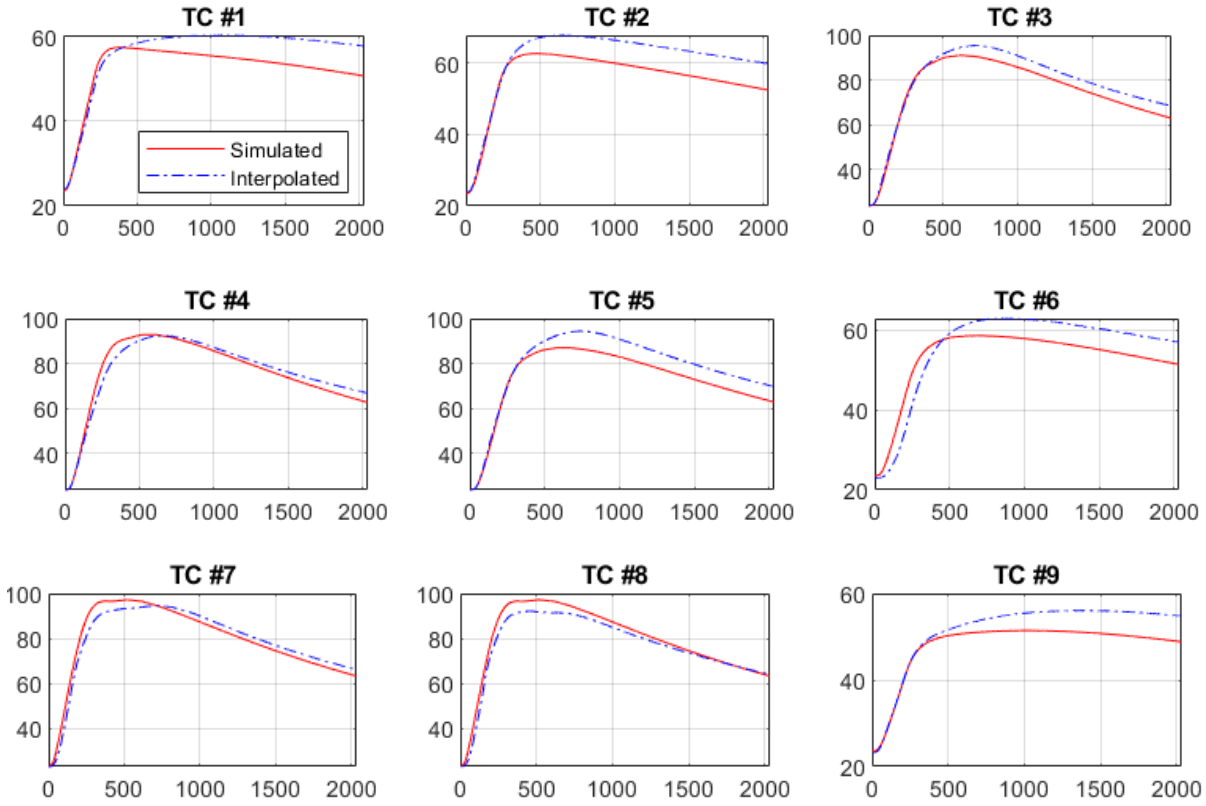

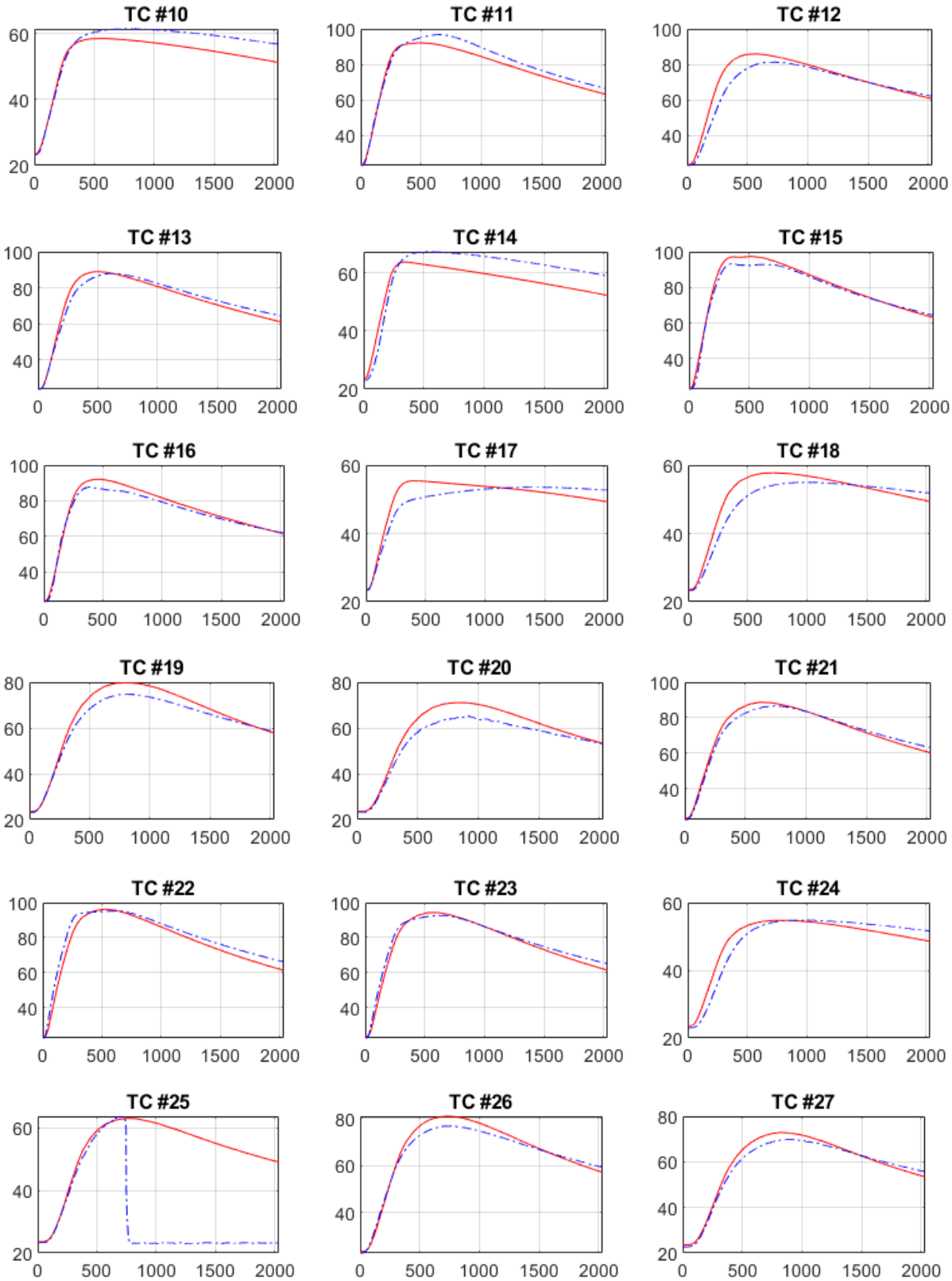
TC #10
TC #11
TC #12
TC #13
TC #14
TC #15
TC #16
TC #17
TC #18
TC #19
TC #20
TC #21
TC #22
TC #23
TC #24
TC #25
TC #26
TC #27

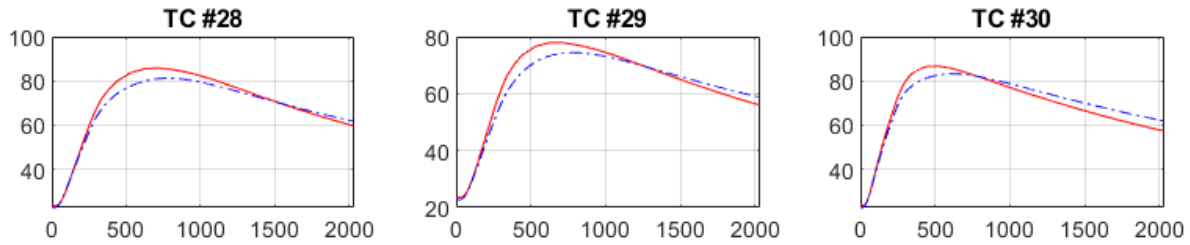

Figure 6-8 Measured and Optimized simulated temperature profiles in ^0C against time in seconds for Test 2

By investigating the repeatability of the optimized welding parameters and their potential for practical implementation in industrial settings, this section provided valuable insights into the reliability and applicability of the optimization results. Understanding the robustness of the optimized parameters allows us to confidently implement them in real-world welding processes, ultimately leading to the production of high-quality and durable TCP joints. The successful integration of the optimized welding parameters into industrial practice fosters advancements in electrofusion welding technology and contributes to the understanding of the heat transfer during the welding process and advancement in designing new EF fitting which will be discussed in Chapter 8, leading to a wider adoption of TCP in multiple infrastructure systems.

6.4.4 Melting zone

Following the process optimization, the simulation of the melting zone pinpointed regions that had attained or surpassed the previously measured melting temperature of PE100 (131.3°C), as identified in Chapter 4. The outcome of this analysis, presented in Figure 6-9, illustrates the extent of the melting region surrounding the heating wires during the heating time in the electrofusion welding process. The observed melt zone length and width was determined to be 58.7 mm and 5.9 mm respectively. The fusion zone length value is 10% higher than those obtained experimentally in Section 4.3.3. Still, this value exceeds the minimum required fusion zone length as instructed in BS EN 1555-3 [73].

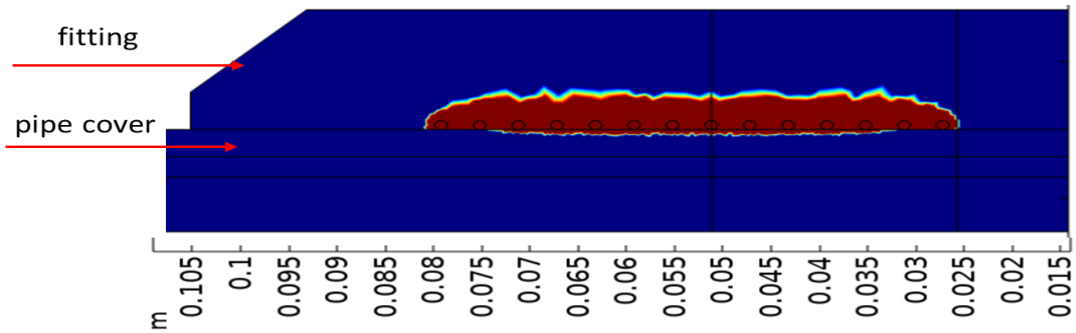

Figure 6-9 Simulated melted zone

The dataset shown in Figure 6-10 tracks the evolution of the fusion zone width and length over time during the welding process. Notably, for the initial 29 seconds, both width and length measurements remained at zero, indicating a lack of fusion and time required to heat the conductive wires. Subsequently, the fusion zone began to form, with the width stabilizing at around 5.9 mm and the length extending to approximately 59 mm. These findings provide valuable insights into the temporal dynamics of the electrofusion welding process, shedding light on when and how fusion occurs.

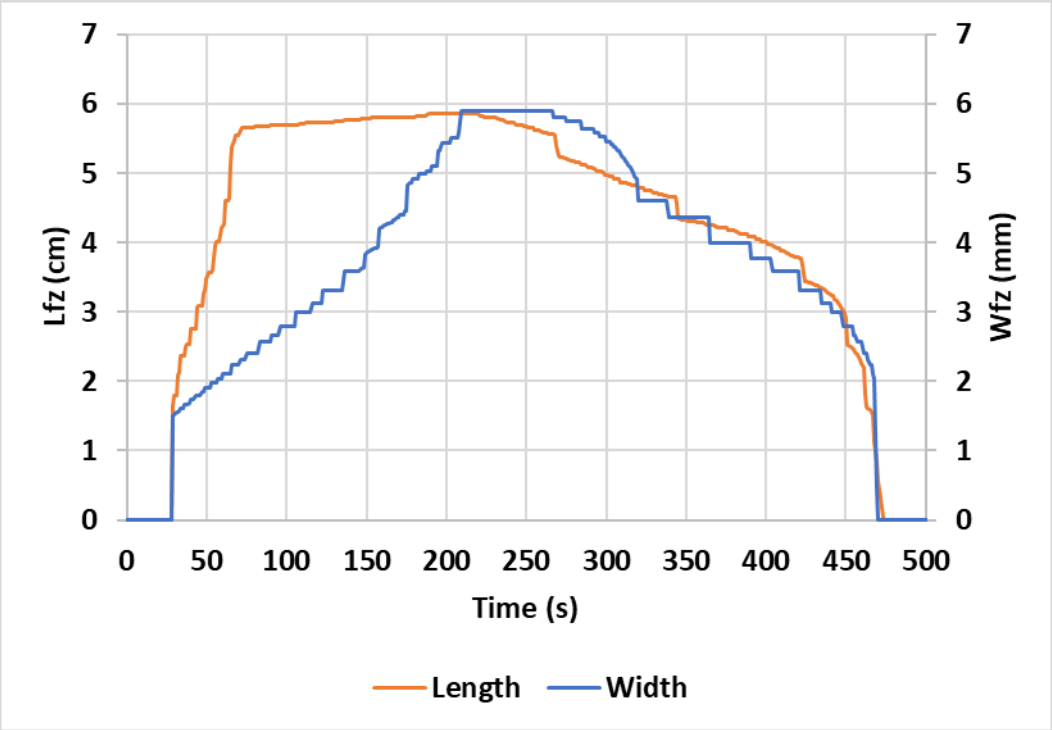

Figure 6-10 simulated length and width of the melting zone over time

6.5 Conclusion

In this chapter, the optimization of process parameters was meticulously assessed, utilizing the least squares method via the COMSOL optimization module. Optimal values of presumed process parameters for Test 1 were determined to be 12.27 and 9.7 for the external and internal

convective heat transfer coefficients, respectively; 0.017 W/m²K for the thermal contact resistance at the welding interface; and 97% for the efficiency of the heat generated at the wires.

A visual examination of the temperature profiles at 30 thermocouple locations, both pre- and post-optimization, was conducted, showcasing a discernible reduction in the overall RMSE value of Test 1. To corroborate the optimal process parameters deduced, a repeated simulation for Test 2 was executed employing these parameter values, and subsequently visually compared. The overall RMSE value for Test 2 was computed to be 3.6 °C.

The robustness of the optimized results was scrutinized in Test 2, aiming to verify the resilience of the optimal solution to minor variations in the initial conditions, especially considering the initial ambient temperature of Test 2 being 2 °C higher than that of Test 1. In conclusion, the post-optimization melting zone was meticulously evaluated and juxtaposed with the values acquired experimentally, affirming the reliability and effectiveness of the optimized process parameters in enhancing the process overall efficiency and accuracy.

Chapter 7

RECOMMENDATIONS OF EF FITTING DESIGN

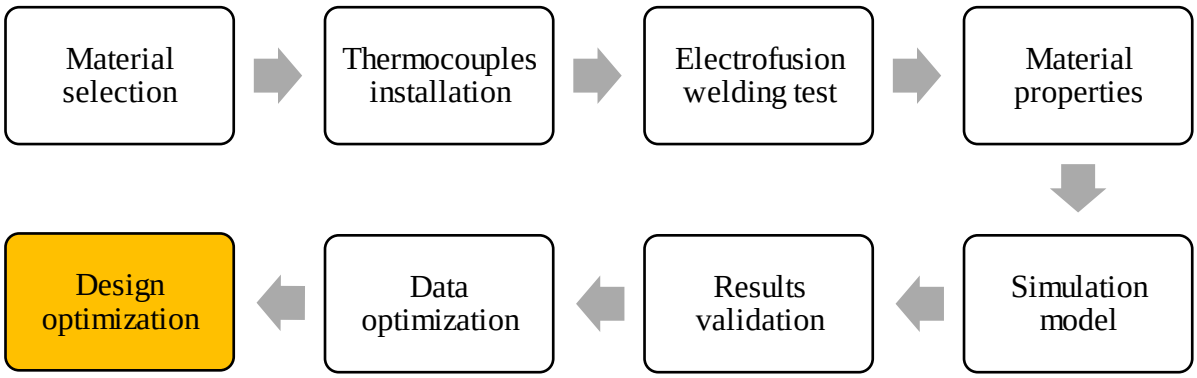

In this chapter, the optimized welding parameters obtained from Chapter 7 were implemented in a new design optimization problem focused on improving the electrofusion fitting for Thermoplastic Composite Pipes (TCP). The design optimization aims to create a fitting that optimally suits TCP, considering various constraints such as temperature limits and stress-related considerations.

7.1 Introduction

In the context of designing optimal solutions for Thermoplastic Composite Pipes (TCP), the integration of advanced simulation techniques holds paramount significance. This study in the field of heat transfer during electrofusion welding have showcased the potential to enhance joint performance through optimized welding parameters. Building upon this foundation, this chapter embarks on a journey of design recommendations of EF fittings for TCP. This chapter uses the calibrated simulation model from Chapters 5 and 6, forged from meticulous mesh sensitivity analysis and validated against experimental data. By merging the insights gained from the optimized welding parameters, the chapter propels the investigation towards the optimization of the electrofusion fitting design for TCP. This approach draws inspiration from the synergy of theoretical rigor and practical applicability, envisioning an electrofusion fitting tailored to the unique demands of TCP applications.

7.2 Fitting design proposals

The EF fitting design problem for TCP commences by proposing distinct fitting designs, each characterized by a unique combination of geometric parameters, welding power, and time settings. These designs are subjected to a rigorous optimization process that involves a computational loop aiming to minimize the differences between simulation-based temperature profiles and the prescribed temperature constraints.

7.2.1 Single fusion zone

The first type of fitting is an innovative design characterized by a single fusion zone presented in Figure 7-1. In this configuration, the fusion zone extends along the entire length of the fitting, forming a seamless connection between the fitting and the outer cover layer of the TCP. The pipes are butt-fused together prior to the electrofusion process with the fitting. The butt-fusion requires machining of the reinforcement and weld the internal and outer layer of the pipes together. The fusion process ensures a robust bonding, enhancing both the thermal integrity and mechanical strength of the joint. The design process for this configuration entails determining the optimal fusion zone length, wire parameters, and welding power and time settings. By establishing a coherent thermal and mechanical connection, the single fusion zone design contributes to the overall reliability and performance of the TCP system.

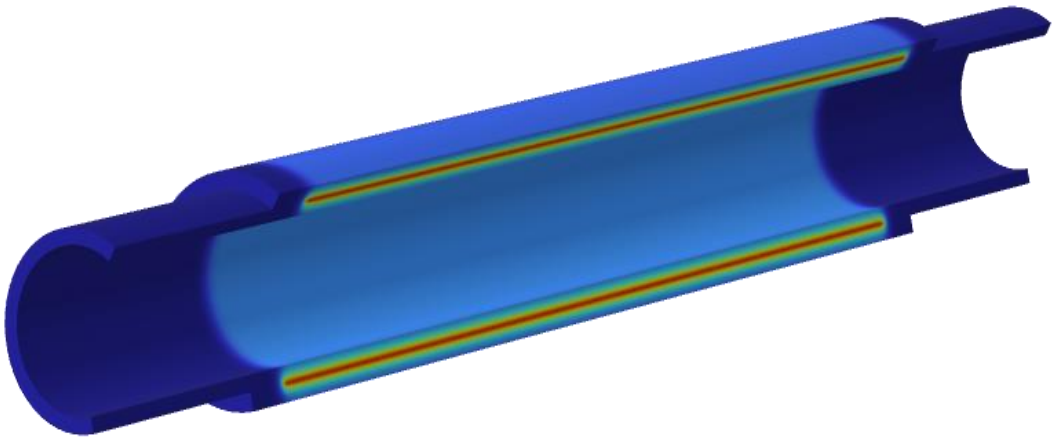

Figure 7-1 Single fusion zone design

7.2.2 Double fusion zone

The second fitting design is characterized by double fusion zones as shown in Figure 7-2. In this design, the fitting is bonded to both the internal layer (liner) and the external cover layer of the Thermoplastic Composite Pipe. This dual-fusion approach results in the creation of four distinct fusion zones, two on each side of the fitting.

The optimization process for the double fusion zone design encompasses the determination of the fusion zone lengths, wire characteristics, and welding power and time settings for both internal and external fusion zones. By capitalizing on the synergy between layers, this design offers an innovative solution that promises heightened thermal and mechanical performance, thereby elevating the overall reliability and durability of the fitting within the TCP system.

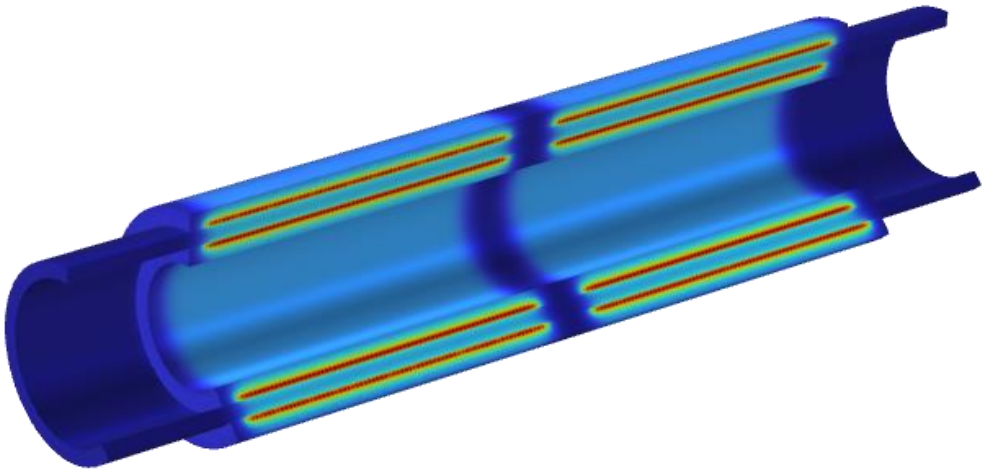

Figure 7-2 Double fusion zone design

7.3 Design Constraints

The design optimization problem is formulated to identify the optimal configuration of the electrofusion fitting for TCP. The objective is to maximize joint strength, improve weld quality, and ensure the fitting's suitability for long-term performance. The design optimization problem is subjected to various constraints to meet the specific requirements of TCP applications.

7.3.1 Welding interface temperature constraint

HDPE properties necessitate a precise range of temperatures to ensure a secure and enduring fusion between pipe sections. As per DVS 2207-1, the suggested welding temperature is between 200 and 220 ^{0}C [75]. Cai et al. (2018) indicates that an optimal temperature range of 210 to 230 ^{0}C in butt-fusion exists at the interface where the polymer chains can entangle for creating a robust, homogenous weld [76]. Any deviation above or below this threshold may compromise the structural integrity, inducing defect formations like voids, non-uniformity, or inadequate bond strength, consequently impacting the reliability and longevity of the weld. This constraint is not merely a technical formality but a critical parameter governing the successful application of electrofusion welding in industries leveraging HDPE.

7.3.2 Temperature Constraint for middle pipe layer

One of the key factors shaping the design optimization is the temperature in the middle layer of the TCP. To ensure the durability and strength of the thermoplastic composite material, it is crucial to keep the temperature in this layer below a certain limit known as $T_{allowable}$. This limit is carefully chosen to match the consolidation temperature of the GF/HDPE tapes and assumed in this analysis as the melting temperature of HDPE (131 ^{0}C). This decision is made to protect the mechanical properties of the GF/HDPE composite material over time and avoid future failures due to delamination of the composite. This temperature limit guarantees that even during welding, the material's strength is not compromised. Adhering to this strict temperature limit ensures that the design of the electrofusion fitting effectively maintains the thermal integrity of the TCP system.

7.3.3 Overall welding temperature constraint

Maintaining the long-term strength and performance of the welded joint is crucial. To prevent any detrimental effects on the thermoplastic composite layer nor the HDPE cover/liner, during fusion, we set a strict limit on the welding temperature. This limit is chosen to be below the degradation temperature of HDPE, known as T_{deg}, which is approximately 330-350°C [45]. By adhering to this constraint, we ensure that the welding process does not subject the HDPE material to conditions that could compromise its structural integrity. This careful approach guarantees the durability and performance of the TCP over time.

7.3.4 Length of melting zone constraint

The dimension of the melting zone within the electrofusion fitting holds a pivotal role in preserving joint integrity and optimizing mechanical performance. The extent of this melting zone is required to be no less than the measurement derived from an independent stress analysis investigation [74]. This stipulation ensures the attainment of adequate material intermixing and the establishment of an optimal fusion bond between the fitting and the TCP. It is noteworthy that a distinct and comprehensive study focused on stress analysis and axial loadings has been undertaken, yielding crucial insights into the minimum requisite length of the fusion zone. This data-driven approach, involving a thorough examination of the operational pipe conditions, solidifies the fusion zone's capability to withstand the loadings and stresses inherent to the functioning of the pipe network.

Thus, the constraint of the length of melting zone can be expressed as:

$$L_{fz} => L_{fz}\ (minimum\ or\ required)$$

For GF/HDPE TCP with 100 bar pressure rating, the minimum fusion zone required is around 64 cm for each pipe in the single fusion zone design, and 32 cm for each in the double fusion zone design [76].

7.4 Design parameters

7.4.1 Design geometry

Within the realm of optimizing the electrofusion fitting design, the geometry of various components holds a significant role in achieving a robust joint. This section explores the geometric aspects that exert a direct influence on the fitting's performance and thermal behaviour. These parameters include the fitting length, wire length (expressed as the number of turns), wire diameter, depth of wire insertion, and the pitch size between successive wire turns.

Fitting Length

In the pursuit of an optimized electrofusion fitting design, the extent of the fusion zone coverage across the fitting's width holds paramount importance. Ensuring the integrity of the joint involves determining an appropriate fitting length that accommodates the entire fusion zone along with necessary safety margins. The recommended fitting length, denoted as L, can be expressed as the fusion zone length supplemented by a safety margin on both sides. A typical safety margin, often ranging between 10% to 20% of the fusion zone length, serves to bolster the joint's robustness. Mathematically, if L_{fz} represents the fusion zone length, the fitting length L can be calculated using the equation:

$$L = L_{fz} + 2(0.10L_{fz}) \tag{7.1}$$

This equation simplifies to:

$$L = 1.20\, L_{fz} \tag{7.2}$$

By adhering to this methodology, the electrofusion fitting's dimensions are meticulously tailored to embrace the fusion zone while ensuring that a prudent safety margin contributes to the overall joint performance.

Wire diameter

The diameter of the heating wire profoundly influences the heat generation and distribution within the electrofusion fitting. A balance must be struck between wire diameter and power input to attain uniform heating, contributing to a well-bonded joint. In this study, wires with diameter of 1.5 and 3 mm which are reasonable assumptions for the size of the pipe considered.

Depth of wire insertion:

The depth to which the heating wire is inserted within the fitting bears a direct impact on the heat transfer efficiency and the extent of material intermixing. Optimizing this depth ensures that the fusion region encompasses the required volume for effective bonding. For this study, exposed wires (at the surface of the fitting) were analysed and then the depth was optimized to meet the constraints requirement by changing the depth to multiples of the diameter of the wire (i.e. depth= D_{wire}, $2D_{wire}$, $3D_{wire}$)

Pitch size between wire turns

The pitch size, indicative of the distance between successive wire turns, contributes to the even distribution of heat and pressure during the welding process. A suitable pitch size aids in achieving consistent fusion quality across the joint interface. The pitch can be expressed as the diameter of the wire in addition to some space *S*.

$$Pitch = D_{wire} + S \tag{8.3}$$

where,

D_{wire} is the diameter of the wire.

S is the distance between two adjacent wire turns in some applications, a space equals to the wire diameter or 2 times the wire diameter (i.e., $S=2\ D_{wire}$) was chosen for simplicity and uniform heating. In such a case substituting in equation 7.3,

$$Pitch= 2D_{wire}\ or\ 3D_{wire} \tag{7.4}$$

Wire length (number of turns):

The wire length, often quantified by the number of turns, holds significance in establishing the extent of heat generation during the welding process. The appropriate number of turns ensures uniform heat distribution along the joint interface, vital for achieving consistent and reliable fusion quality. The number of wires can be initially approximated as,

$$N_{wires}= L_f /Pitch \tag{7.5}$$

Substituting the relation from the pitch definition from equation 7.4,

$$N_{wires} = L_f / 3D_{wire} \quad (7.6)$$

It is important to mention while the pitch largely determines the length of the fusion zone, the effective melting and bonding will also be influenced by the current passed through the wire, heating time, wire material, and the plastic material being fused.

The chosen gap between turns will also play a role in determining the evenness of the heat distribution. A smaller gap results in more uniform heating but might require more precise manufacturing controls. On the other hand, a larger gap results in cooler spots between the turns as discussed earlier in Section 2.3.3.

7.4.2 Welding power and time

This section explores the intricate interplay between two critical design control parameters, namely welding power and time, that profoundly influence the electrofusion welding process. The welding power input and heating duration are pivotal factors shaping the distribution of heat along the joint interface during the fusion process. By effectively manipulating these parameters, the fusion process can be optimized to achieve ideal heat generation and material intermixing, ultimately contributing to the quality and integrity of the joint. This investigation serves as a foundational step towards enhancing the understanding of the combined influence of welding power and time on the intricate thermal dynamics of the electrofusion welding process for TCP.

Welding Power

The influence of welding power as a control parameter on the electrofusion welding process is significant. By adjusting the welding power, the amount of heat generated during the process can be finely tuned. This directly affects the temperature distribution, material intermixing, and ultimately, the quality of the joint. Proper modulation of welding power allows for precise control over the fusion process, ensuring optimal bonding and thermal distribution within the fitting and TCP.

Welding time

In the realm of electrofusion welding, time functions as a pivotal control parameter with a pronounced impact on joint quality. The duration for which the welding process is maintained affects the heat input, material intermixing, and the extent of fusion. Adjusting the welding time can lead to variations in temperature profiles and heat penetration depths.

In electrofusion welding, the time required to achieve complete melting is intrinsically linked to the power supplied by the welding machine and how this power is distributed across each individual wire.

7.5 EF fitting designs optimization

This section delves into the pivotal phase of the fitting design optimization process, presenting a systematic formulation of the optimization problem. The objective is to tailor the electrofusion fitting design to best accommodate the intricate demands outlined in the earlier sections while adhering to the established design constraints. This encompasses the parameters related to geometry, welding power and time, and the critical temperature constraints within the TCP system.

To commence the design optimization process, it is imperative to first address an initial estimation problem, as delineated in the design parameters found in Section 6.4. Upon obtaining the results, one should cross-reference them with the design constraints outlined in Section 7.3. If the outcomes are in alignment with these constraints, it signifies a satisfactory progression. Conversely, if they do not meet the stipulated criteria, it becomes necessary to undertake further optimization. This can be achieved by adjusting the relevant design control parameters.

To unravel the optimization process, a comprehensive flowchart in Figure 7-3 is presented, outlining the sequential steps. This chart details the iterative nature of the optimization, encompassing the evaluation of fitting designs, comparison with design constraints, adjustment of parameters, and further iterations until an optimal solution is achieved.

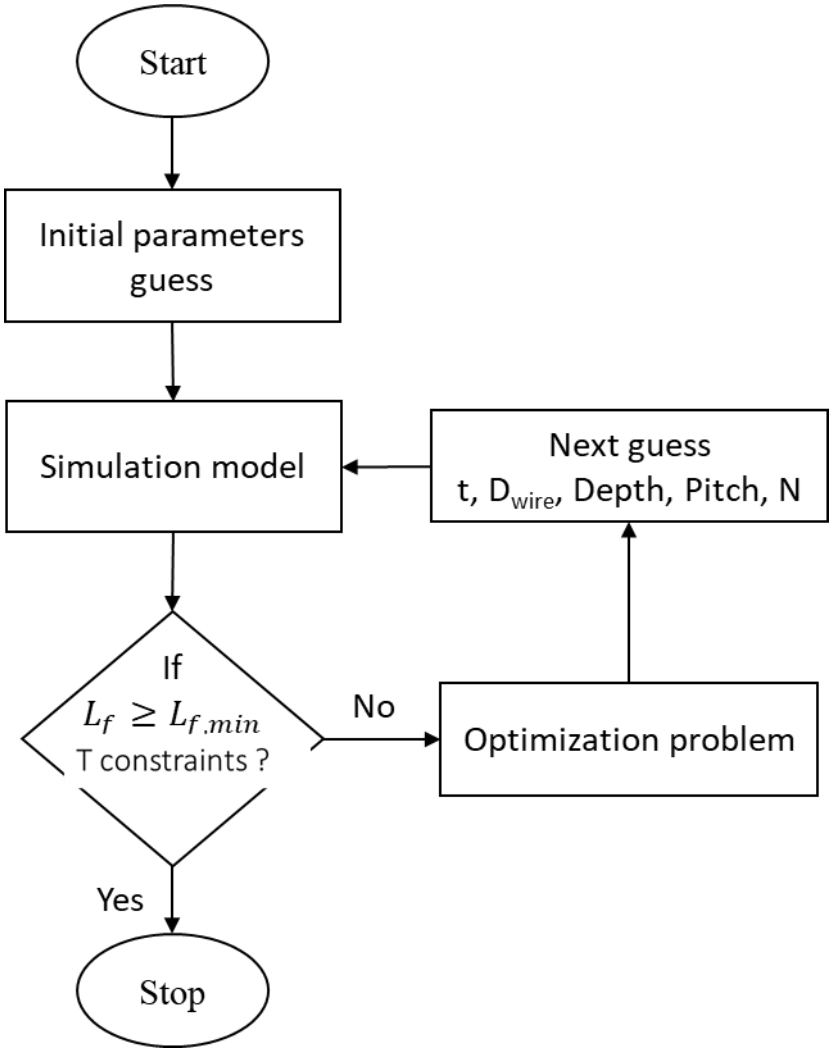

Figure 7-3 Design optimization process

Solving settings encompassing the meshing strategy, time-dependent solver, and convergence criteria are configured to facilitate precise determination of heat transfer during electrofusion welding for each proposed fitting design. This iterative process ensures that the selected designs exhibit exceptional thermal integrity, attesting to their ability to perform within specified constraints.

By encapsulating the formulation of the optimization problem, the intricate process of proposing, evaluating, and refining fitting designs is systematically elucidated. This section serves as a bridge between theoretical understanding and practical application, demonstrating how advanced simulation methodologies can culminate in fitting designs that harmoniously align with the multifaceted demands of the TCP system.

7.6 Results

7.6.1 Single fusion zone

In this section the temperature behaviour at critical locations during the electrofusion welding of the single fusion zone design concept was analysed. Meeting the design constraint presented earlier in Section 7.3 is crucial for ensuring the quality of the welded joint. The assumptions presented in Table 22 are the result of an iterative process to match the design requirement for the single fusion zone fitting concept.

Table 22 Design parameters for single fusion zone fitting design

Parameter	Value
Pressure	100 bar *
$L_{f,min}$	64 cm for each pipe **
Wire diameter	1.5 mm
Pitch	4.5 mm
Number of wire turns	144*2
Depth of wire	0.75 mm (exposed wires)

* Pressure requirement for the new design of electrofusion fitting

** Fusion zone length requirement from the strength analysis study to match the pressure rating

The required power and time based on commercially available electrofusion welding machine is presented in Table 23 with the aim to meet the design constraints reached by the iterative design optimization process.

Table 23 Power and time requirement for single fusion fitting design

Parameter	Value
Welding power	15 kW*
Welding time	240 s
Cooling time	15 minutes

*The welding power 15 kW is around 6.25 higher than the ECU used in the physical test in Chapter 4.

- **The length of fusion zone**

The fusion zone length shown in Figure 7-4 clearly indicates that the set of used design geometry and power input have met the required fusion zone length of 64 cm for each pipe. The time taken to the actual start of melting the polymer is around 100 seconds this includes heating the wires and the energy needed for phase change. The time to reach the required fusion length is about 180 seconds of heating. It was not possible to stop heating at 180 seconds to account for meeting other constraints.

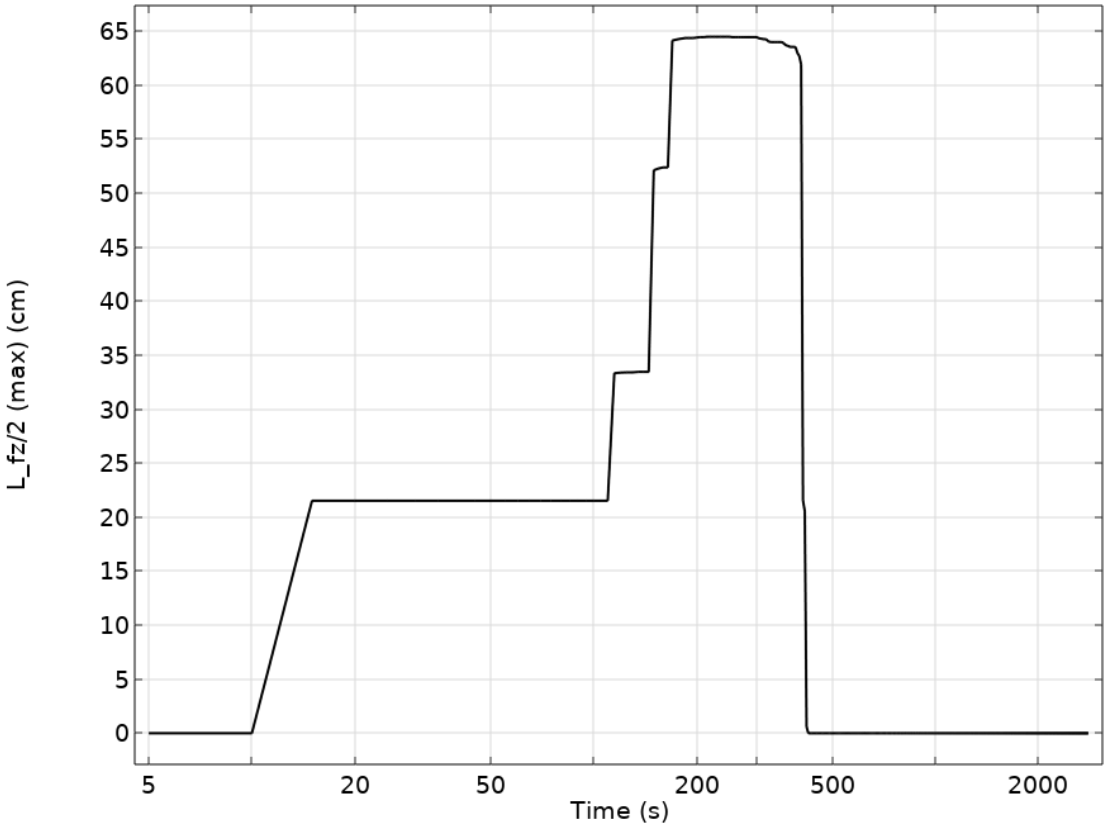

Figure 7-4 The simulated fusion zone length of each pipe

- **The welding interface temperature**

The joint interface temperature shown in Figure 7-5 indicates that the set of used design geometry and power input have met the required welding interface temperature as indicated in section 7.3.1. The peak temperature is slightly above 200 ^{0}C which fall in the range of 200-220 ^{0}C as per DVS 2207-1.

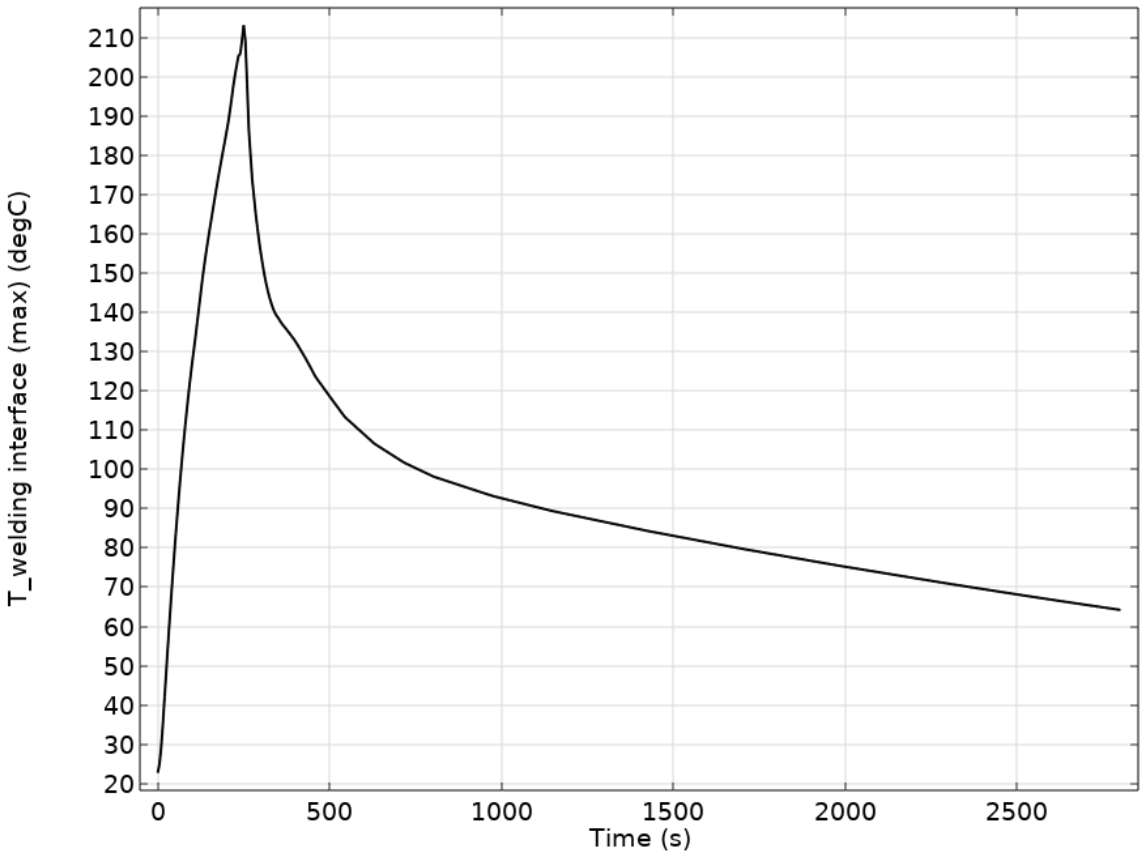

Figure 7-5 The simulated temperature at the welding interface

- **The overall maximum temperature in the HDPE at the boundaries of the wires**

The temperature of the adjacent polymer to the wires shown in Figure 7-6 indicates that the set of used design geometry and power input have met the required overall maximum temperature as indicated in section 7.3.3. The peak temperature is slightly above 340 ^{0}C which is at the upper bound of the allowable temperature to avoid polymer degradation.

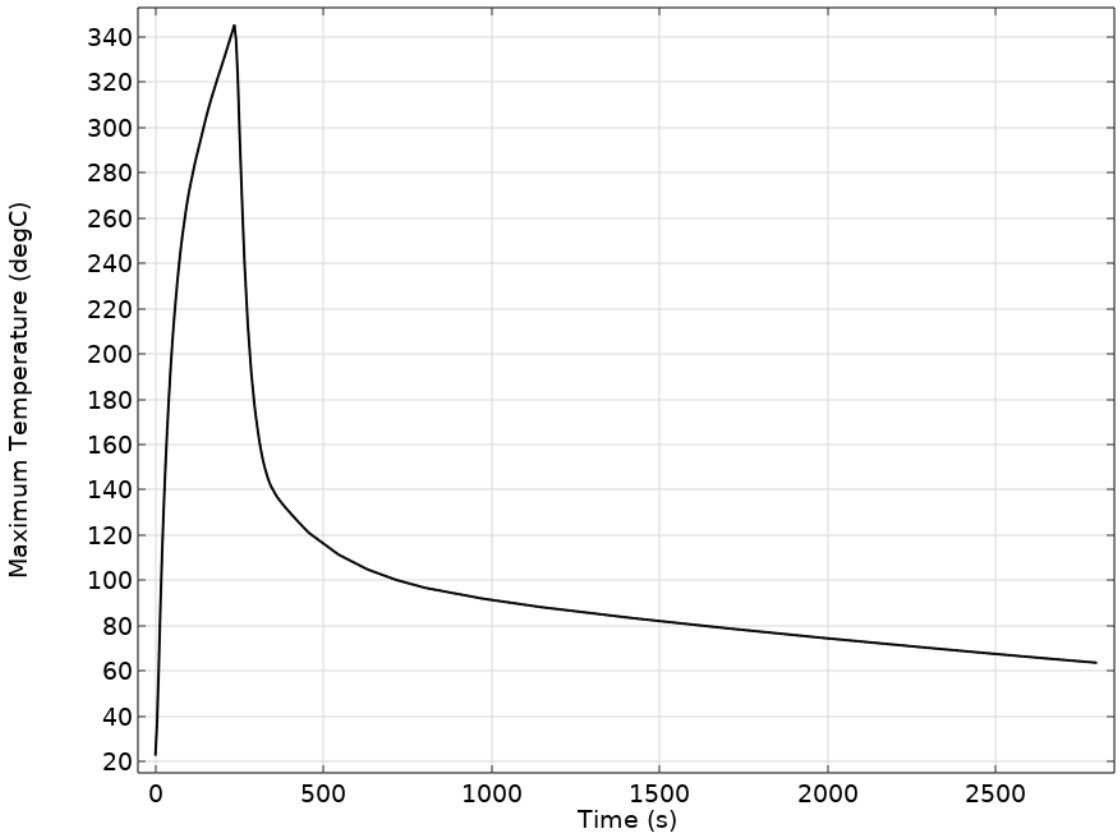

Figure 7-6 The simulated maximum temperature at the wires boundaries

- **The reinforcement GF/HDPE laminate temperature**

The maximum temperature at the GF/HDPE reinforcement shown in Figure 7-7 indicates that the set of used design geometry and power input have met the allowable temperature for the laminate as indicated in section 7.3.2. The peak temperature is slightly above 105 ^{0}C which is at the acceptable levels to maintain the integrity and mechanical performance of the pipe's middle layer.

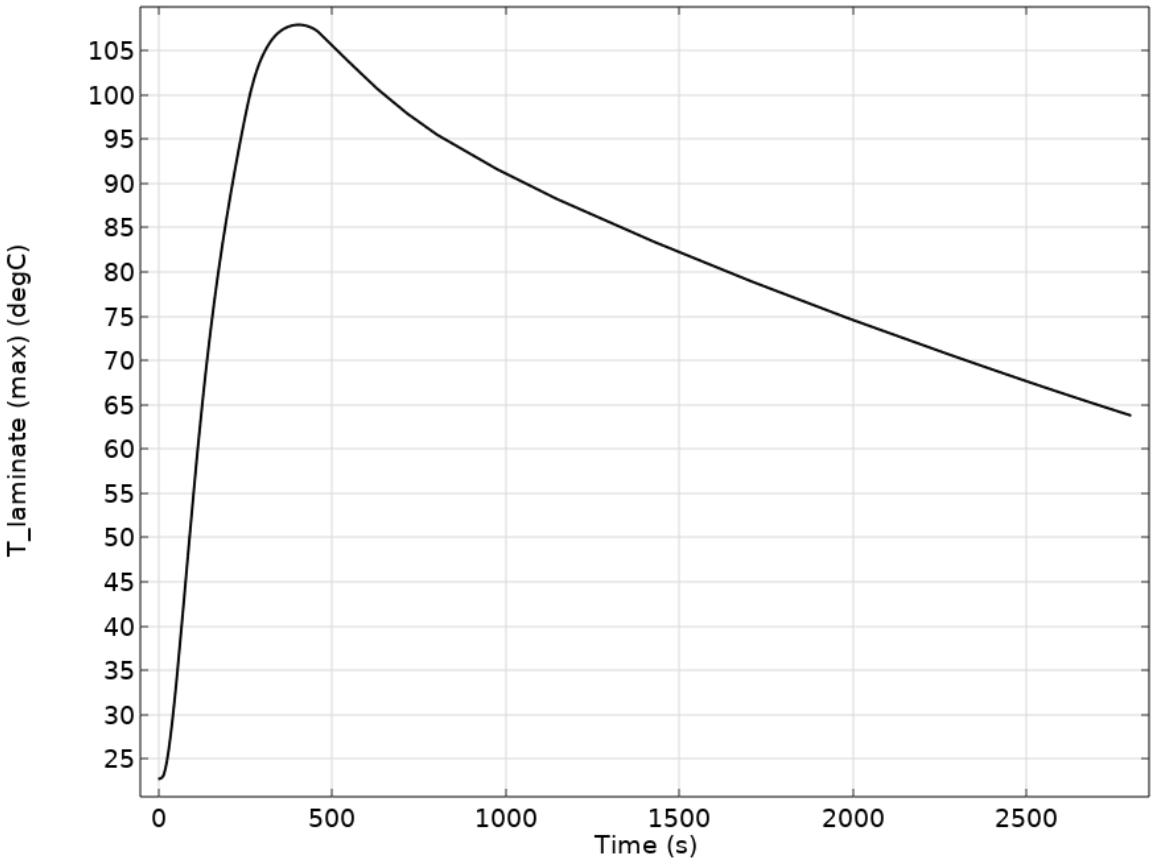

Figure 7-7 The simulated temperature at the laminate interface

- **The external fitting temperature**

The maximum temperature at the fitting external surface shown in Figure 7-8 indicates that the set of used design geometry and power input have met the allowable temperature for the fitting external surface at lower than 80 ^{0}C matching the recommended temperature from literature.

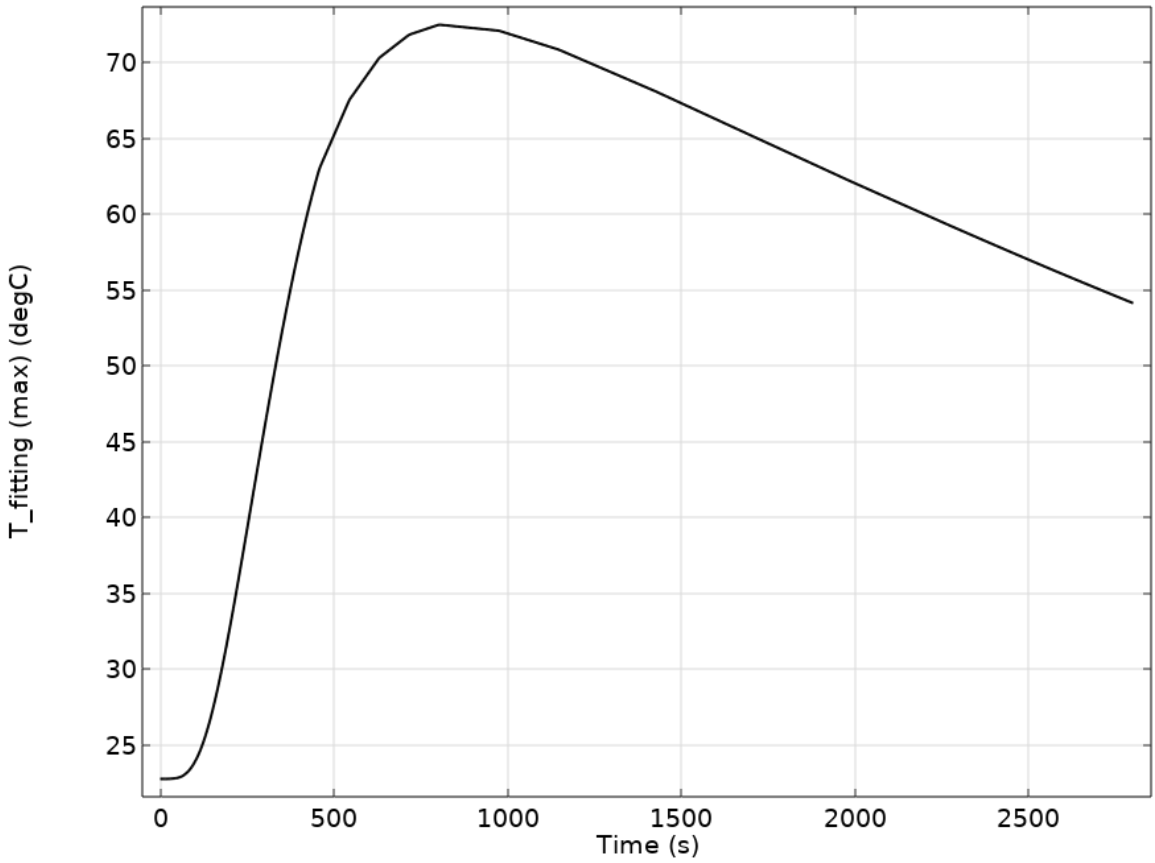

Figure 7-8 The simulated temperature at the external surface of the fitting

7.6.2 Double fusion zone results

In the case of the double fusion zone design concept, the iteration process had been more complicated compared to the single fusion zone design. The rationale for this was the accumulative heat transfer to the laminate surface from both sides of the fitting, namely the cover and the liner. In figure 7-9, it was clear how the heat transferred through the fitting surface, with the arrow lines indicating the local flow direction of heat transfer at the surface. This risk had been incidentally discussed in section 2.1.5, and it was now substantiated by the developed heat transfer FEA. Thus, careful wiring placement was studied, and the outcome was to have different depths of wires at the cover and the liner. Alternatively, it was crucial to augment the thickness of the TCP cover layer to preclude excessive heating to the GF/HDPE laminate.

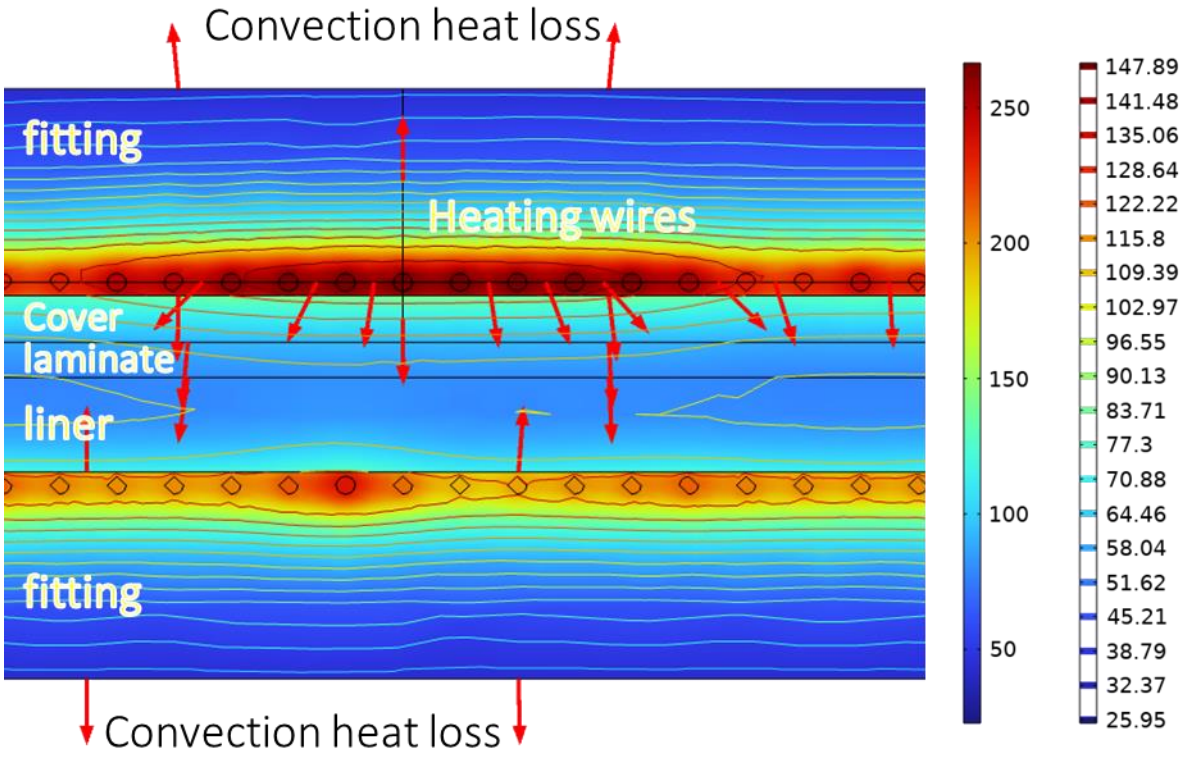

Figure 7-9 Surface temperature and arrow lines in the double fusion zone concept

In this section the temperature behaviour at critical locations during the electrofusion welding of the double fusion zone design concept was analysed. Meeting the design constraint presented earlier in Section 7.3 is crucial for ensuring the quality of the welded joint. The assumptions presented in Table 24 are the result of an iterative process to match the design requirement for the single fusion zone fitting concept.

Table 24 Design parameters for double fusion zone fitting design

Parameter	Value
Pressure	100 bar*
$L_{f,min}$	32 cm for each pipe**
Wire diameter	1.5 mm
Pitch	4.5 mm
Number of wire turns	73 * 4
Depth of wire at the cover	1.125 mm
Depth of wires at the liner	0.75 (exposed wires)

* Pressure requirement for the new design of electrofusion fitting

** Fusion zone length requirement from the strength analysis study to match the pressure rating

The required power and time based on commercially available electrofusion welding machine with the aim to match the design constraints accomplished by the iterative design optimization process are the same used for the first concept in Section 7.6.1 with slightly less heating time difference of 10 seconds as presented in table 25.

Table 25 Power and time requirement for double fusion fitting design

Parameter	Value
Welding power	15 kW*
Welding time	230 s
Cooling time	15 minutes

*The welding power 15 kW is around 6.25 higher than the ECU used in the physical test in Chapter 4.

- **The length of fusion zone**

The fusion zone length shown in Figure 7-10 clearly indicates that the set of used design geometry and power input have met the required fusion zone length of 32 cm for each pipe. The time taken to the actual start of melting the polymer is around 50 seconds this includes heating the wires and the energy needed for phase change. The time to reach the required fusion length is about 130 seconds of heating.

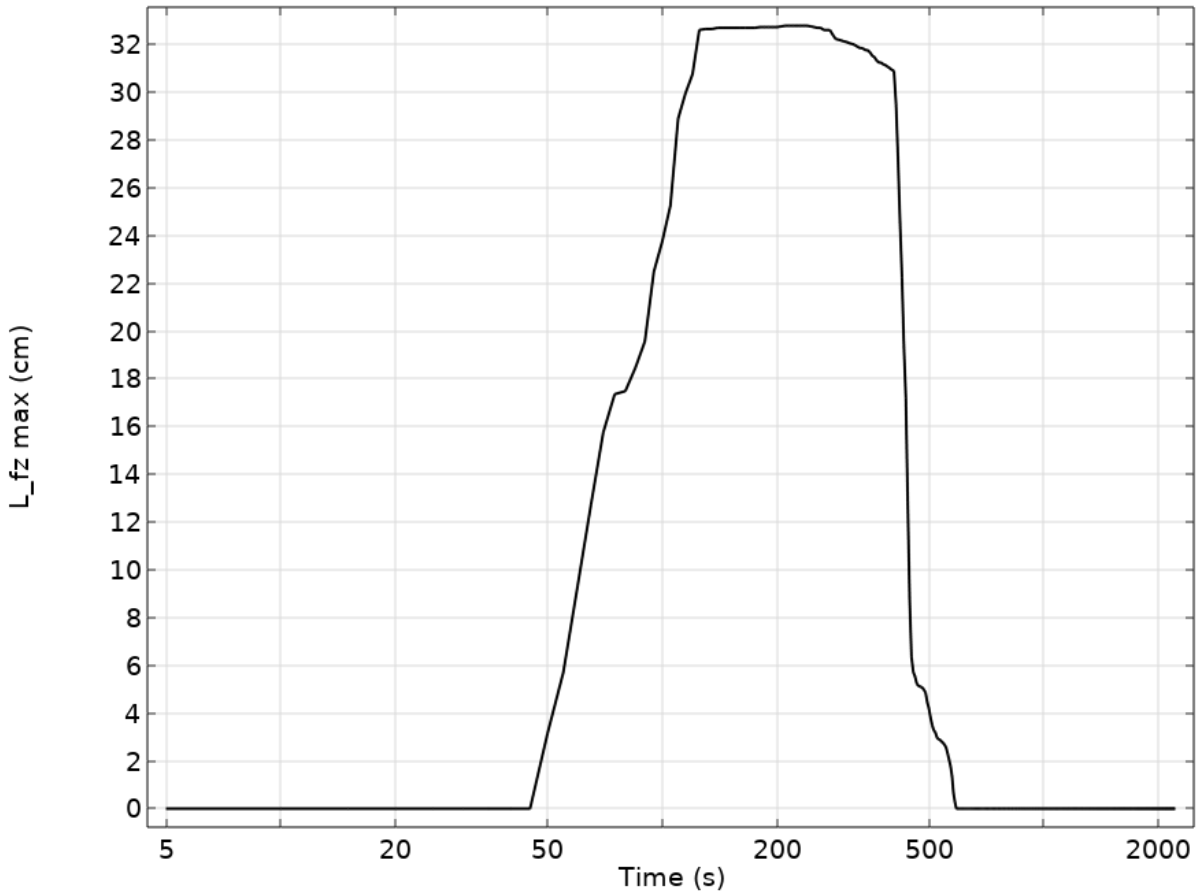

Figure 7-10 Simulated fusion zone length.

- **The welding interface temperature**

The joint interface temperature at both the cover and the liner interfaces shown in Figures 7-10 and 7-11 indicates that the set of used design geometry and power input have met the required welding interface temperature as indicated in section 7.3.1. The peak temperature is slightly above 200 ^{0}C at the cover interface and slightly above 220 ^{0}C at the liner interface.

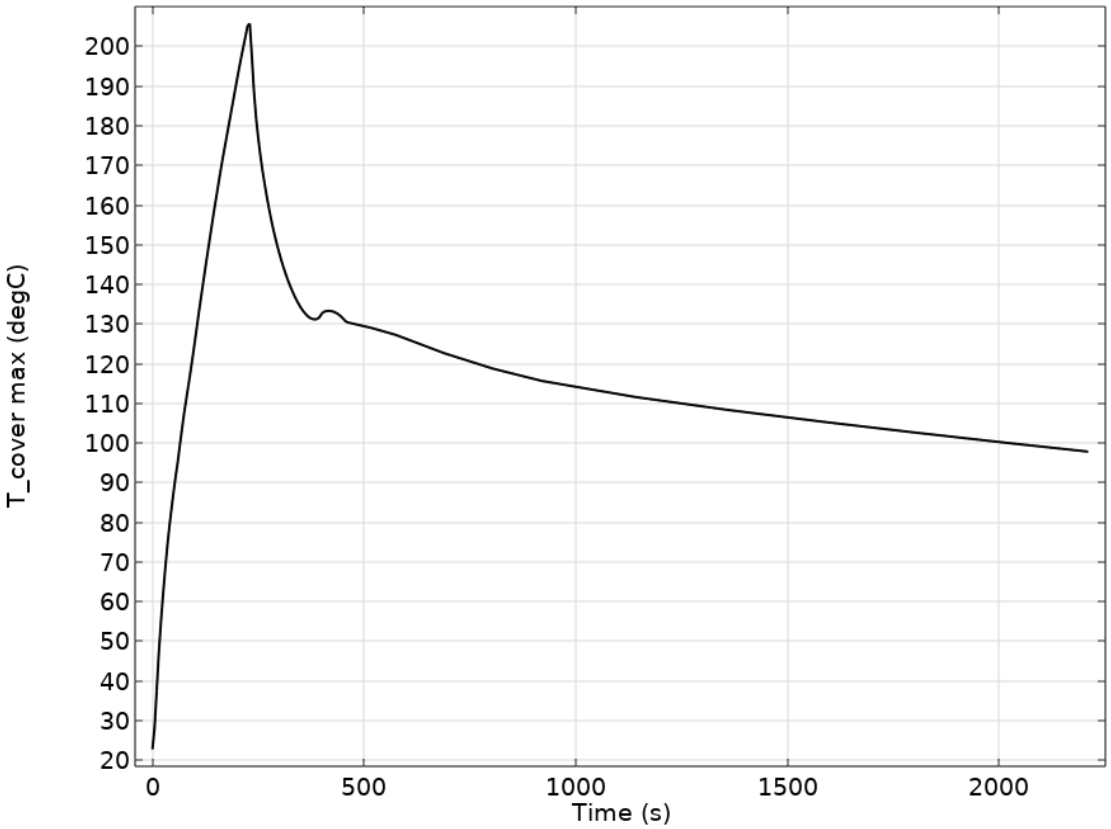

Figure 7-11 Simulated temperature at the welding interface of the cover

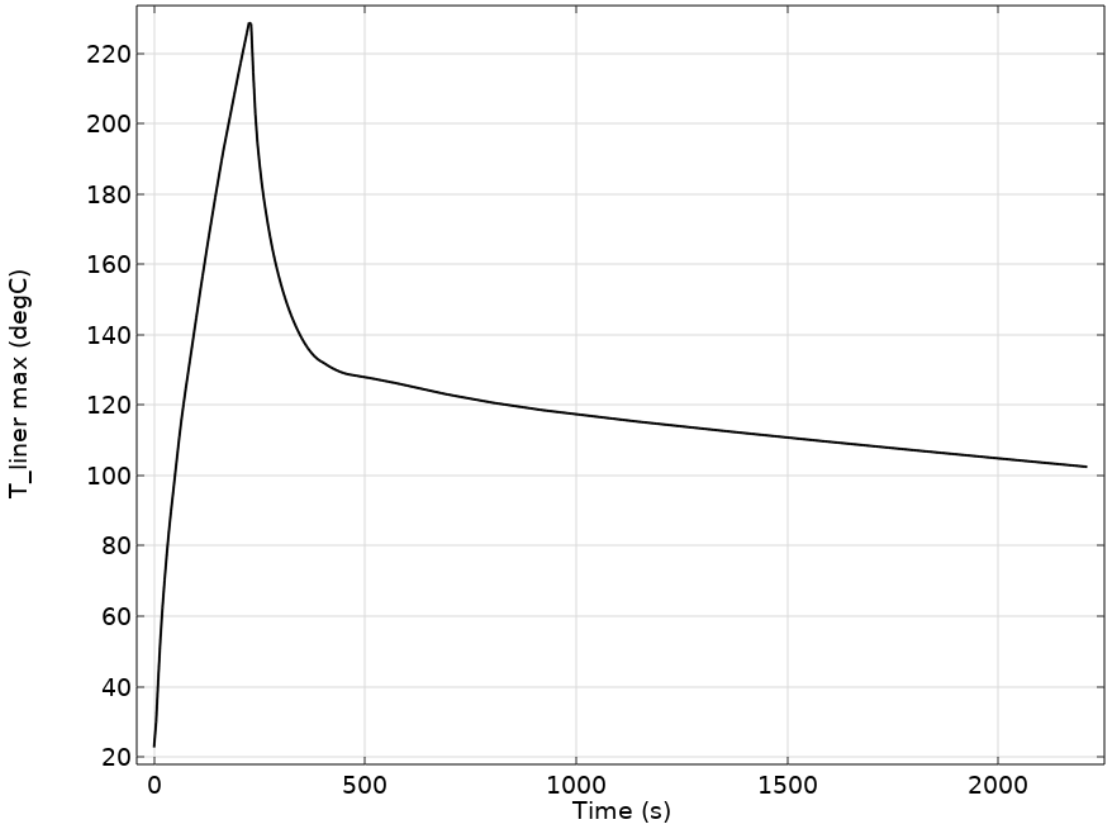

Figure 7-12 Simulated temperature at the welding interface of the liner

- **The reinforcement GF/HDPE laminate temperature**

The maximum temperature at the GF/HDPE reinforcement shown in Figure 7-13 indicates that the set of used design geometry and power input have met the allowable temperature for the laminate as indicated in section 7.3.2. The peak temperature is around 120 ^{0}C which is at the acceptable levels to maintain the integrity and mechanical performance of the pipe's middle layer.

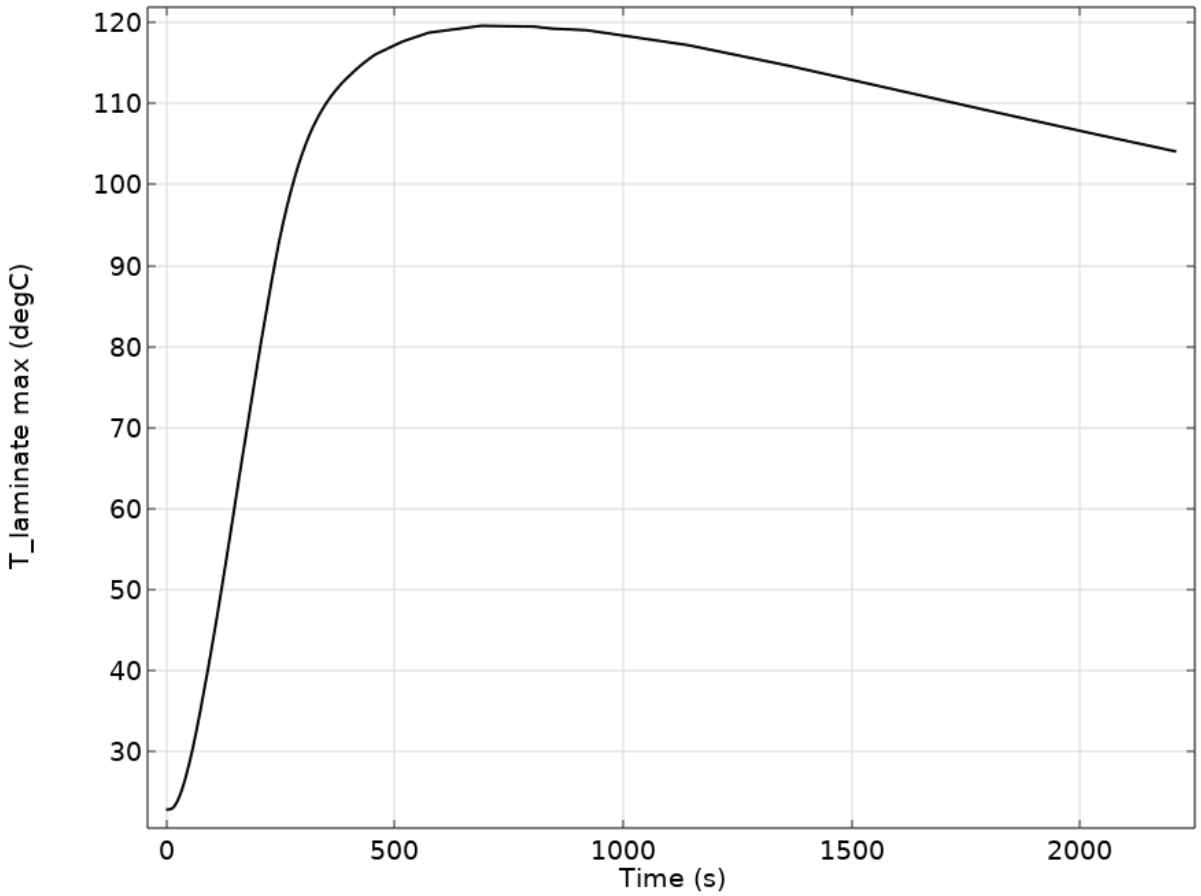

Figure 7-13 Simulated maximum temperature at the laminate surface

- **The overall maximum temperature in the HDPE at the boundaries of the wires**

The temperature of the adjacent polymer to the wires shown in Figure 7-14 indicates that the set of used design geometry and power input have met the required overall maximum temperature as indicated in section 7.3.3. The peak temperature is slightly above 310 ^{0}C which is at the acceptable levels of the allowable maximum temperature to avoid polymer degradation.

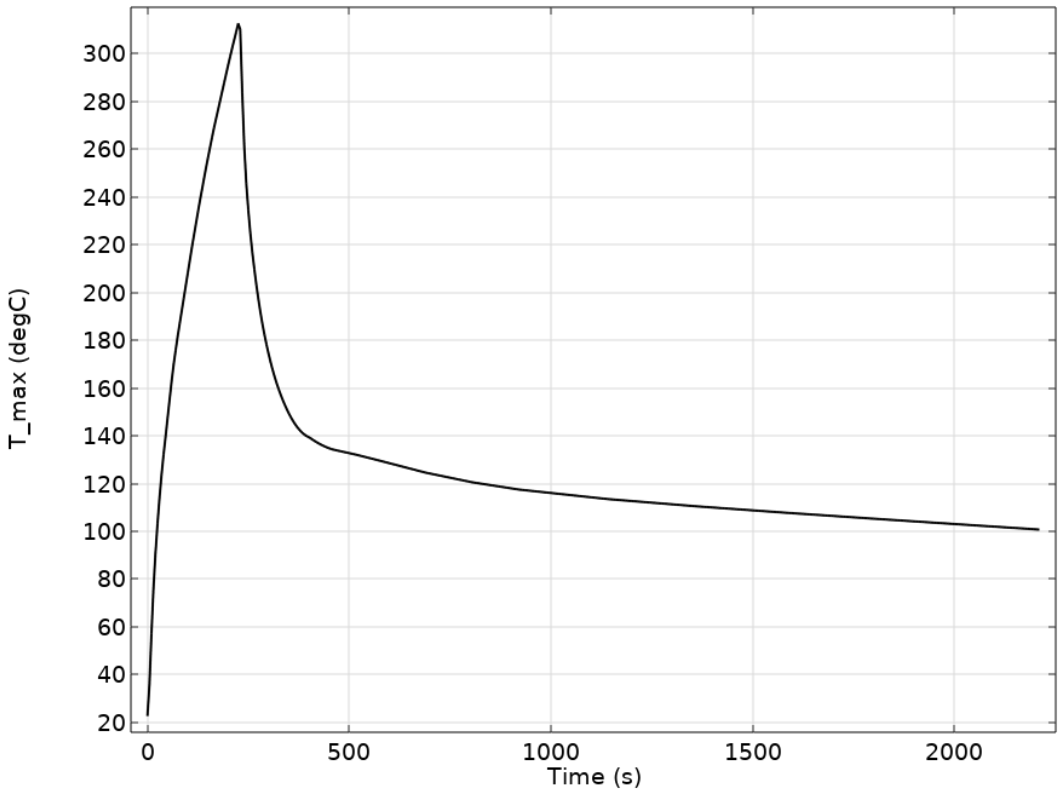

Figure 7-14 Simulated maximum temperature at the boundaries of the wires

- **The external fitting temperature**

The maximum temperature at the fitting external surface shown in Figure 7-15 indicates that the set of used design geometry and power input almost met the allowable temperature for the fitting external surface at slightly above 80 ^{0}C being close to the recommended temperature from literature.

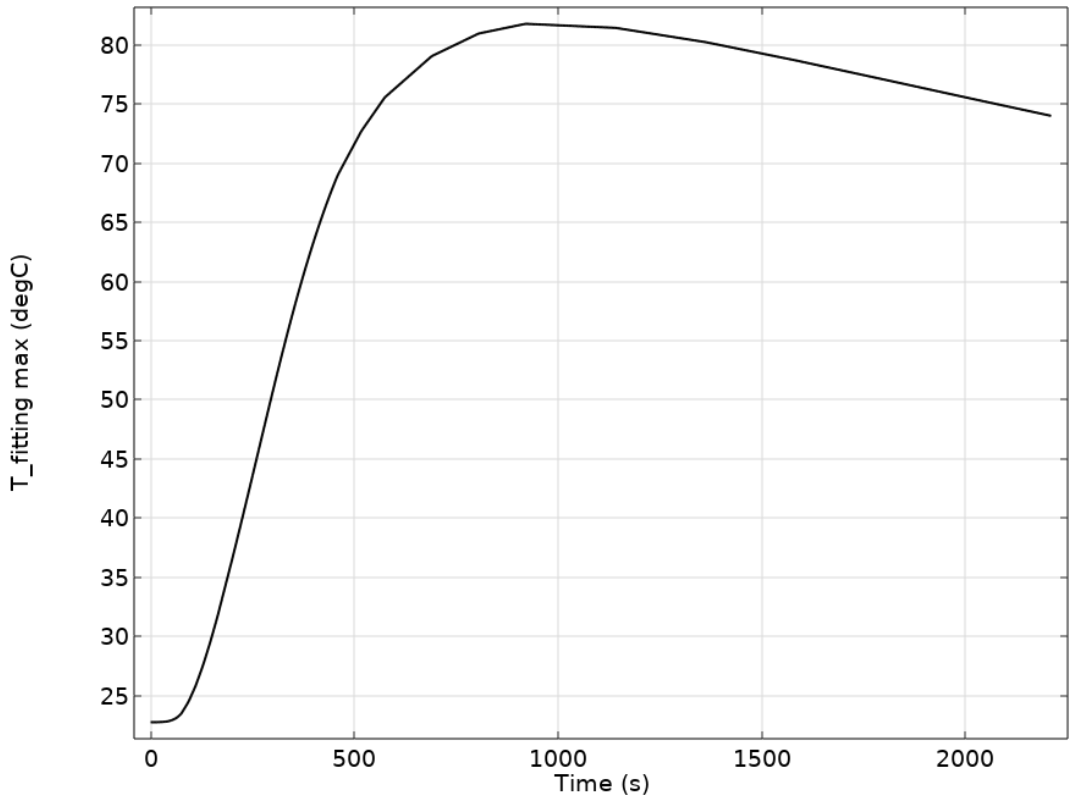

Figure 7-15 Simulated maximum temperature at the fitting surface

7.7 Conclusion

This Chapter illustrated the design optimization requirements for two distinct design concepts of FE fitting to join TCP, specifically focusing on single and double fusion zones. The necessary length of the fusion zone was obtained through separate strength analysis, with the study mainly concentrating on the heat transfer aspect of the design concept. The principal constraints included the welding temperature at the welding interface, the maximum permissible temperature within the polymer, and the peak allowable temperature at the GF/HDPE reinforcement. To streamline the design optimization problem, assumptions regarding the design geometry, specifically the length of the fitting, wire diameter, and pitch, were established. Nevertheless, the depth of the wire had to be factored into the iterative design optimization problem, in tandem with the power and time necessary for heating. Conclusively, a distinct design was offered for each of the design concepts, with the ensuing temperature constraints output appearing promising for both designs and satisfying all the stipulated design requirements.

Chapter 8

DISCUSSION, CONCLUSIONS & FUTURE WORK

This research investigated the complex aspects of heat transfer during electrofusion welding of Glass/HDPE Thermoplastic Composite Pipes (TCP). The main goal was to enhance the welding process parameters and coupler design to ensure lasting and high performing welded joints. By combining knowledge, experimental validation, and advanced simulation techniques this study has made significant contributions towards understanding the mechanisms of heat transfer, in TCP welding. The research on electrofusion welding of TCPs has unveiled several critical insights that bear significant implications for both the understanding and practical application of this welding technique.

8.1 Discussion

This study started with a literature review and market research for current and potential joining methods for TCP. After this electrofusion was chosen as a potential joining method suitable for the oil and gas application to replace the currently used metallic connecter and have a leak-proof thermoplastic connecter to eliminate any corrosion issues for the service life of the pipe. Electrofusion welding although it has been used for decades to join single layer thermoplastic pipes, however, risk is still present in handling the high operating pressure of TCP. Another risk is related to the heating process of electrofusion and associated danger of excessively heating the reinforcement layer, which may cause mechanical defects on this reinforcement, and thus, affecting the overall mechanical properties of the TCP.

The electrofusion welding physical test was a novel comprehensive procedure that integrated the pre-welding to the post-welding steps. The thermocouples installation process allowed for installation of thermocouples to capture the temperature readings on multiple locations in the pipe and fitting (Section 4.1). The IR camera allowed to capture the surface temperature at the fitting, confirming inconsistency of temperature readings along the circumference, suggesting the presence of air gaps or variable thermal contact resistances at the welding interface.

The post-welding CT scan allow the determination of the actual locations of these thermocouples after the test in addition to the observation of delamination among several areas in between the TCP layers. One paramount observation is the substantial influence of the pipe's initial quality on the welding process. The use of non-fresh pipe samples with a prolonged storage time led to suboptimal results, with visible cracks and inadequate bonding of the TCP layer. This underscores the importance of adhering to industry best practices, which stipulate that TCP should ideally be cut and joined within one hour to ensure the integrity of the composite layers.

The occurrence of pipe delamination a problem in composite pipes has been observed, although the exact causes are not yet fully understood. Several factors, such as cutting methods, manufacturing processes, thermocouple placements and weak bonding due to pressure accumulation during welding could contribute to this issue. A possible cause of delamination in TCP can be due to the release of build-up interlaminar stresses from spooling the pipe. Therefore, it is important for research efforts to focus on thorough investigations aimed at identifying the underlying reasons behind delamination.

The placement of thermocouples was found to affect the roundness of the pipe. Uncertainty arose regarding the location of these thermocouples particularly within the fitting area where many thermocouples became dislodged during transient CT scan analysis. It was apparent that the sealing material used for these thermocouples was not suitable for this application and that the connection of thermocouple wires was delicate. Optimizing these installation procedures is essential, for maintaining accuracy.

The 2D axisymmetric simulation model that was developed had a feature; it could accurately capture the temperature profile at various points on the TCP even though it primarily considered heat transfer through conduction and temperature gradients. To enhance the simulation model a process parameter estimation was performed using optimization with the least squares method. However, it is evident that incorporating factors like melting phenomena, thermal stresses, deformation, variations in ovality and potential air gaps can greatly improve the accuracy and predictive capabilities of the model.

Extensive research was conducted on the fusion zone using both an optimized simulation model and experimental measurements. Furthermore, there is room for exploration of material properties such, as density and reinforcement characteristics to refine the welding process and achieve desired fusion zone lengths. It should be noted that in a scenario where pipes are fully bonded together fusion zone length requirements would decrease, potentially resulting in smaller fittings and reduced power consumption. However, the proposed model and design were tailored to accommodate pipe conditions while also providing flexibility to adapt to different input data and temperature constraints during welding processes.

Finally, design optimization was considered, emphasizing the potential benefits of higher power requirement, albeit without considerations for real-world factors like wind speed. This highlights the need for an adaptive approach to electrofusion welding, accounting for environmental variables to ensure consistent and reliable results in practical applications. The less the power input had longer time to match the required temperature constraints.
Although it was found that longer heating time has higher effect on the GF/HDPE laminate temperature. In figure 8-1 the temperature constraints for the double fusion zone is presented. In this design concept higher temperature gradient to the reinforcement was observed, thus the wiring depth were carefully mounted in the simulation model. The different wiring configuration could have negative impact on the complexity of the fitting production process.

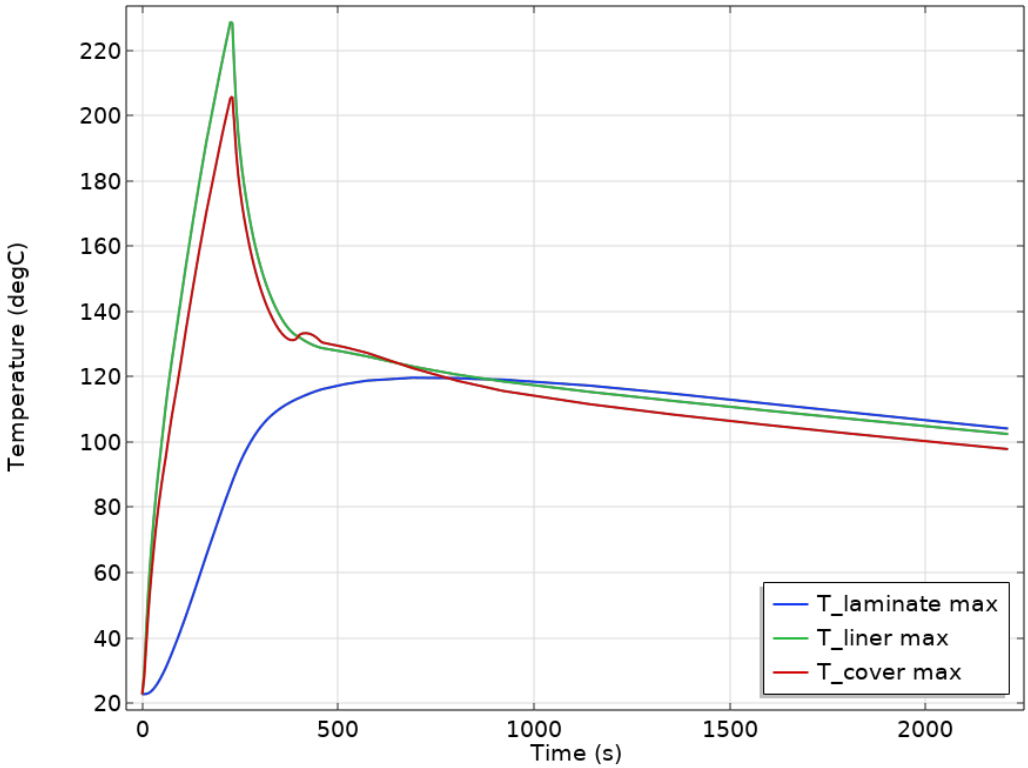

Figure 8-1 Simulated temperatures for the double fusion zones EF fitting concept

The entire design optimization problem was indeed had a promising outcome to set the foundation for designing an electrofusion fitting for TCP, saving time, equipment and cost by the utilization of advanced simulations.

However, the whole design optimization problem can be enhanced with coupling both the heat transfer model with the strength analysis model to run one entire design optimizing problem that can potentially optimize the overall geometry of the fitting and reduce the cost of material and manufacturing. Exploration of further materials with enhanced properties could significantly enhance the fitting using reinforcement or additives.

Finally, further industrial collaboration to produce and pilot test this advancement in technology is required to accelerate the adopting of EFW technology for high pressure TCP applications in oil and gas and other sectors. This heat transfer study combined with the strength analysis study on EFW of TCP had brought insights, discussed associated problems and open a new area of research to be

In conclusion, this research lays the foundation for further investigations and refinements in electrofusion welding techniques for TCP, with a focus on improving both the theoretical understanding and practical implementation of this crucial technology.

8.2 Evaluation of research objectives

The research objectives outlined in Chapter 1 were systematically pursued and evaluated to achieve a comprehensive understanding of heat transfer dynamics during electrofusion welding of Glass-HDPE Thermoplastic Composite Pipes (TCP)

1. To investigate existing commercial coupler designs to analyse their performance and identify potential areas for improvement.

During the investigation of existing commercial coupler designs, insights into their performance was gained and areas where improvements could be made were identified. This examination served as a starting point for refining the coupler design to achieve joint integrity. To enhance this assessment, a market research was conducted to review recent literature and explore innovative techniques like butt fusion and electrofusion welding with metallic free fittings .

2. To develop a reliable model for heat transfer during electrofusion welding of TCP, considering the complexities of the composite material and the welding process.

One notable achievement was the development of a heat transfer model specifically for TCP electrofusion welding. This model took into consideration the dynamics between composite materials and the welding process resulting in more accurate predictions and advancing the understanding of this field. Creating this model was a step forward both in terms of enhancing the knowledge of the process and pioneering new modelling methods, for TCP electrofusion welding.

3. To measure the required material thermal properties to accurately incorporate them into the model and improve the accuracy of predictions.

The model's accuracy was enhanced by incorporating the thermal properties of materials using meticulous measurements. Various thermal tests, such as LFA, TPS and DSC were conducted to determine factors like thermal conductivity, specific heat capacity and melting temperature. This high level of precision did not improve the models predictive capabilities but also ensured that theoretical simulations aligned well with real world observations.

4. To conduct experimental testing to validate the developed model and verify the effectiveness of the optimized process parameters.

In this research experimental testing played a role in validating the developed model. By subjecting the models' predictions to examination, we not only confirmed its effectiveness but also established a strong foundation for future optimization efforts. It is worth mentioning that we implemented a method for installing thermocouples allowing comprehensive temperature measurements, across different locations during two separate physical tests.

5. To perform a sensitivity analysis on critical welding parameters to understand their influence on heat transfer and joint quality.

Alongside the visual comparison of simulated and experimental data, a comprehensive statistical analysis was undertaken to establish a foundation for optimizing control parameters. Additionally, a sensitivity analysis was executed on pivotal welding parameters, shedding light on their influence on the heat transfer during welding. This exploration not only enriched the comprehension of the significance of these parameters but also served as a guiding compass for subsequent optimization initiatives.

6. To analyse the melting area and define the temperature distribution and behaviour around the composite laminate during the welding process

By examining the melting region and temperature distribution surrounding the composite laminate, valuable insights were gained into the fusion length and width. This in depth understanding played a role, in the optimization process enabling to tailor solutions that enhance joint strength and overall reliability.

7. To optimize the welding process parameters to achieve the desired joint strength, integrity, and long-term performance.

The successful optimization of welding process parameters aimed to achieve specific joint characteristics, aligning with strength requirements established through comprehensive strength analyses across various pressure-rated pipes. This accomplishment underscores the harmonization of theoretical understanding, empirical validation, and sophisticated modelling approaches, all dedicated to enhancing welding outcomes. These optimized outcomes have been seamlessly integrated into two distinct electrofusion fitting designs.

8. To achieve a reliable design of electrofusion fitting for TCP based on the research findings, incorporating the optimized process parameters and coupler design recommendations.

The successful integration between strength analysis and heat transfer analysis put the stone in achieving and suggesting multiple suitable EF fitting designs for TCP. A design problem formulation and requirements were developed by the clear understanding of the system design constraints. The final design parameters for the two design concepts for EFW of 100 bar TCP using 15 kW ECU unit, 1.5 mm wire diameter and 4.5 mm pitch are as follow,

For the single fusion zone EF fitting design,

Wire depth = 0.75 mm (exposed)

Number of wire turns = 144*2

Heating time = 240 seconds

For the double fusion zone EF fitting design,

Wire depth at the TCP cover = 1.125 mm

Wire depth at the TCP liner = 0.75 mm (exposed)

Number of wire turns = 73 * 4

Heating time = 230 seconds

In summation, the evaluation of these research objectives underscores the comprehensive nature of this study, which amalgamated theoretical, experimental, and simulation methodologies to advance the understanding and practice of TCP electrofusion welding. Each objective's attainment adds to the broader knowledge in this domain and contributes insights with relevance to industries reliant on robust welded joints.

8.3 Contribution to the knowledge

This research has significantly advanced the understanding of electrofusion welding processes for (GF/HDPE) thermoplastic composite pipes. The contributions made in this study encompass,

First-of-its-Kind TCP EFW FEA model

A groundbreaking FEA model has been developed specifically for EFW processes allowing for simulation of heat transfer through the three distinct layers of HDPE/GF TCP. This innovative model not provides valuable insights into the complex dynamics of the welding process but also establishes a foundation for future research in this field.

Comprehensive experimental study

An extensive and meticulous experimental study on EFW has been conducted, incorporating the installation of thermocouples in an innovative manner. The procedures have been outlined within a framework providing a comprehensive approach that generates a rich dataset, for further analysis and enhances the reliability of the research findings.

Methodological data comparison and validation

A systematic and methodological procedure has been devised to compare and validate data obtained from simulations and experiments. This ensures that the simulation model is not theoretical but closely aligns with real world observations contributing to the robustness of the research.

Optimization driven design

A notable contribution is integrating the validated heat transfer simulation model with requirements derived from stress analysis results. This unique approach enables the design of EFW fittings that're both thermally efficient and structurally robust catering to diverse industry applications.

Practical Relevance

In addition to providing insights this research aims to bridge the gap between academic findings and industry applications. By conducting experiments and prioritizing collaboration with industrial partners the outcomes of this study have immediate practical importance. They address the needs and challenges faced by the industry in TCP welding processes.

In summary, this research represents an advancement in the understanding of EFW processes, for GF/HDPE TCP. It offers both contributions and practical solutions that can benefit the industry. The integration of FEA modelling, experimentation, data validation and optimization driven design highlights the multidisciplinary significance of this work and its potential to shape the field of thermoplastic composite pipe welding.

8.4 Recommendation for future work

Validation through Varied Test conditions

To validate the reliability and adaptability of the simulation model we should expand the range of tests to include various environmental conditions like temperature and humidity fluctuations. It is also important to examine how different fitting sizes affect the electrofusion welding process. These comprehensive experiments will help us verify that the simulation model can effectively simulate real world scenarios.

Simulation model enhancement

Enhance the simulation model by considering the complexities associated with gap clearance situations. This involves incorporating melting phenomena, mechanisms for closing gaps and conducting 3D simulations. Furthermore, it would be beneficial to integrate coupled analyses that encompass both deformation and thermal stresses. This will provide a comprehensive understanding of the process.

High-Performance Computing utilization

To expedite and improve the accuracy of the optimization process we should utilize high performance computing capabilities to implement algorithms. These algorithms will not speed up optimization but also ensure precise determination of optimal welding parameters in a more efficient manner.

Field testing and industrial collaboration

In order to broaden the scope of this research it is essential to conduct full scale field testing for evaluating pipe performance across various applications and environmental conditions. Establishing partnerships with industrial collaborators will enable us to implement and validate the research outcomes in practical real-world settings. By adopting this approach, we can ensure that the research findings are not just theoretical but also robust and applicable, in meeting industry needs.

Exploration of reinforced fittings

Investigate the potential of designing electrofusion fittings with reinforcement materials or additives to enhance their mechanical strength. Analyse how these modifications may impact heat transfer within the fitting and at the welding interface. This exploration could uncover innovative approaches to improving joint performance.

REFERENCES

1- Da Costa, A. P., Botelho, E. C., Costa, M. L., Narita, N. E., & Tarpani, J. R. (2012). A review of welding technologies for thermoplastic composites in aerospace applications. *Journal of Aerospace Technology and Management*, *4*(3), 255–265. https://doi.org/10.5028/jatm.2012.04033912

2- Alshammari BA, Alsuhybani MS, Almushaikeh AM, Alotaibi BM, Alenad AM, Alqahtani NB, Alharbi AG. Comprehensive Review of the Properties and Modifications of Carbon Fiber-Reinforced Thermoplastic Composites. Polymers (Basel). 2021 Jul 27;13(15):2474. doi: 10.3390/polym13152474

3- Yangye He, Murilo Augusto Vaz, Marcelo Caire. (2021),Stress and failure analyses of thermoplastic composite pipes subjected to torsion and thermomechanical loading, Marine Structures,Volume 79,2021,103024,ISSN 0951-8339, https://doi.org/10.1016/j.marstruc.2021.103024.

4- A. Zubail, A. Traidia, M. Masulli, K. Vatopoulos, T. Villette, I. Taie, Carbon and energy footprint of nonmetallic composite pipes in onshore oil and gas flowlines,Journal of Cleaner Production,Volume 305,2021,ISSN 0959-6526. https://doi.org/10.1016/j.jclepro.2021.127150.

5- Wang, S. Q., Yao, L., & Meng, X. J. (2018). Bending mechanical behavior analysis of glass-fiber reinforced thermoplastic pipe based on a nonlinear solid element model. *Journal of Marine Science and Technology (Taiwan)*, *26*(4), 575–586. https://doi.org/10.6119/JMST.201808_26(4).0010

6- Wilkins, J. (2018). Qualification of thermoplastic composite pipes. *Proceedings of the International Conference on Offshore Mechanics and Arctic Engineering - OMAE*, *5*, 1–7. https://doi.org/10.1115/OMAE2018-77014

7- James C. Hastie, Maria Kashtalyan, Igor A. Guz, Failure analysis of thermoplastic composite pipe (TCP) under combined pressure, tension and thermal gradient for an offshore riser application,International Journal of Pressure Vessels and Piping,Volume 178, 2019, ISSN 0308-161, https://doi.org/10.1016/j.ijpvp.2019.103998.

8- Yu K, Morozov EV, Ashraf MA, Shankar K. A review of the design and analysis of reinforced thermoplastic pipes for offshore applications. *Journal of Reinforced Plastics and Composites*. 2017;36(20):1514-1530. doi:10.1177/0731684417713666

9- Yangye He, Murilo Augusto Vaz, Marcelo Caire,Stress and failure analyses of thermoplastic composite pipes subjected to torsion and thermomechanical loading, Marine Structures,Volume 79,2021,103024,ISSN 0951-8339, https://doi.org/10.1016/j.marstruc.2021.103024

10- James C. Hastie, Igor A. Guz, Maria Kashtalyan, Effects of thermal gradient on failure of a thermoplastic composite pipe (TCP) riser leg,International Journal of Pressure Vessels and Piping,Volume 172,2019,Pages 90-99,ISSN 0308-0161, https://doi.org/10.1016/j.ijpvp.2019.03.027.

11- Qi, G., Wu, Y., Qi, D., Wei, B., Li, H., Ding, N., & Cai, X. (2015). Experimental study on the thermostable property of aramid fiber reinforced PE-RT pipes. *Natural Gas Industry B*, *2*(5), 461–466. https://doi.org/10.1016/j.ngib.2015.09.023

12- Toh, W., Tan, L. Bin, Jaiman, R. K., Tay, T. E., & Tan, V. B. C. (2018). A comprehensive study on composite risers: Material solution, local end fitting design and global response. Marine Structures, 61(May), 155–169. https://doi.org/10.1016/j.marstruc.2018.05.005

13- Kiani, M., Parvaneh, V., Dadrasi, A. et al. Evaluating Tensile Strength in Butt Fusion and Electrofusion Joints in Nanocomposite HDPE Pipes. Exp Tech 46, 191–202 (2022). https://doi.org/10.1007/s40799-021-00477-x

14- Wenshu Liu, Yong Bai, Yifan Gao, Xianni Song & Zhiping Han (2022) Analysis of the mechanical properties of a reinforced thermoplastic composite pipe joint, Ships and Offshore Structures, 17:7, 1515-1521, DOI: 10.1080/17445302.2021.1932024

15- Liu, W.; Gao, Y.; Shao, Q.; Cai, W.; Han, Z.; Chi, M. Design and analysis of joints in reinforced thermoplastic composite pipe under internal pressure. *Ships Offshore Struct.* **2022**, *17*, 1276–1285, https://doi.org/10.1080/17445302.2021.1907065

16- *High pressure (sandwich) ef coupler pe100 / yüksek basinçli ef manşon pe100 | tega mühendislik*. (n.d.). high pressure (sandwich) ef coupler pe100.. http://www.tega.com.tr/product-detail/high-pressure-sandwich-ef-coupler-pe100-yuksek-basincli-ef-manson-pe100/

17- Electrofusion fittings. (2021, January 27). Soluforce. https://www.soluforce.com/product-overview/fittings/electrofusion-fittings.html

18- Bowman, J. (1997). A Review of the Electrofusion Joining Process for Polyethylene Pipe Systems. *Radius*, *5*(3), 2–54.

19- Rosala, G. F., Day, A. J., & Wood, A. S. (1997). A finite element model of the electrofusion welding of thermoplastic pipes. *Proceedings of the Institution of Mechanical Engineers, Part E: Journal of Process Mechanical Engineering*, *211*(2), 137–146. https://doi.org/10.1243/0954408971529629

20- Gierulski MP, Tomlinson R, Troughton M. Electrofusion welding and reinforced thermoplastic pipes – A review. *Journal of Reinforced Plastics and Composites*. 2022;41(3-4):147-163. doi:10.1177/07316844211051207

21- *Radius Systems*. Product Page - Radius Systems. https://www.radius-systems.com/products/gas/electrofusion-fittings-gas-applications

22- GillesRégnier, StevenLeCorre. Modeling of Thermoplastic Welding. Nicolas Boyard. Heat Transfer in Polymer Composite Materials: Forming Processes,Wiley, pp.235-268,2016,978-111911628-8;978184821761-4. 10.1002/9781119116288.ch8. hal-02591944

23- F. Yang and R. Pitchumani. Healing of Thermoplastic Polymers at an Interface under Nonisothermal Conditions,Macromolecules 2002 35 (8), 3213-3224, ISSN0024-9297, DOI:10.1021/ma010858o

24- Julien Avenet, Thomas A. Cender, Steven Le Corre, Jean-Luc Bailleul, Arthur Levy, Experimental correlation of rheological relaxation and interface healing times in welding thermoplastic PEKK composites,Composites Part A: Applied Science and Manufacturing,Volume 149,2021,106489,ISSN 1359-835X, https://doi.org/10.1016/j.compositesa.2021.106489

25- Fujikake, M., Fukumura, M., & Kitao, K. (1997). Analysis of the electrofusion joining process in polyethylene gas piping systems. *Computers and Structures*, *64*(5–6), 939–948. https://doi.org/10.1016/S0045-7949(97)00008-4

26- Shi, J., Zheng, J., Guo, W. and Qin, Y. (2012), Defects classification and failure modes of electrofusion joint for connecting polyethylene pipes. J. Appl. Polym. Sci., 124: 4070-4080. https://doi.org/10.1002/app.35013

27- Ge, Z, Yao, R, Shi, J, & Zheng, J. "A Comprehensive Review on Failure Analysis of Electrofusion Joint For Plastic Pipes." *Proceedings of the . Volume 2: Computer Technology and Bolted Joints; Design and Analysis*. Virtual, Online. July 13–15, 2021. V002T03A013. ASME. https://doi.org/10.1115/PVP2021-62132

28- Plastics Industry Pipe Association of Australia (PIPA). (2021). POP001 – Electrofusion Jointing of PE Pipes and Fittings for Pressure Applications (Issue 8.1).

29- Troughton, M., & Brown, C. (2011). *Comparison of long-term and short-term tests for electrofusion joints in PE pipes (Octobe ... Page 1 of 10 Comparison of long-term and short-*

term tests for electrofusion joints in PE pipes Comparison of long-term and short-term tests for electrofusion jo. *08*(1), 1–10.

30- R. Kafieh, T. Lotfi, Rassoul Amirfattahi, Automatic detection of defects on polyethylene pipe welding using thermal infrared imaging, Infrared Physics & Technology, Volume 54, Issue 4, 2011, Pages 317-325, ISSN 1350-4495, https://doi.org/10.1016/j.infrared.2010.12.010.

31- Abolfazl Tutunchi, Mehdi Eskandarzade, Reza Aghamohammadi, Tahereh Masalehdan, Karim Osouli-Bostanabad,Risk assessment of electrofusion joints in commissioning of polyethylene natural gas networks, International Journal of Pressure Vessels and Piping, Volume 196, 2022, 104627, ISSN 0308-161, https://doi.org/10.1016/j.ijpvp.2022.104627.

32- Tayefi, P., Beck, S.B.M. orcid.org/0000-0003-2673-4179 and Tomlinson, R.A. (2015) Fatigue Failure of Polyethylene Electrofusion Joints Subject to Contamination. . 2014 Annual Conference on Experimental and Applied Mechanics Conference Proceedings of the Society for Experimental Mechanics Series, 5 . Springer International Publishing , pp. 197-202. ISBN 9783319069760 https://doi.org/10.1007/978-3-319-06977-7_26

33- Sarambale, D & Shinde, Dattaji. (2017). Electro-Fusion Joint Failure Polyethylene Pipes Analysis and its Simulation using Finite Element Analysis. International Journal of Food Engineering. 5. 51-55.

34- Barton, N.A., Farewell, T.S. & Hallett, S.H. Using generalized additive models to investigate the environmental effects on pipe failure in clean water networks. npj Clean Water 3, 31 (2020). https://doi.org/10.1038/s41545-020-0077-3

35- Gao, Guanling & Tian, Xiaojiang & Luo, Tao & Li, Chao & Gao, Jin. (2023). Study on Structural Aging and Gas Leakage Failure Behavior of Electrofusion Socket of Buried Polyethylene Gas Pipes. Journal of Physics: Conference Series. 2468. 012119. 10.1088/1742-6596/2468/1/012119.

36- Ageorges, C., Ye, L., & Hou, M. (2001). Advances in fusion bonding techniques for joining thermoplastic matrix composites: A review. *Composites - Part A: Applied Science and Manufacturing*, *32*(6), 839–857. https://doi.org/10.1016/S1359-835X(00)00166-4

37- Ezekoye, O.A., Lowman, C.D., Fahey, M.T. and Hulme-Lowe, A.G. (1998), Polymer weld strength predictions using a thermal and polymer chain diffusion analysis. Polym Eng Sci, 38: 976-991. https://doi.org/10.1002/pen.10266

38- Pitman, G. L. (1985). Electrofusion Welding Prediction and Computer-Aided Design of Fittings. International Conference - Plastics Pipes.

39- Shi, J., Zheng, J., & Guo, W. (2008). A model for predicting temperature of electrofusion joints for polyethylene pipes. American Society of Mechanical Engineers, Pressure Vessels and Piping Division (Publication) PVP, 5(December), 303–313. https://doi.org/10.1115/PVP2008-61724
40- Rajabi, A. & Alinejad, Javad. (2018). Simulation of Melting in an Electrofusion Joint Using Lattice Boltzmann Method. Journal of Thermophysics and Heat Transfer. 33. 1-9. 10.2514/1.T5507.
41- Nakashiba, A., Nishimura, H., Inoue, F., Nakagawa, T., Homma, K., & Nakazato, H. (1993). Fusion simulation of electrofusion polyethylene joints for gas distribution. Polymer Engineering and Science, 33(17), 1146–1151. doi:10.1002/pen.760331708
42- Nishimura, H., Inoue, F., Nakashiba, A., & Ishikawa, T. (1994). Design of electrofusion joints and evaluation of fusion strength using fusion simulation technology. Polymer Engineering and Science, 34(20), 1529–1534. doi:10.1002/pen.760342003
43- Fujikake, M., Fukumura, M., & Kitao, K. (1997). Analysis of the electrofusion joining process in polyethylene gas piping systems. Computers and Structures, 64(5–6), 939–948.
44- Ziad Chebbo, Michel Vincent, Adil Boujlal, Dominique Gueugnaut, Yannick Tillier. Numerical and experimental study of the electrofusion welding process of polyethylene pipes. Polymer Engineering and Science, 2015, 55 (1), pp.123-131. ⟨10.1002/pen.23878⟩. ⟨hal-00954554⟩
45- Zheng, J., Zhong, S., Shi, J., & Guo, W. (2015). Study on the allowable temperature for preventing over welding during thermal welding of polyethylene pipe. Journal of Pressure Vessel Technology, Transactions of the ASME, 137(2).
46- NP Starostin and RS Tikhonov. Thermoelastic state during electrofusion welding of polyethylene pipes at different ambient temperatures, 2022 *IOP Conf. Ser.: Earth Environ. Sci.* 991 012011 DOI:10.1088/1755-1315/991/1/012011
47- N. P. Starostin, O. A. Ammosova; Calculation of the technological parameters of electrofusion welding of polyethylene pipes at low temperatures. AIP Conf. Proc. 12 December 2017; 1915 (1): 040057. https://doi.org/10.1063/1.5017405
48- Rosala, G.F., (1995). THE PROCESS MECHANICS OF POLYMER PIPES WELDING BY ELECTRO-FUSION. PhD thesis
49- Riahi, M., Arab, H. & Ghanati, M.F. Analysis of pressure exertion's effect on electrofusion welding process of polymer pipes. Int J Adv Manuf Technol 57, 183–188 (2011). https://doi.org/10.1007/s00170-011-3287-5

50- Sima Mansouri, M. Sadegh Tavallali, Heat transfer approximate modeling, parameter estimation and thermography of thermal pulsing in electrofusion joints of gas pipelines, Infrared Physics & Technology, Volume 98, 2019, Pages 354-363, ISSN 1350-4495, https://doi.org/10.1016/j.infrared.2019.03.002.
51- M. Javadi Azad, M. Sadegh Tavallali, A novel computational supplement to an IR-thermography based non-destructive test of electrofusion polyethylene joints, Infrared Physics & Technology, Volume 96, 2019,Pages 30-38, ISSN 1350-4495, https://doi.org/10.1016/j.infrared.2018.10.031.
52- Zhiyong Jiang, Yujing Tang, Jens Rieger, Hans-Friedrich Enderle, Dieter Lilge, Stephan V. Roth, Rainer Gehrke, Zhonghua Wu, Zhihong Li, Yongfeng Men,Structural evolution of tensile deformed high-density polyethylene at elevated temperatures: Scanning synchrotron small- and wide-angle X-ray scattering studies,Polymer,Volume 50, Issue 16,2009,Pages 4101-4111,ISSN 0032-3861, https://doi.org/10.1016/j.polymer.2009.06.063.
53- Yu Jia, Zepeng Mao, Wenxin Huang, Jun Zhang, Effect of temperature and crystallinity on the thermal conductivity of semi-crystalline polymers: A case study of polyethylene, Materials Chemistry and Physics, Volume 287, 2022,126325, ISSN 0254-0584, https://doi.org/10.1016/j.matchemphys.2022.126325.
54- International Organization for Standardization. ISO 8894-2:2007 Refractory materials. Determination of thermal conductivity. Hot-wire method (parallel)
55- International Organization for Standardization. BS EN ISO 22007-2:2022 Plastics. Determination of thermal conductivity and thermal diffusivity. Transient plane heat source (hot disc) method
56- International Organization for Standardization. BS EN ISO 8302:1991 Thermal insulation. Determination of steady-state thermal resistance and related properties. Guarded hot plate apparatus.
57- International Organization for Standardization. BS EN ISO 11357-4:2021 Plastics. Differential scanning calorimetry (DSC). Determination of specific heat capacity
58- International Organization for Standardization. BS EN ISO 19935-2:2020 Plastics. Temperature modulated DSC. Measurement of specific heat capacity
59- International Organization for Standardization. BS EN ISO 11357-3:2018 Plastics. Differential scanning calorimetry (DSC). Determination of temperature and enthalpy of melting and crystallization

60- International Organization for Standardization. BS ISO 11359-2:2021 Plastics. Thermomechanical analysis (TMA). Determination of coefficient of linear thermal expansion and glass transition temperature
61- S. Min, J. Blumm, A. Lindemann, A new laser flash system for measurement of the thermophysical properties, Thermochimica Acta, Volume 455,Issues 1–2,2007,Pages 46-49, ISSN 0040-6031,https://doi.org/10.1016/j.tca.2006.11.026.
62- Takizawa, Yoshihiro & Chung, Deborah. (2016). Through-thickness thermal conduction in glass fiber polymer–matrix composites and its enhancement by composite modification. Journal of Materials Science. 51. 10.1007/s10853-015-9665-x.
63- Hsuan-Yu Chen, Chiachung Chen,Determining the emissivity and temperature of building materials by infrared thermometer, Construction and Building Materials, Volume 126, 2016, Pages 130-137, ISSN 0950-0618, https://doi.org/10.1016/j.conbuildmat.2016.09.027
64- Caravaca, D & Bird, C & Kleiner, D. (2007). Ultrasonic phased array inspection of electrofusion joints in polyethylene pipes. Insight - Non-Destructive Testing and Condition Monitoring. 49. 83-86. 10.1784/insi.2007.49.2.83.
65- A. S. WOOD, G. F. ROSALA and A. J. DAY, "Control-volume simulation of the electrofusion welding process," in IMA Journal of Management Mathematics, vol. 9, no. 1, pp. 65-88, Jan. 1998, doi: 10.1093/imaman/9.1.65.
66- Samat A. Kassabek, Durvudkhan Suragan,Two-phase inverse Stefan problems solved by heat polynomials method,Journal of Computational and Applied Mathematics,Volume 421, 2023, 114854, ISSN 0377-0427, https://doi.org/10.1016/j.cam.2022.114854.
67- Muhieddine, Mohamad & Canot, Edouard & March, Ramiro. (2009). Various Approaches for Solving Problems in Heat Conduction with Phase Change. International Journal On Finite Volumes. 6.
68- COMSOL Multiphysics Reference Manual
69- Tian Zhou, Yejing Zhao, Zhenghua Rao, Fundamental and estimation of thermal contact resistance between polymer matrix composites: A review, International Journal of Heat and Mass Transfer, Volume 189, 2022, 122701, ISSN 0017-9310, https://doi.org/10.1016/j.ijheatmasstransfer.2022.122701.
70- Colaco, Marcelo & Orlande, Helcio & Dulikravich, George. (2006). Inverse and Optimisation Problems in Heat Transfer. Journal of the Brazilian Society of Mechanical Sciences and Engineering. XXVIII. 10.1590/S1678-58782006000100001.

71- Miao Cui, Wei-wei Duan, Xiao-wei Gao, A new inverse analysis method based on a relaxation factor optimization technique for solving transient nonlinear inverse heat conduction problems,International Journal of Heat and Mass Transfer,Volume 90, 2015, Pages 491-498, ISSN 0017-9310, https://doi.org/10.1016/j.ijheatmasstransfer.2015.07.009.
72- Miao Cui, Wei-wei Duan, Xiao-wei Gao, A new inverse analysis method based on a relaxation factor optimization technique for solving transient nonlinear inverse heat conduction problems,International Journal of Heat and Mass Transfer, Volume 90, 2015, Pages 491-498, ISSN 0017-9310, https://doi.org/10.1016/j.ijheatmasstransfer.2015.07.009.
73- British Standards Institution (BSI). BS EN 1555-3:2021, Plastics piping systems for the supply of gaseous fuels - Polyethylene (PE) - Part 3: Fittings.
74- Maciej P Gierulski, Electrofusion joining of thermoplastic composite pipes, PhD thesis, The University of Sheffield
75- DVS 2207-1, Welding of Thermoplastics - Heated Element Welding of Pipes, Piping Parts, and Panels Made Out of Polyethylene
76- Zhiqiang Cai, Hongbin Dai, Xibin Fu, Investigation on the hot melting temperature field simulation of HDPE water supply pipeline in gymnasium pool, Results in Physics, Volume 9, 2018, Pages 1050-1056, ISSN 2211-3797, https://doi.org/10.1016/j.rinp.2018.04.019.
77- Okolie, O., Latto, J., Faisal, N. et al. Manufacturing Defects in Thermoplastic Composite Pipes and Their Effect on the in-situ Performance of Thermoplastic Composite Pipes in Oil and Gas Applications. Appl Compos Mater 30, 231–306 (2023). https://doi.org/10.1007/s10443-022-10066-9

APPENDIX A

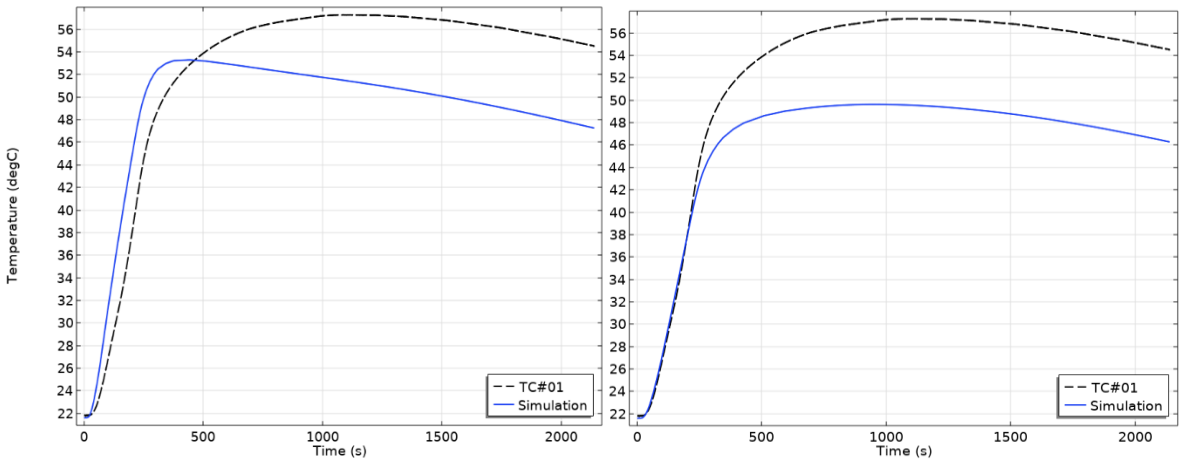

Figure A-1 TC#1 Simulated and experimental temperature over time a) before b) after optimization

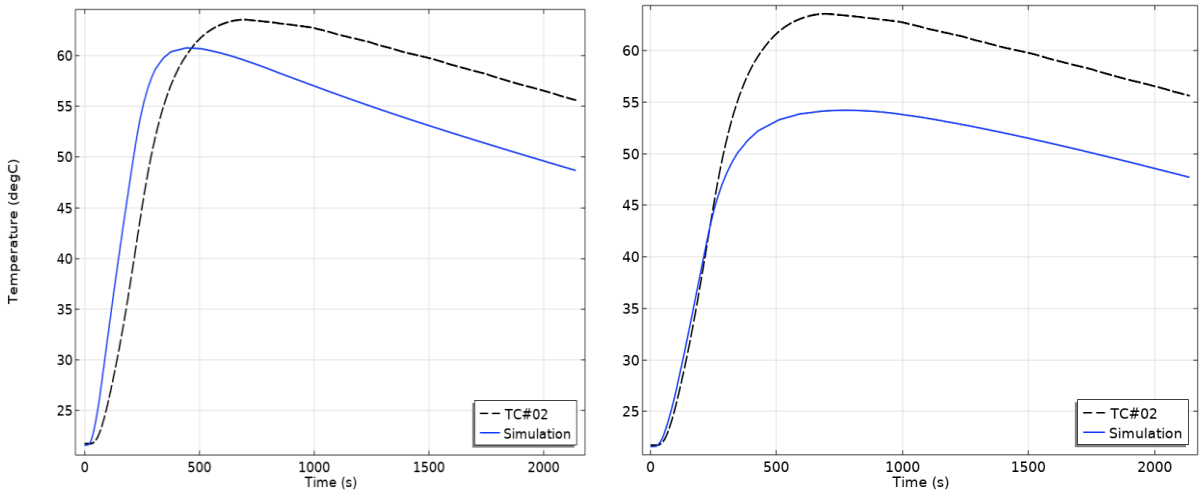

Figure A-2 TC#2 Simulated and experimental temperature over time a) before b) after optimization

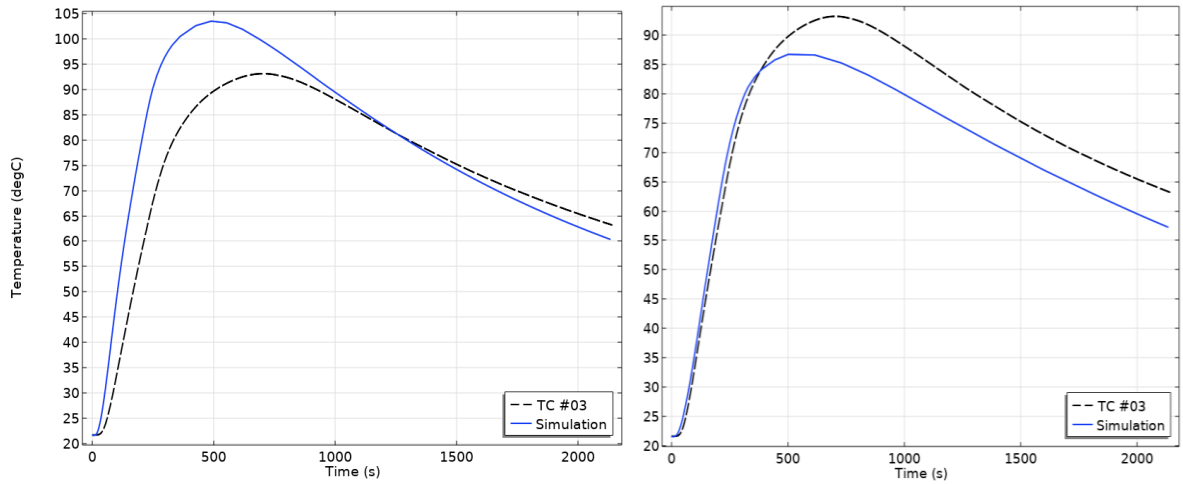

Figure A-3 TC#03 Simulated and experimental temperature over time a) before b) after optimization

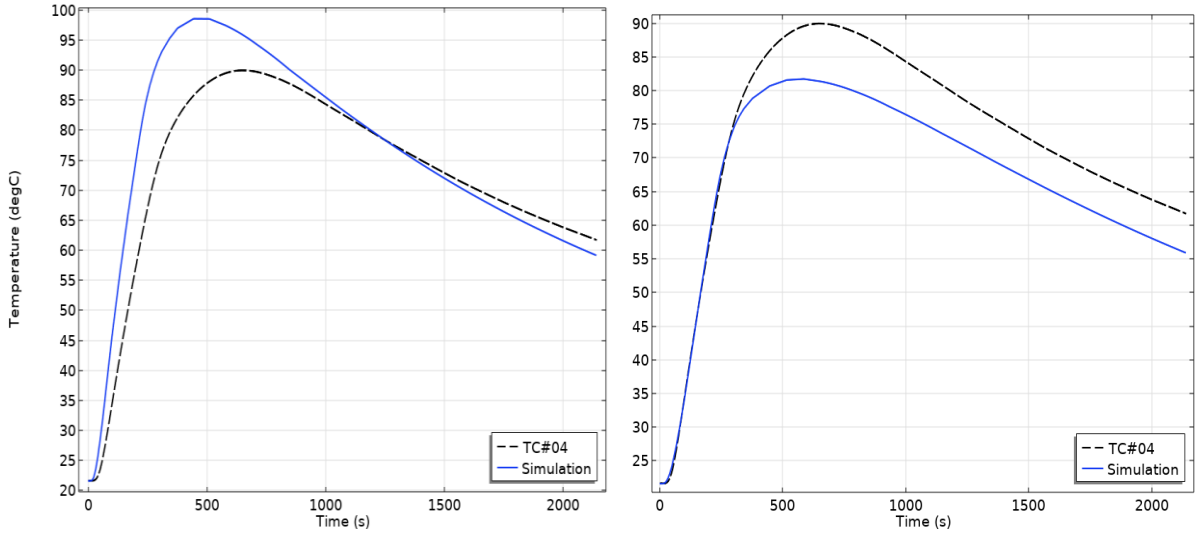

Figure A-4 TC#04 Simulated and experimental temperature over time a) before b) after optimization

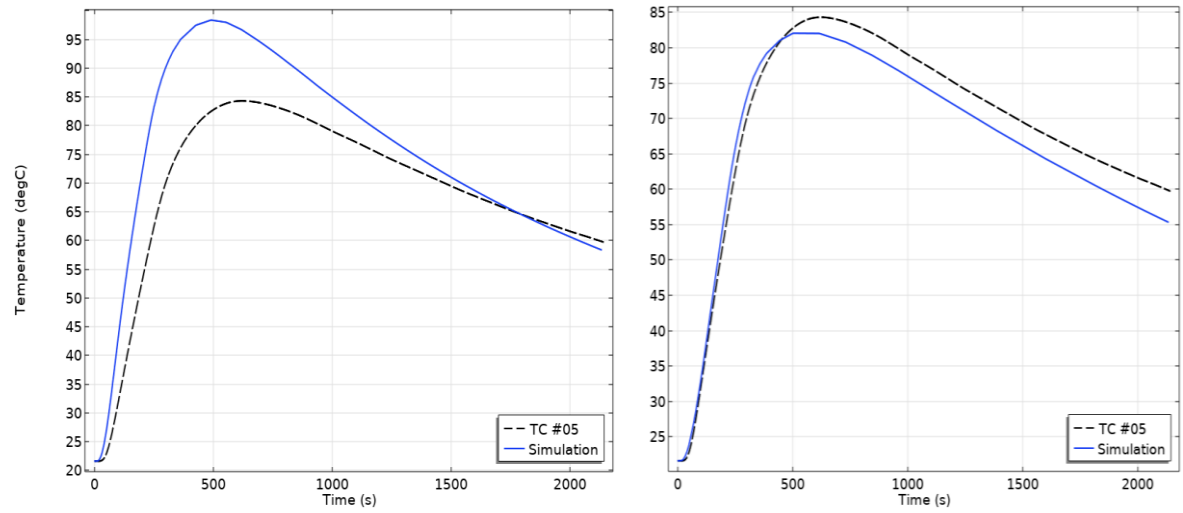

Figure A-5 TC#05 Simulated and experimental temperature over time a) before b) after optimization

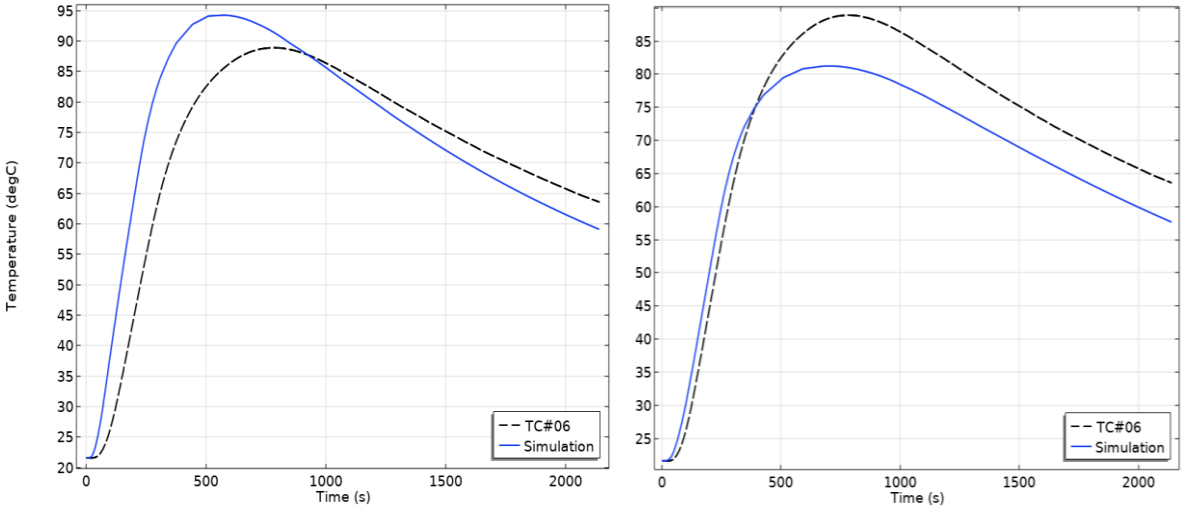

Figure A-6 TC#06 Simulated and experimental temperature over time a) before b) after optimization

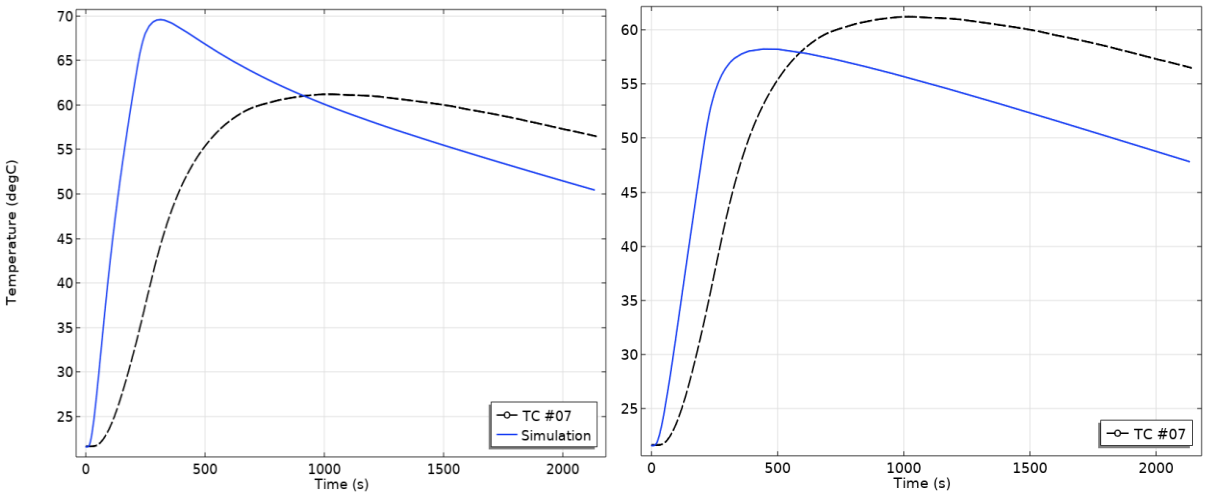

Figure A-7 TC#07 Simulated and experimental temperature over time a) before b) after optimization

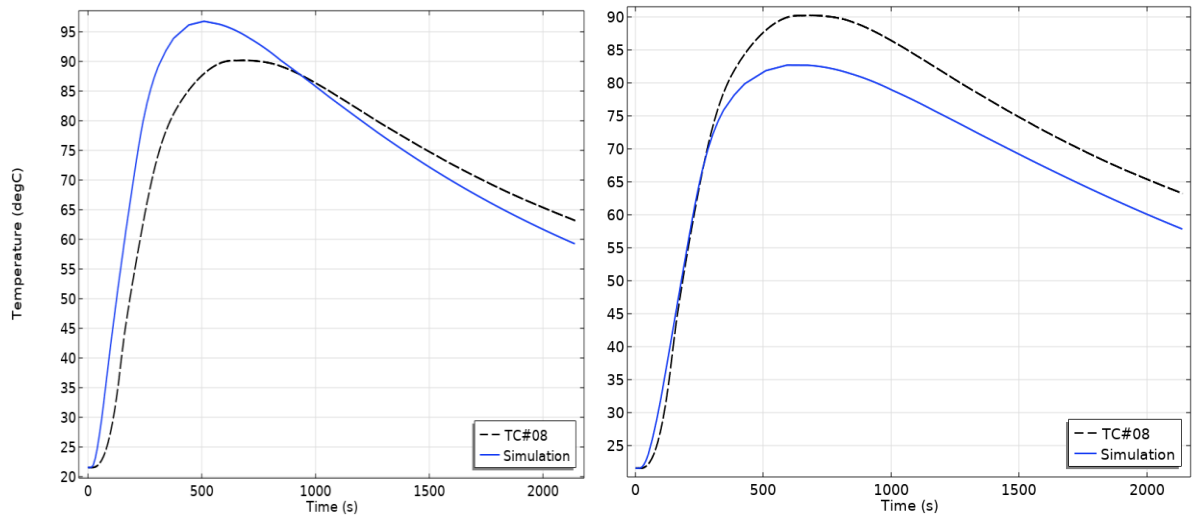

Figure A-8 TC#08 Simulated and experimental temperature over time a) before b) after optimization

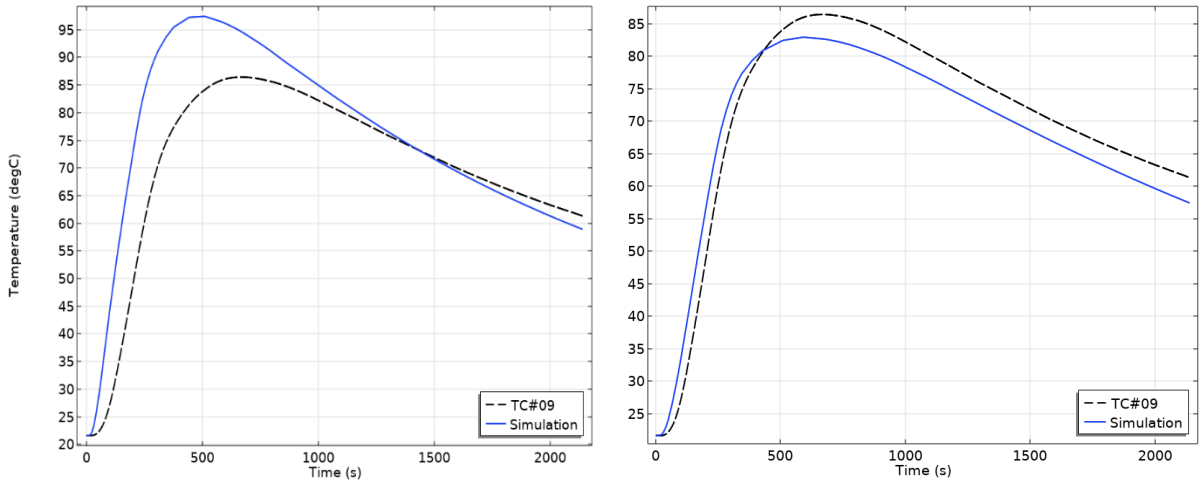

Figure A-9 TC#09 Simulated and experimental temperature over time a) before b) after optimization

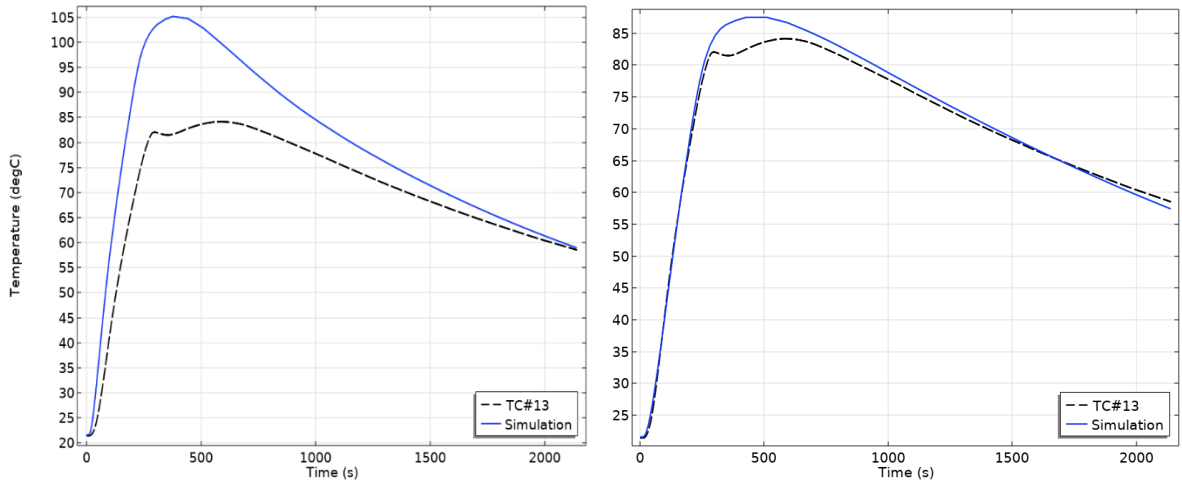

Figure A-10 TC#13 Simulated and experimental temperature over time a) before b) after optimization

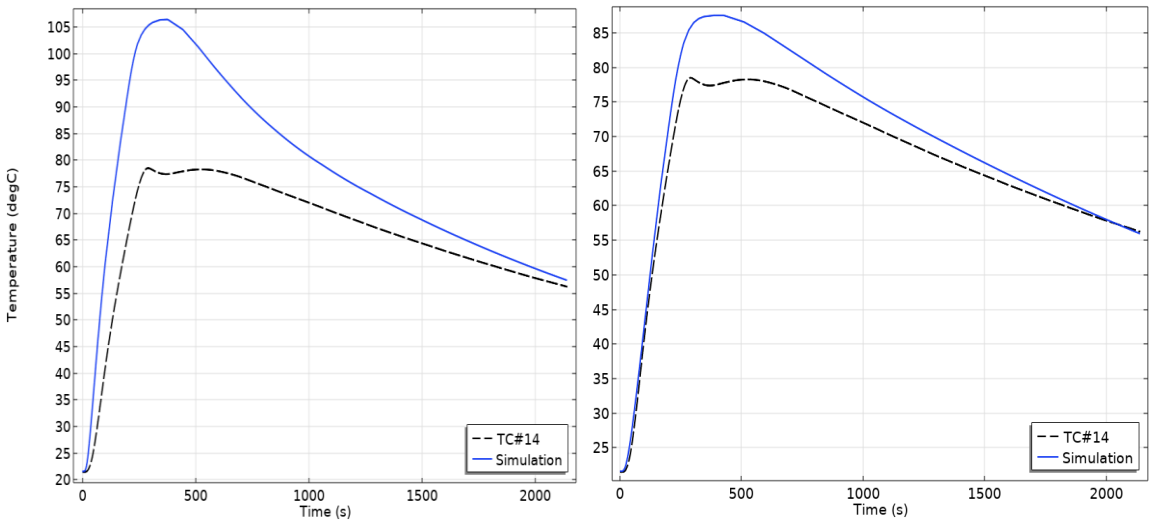

Figure A-11 TC#14 Simulated and experimental temperature over time a) before b) after optimization

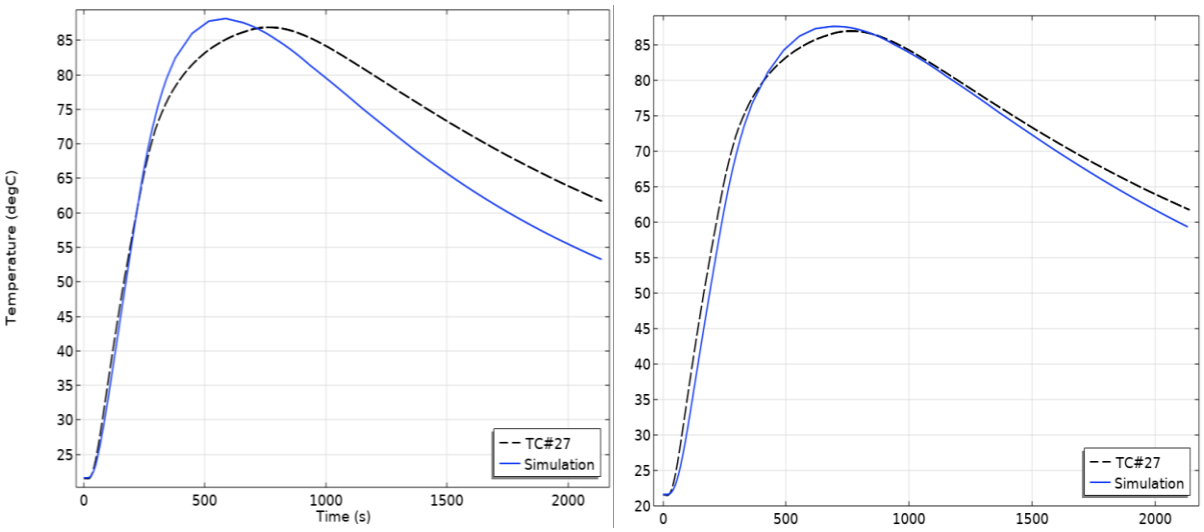

Figure A-12 TC#27 Simulated and experimental temperature over time a) before b) after optimization

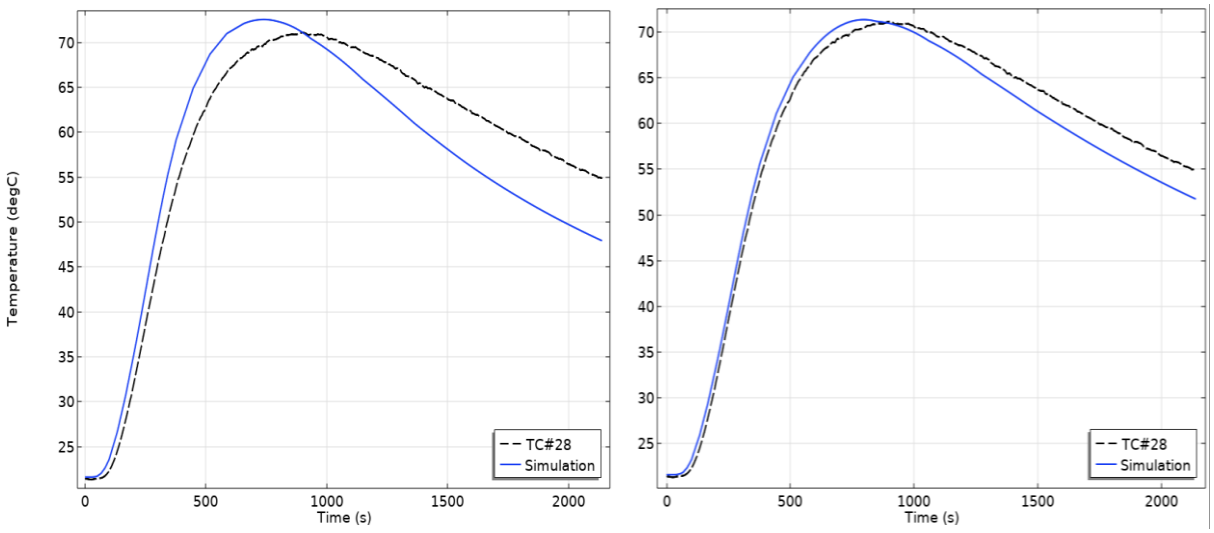

Figure A-13 TC#28 Simulated and experimental temperature over time a) before b) after optimization

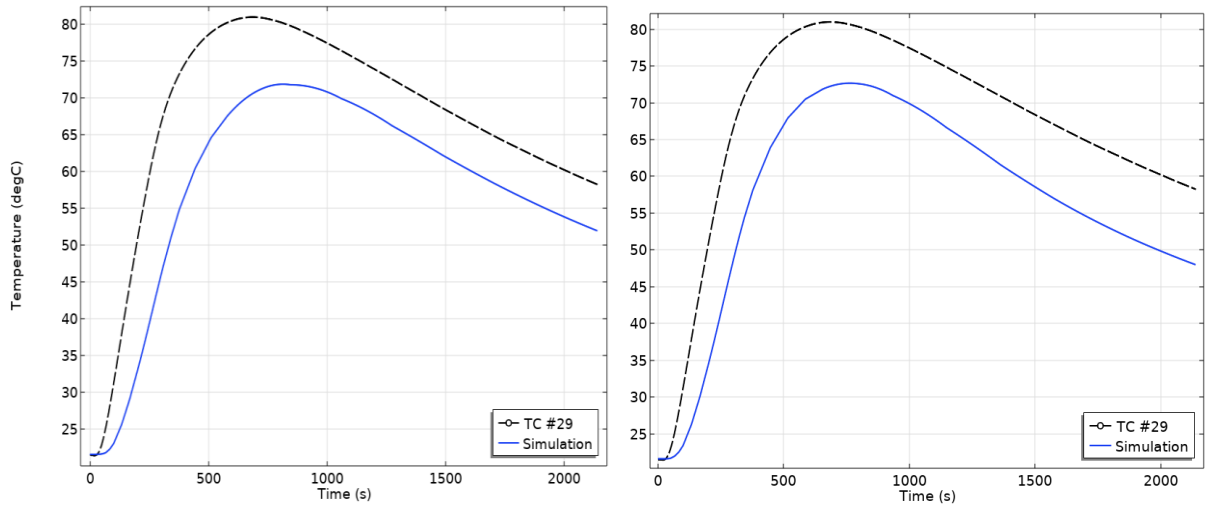

Figure A-14 TC#29 Simulated and experimental temperature over time a) before b) after optimization

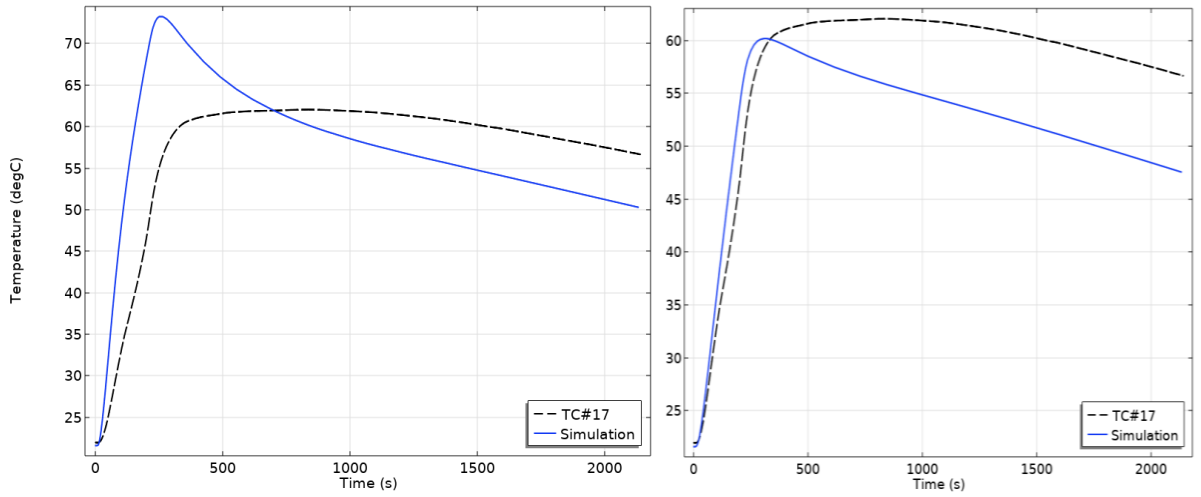

Figure A-15 TC#17 Simulated and experimental temperature over time a) before b) after optimization

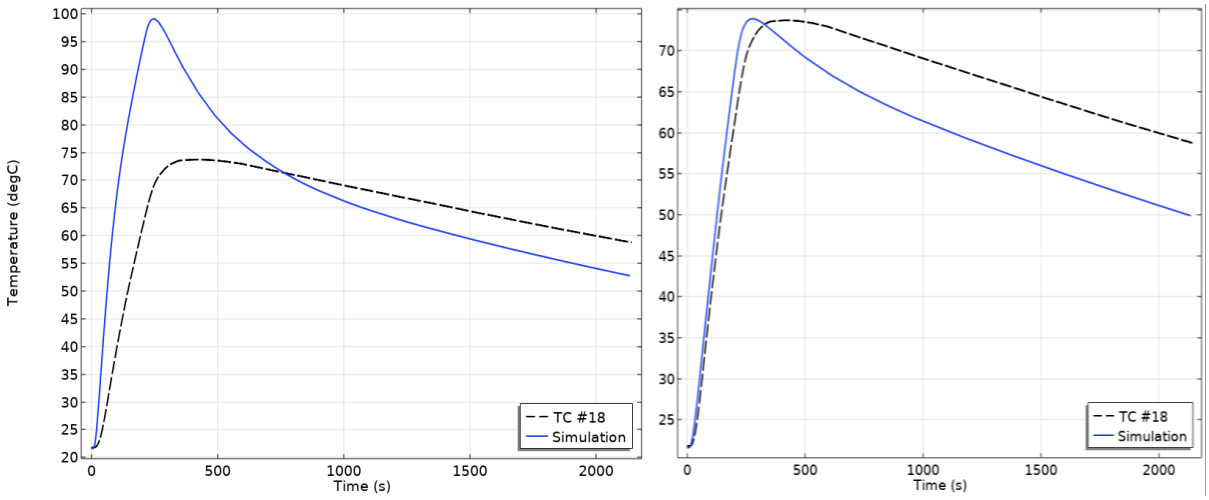

Figure A-16 TC#18 Simulated and experimental temperature over time a) before b) after optimization

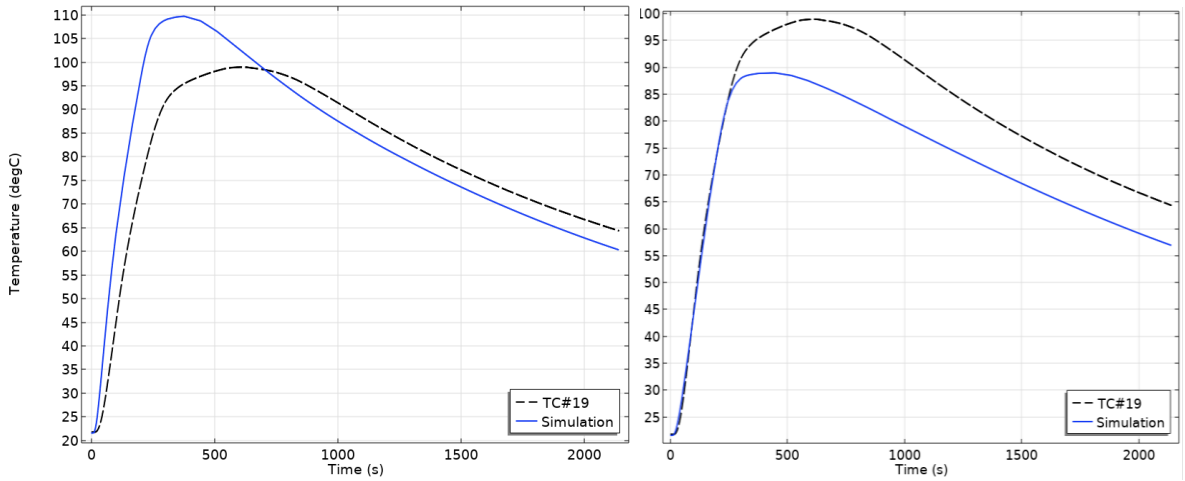

Figure A-17 TC#19 Simulated and experimental temperature over time a) before b) after optimization

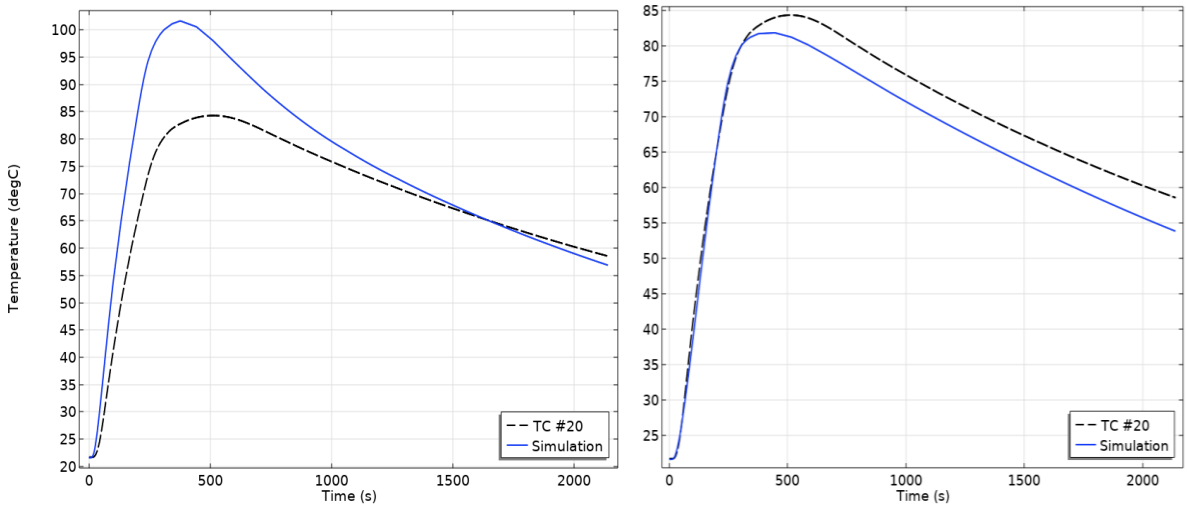

Figure A-18 TC#20 Simulated and experimental temperature over time a) before b) after optimization

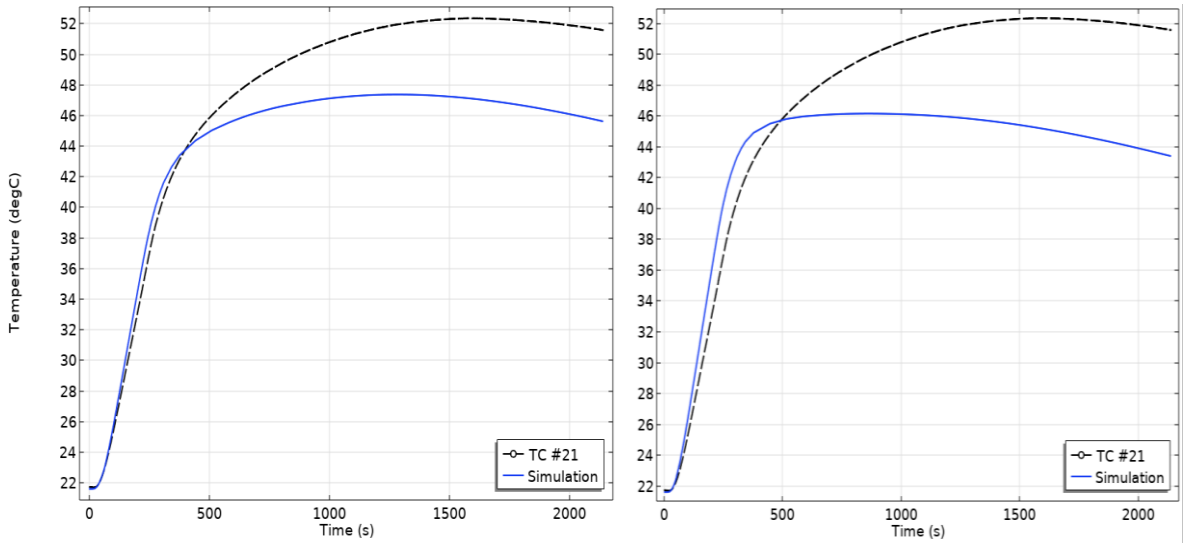

Figure A-19 TC#21 Simulated and experimental temperature over time a) before b) after optimization

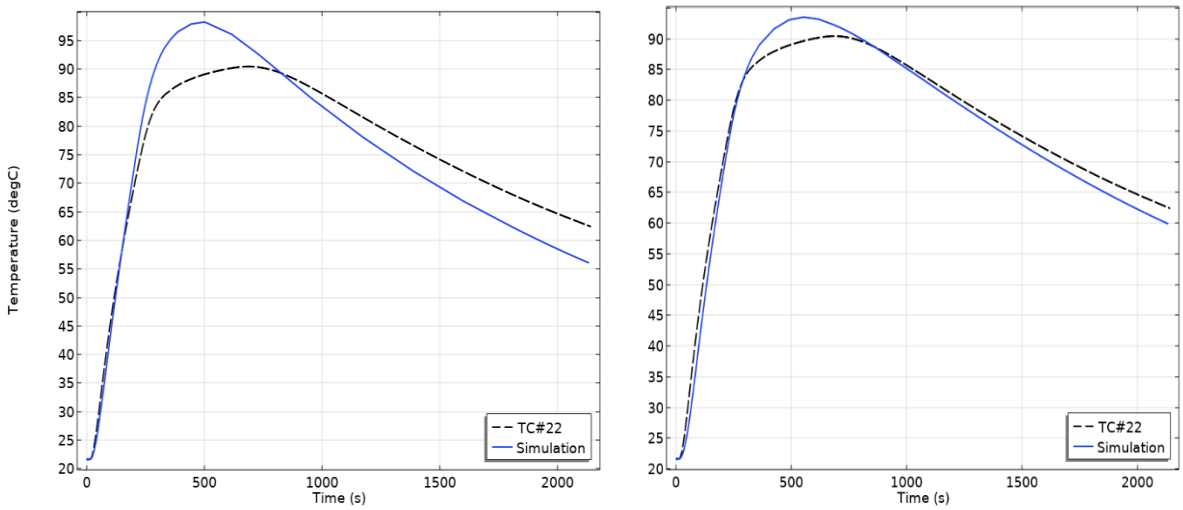

Figure A-20 TC#22 Simulated and experimental temperature over time a) before b) after optimization

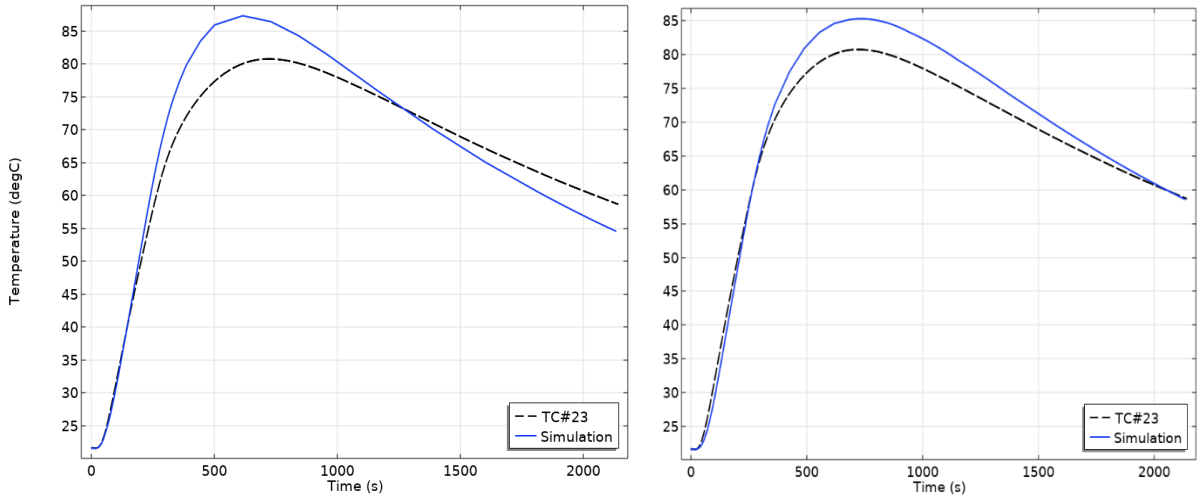

Figure A-21 TC#23 Simulated and experimental temperature over time a) before b) after optimization

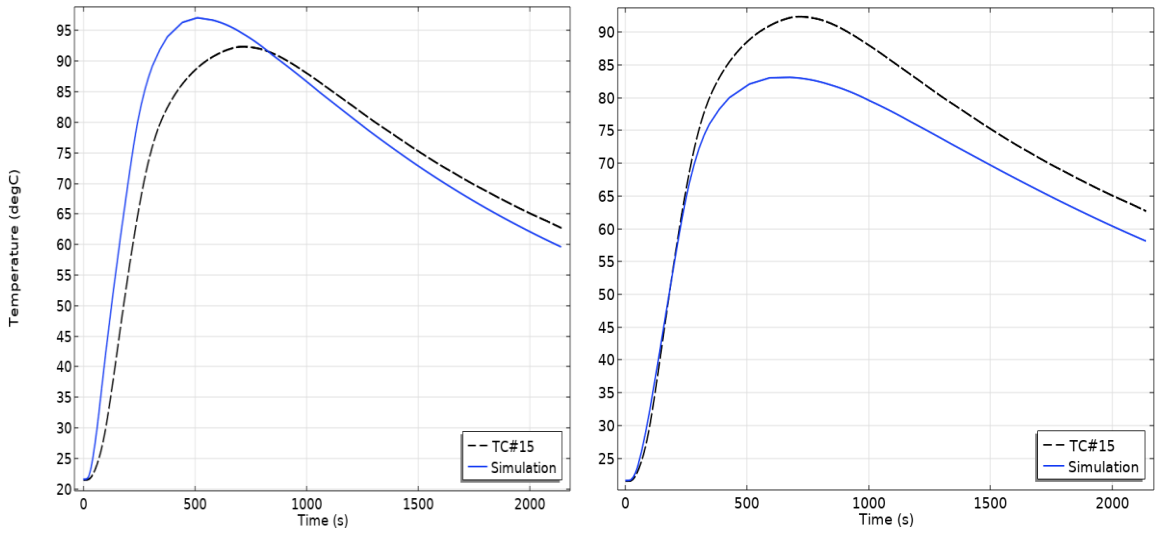

Figure A-22 TC#15 Simulated and experimental temperature over time a) before b) after optimization

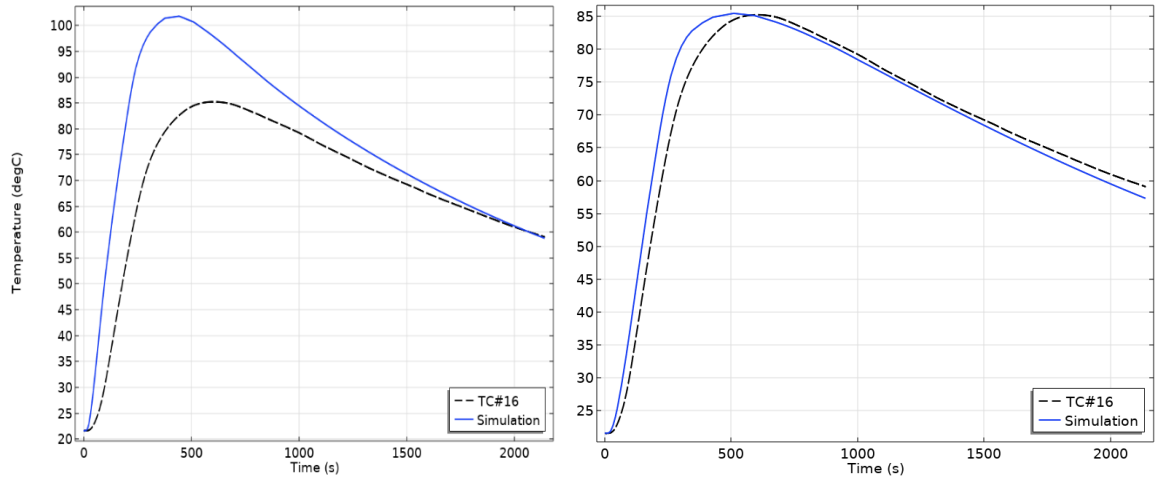

Figure A-23 TC#16 Simulated and experimental temperature over time a) before b) after optimization

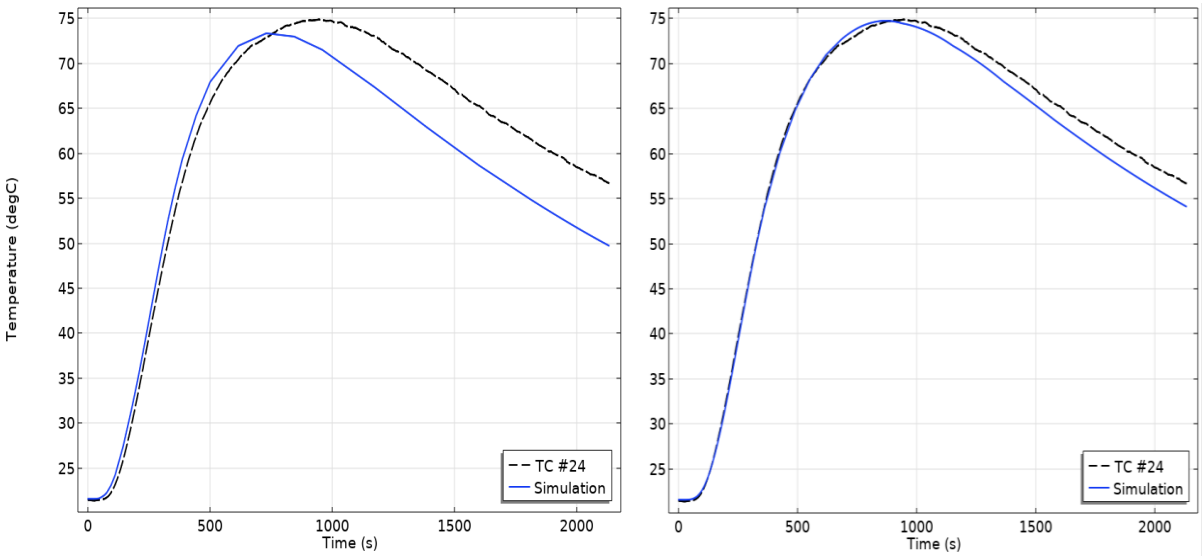

Figure A-24 TC#24 Simulated and experimental temperature over time a) before b) after optimization

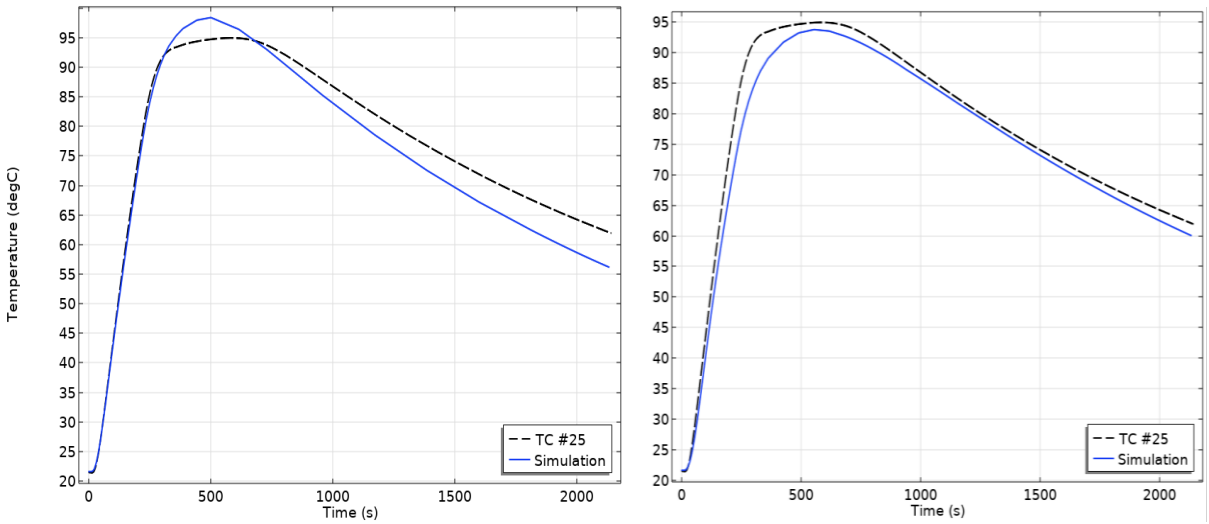

Figure A-25 TC#25 Simulated and experimental temperature over time a) before b) after optimization

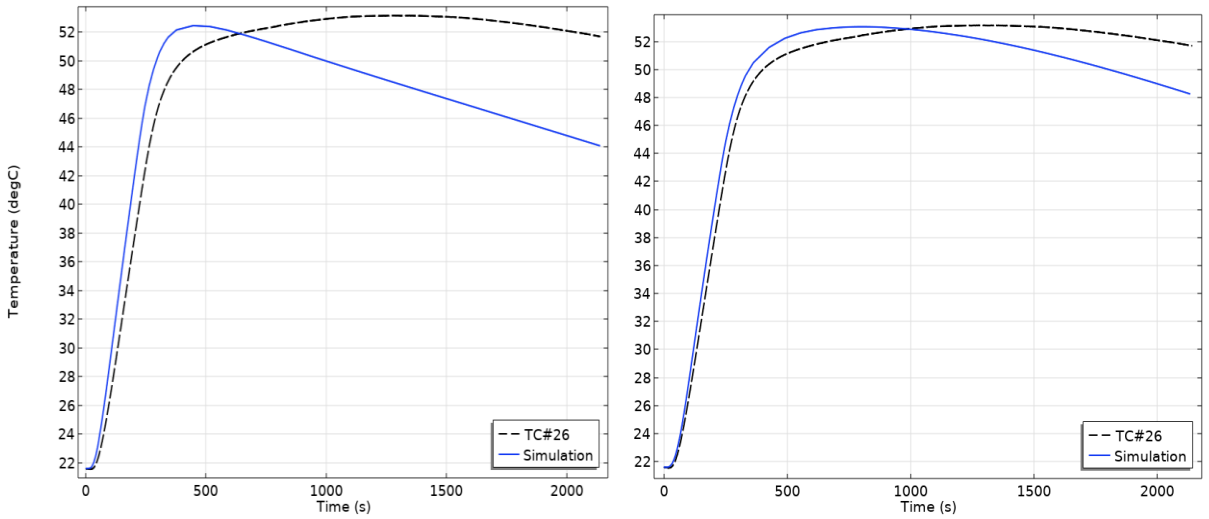

Figure A-26 TC#26 Simulated and experimental temperature over time a) before b) after optimization